A General Effective Action for Quark Matter and its Application to Color Superconductivity

von
Philipp Tim Reuter
aus Bonn

vom Fachbereich Physik der Johann Wolfgang Goethe–Universität
als Dissertation angenommen.

Dekan: Prof. Dr. W. Aßmus

Gutachter: Prof. Dr. D.-H. Rischke, HD Dr. J. Schaffner-Bielich

Datum der Disputation: 30.11.2005

Contents

List of Figures

List of Tables

Chapter 1

Introduction

1.1 Quark matter and strong interactions

In contrast to philosophers who search for meaning in nature, physicists investigate the properties of nature and search for the laws that inanimate nature obeys. Apparently, the properties of any given piece of (known) matter depend on its temperature and its density. It is therefore not at all a naive question to ask: "What happens to some piece of matter if I heat and squeeze it...further and further?" One correct answer could be: "You may use QCD to describe it." At least this applies to "normal" matter made of atoms. Atoms have a nucleus, which is composed of neutrons and protons, which in turn consist of quarks. Quarks are fermions and interact with each other by exchanging gluons, which mediate the strong interaction. The charge corresponding to the strong interaction is called color and the quantum field theory describing this interaction Quantum Chromodynamics (QCD). Generally, all particles that interact strongly are composed of quarks and called hadrons. Those hadrons, which are composed of a quark and an antiquark, are called mesons and those composed of three quarks, as the neutrons and protons mentioned above, baryons. While all quarks carry color charge, all hadrons are in total color neutral.

As long as the temperature and density of the considered system are not too large, i.e. below the scale $\Lambda_{\rm QCD} \simeq 200$ MeV, quarks are strongly coupled and always confined into these color neutral hadrons. As a consequence of this strong coupling perturbative approaches are impossible. The quarks are deconfined at temperatures or densities above $\Lambda_{\rm QCD}$. Well above this scale the strong interaction exhibits the phenomenon of asymptotic freedom [1], where QCD becomes weakly coupled. In this regime all hadrons vanish and quarks and gluons form a state called the quark-gluon plasma or simply quark matter [2].

Quarks also feel the electroweak and the gravitational force. The first one is described by a quantum field theory, which comprises electromagnetic and weak interactions. The theory for the latter, general relativity, describes gravitation in terms of the curvature of space-time and is a classical field theory. Due to their relative weakness as compared to the strong force it is often justified to neglect the gravitional and the electroweak against the strong interaction and describe the considered matter by QCD only. As a counter example related to this work, where QCD alone is not sufficient, one may allude to neutron stars. These are the compact remnants

of supernova explosions of type II [3, 4, 5]. They have extremely large masses comparable to the mass of our sun, but only very small radii of several kilometers. The density in their inner cores are possibly sufficient to deconfine the quarks. Since these stellar objects have to be electrically neutral and β−equilibrated, electroweak processes have to be considered. Furthermore, neutron stars are held together gravitationally. In order to describe their bulk properties adequately, one therefore has to account for gravity as well.

In the present work, however, only the strong interaction will be accounted for and, moreover, only its weak coupling regime will be considered. The aim is to derive an effective action for strongly interacting matter in the deconfined phase, i.e. for quark matter [6]. This motivated by the occurence of several well seperated momentum scales at high temperatures and/or baryonic densities, cf. Sec. 1.3. The derivation is performed in Sec. 2.1. The field of application comprises low energy phenomena in weakly coupled quark matter. By construction this action will only contain low energy quark and gluon modes as explicit degrees of freedom. At large temperatures such modes are, e.g., long wave-length collective excitations [7, 8, 9]. At large quark densities and low temperatures only those quarks, which are located close to the Fermi surface, are relevant degrees of freedom. The derived action can be adjusted to different high temperature and/or density regimes by a suitable choice of the projection operators, which separate high energy from low energy quark and gluon modes. These projection operators contain two independent cutoff parameters, Λ_q for quarks and Λ_{gl} for gluons. In Sec. 2.2 it is shown that well-known effective theories for strongly interacting quark matter can be assigned to special choices of these cutoff parameters in this general effective action. In chapter 3 the phenomenon of color superconductivity in quark matter will serve as a physical application to demonstrate the usefulness of the derived action in a semi-perturbative context.

Before going into more details, however, it is first necessary to provide an introductory overview of the basic principles of QCD and its phase diagram. This will be done in the remainder of this section. In Sec. 1.2 the phenomenon of color superconductivity will be introduced. In Sec. 1.3 the general concepts of effective theories are explained and some caveats with respect to quark matter are pointed out. Finally, the specific features of the effective approach developed in this work are discussed.

QCD: Asymptotic freedom, symmetries, and the phase diagram

QCD is a non-Abelian gauge theory with the gauge group $SU(N_c)_c$, where the index c refers to color and N_c is the number of quark colors. The quarks correspond to the fundamental representation of $SU(N_c)_c$, whereas the gluons are the gauge bosons and belong to the adjoint representation of $SU(N_c)_c$. Apart from the color index, $1 \leq c \leq N_c$, quarks also carry a flavor quantum number, $1 \leq f \leq N_f$. Suppressing all quark indices for simplicity the Lagrange density for QCD reads [10, 11, 12, 13]

$$\mathcal{L}_{QCD} = \bar{\psi} \left(i\gamma^\mu D_\mu - m \right) \psi - \frac{1}{4} F_a^{\mu\nu} F_{\mu\nu}^a + \mathcal{L}_{gf} + \mathcal{L}_{ghost} \ . \tag{1.1}$$

Since quarks are fermions with spin 1/2 their wave functions ψ are $4N_cN_f$-dimensional spinors. The Dirac conjugate spinor is defined by $\bar{\psi} \equiv \psi^\dagger \gamma_0$, where γ^μ are the Dirac matrices and m is the current quark mass, which is a diagonal matrix in flavor space, $m \equiv m_{ij} \, \delta_{ij}$. The six known

flavors are called up (u), down (d), strange (s), charmed (c), bottom (b), and top (t). Their masses are ordered as $m_u \simeq m_d \ll m_s \ll m_c \ll m_b \ll m_t$. Explicitly, the current quark masses appearing in $\mathcal{L}_{\mathrm{QCD}}$ for the three lightest quark flavors are $m_u \simeq 5$ MeV, $m_d \simeq 10$ MeV, and $m_s \simeq 100$ MeV [14]. The masses for the three remaining quark flavors are so much larger that these flavors will not play any role in the following.

The covariant derivative is defined as $D_\mu = \partial_\mu - ig A_\mu^a T_a$, with the strong coupling constant g. The vector fields A_a^μ represent the gluons, where the adjoint color index a runs from 1 to $N_c^2 - 1$. The $N_c \times N_c$ matrices T_a are the generators of the local $SU(N_c)_c$ gauge symmetry. Throughout this work I use the representation $T_a \equiv \lambda_a/2$, where λ_a are the Gell-Mann matrices. The gluonic field strength tensor is defined as

$$F_a^{\mu\nu} = \partial^\mu A_a^\nu - \partial^\nu A_a^\mu + g f_{abc} A_b^\mu A_c^\nu \;, \tag{1.2}$$

where f_{abc} are the structure constants of $SU(N_c)_c$. They are defined through $i f_{abc} T_c \equiv [T_a, T_b]$. In the non-linear terms in Eq. (1.2) proportional to f_{abc} the non-Abelian character of QCD manifests itself: the gluons carry color charge and couple to themselves. This ultimately gives rise to the numerous non-trivial features of this theory. The terms $\mathcal{L}_{\mathrm{gf}}$ and $\mathcal{L}_{\mathrm{ghost}}$ in Eq. (1.1) contain gauge fixing terms and the contribution of the Faddeev-Popov ghosts. Since they are of no further relevance for this work I will not specify them here.

The QCD Lagrange density given in Eq. (1.1) is needed to calculate the grand canonical partition function of QCD [9, 15]

$$\mathcal{Z}(T, V, \mu) = \int \mathcal{D}\bar{\psi}\,\mathcal{D}\psi\,\mathcal{D}A_a^\mu \;\exp\{S_{\mathrm{QCD}}[\bar{\psi}, \psi, A]\} \tag{1.3}$$

with the tree-level action of QCD at quark chemical potential μ

$$S_{\mathrm{QCD}}[\bar{\psi}, \psi, A] \equiv \left[\int_X (\mathcal{L} + \mu \mathcal{N})\right] \;. \tag{1.4}$$

The quark chemical potential is associated with the net quark number conservation. The number density operator of the conserved net quark number is $\mathcal{N} \equiv \bar{\psi}\gamma_0\psi$. From Eq. (1.3) one can derive thermodynamical quantities such as pressure, $p(T, \mu)$, entropy density, $s(T, \mu)$, and particle number density, $n(T, \mu)$,

$$p(T, \mu) = T \left.\frac{\partial \ln \mathcal{Z}(T, \mu)}{\partial V}\right|_{T,\mu} \;, \quad s(T, \mu) = \left.\frac{\partial p(T, \mu)}{\partial T}\right|_\mu \;, \quad n(T, \mu) = \left.\frac{\partial p(T, \mu)}{\partial \mu}\right|_T \;. \tag{1.5}$$

In particular, the quark number density $n(T, \mu)$ for massless quarks and at $T \ll \mu$ is proportional to the third power of μ, $n \sim \mu^3$. Note that in the thermodynamical limit, $V \to \infty$, $\ln \mathcal{Z}(T, \mu)$ becomes an extensive quantity and as such is simply proportional to V. Therefore, the dependence of the pressure on the volume cancels out. In order to calculate the expectation value of any given operator $\mathcal{O}$ in the grand canonical ensemble one employs the following averaging prescription

$$\langle \mathcal{O} \rangle \equiv \frac{1}{\mathcal{Z}} \int \mathcal{D}\bar{\psi}\,\mathcal{D}\psi\,\mathcal{D}A_a^\mu\;\mathcal{O}\;\exp\{S_{\mathrm{QCD}}[\bar{\psi}, \psi, A]\} \;. \tag{1.6}$$

Since QCD is a quantum field theory the vacuum is treated as a polarizable medium. Consequently, the result of any experiment that measures the effective color charge in the coupling

constant $\alpha_s \equiv g^2/4\pi$ of two strongly interacting quarks will depend on the energy scale of the experiment. This dependence on the scale Q is expressed by the $\beta-$function of QCD [10, 11, 12]. In the so called $\overline{\text{MS}}$-scheme at the three loop level one finds for the scale Q [16]

$$Q\frac{\partial \alpha_s}{\partial Q} = 2\beta(\alpha_s) = -\frac{\beta_0}{2\pi}\alpha_s^2 - \frac{\beta_1}{4\pi^2}\alpha_s^3 - \frac{\beta_2}{64\pi^3}\alpha_s^4 - \dots \tag{1.7}$$

where

$$\beta_0 = 11 - \frac{2}{3}N_f , \qquad \beta_1 = 51 - \frac{19}{3}N_f , \qquad \beta_2 = 2857 - \frac{5033}{9}N_f + \frac{325}{27}N_f^2 . \tag{1.8}$$

Since in nature the number of quark flavors is $N_f = 6$ it follows that $\beta < 0$ and QCD is indeed an asymptotically free theory as already mentioned above, cf. left diagram in Fig. 1.1. For a
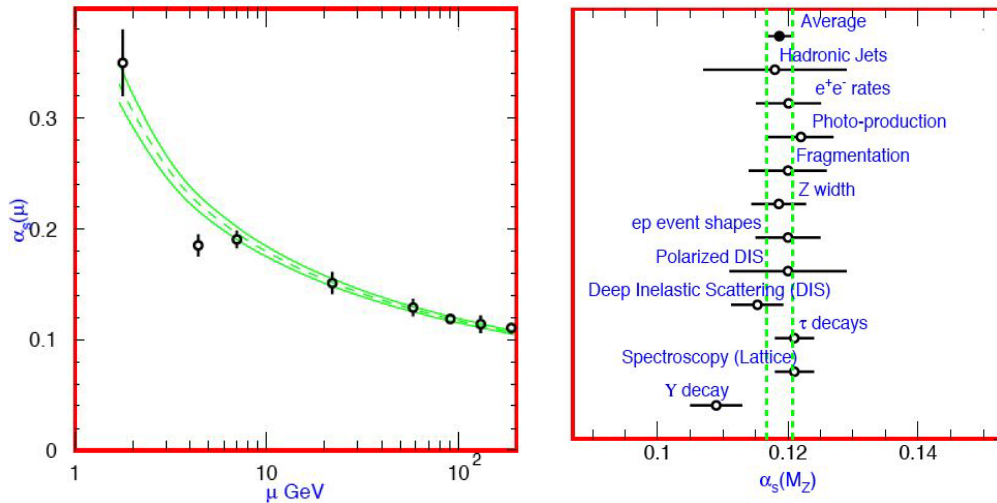
Figure 1.1: The experimental and theoretical dependence of $\alpha_s(Q)$ on the considered energy scale $Q \equiv \mu$ (left figure). Experimental values for $\alpha_s(M_Z)$ (right figure), [14].

more quantitative analysis one has to solve the renormalization group equations. At three-loop order one finds [16]

$$\alpha_s(Q) = \frac{4\pi}{\beta_0 \log(Q^2/\Lambda_{\text{QCD}}^2)}\left[1 - \frac{2\beta_1}{\beta_0^2}\frac{\log\left[\log(Q^2/\Lambda_{\text{QCD}}^2)\right]}{\log(Q^2/\Lambda_{\text{QCD}}^2)} + \frac{4\beta_1^2}{\beta_0^4 \log^2(Q^2/\Lambda_{\text{QCD}}^2)}\right. \tag{1.9}$$

$$\times \left.\left(\left(\log\left[\log(Q^2/\Lambda_{\text{QCD}}^2)\right] - \frac{1}{2}\right)^2 + \frac{\beta_2\beta_0}{8\beta_1^2} - \frac{5}{4}\right)\right] . \tag{1.10}$$

This solution may be used to compare the values of $\alpha_s(Q)$ and Λ_{QCD} from different experiments. With Eq. (1.10) one may first calculate the scale Λ_{QCD} by matching it to the measured $\alpha_s(Q)$ and then use it to extrapolate α_s to one standard reference scale, say to the mass of the Z boson, $M_Z = 91.1876 \pm 0.0021$ GeV. This of course depends on the number of flavors used in

Eq. (1.10). For energies not much larger than M_Z one may restrict oneself to $N_f = 5$ active flavors and finds for Λ_{QCD} the value [14]

$$\Lambda_{\overline{\mathrm{MS}}}^{(5)} = 217_{-23}^{+25} \text{ MeV} . \tag{1.11}$$

For $\alpha_s(M_Z)$ one obtains [14]

$$\alpha_s(M_Z) = 0.1187 \pm 0.002 , \tag{1.12}$$

cf. right diagram in Fig. 1.1. Decreasing the scale Q, the coupling $\alpha_s(Q)$ grows very large for $Q \to \Lambda_{\mathrm{QCD}}$. Such a divergency of the coupling is sometimes called a Landau pole. In the case of quantum electrodynamics (QED) the Landau pole appears at very large energy scales, whereas the coupling is perturbatively small at low energies.

Turning to the symmetries of the QCD Lagrangian given in Eq. (1.1) one observes that $\mathcal{L}_{\mathrm{QCD}}$ is invariant under Lorentz transformations and translations in space-time. Furthermore, it respects charge conjugation, parity and time-reversal invariance. Another symmetry is its invariance under gauge transformations, which are generally local, i.e. dependent of space-time, $U(x) \in SU(N_c)_c$

$$\psi(x) \to U(x)\psi(x) , \quad A^\mu(x) \to U(x)A^\mu(x)U^\dagger(x) + iU(x)\partial^\mu U^\dagger(x) , \tag{1.13}$$

where $A^\mu \equiv A_a^\mu T_a$. A further symmetry is the global (i.e. independent on space-time) quark flavor symmetry of $\mathcal{L}_{\mathrm{QCD}}$. To elaborate this, one may decompose the quark fields with respect to their chirality

$$\psi \equiv \psi_r + \psi_\ell , \quad \psi_{r,\ell} \equiv \mathcal{P}_{r,\ell}\,\psi , \quad \mathcal{P}_{r,\ell} \equiv \frac{1 \pm \gamma_5}{2} , \tag{1.14}$$

where $\mathcal{P}_{r,\ell}$ are the chirality projectors. One observes that in $\mathcal{L}_{\mathrm{QCD}}$ only the mass term mixes quarks with different chirality

$$\bar{\psi}^i\, m_{ij}\, \psi^j \equiv \bar{\psi}_r^i\, m_{ij}\, \psi_\ell^j + \bar{\psi}_\ell^i\, m_{ij}\, \psi_r^j , \tag{1.15}$$

where use was made of the orthogonality of $\mathcal{P}_r$ and $\mathcal{P}_\ell$ and of $\mathcal{P}_{r,\ell}\gamma_0 = \gamma_0\mathcal{P}_{\ell,r}$. Hence, assuming zero quark masses for all flavors, $m \equiv 0$, $\mathcal{L}_{\mathrm{QCD}}$ becomes chirally symmetric, i.e. invariant under global chiral $U(N_f)_r \otimes U(N_f)_\ell$ transformations given by

$$\psi_{r,\ell} \to U_{r,\ell}\,\psi_{r,\ell} , \quad U_{r,\ell} \equiv \exp\left(i\sum_{a=0}^{N_f^2-1} \alpha_{r,\ell}^a\, T_a\right) \in U(N_f)_{r,\ell} . \tag{1.16}$$

Here, the $\alpha_{r,\ell}^a$ are the parameters and T_a the generators of $U(N_f)_{r,\ell}$ with $T_0 \sim \mathbf{1}$. While the kinetic and interaction parts of $\mathcal{L}_{\mathrm{QCD}}$ are generally invariant under arbitrary transformations of $U(N_f)_r \otimes U(N_f)_\ell$, the mass term is only invariant in the case that the parameters α_r^a and α_ℓ^a of the given transformations U_r and U_ℓ are equal, $\alpha_r^a = \alpha_\ell^a$. One therefore introduces the vectorial group $U(N_f)_V \subset U(N_f)_r \otimes U(N_f)_\ell$ with elements that fulfill $U_r = U_\ell$, which is often denoted as $U(N_f)_V \equiv U(N_f)_{r+\ell}$. These vectorial transformations leave $\mathcal{L}_{\mathrm{QCD}}$ invariant if all masses are equal. In nature, however, only the two lightest quarks have approximately equal

masses, which reduces the vector symmetry to an approximative $U(2)_V$ symmetry. Analogously one recovers an approximative $U(3)_V$ symmetry, if one considers energies much larger than m_s. The subset $U(N_f)_A = U(N_f)/U(N_f)_V$ comprises all transformations fulfilling $U_r = U_\ell^\dagger$. Hence, the symmetry of these so-called axial transformations is always explicitly broken by the quark masses.

Since any unitary transformation can be decomposed into the product of a special unitary transformation and a complex phase one may finally write $U(N_f)_r \otimes U(N_f)_\ell$ as $SU(N_f)_r \otimes SU(N_f)_\ell \otimes U(1)_V \otimes U(1)_A$. The phase factors due to $U(1)_V$ correspond to an exact symmetry (independent of the quark masses) of QCD, corresponding to the conservation of baryonic charge, i.e. of quark numbers, and is often denoted as $U(1)_B$. The $U(1)_A$ symmetry is explicitly broken by an anomaly at the quantum level of QCD [17]. In hot and/or dense matter the instantons corresponding to this anomaly are screened [18] so that the $U(1)_A$ symmetry may become effectively restored again in matter.

Below some critical density and temperature of the order of magnitude of $\Lambda_{\rm QCD}$ the true ground state of the vacuum is populated by the so called chiral condensate. In Fig. 1.2 the corresponding region is labelled by χSB. Often it is also referred to as the hadronic phase. It is described by the order parameter

$$\Phi^{ij} \sim \langle \bar{\psi}_\ell^i \psi_r^j \rangle + {\rm h.\,c.} \neq 0 \,. \tag{1.17}$$

Its structure in flavor space connects right and left handed quarks. In the chiral limit of zero quark masses the difference among the quark flavors vanishes and $\Phi^{ij} = \delta^{ij}\Phi$, i.e. the order parameter of the chiral condensate becomes diagonal in flavor space just as the mass matrix discussed above. It follows analogosly that the chiral condensate spontaneously breaks the (approximate) axial part of the chiral symmetry. Since the broken symmetry is global, Goldstone's theorem [10, 11, 12] applies and massless Goldstone bosons are created. Their number is given by the number of broken generators. Since in the considered case the chiral condensate breaks the $SU(N_f)_A$ symmetry, $N_f^2 - 1$ Goldstone bosons are generated. In the case of $N_f = 2$ (considering only up and down quarks) this corresponds to the generation of the three pseudoscalar pions. These are not exactly massless, since the symmetry was already explicitly broken by the up and down quark masses and therefore it was only an approximate symmetry. Generally, one calls the massive Goldstone bosons corresponding to the breaking of approximate global symmetries pseudo-Goldstone bosons. For $N_f = 3$ also the heavier strange quark is involved, which makes the spontaneously broken symmetry even more approximate as in the case of $N_f = 2$. Consequently, the created pseudo-Goldstone bosons are more massive. They correspond to the pseudoscalar meson octet made of pions, kaons, and the eta meson. Since all these mesons consist of a quark-antiquark pair, the quark number symmetry $U(1)_V$ and the gauge symmetry of electromagnetism $U(1)_{em}$ remain intact,

$$\chi{\rm SB}: \quad SU(3)_c \otimes SU(3)_V \otimes U(1)_B \otimes U(1)_{em} \,. \tag{1.18}$$

Inside this hadronic phase the ground state of (infinite) nuclear matter with baryonic density $n_0 \simeq 0.15\ {\rm fm}^{-3}$ is located at $T = 0$ and $\mu = 308$ MeV. The value of the chemical potential is given by the mass of the neutron, $m_N = 939$ MeV, reduced by the average binding energy per nucleon in nuclear matter, $B_0 = 16$ MeV/A [19]. One obtains $\mu_B \equiv 939$ MeV – 16 MeV = 923
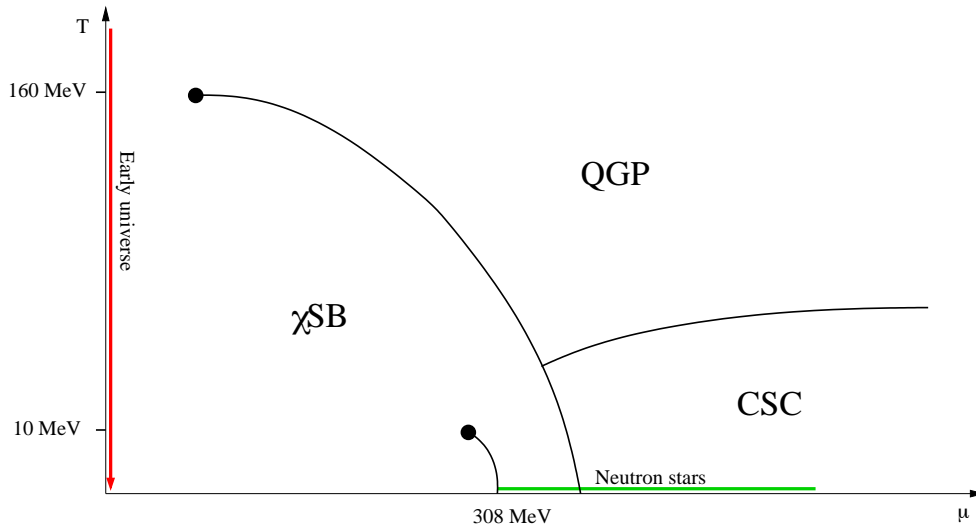
Figure 1.2: The phase diagram of strongly interacting matter.

MeV $= 3\mu$. The factor 3 arises from the fact that a nucleon is a baryon with baryonic charge 1 and as such consists of three (up and down) quarks each carrying baryonic charge 1/3. These quarks are dressed by their strong interaction with the chiral condensate, so that the quark masses become proportional to the expectation value of the chiral condensate. This effectively gives them much larger constituent masses as compared to the respective current quark masses m in $\mathcal{L}_{\text{QCD}}$.

The line emerging from the point of infinite nuclear matter separates the gaseous from the liquid phase of hadronic matter and corresponds to a first order phase transition [20, 21]. At its endpoint at $T \approx 10$ MeV it becomes of second order exhibiting critical phenomena similarly to normal water [22, 23, 24, 25, 26, 27].

The evolution of strongly interacting matter in the early universe corresponds to the red line at zero net baryonic density, $\mu = 0$, in Fig. 1.2. For small values of μ the numerical lattice simulations of QCD [28, 29] predict that the transition from the quark-gluon phase to the hadronic phase is a crossover [30, 31]. These analyses fail so far in the regime $\mu > T$: lattice simulations are based on Monte Carlo importance sampling and rely on the probabilistic interpretation of the weight in the path integral. For $\mu > 0$ the fermion determinant becomes complex, which causes the famous sign problem [28, 29]. For small values of μ a Taylor expansion technique has been proposed to investigate the critical endpoint of the chiral phase transition [32]. For recent experimental and theoretical progress on the properties of the confined and deconfined phases and the transitions among them see [33, 34]. As this field is not yet settled, the location of the line of the chiral phase transition and its critical endpoint in Fig. 1.2 are only approximate.

Also the boundaries around the color superconducting regime [13, 35, 36, 37] labelled by CSC are essentially unknown. Only in the limit of asymptotically large quark chemical potentials where QCD becomes weakly coupled it can be rigorously proven that the true ground state is color superconducting at sufficiently low temperatures. In this limit even the specific color

superconducting phase is known. It is the so-called CFL phase, which breaks again the chiral symmetry, cf. Sec. 1.2. At chemical potentials and densities of physical relevance, however, the the situation becomes less transparent. The densities inside neutron stars are bounded by the condition of hydrostatic stability to be $n \lesssim 10\,n_0$ [37]. This corresponds to $\mu \lesssim 500$ MeV, cf. the green line in Fig. 1.2 where QCD is not weakly coupled anymore. It is believed, however, that inside the cores of some neutron stars color superconductivity might occur and have observable effects on their properties [38, 39, 40]. The critical temperature and density for the onset of color superconductivity can only be estimated to be roughly of the order $\mu_c \gtrsim 400$ and $T_c \lesssim 50$ MeV. Furthermore, the search for the most dominant color superconducting phase for given T and μ is still ongoing wherefore the presumably complex structure inside the CSC region in Fig. 1.2 is essentially unknown. These issues will be elaborated further in the following section.

1.2   Color superconductivity

The discovery of color superconductivity goes back to the late 1970's [35]. However, wider interest in the phenomenon of color superconductivity has only recently been generated by the observation that, within a simple Nambu–Jona-Lasinio (NJL) – type model [41] for the quark interaction, the so-called color-superconducting gap parameter ϕ assumes values of the order of 100 MeV [42]. The gap parameter ϕ appears in the dispersion relation of the gapped, i.e. Cooper paired quarks in the color superconducting medium

$$\epsilon_{k,r} = \sqrt{(k-\mu)^2 + \lambda_r \phi^2} \,, \tag{1.19}$$

where k is the modulus of the 3-momentum of the quark. The index r specifies the color and the flavor of the considered quark. In the special case that $\lambda_r = 0$ the quark is ungapped. It follows that gapped quarks carry a non-zero amount of energy $\epsilon_{\mu,r} = \sqrt{\lambda_r}\,\phi$ even on the Fermi surface, $k = \mu$. Therefore, to excite (generate) a pair of gapped quarks costs at least the energy $2\sqrt{\lambda_r}\,\phi$. Such an excitation process can be interpreted as the break-up of a Cooper pair and the required energy as the Cooper pair binding energy [43, 44, 45, 46, 47].

  Gap parameters of ~ 100 MeV would have important phenomenological consequences for the physics of neutron stars [38, 39, 40]. It is therefore of paramount importance to put the estimates from NJL-type models [48, 49, 50, 51, 52] on solid ground and obtain a more reliable result for the magnitude of the gap parameter based on first principles. To this end, the color-superconducting gap parameter was also computed in QCD [53, 54, 55, 56, 57]. In this section a short review on color superconductivity is given including the mechanism of Cooper pairing in QCD, the different symmetry breaking patterns for various color superconducting phases, and some implications on the observables of neutron stars. At the end of this section a schematic version of the QCD gap equation in the weak coupling limit will be presented. It is suitable to identify and power-count the various terms that arise from the different gluon sectors.

  As already explained, at high densities the quarks are deconfined and free to move individually. Since quarks are fermions, Pauli blocking forces them to build up a Fermi sea, where only quarks at the Fermi surface with Fermi momentum $k_F \equiv \sqrt{\mu^2 - m^2}$ are able to interact and exchange momenta. For $\mu \gg m$ the typical momentum scale of these quarks is given by μ. Hence, for $\mu \gg \Lambda_{\mathrm{QCD}}$ the strong interaction becomes weakly coupled and single gluon exchange,

cf. Fig. 1.3, becomes dominant. The quark-quark scattering amplitude for one-gluon exchange is proportional to [13, 37]

$$\sum_{a=1}^{N_c^2-1} T_{ii'}^a T_{jj'}^a = -\frac{N_c+1}{4N_c}\left(\delta_{ii'}\delta_{jj'} - \delta_{ij'}\delta_{i'j}\right) + \frac{N_c-1}{4N_c}\left(\delta_{ii'}\delta_{jj'} + \delta_{ij'}\delta_{i'j}\right) \; . \tag{1.20}$$

The indices i, j are the fundamental colors of the two quarks in the incoming channel, and i', j' the respective colors in the outgoing channel. If one interchanges two color indices in the incoming or in the outgoing channel the sign of the first term changes while the second term remains intact. The minus sign in front of the first, antisymmetric term indicates that this channel is attractive, whereas the other, symmetric term is repulsive. In terms of representation theory,
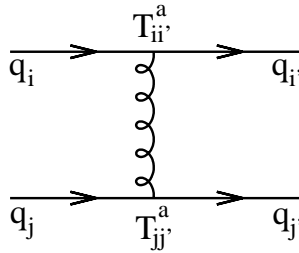
Figure 1.3: Feynman diagram for one gluon exchange among two quarks.

Eq. (1.20) corresponds to the coupling of two fundamental color triplets to the antisymmetric color antitriplet and the symmetric color sextet

$$[3]_c \otimes [3]_c = [\bar{3}]_c^a \oplus [6]_c^s \; . \tag{1.21}$$

Hereby, the 9-dimensional direct product of two 3-dimensional representations of $SU(3)_c$ has been uniquely decomposed into a direct sum of one 3-dimensional and one 6-dimensional representation. The term $[\bar{3}]_c^a$ corresponds to the first term in Eq. (1.20) and $[6]_c^s$ to the second.

The presence of an attraction among quarks is crucial. According to Cooper's theorem [43] any attractive interaction destabilizes the Fermi surface in favor of the formation of Cooper pairs [44, 45, 46, 47]. Also for $\mu \sim 400 - 500$ MeV, where the theory is not yet in its weak coupling limit, $\alpha_s(\mu) \sim 1$, one expects the anti-triplet channel to be attractive. However, then it would be mediated by instantons [42] rather than by one-gluon exchange.

As in the case of the chiral condensate, the Cooper pairs spontaneously reduce the symmetry of the system. Normal quark matter without any condensate is invariant under arbitrary

$$\text{NQ}: \quad SU(3)_c \otimes SU(N_f)_V \otimes SU(2)_J \otimes U(1)_B \otimes U(1)_{em} \tag{1.22}$$

transformations, where also the global spin group $SU(2)_J$ is included with the total quark spin $J = S + L$. N_f is the number of quark flavors with approximately equal masses. The residual symmetry of the system in the presence of a Cooper pair condensate is given by the symmetry of the order parameter Φ, i.e. that of the Cooper pair wave function. Already from the symmetry breaking pattern of a specific color superconducting phase one can draw some

important conclusions for its key properties. In this context, however, it is necessary to remember the Anderson-Higgs mechanism [58, 59]. It is roughly speaking the transfer of Goldstone's theorem onto gauge symmetries: if a gauge symmetry is spontaneously broken then those gauge bosons, which correspond to the broken generators, acquire masses. In this way they absorb the degrees of freedom, which would have been occupied by the Goldstone bosons if the broken symmetries had been global. One jargonizes this by saying that these gauge bosons "eat up the would-be-Goldstone-bosons and therefore become massive." (Strictly speaking, a gauge symmetry must first be fixed before it can be broken [60]. After its fixing the gauge the symmetry has become global and the occurring breaking is explicit. The corresponding Goldstone bosons depend on the choosen gauge and are therefore non-physical. The masses of the gauge bosons, however, are independent of the gauge and are physical.)

One canonical example for the Anderson-Higgs mechanism is the Weinberg-Salam model for the electroweak interactions [61], which has a $SU(2)_I \otimes U(1)_Y$ gauge symmetry. The index I stands for the isospin and Y for the hypercharge of the left-handed leptons and quarks. One introduces the so-called Higgs field [59], which spontaneously breaks the gauge symmetries to a residual $U(1)_{I+Y}$. Physically one interprets this residual group as the gauge group $U(1)_{em}$ of electromagnetism with one massless gauge boson A, the photon. The three massive gauge bosons that emerge are identified with the $W^\pm$ and the Z boson of the weak interaction. Since the remaining gauge group $U(1)_{I+Y}$ consists of joint rotations in isospin and hypercharge space, the Z and the A bosons must be generated by a "rotation" in the space of the gauge boson of the original $U(1)_Y$ group with one of the gauge bosons of the original $U(1)_I$ group. Those "original" gauge bosons on the other hand become meaningless in the phase of the broken symmetries, for details see e.g. [10, 11, 12].

In the case of color superconductivity the Cooper pairs always carry color charge. Depending on the considered colorsperconducting phase, they therefore reduce the color gauge symmetry to either $SU(2)_c$ and give masses to five gluons, or break the color gauge symmetry completely. Then all eight gluons become massive. The respective gluon masses are called color Meissner masses and lead to the color Meissner effect: the respective magnetic gluon fields are expelled from the color superconducting medium. This is analogous to the more familiar electromagnetic Meissner effect, which occurs in electric superconductors. In that case the $U(1)_{em}$ gauge symmetry is spontaneously broken and the photons attain a Meissner mass. Since Cooper pairs of quarks are also electrically charged, a color superconductor may also be an electromagnetic superconductor depending on the breaking of the electromagnetic gauge symmetry in the considered phase [72]. Analogously, the baryon number symmetry may be broken, since Cooper pairs have nonzero baryonic charge. A breaking of this symmetry is connected to the onset of superfluidity.

In the following, the requirement of antisymmetry of the Cooper pair wave function will be used to analyze different symmetry breaking patterns. This approach, however, cannot give any information on the breaking of the $U(1)_B$ and $U(1)_{em}$ symmetries. This as well as the values of the Meissner masses require more intensive calculations, which shall not be presented here. As shown above, the order parameter is an element of the representation $[\bar{3}]_c^a$ of $SU(3)_c$ and is therefore antisymmetric in color space. In the case that the Cooper pair is a spin singlet, $J = 0$, the wave function must be an element of the antisymmetric representation $[1]_J^a$ of $SU(2)_J$. If, however, it is a spin triplet, $J = 1$, the corresponding representation of $SU(2)_J$ is $[3]_J^s$, which

is symmetric. Therefore, its representation with respect to $SU(N_f)_V$ must be antisymmetric if $J = 0$, and symmetric if $J = 1$.

Starting with $J = 0$ it follows that the Cooper pairs have to consist of two quarks with different flavors in order to fulfill antisymmetry. Assuming that only two flavors, i.e. up and down, participate in the pairing, $N_f = 2$, one finds $[1]_f^a$ as the corresponding antisymmetric representation, since analogosly to the spin one has in flavor space

$$[2]_V \otimes [2]_V = [1]_V^a \oplus [3]_V^s \ . \tag{1.23}$$

In color and flavor the most general ansatz for the order parameter reads

$$\Phi_{ij}^{fg} = \epsilon_{ijk}\epsilon^{fg}\,\Phi_k \ , \tag{1.24}$$

where the indices i, j are the color and f, g the flavor indices of the two quarks and the quantities ϵ_{ijk} and ϵ^{fg} are totally antisymmetric tensors of rank 3 in color and and of rank 2 in flavor space, respectively. It follows that the order parameter is a (complex) 3-vector in the fundamental color space. By a global color rotation one may transform the order parameter Φ_k to point into the (anti-)3 direction in color space. Then only those quarks carrying (transformed) colors 1 and 2 participate in the pairing. This demonstrates that in this phase the $SU(3)_c$ gauge symmetry is broken down to $SU(2)_c$. It follows that five of the eight gluons acquire a Meissner mass in this phase. The remaining three gluons do not interact with the anti-triplett Cooper pairs and remain massless. One finally finds that for this phase, which is called the 2SC phase (indicating that only two quark flavors participate in the pairing), the residual symmetry is given by

$$\text{2SC}: \quad SU(2)_c \otimes SU(2)_V \otimes U(1)_{B+c} \otimes U(1)_{em+c} \tag{1.25}$$

Here, from the outset only the isospin symmetry $SU(2)_V$ was assumed, which is found unbroken. Furthermore, the condensate is invariant under joint rotations of $U(1)_B$ and $U(1)_{em}$ as well as under joint rotations of $SU(2)_c$ and $U(1)_{em}$ [62, 63]. Since the latter two are both gauge groups this implies that, as in the Weinberg-Salam model, the photon is only rotated but remains massless [66]. Therefore the 2SC phase is no electromagnetic superconductor. The presence of the symmetry group $U(1)_{B+c}$ suggests that this phase exhibits nontrivial features concerning superfluidity. In helium-3 one encounters similar symmetry breaking patterns where the particle number conservation group is locked with rotations in spin or angular momentum space [47].

Assuming quark chemical potentials much larger than the strange quark mass one may consider the case that up, down, and strange quarks equally participate in the pairing. Then, for $N_f = 3$, it is

$$[3]_V \otimes [3]_V = [\bar{3}]_V^a \oplus [6]_V^s \ , \tag{1.26}$$

wherefore the desired antisymmetric representation of $SU(3)_V$ is $[\bar{3}]_J^a$. Consequently, in Dirac and flavor space the ansatz for the condensate reads

$$\Phi_{ij}^{fg} = \epsilon_{ijk}\epsilon^{fgh}\Phi_k^h \ . \tag{1.27}$$

It has a similar structure as the order parameter of superfluid helium-3 with spin $S = 1$ and angular momentum $L = 1$, which breaks the global $SO(3)_S$ and $SO(3)_L$ symmetries. There

one encounters a multitude of different phases [47]. In the present case of $SU(3)_c$ and $SU(3)_V$ symmetry breaking, however, it turns out that the following ansatz for Φ_k^h is dominant [64, 65]

$$\Phi_k^h = \delta_k^h \, \Phi \; . \tag{1.28}$$

This ansatz is similar to the order parameter of the chiral condensate, cf. Eq. (1.17), in the chiral limit of zero quark masses, where the different flavors have identical properties and consequently $\Phi^{ij} = \delta^{ij}\Phi$. This order parameter simultaneously breaks the two global flavor symmetries $SU(3)_r \otimes SU(3)_\ell$ to the one global vectorial symmetry $SU(3)_V$. In the present case the global vectorial symmetry $SU(3)_V$ and the local symmetry $SU(3)_c$ are simultaneously broken to one global $SU(3)_{c+V}$ symmetry. Accordingly, the system is invariant under "locked" rotations in color and flavor space. This phase is therefore called the color-flavor-locked or CFL phase. All in all, it is invariant under

$$\text{CFL}: \quad SU(3)_{c+V} \otimes SU(2)_J \otimes U(1)_{c+em} \; . \tag{1.29}$$

In contrast to the 2SC phase all three colors and flavors participate in the pairing and one therefore expects all gluons to interact with the Cooper pair condensate and attain a Meissner mass. This is in fact true, since the remaining color symmetry is only global. Furthermore, since $U(1)_{c+em}$ is a gauge group the photon remains massless. However, it is mixed with one of the gluons. Therefore, the CFL phase is no electromagnetic superconductor, i.e. the Cooper pairs are neutral with respect to the rotated electric charge [66]. Due to the broken $U(1)_B$ it is a superfluid. In rotating systems as neutron stars superfluidity may result in vortices, through which magnetic fields can enter the superconducting phase in so called flux-tubes [67]. These vortices stick to the star's crust and and carry some amount of the stars total angular momentum. When the rotational velocity of the star gradually decreases due to electromagnetic radiation these vortices eventually rearrange and transfer some of the angular momentum to the star. As a consequence the rotational frequency is expected to suddenly increase leading to observable "glitches" [68].

As mentioned above, the CFL phase is physically significant only for $\mu \gg m_s$. For such large chemical potentials one could in principle neglect all masses and assume invariance under chiral symmetry rotations, $SU(3)_r \otimes SU(3)_\ell$ instead of the vectorial $SU(3)_V$. In the CFL phase left and right handed quarks separately form Cooper pair condensates, which corresponds to the breaking pattern $SU(3)_{r+c} \otimes SU(3)_{\ell+c} \hat{=} SU(3)_{r+\ell+c}$. Therefore, also in the limit of very large densities the chiral symmetry is broken, however, not by the quark masses or the chiral condensate but by the CFL phase [69].

In the case that the Cooper pair carries spin 1, $J = 1$, it may consist of two quarks of the same flavor [35, 70, 71, 72, 73, 74]. For simplicity one first considers the case that there is only one quark flavor in the system, $N_f = 1$. As an element of $[3]_J^s$ the order parameter is a 3-vector in momentum space with components $a = x, y, z$. The most general ansatz for the order parameter reads in spin and color space [35, 55, 75, 76]

$$\Phi_{ij}^a = \epsilon_{ijk} \, \Phi_k^a \; , \tag{1.30}$$

which generally breaks the $SU(3)_c \otimes SU(2)_J$ symmetry and allows for a multitude of possible phases [73, 74]. Here, only two special phases shall be analyzed, which are interesting due to

their analogy to the 2SC and the CFL phases of spin-0 color superconductors. These are the color-spin-locked or CSL phase

$$\Phi_k^a = \delta_k^a \, \Phi \; , \tag{1.31}$$

and the polar phase, where

$$\Phi_k^a = \delta_{k3} \, \delta^{az} \, \Phi \; . \tag{1.32}$$

In the first the color gauge group $SU(3)_c$ and the global spin group $SU(3)_J$ are simultaneously broken to the global $SU(3)_{c+J}$ group, which "locks" color and spin rotations. One has in total

$$\text{CSL}: \quad SU(3)_{c+J} \otimes U(1)_V \; . \tag{1.33}$$

As in the CFL phase all gluons and the photon become massive. In contrast to the CFL phase, however, the $U(1)_B$ and the $U(1)_{em}$ symmetry are broken. Hence, the CSL phase is a superfluid and a electromagnetic superconductor. The implications of the electromagnetic superconductivity on the observables of a neutron star are discussed in [72].

The polar phase is similar to the 2SC phase with $SU(3)_c \otimes SU(2)_J$ breaking down to $SU(2)_c \otimes U(1)_J$. One finds for the residual symmetry group

$$\text{polar}: \quad SU(2)_c \otimes U(1)_J \otimes U(1)_V \otimes U(1)_{B+c} \otimes U(1)_{em+c} \; . \tag{1.34}$$

Consequently, in the polar phase five gluons become massive. The condensate leaves rotational invariance in momentum space only with respect to one fixed axis. Indeed, the color superconducting gap parameter, see below, exhibits only an axial symmetry [76]. The $U(1)_{em}$ remains unbroken, wherefore the polar phase is no electromagnetic superconductor. However, a many flavor system, where each flavor separately forms a polar spin-1 gap, can be shown to be electromagnetically superconducting [76].

The physical significance of one-flavor color superconductors is that in neutron stars the Fermi momenta of quarks with different flavors may become sufficiently different to rule out the normal BCS pairing mechanism, which requires exactly opposite quark momenta. Such a mismatch of Fermi surfaces indeed occurs in neutron stars if one respects its electrical neutrality and $\beta-$equilibrium [37, 77, 78, 79, 80, 81, 82]. Total electric and color charge neutrality has to be fulfilled in order to allow for the gravitational binding of the star. Electrical charge neutrality for a two flavor system neglecting electrons, e.g., requires $n_d \approx 2n_u$, since the electrical charge of an up quark is $Q_u = 2/3$, whereas $Q_d = -1/3$ for a down quark. With $n_{u,d} \sim \mu_{u,d}^3$ it therefore follows $\mu_d \approx 2^{1/3}\mu_u \approx 1.26\mu_u$. In this simple case of two flavors, the requirement of $\beta-$equilibrium will not change this estimate much, cf. [37].

In spin-1 color superconductors quarks of the same flavor may pair, wherefore the BCS-pairing mechanism remains always intact. Alternatively, other color superconducting phases are proposed with different pairing mechanisms. In the so-called interior gap or breached pairing the quarks with the smaller Fermi momentum are excited to a higher energy state in order to form Cooper pairs with the quarks with larger Fermi momentum [83, 84]. Also displacements [85, 86] (LOFF phases) and deformations of the Fermi surfaces [87] are discussed to allow for Cooper pairing. The breached pairing mechanism has been shown to lead to Cooper pairs with gapless spectra [88, 89, 90, 91], which however appear to be unstable [92, 93, 94, 95, 96].

To decide which of the many possible phases is favorable at given T and μ one has to determine the phase with the largest pressure. Generally, the pressure grows with the gain of condensation energy of the Cooper pairs. This in turn depends on the number of quark degrees of freedom, which participate in the Cooper pairing, and on the magnitude of the respective color superconducting gap parameters. The gap parameter is determined from the gap equation. For a general derivation see [13] and references therein. In Sec. 3.1 the gap equation is rederived within the new effective formalism. In the following it is sufficient to concentrate on the gap equation in the schematic form

$$\phi = g^2\,\phi\left[\zeta\,\ln^2\left(\frac{\mu}{\phi}\right) + \beta\,\ln\left(\frac{\mu}{\phi}\right) + \alpha\right] \tag{1.35}$$

to discuss the various contributions from different gluon sectors and their respective orders of magnitude. To derive it one has to assume zero temperature, $T = 0$, weak coupling, $g \ll 1$, and apply the mean-field approximation. The solution is

$$\phi = 2\,b\,\mu\,\exp\left(-\frac{c}{g}\right)[1 + O(g)]\ . \tag{1.36}$$

The first term in Eq. (1.35) is of *leading* order since, according to Eq. (1.36), $g^2\ln^2(\mu/\phi) \sim 1$. It originates from the exchange of almost static, long-range, Landau-damped magnetic gluons [53]. One factor $\ln(\mu/\phi)$ is the standard BCS logarithm, which arises when integrating over quasiparticle modes from the bottom to the surface of the Fermi sea, $\int dq/\epsilon_q \sim \ln(\mu/\phi)$. (In fact, as will be shown in Sec. 3.2.2, integrating over quasiparticle modes inside a layer around the Fermi surface of an "intermediate" width is sufficient to build up a BCS log.) The second factor $\ln(\mu/\phi)$ comes from a collinear enhancement $\sim \ln(\mu/\epsilon_q)$ in the exchange of almost static magnetic gluons. The coefficient ζ determines the constant c in the exponent in Eq. (1.36). As was first shown by Son [53],

$$c \equiv \frac{3\pi^2}{\sqrt{2}}\ . \tag{1.37}$$

The second term in Eq. (1.35) is of *subleading* order, $g^2\ln(\mu/\phi) \sim g \ll 1$. It originates from two sources. The first is the exchange of electric and non-static magnetic gluons [54, 55, 56, 57]. In this case, the single factor $\ln(\mu/\phi)$ is the standard BCS logarithm. The second source is the quark wave-function renormalization factor in dense quark matter [97, 98]. Here, the BCS logarithm does not arise, but the wave-function renormalization contains an additional $\ln(\mu/\epsilon_q)$ which generates a $\ln(\mu/\phi)$. The coefficient β determines the prefactor b of the exponent in Eq. (1.36). For a two-flavor color superconductor,

$$b \equiv 256\,\pi^4\left(\frac{2}{N_f\,g^2}\right)^{5/2}\exp\left(-\frac{\pi^2 + 4}{8}\right)\ , \tag{1.38}$$

where N_f is the number of (massless) quark flavors participating in screening the gluon exchange interaction. The third term in Eq. (1.35) is of *sub-subleading* order, $\sim g^2$. The coefficient α determines the $O(g)$ correction to the prefactor of the color-superconducting gap parameter in Eq. (1.36). Since α has not yet been determined, the gap parameter can be reliably computed only in weak coupling, i.e., when the $O(g)$ corrections to the prefactor are small.

Weak coupling, $g \ll 1$, however, requires asymptotically large quark chemical potentials, $\mu \gg \Lambda_{\mathrm{QCD}}$. The range of μ values of phenomenological importance is, however, $\lesssim 1$ GeV. Although the quark density n is already quite large at such values of μ, $n \sim 10$ times the nuclear matter ground state density, the coupling constant is still not very small, $g \sim 1$. It is therefore of interest to determine the coefficient of g in the $O(g)$ corrections to the prefactor in Eq. (1.36). If it turns out to be small, one gains more confidence in the extrapolation of the weak-coupling result (1.36) to chemical potentials of order ~ 1 GeV.

It is worthwhile mentioning that an extrapolation of the weak-coupling result (1.36) for a two-flavor color superconductor, neglecting sub-subleading terms altogether and assuming the standard running of g with the chemical potential μ, yields values of ϕ of the order of ~ 10 MeV at chemical potentials of order ~ 1 GeV, cf. Ref. [13]. This is within one order of magnitude of the predictions based on NJL-type models and thus might lead one to conjecture that the true value of ϕ will lie somewhere in the range $\sim 10 - 100$ MeV.

However, in order to confirm this and to obtain a more reliable estimate of ϕ at values of μ of relevance in nature, one ultimately has to compute all terms contributing to sub-subleading order. In the following section the approach to this problem by an effective theory will be motivated.

1.3   Search for an *effective* approach

Although possible in principle, the task to calculate the sub-subleading order contributions to the color superconducting gap parameter is prohibitively difficult within the standard solution of the QCD gap equation in weak coupling. So far, in the course of this solution terms contributing at leading and subleading order have been identified, cf. discussion after Eq. (1.36). However, up to date it remained unclear which terms one would have to keep at sub-subleading order. Moreover, additional contributions could in principle arise at any order from diagrams neglected in the mean-field approximation [97, 99]. Therefore, it would be *ideal* to have a computational scheme, which allows one to determine *a priori*, i.e., at the outset of the calculation, which terms contribute to the gap equation at a given order.

As a first step towards this goal, note that there are several scales in the problem. Besides the chemical potential μ, there is the inverse gluon screening length, which is of the order of the gluon mass parameter m_g. At zero temperature and for N_f massless quark flavors [9],

$$m_g^2 = N_f \, \frac{g^2 \mu^2}{6\pi^2} \; , \tag{1.39}$$

i.e., $m_g \sim g\mu$. Finally, there is the color-superconducting gap parameter ϕ, cf. Eq. (1.36). In weak coupling, $g \ll 1$, these three scales are naturally ordered, $\phi \ll g\mu \ll \mu$. This ordering of scales implies that the modes near the Fermi surface, which participate in the formation of Cooper pairs and are therefore of primary relevance in the gap equation, can be considered to be independent of the detailed dynamics of the modes deep in the Fermi sea. This suggests that the most efficient way to compute properties such as the color-superconducting gap parameter is via an *effective theory for quark modes near the Fermi surface*. Such an effective theory has been originally proposed by Hong [100, 101] and was subsequently refined by others [102, 103, 104, 105].

At this point it is worthwhile reviewing the standard approach to derive an effective theory [107, 108, 109]. In the most simple case, one has a single scalar field, ϕ, and a single momentum scale, Λ, which separates relevant modes, φ, from irrelevant modes, ψ, $\phi = \varphi + \psi$. The relevant modes live on spatial scales $L \gg 1/\Lambda$, while the irrelevant modes live on scales $l \lesssim 1/\Lambda \ll L$, cf. Fig. 1.4. In the derivation of the effective action, one is supposed to integrate out the microscopic,
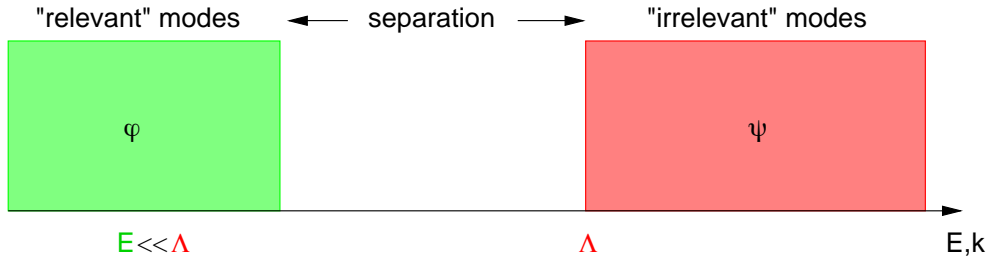
Figure 1.4: The separation of scales.

irrelevant modes. Usually, however, this is not done explicitly. Instead, one constructs all possible operators $\mathcal{O}_i$ composed of powers of the field φ and its derivatives, which are consistent with the symmetries of the underlying theory, and writes the effective action as [108]

$$S_{\text{eff}}[\varphi] = \int_X \sum_i g_i \mathcal{O}_i(\varphi) \,. \tag{1.40}$$

The coefficients, or *vertices*, g_i determine the interactions of the relevant modes φ. A priori, they are unknown functions of the single scale Λ, $g_i = g_i(\Lambda)$. All information about the microscopic scale l is contained in these vertices. Since the microscopic scale $l \ll L$, the operators $\mathcal{O}_i$ are assumed to be *local* on the scale L.

The effective action (1.40) contains infinitely many terms. In order to calculate physical observables within the effective theory, one has to truncate the expansion after a finite number of terms. One can determine the order of magnitude of various terms in the expansion (1.40) via a dimensional scaling analysis, which allows to classify the operators as *relevant* (they become increasingly more important as the scale L increases), *marginal* (they do not change under scale transformations), and *irrelevant* (they become increasingly less important as the scale L increases). To this end, one determines the naive scaling dimension of the fields, $\dim(\varphi) \equiv \delta$, from the free term in the effective action. Then, if the operator $\mathcal{O}_i$ consists of M fields φ and N derivatives, its scaling dimension is $\dim(\mathcal{O}_i) \equiv \delta_i = M\delta + N$. The operator $\mathcal{O}_i$ is then of order $\sim L^{-\delta_i}$. For dimensional reasons the constant coefficients g_i must then be of order $\sim \Lambda^{d-\delta_i}$, where d denotes the dimensionality of space-time. Including the integration over space-time, the terms in the expansion (1.40) are then of order $\sim (L\Lambda)^{d-\delta_i}$. Consequently, relevant operators must have $\delta_i < d$, marginal operators $\delta_i = d$, and irrelevant operators $\delta_i > d$. At a given scale L, one has to take into account only relevant, or relevant and marginal, or all three types of operators, depending on the desired accuracy of the calculation. To calculate a process at energy $E = s\Lambda$ with $s \ll 1$ and error of order s^{n+1} one only needs operators $\mathcal{O}_i$ with dimension $\delta_i \leq D + n$. The final result still depends on Λ through the coefficients $g_i(\Lambda)$. This dependence is eliminated by computing a physical observable in the effective theory and in the underlying microscopic theory, and matching the result at the scale Λ.

There are, however, cases where this naive dimensional scaling analysis fails to identify the correct order of magnitude, and thus the relevance, of terms contributing to the effective action. In the following, three examples shall be discussed briefly. For the first example, consider effective theories where, in contrast to the above assumption, the vertices g_i are in fact *non-local* functions. Such theories are, for instance, given by the "Hard Thermal Loop" (HTL) or "Hard Dense Loop" (HDL) effective actions [7, 9]. In these effective theories, valid at length scales $L \sim 1/(gT)$ or $\sim 1/(g\mu)$, respectively, there are terms $g_n A^n$ in the effective action, which are constructed from a quark or gluon (or ghost) loop with n external gluon legs; A is the external gluon field with $\delta = 1$. The coefficients g_n are non-local and do not only depend on the scale $\Lambda \lesssim T$, or $\lesssim \mu$, but also on the relevant momentum scale $1/L \sim gT$, or $\sim g\mu$. Naively, one would expect g_n to belong to a local n-gluon operator and to scale like Λ^{4-n}. Instead, it scales like L^{n-4} [7]. For arbitrary n, the corresponding term $g_n A^n$ in the effective action then scales like L^4, independent of the number n of external gluon legs.

The second example pertains to the situation when there is more than one single momentum scale Λ. As explained above, for a single scale Λ and a given length scale L, the naive dimensional scaling analysis unambiguously determines the order of magnitude of the terms in the expansion (1.40). Now suppose that there are two scales, Λ_1 and Λ_2. Then, the vertices g_i may no longer be functions of a single scale, say Λ_1, but could also depend on the ratio of Λ_2/Λ_1. Two scenarios are possible: (a) two terms in the expansion (1.40), say $g_n \mathcal{O}_n$ and $g_m \mathcal{O}_m$, with the *same* scaling behavior may still be of a *different* order of magnitude, or (b) the two terms can have a *different* scaling behavior, but may still be of the *same* order of magnitude. In case (a), all that is required is that the operators $\mathcal{O}_n$ and $\mathcal{O}_m$ scale in the same manner, say L^{-k}, and that $g_n \sim \Lambda_2^{d-k}$, but $g_m \sim \Lambda_1^{d-k}$. If $\Lambda_1 \ll \Lambda_2$, $g_m \gg g_n$, and thus the two terms are of different order of magnitude. In case (b), assume $1/L \ll \Lambda_1 \ll \Lambda_2$, with $\Lambda_1/\Lambda_2 \sim 1/(\Lambda_1 L) \sim \epsilon \ll 1$ and let take the fields φ to have naive scaling dimension $\delta = 1$. Then, at a given length scale L, a term $g_n \varphi^n$, with a coefficient g_n of order Λ_2^{d-n}, can be of the same order of magnitude as a term $g_m \varphi^m$, $m \neq n$, if the coefficient $g_m \sim \Lambda_1^{d-m}(\Lambda_2/\Lambda_1)^k$ with $k = d + m - 2n$. Although the scaling behavior of the two terms is quite different as L increases, they can be of the same order of magnitude, if the interesting scale L happens to be $\sim \Lambda_2/\Lambda_1^2$. In both cases (a) and (b) the naive dimensional scaling analysis fails to correctly sort the operators $\mathcal{O}_i$ with respect to their order of magnitude.

The third example where the naive dimensional scaling analysis fails concerns quantities, which have to be calculated self-consistently. Such a quantity is, for instance, the color-superconducting gap parameter, which is computed from a Dyson-Schwinger equation within a given many-body approximation scheme. In this case, the self-consistent solution scheme leads to large logarithms, like the BCS logarithm in Eq. (1.35). These logarithms cannot be identified *a priori* on the level of the effective action, but only emerge *in the course* of the calculation [55].

In order to avoid these failures of the standard approach, in this work I pursue a different venue to construct an effective theory. I introduce cut-offs in momentum space for quarks, Λ_q, and gluons, Λ_{gl}. These cut-offs separate relevant from irrelevant quark modes and soft from hard gluon modes. I then explicitly integrate out irrelevant quark and hard gluon modes and derive a *general* effective action for hot and/or dense quark-gluon matter. One advantage of this approach is that I do not have to guess the form of the possible operators $\mathcal{O}_i$ consistent with the symmetries of the underlying theory. Instead, they are exactly derived from first principles. Simultaneously, the vertices g_i are no longer unknown, but are completely determined. Moreover,

in this way I construct *all* possible operators and thus do not run into the danger of missing a potentially important one.

I shall show that the standard HTL and HDL effective actions are contained in the general effective action for a certain choice of the quark and gluon cut-offs Λ_q, Λ_{gl}. Therefore, the new approach naturally generates non-local terms in the effective action, including their correct scaling behavior, which, as mentioned above, does not follow the rules of the naive dimensional scaling analysis. I also show that the action of the high-density effective theory derived by Hong and others [100, 101, 102, 103, 104, 105] is a special case of the general effective action. In this case, relevant quark modes are located within a layer of width $2\Lambda_q$ around the Fermi surface.

The two cut-offs, Λ_q and Λ_{gl}, introduced in the present approach are in principle different, $\Lambda_q \neq \Lambda_{gl}$. The situation is then as in the second example mentioned above, where the naive dimensional scaling analysis fails to unambiguously estimate the order of magnitude of the various terms in the effective action. Within the present approach, this problem does not occur, since all terms, which may occur in the effective action, are automatically generated and can be explicitly kept in the further consideration. I shall show that in order to produce the correct result for the color-superconducting gap parameter to subleading order in weak coupling, one has to demand $\Lambda_q \lesssim g\mu \ll \Lambda_{gl} \lesssim \mu$, so that $\Lambda_q/\Lambda_{gl} \sim g \ll 1$. Only in this case, the dominant contribution to the QCD gap equation arises from almost static magnetic gluon exchange, while subleading contributions are due to electric and non-static magnetic gluon exchange. The fact that $\Lambda_q \ll \Lambda_{gl}$ is not entirely unexpected: at asymptotically large densities, where the scale hierarchy is $\phi \ll g\mu \sim m_g \ll \mu$, the dominant contribution in the QCD gap equation arises from gluons with momenta of order $\sim (m_g^2\phi)^{1/3}$ [53, 54, 55], while typical quark momenta lie in a shell of thickness $\sim 2\,\phi \ll (m_g^2\phi)^{1/3}$ around the Fermi surface.

The color-superconducting gap parameter is computed from a Dyson-Schwinger equation for the quark propagator. In general, this equation corresponds to a self-consistent resummation of all one-particle irreducible (1PI) diagrams for the quark self-energy. A particularly convenient way to derive Dyson-Schwinger equations is via the Cornwall-Jackiw-Tomboulis (CJT) formalism [106]. In this formalism, one constructs the set of all two-particle irreducible (2PI) vacuum diagrams from the vertices of a given tree-level action. The functional derivative of this set with respect to the full propagator then defines the 1PI self-energy entering the Dyson-Schwinger equation. Since it is technically not feasible to include all possible diagrams, and thus to solve the Dyson-Schwinger equation exactly, one has to resort to a many-body approximation scheme, which takes into account only particular classes of diagrams. The advantage of the CJT formalism is that such an approximation scheme is simply defined by a truncation of the set of 2PI diagrams. However, in principle there is no parameter, which controls the accuracy of this truncation procedure.

The standard QCD gap equation in mean-field approximation studied in Refs. [54, 55, 56] follows from this approach by including just the sunset-type diagram, which is constructed from two quark-gluon vertices of the QCD tree-level action (see, for instance, Fig. 3.1 in Sec. 3.1.1). I also employ the CJT formalism to derive the gap equation for the color-superconducting gap parameter. However, I construct all diagrams of sunset topology from the vertices of the general *effective* action derived in this work. The resulting gap equation is equivalent to the gap equation in QCD, and the result for the gap parameter to subleading order in weak coupling is identical to that in QCD, provided $\Lambda_q \lesssim g\mu \ll \Lambda_{gl} \lesssim \mu$. The advantage of using the effective theory is

that the appearance of the two scales Λ_q and Λ_gl considerably facilitates the power counting of various contributions to the gap equation as compared to full QCD. I explicitly demonstrate this in the course of the calculation and suggest that, within this approach, it should be possible to identify the terms, which contribute beyond subleading order to the gap equation. Of course, for a complete sub-subleading order result one cannot restrict oneself to the sunset diagram, but would have to investigate other 2PI diagrams as well. This again shows that an *a priori* estimate of the relevance of different contributions on the level of the effective action does not appear to be feasible for quantities, which have to be computed self-consistently.

This work is organized as follows. In Sec. 2.1 I derive the general effective action by explicitly integrating out irrelevant quark and hard gluon modes. In Sec. 2.2 I show that the well-known HTL/HDL effective action, as well as the high-density effective theory proposed by Hong and others, are special cases of this general effective action for particular choices of the quark and gluon cut-offs Λ_q and Λ_gl, respectively. Furthermore, I power count one special subset of diagrams, loops of irrelevant quark modes, analogously to the HTL power counting scheme [7] for the choice $\phi \ll \Lambda_\mathrm{q} \ll g\mu \ll \Lambda_\mathrm{gl} \lesssim \mu$.

Section 3.1 contains the application of the general effective action to the computation of the real part of the color-superconducting gap parameter. In Sec. 3.2 I consider the energy dependence of the gap function within the effective theory and compute its imaginary part for quarks near the Fermi surface. In Sec. 4 I conclude this work with a summary of the results and an outlook.

The units I use are $\hbar = c = k_B = 1$. 4-vectors are denoted by capital letters, $K^\mu = (k_0, \mathbf{k})$, with $\mathbf{k}$ being a 3-vector of modulus $|\mathbf{k}| \equiv k$ and direction $\hat{\mathbf{k}} \equiv \mathbf{k}/k$. For the summation over Lorentz indices, I use a notation familiar from Minkowski space, with metric $g^{\mu\nu} = \mathrm{diag}(+, -, -, -)$, although I exclusively work in compact Euclidean space-time with volume V/T, where V is the 3-volume and T the temperature of the system. Space-time integrals are denoted as $\int_0^{1/T} d\tau \int_V d^3\mathbf{x} \equiv \int_X$. Since space-time is compact, energy-momentum space is discretized, with sums $(T/V)\sum_K \equiv T\sum_n (1/V)\sum_\mathbf{k}$. For a large 3-volume V, the sum over 3-momenta can be approximated by an integral, $(1/V)\sum_\mathbf{k} \simeq \int d^3\mathbf{k}/(2\pi)^3$. For bosons, the sum over n runs over the bosonic Matsubara frequencies $\omega_n^\mathrm{b} = 2n\pi T$, while for fermions, it runs over the fermionic Matsubara frequencies $\omega_n^\mathrm{f} = (2n+1)\pi T$. In a Minkowski-like notation for four-vectors, $x_0 \equiv t \equiv -i\tau$, $k_0 \equiv -i\omega_n^\mathrm{b/f}$. The 4-dimensional delta-function is conveniently defined as $\delta^{(4)}(X) \equiv \delta(\tau)\,\delta^{(3)}(\mathbf{x}) = -i\,\delta(x^0)\,\delta^{(3)}(\mathbf{x})$.

Chapter 2

A general effective action for quark matter

2.1 Deriving the effective action

In this section, I derive a general effective action for hot and/or dense quark matter. I start from the QCD partition function in the functional integral representation (Sec. 2.1.1). I first integrate out irrelevant fermion degrees of freedom (Sec. 2.1.2) and then hard gluon degrees of freedom (Sec. 2.1.3). The final result is Eq. (2.46) in Sec. 2.1.4. I remark that the same result could have been obtained by first integrating out hard gluon modes and then irrelevant fermion modes, but the intermediate steps leading to the final result are less transparent.

2.1.1 Setting the stage

As discussed in the introduction, cf. Eq. (1.1-1.4), the partition function for QCD in the absence of external sources may be written as

$$\mathcal{Z} = \int \mathcal{D}A \, \exp\left\{S_A[A]\right\} \, \mathcal{Z}_q[A] \, , \tag{2.1}$$

where for convenience the pure (gauge-fixed) gluon action has been introduced

$$S_A[A] = \int_X \left[-\frac{1}{4} F_a^{\mu\nu}(X) \, F_{\mu\nu}^a(X)\right] + S_{\mathrm{gf}}[A] + S_{\mathrm{ghost}}[A] \, . \tag{2.2}$$

The partition function for quarks in the presence of gluon fields is

$$\mathcal{Z}_q[A] = \int \mathcal{D}\bar\psi \, \mathcal{D}\psi \, \exp\left\{S_q[A, \bar\psi, \psi]\right\} \, , \tag{2.3}$$

where the quark action is

$$S_q[A, \bar\psi, \psi] = \int_X \bar\psi(X) \, (i\slashed{D}_X + \mu\gamma_0 - m) \, \psi(X) \, . \tag{2.4}$$

In fermionic systems at nonzero density, it is advantageous to additionally introduce charge-conjugate fermionic degrees of freedom,

$$\psi_C(X) \equiv C \, \bar{\psi}^T(X) \; , \quad \bar{\psi}_C(X) \equiv \psi^T(X) \, C \; , \quad \psi(X) \equiv C \, \bar{\psi}_C^T(X) \; , \quad \bar{\psi}(X) \equiv \psi_C^T(X) \, C \; , \tag{2.5}$$

where $C \equiv i\gamma^2\gamma_0$ is the charge-conjugation matrix, $C^{-1} = C^\dagger = C^T = -C$, $C^{-1}\gamma_\mu^T C = -\gamma_\mu$; a superscript T denotes transposition. I may then rewrite the quark action in the form

$$S_q[A, \bar{\Psi}, \Psi] = \frac{1}{2} \int_{X,Y} \bar{\Psi}(X) \, \mathcal{G}_0^{-1}(X,Y) \, \Psi(Y) + \frac{g}{2} \int_X \bar{\Psi}(X) \, \hat{\Gamma}_a^\mu A_\mu^a(X) \, \Psi(X) \; , \tag{2.6}$$

where I defined the Nambu-Gor'kov quark spinors

$$\Psi \equiv \begin{pmatrix} \psi \\ \psi_C \end{pmatrix} \; , \quad \bar{\Psi} \equiv (\bar{\psi}, \bar{\psi}_C) \; , \tag{2.7}$$

and the free inverse quark propagator in the Nambu-Gor'kov basis

$$\mathcal{G}_0^{-1}(X,Y) \equiv \begin{pmatrix} [G_0^+]^{-1}(X,Y) & 0 \\ 0 & [G_0^-]^{-1}(X,Y) \end{pmatrix} \; , \tag{2.8}$$

with the free inverse propagator for quarks and charge-conjugate quarks

$$[G_0^\pm]^{-1}(X,Y) \equiv (i\slashed{\partial}_X \pm \mu\gamma_0 - m) \, \delta^{(4)}(X - Y) \; . \tag{2.9}$$

The quark-gluon vertex in the Nambu-Gor'kov basis is defined as

$$\hat{\Gamma}_a^\mu \equiv \begin{pmatrix} \gamma^\mu T_a & 0 \\ 0 & -\gamma^\mu T_a^T \end{pmatrix} \; . \tag{2.10}$$

As I shall derive the effective action in momentum space, I Fourier-transform all fields, as well as the free inverse quark propagator,

$$\Psi(X) = \frac{1}{\sqrt{V}} \sum_K e^{-iK\cdot X} \, \Psi(K) \; , \tag{2.11a}$$

$$\bar{\Psi}(X) = \frac{1}{\sqrt{V}} \sum_K e^{iK\cdot X} \, \bar{\Psi}(K) \; , \tag{2.11b}$$

$$\mathcal{G}_0^{-1}(X,Y) = \frac{T^2}{V} \sum_{K,Q} e^{-iK\cdot X} e^{iQ\cdot Y} \, \mathcal{G}_0^{-1}(K,Q) \; , \tag{2.11c}$$

$$A_a^\mu(X) = \frac{1}{\sqrt{TV}} \sum_P e^{-iP\cdot X} \, A_a^\mu(P) \; . \tag{2.11d}$$

The normalization factors are chosen such that the Fourier-transformed fields are dimensionless quantities. The Fourier-transformed free inverse quark propagator is diagonal in momentum space, too,

$$\mathcal{G}_0^{-1}(K,Q) = \frac{1}{T} \begin{pmatrix} [G_0^+]^{-1}(K) & 0 \\ 0 & [G_0^-]^{-1}(K) \end{pmatrix} \delta_{K,Q}^{(4)} \; , \tag{2.12}$$

where $[G_0^\pm]^{-1}(K) \equiv K\!\!\!/ \pm \mu\gamma_0 - m$.

Due to the relations (2.5), the Fourier-transformed charge-conjugate quark fields are related to the original fields via $\psi_C(K) = C\bar\psi^T(-K)$, $\bar\psi_C(K) = \psi^T(-K)C$. The measure of the functional integration over quark fields can then be rewritten in the form

$$
\begin{aligned}
\mathcal{D}\bar\psi\,\mathcal{D}\psi &\equiv \prod_K d\bar\psi(K)\,d\psi(K) = \mathcal{N}\prod_{(K,-K)} d\bar\psi(K)\,d\psi(K)\,d\bar\psi(-K)\,d\psi(-K) \\
&= \mathcal{N}'\prod_{(K,-K)} d\bar\psi(K)\,d\psi(K)\,d\bar\psi_C(K)\,d\psi_C(K) = \mathcal{N}''\prod_{(K,-K)} d\bar\Psi(K)\,d\Psi(K) \\
&\equiv \mathcal{D}\bar\Psi\,\mathcal{D}\Psi \ ,
\end{aligned}
\tag{2.13}
$$

with the constant normalization factors $\mathcal{N}$, $\mathcal{N}'$, $\mathcal{N}''$. The last identity has to be considered as a definition for the expression on the right-hand side.

Inserting Eqs. (2.11) – (2.13) into Eq. (2.3), the partition function for quarks becomes

$$
\mathcal{Z}_q[A] = \int \mathcal{D}\bar\Psi\,\mathcal{D}\Psi \exp\left[\frac{1}{2}\,\bar\Psi\left(\mathcal{G}_0^{-1} + g\mathcal{A}\right)\Psi\right] \ .
\tag{2.14}
$$

Here, I employ a compact matrix notation,

$$
\bar\Psi\left(\mathcal{G}_0^{-1} + g\mathcal{A}\right)\Psi \equiv \sum_{K,Q} \bar\Psi(K)\left[\mathcal{G}_0^{-1}(K,Q) + g\mathcal{A}(K,Q)\right]\Psi(Q) \ ,
\tag{2.15}
$$

with the definition

$$
\mathcal{A}(K,Q) \equiv \frac{1}{\sqrt{VT^3}}\,\hat\Gamma_a^\mu A_\mu^a(K-Q) \ .
\tag{2.16}
$$

The next step is to integrate out irrelevant quark modes.

2.1.2 Integrating out irrelevant quark modes

Since I work in a finite volume V, the 3-momentum $\mathbf{k}$ is discretized. Let us for the moment also assume that there is an ultraviolet cut-off (such as in a lattice regularization) on the 3-momentum, i.e., the space of modes labelled by 3-momentum has dimension $D < \infty$. I define projection operators $\mathcal{P}_1$, $\mathcal{P}_2$ for relevant and irrelevant quark modes, respectively,

$$
\Psi_1 \equiv \mathcal{P}_1\Psi \ , \quad \Psi_2 \equiv \mathcal{P}_2\Psi \ , \quad \bar\Psi_1 \equiv \bar\Psi\,\gamma_0\mathcal{P}_1\gamma_0 \ , \quad \bar\Psi_2 \equiv \bar\Psi\,\gamma_0\mathcal{P}_2\gamma_0 \ .
\tag{2.17}
$$

The subspace of relevant quark modes has dimension N_1 in the space of 3-momentum modes, the one for irrelevant modes dimension N_2, with $N_1 + N_2 = D$.

At this point, it is instructive to give an explicit example for the projectors $\mathcal{P}_{1,2}$. In the effective theory for cold, dense quark matter, which contains the high-density effective theory [100, 101, 102, 103, 104, 105] discussed in Sec. 2.2.2 as special case and which I shall apply in Sec. 3.1 to the computation of the gap parameter, the projectors are chosen as

$$
\mathcal{P}_1(K,Q) \equiv \begin{pmatrix} \Lambda_{\mathbf{k}}^+ & 0 \\ 0 & \Lambda_{\mathbf{k}}^- \end{pmatrix} \Theta(\Lambda_{\mathrm{q}} - |k - k_F|)\,\delta_{K,Q}^{(4)} \ ,
\tag{2.18a}
$$

$$
\mathcal{P}_2(K,Q) \equiv \begin{pmatrix} \Lambda_{\mathbf{k}}^- + \Lambda_{\mathbf{k}}^+\,\Theta(|k - k_F| - \Lambda_{\mathrm{q}}) & 0 \\ 0 & \Lambda_{\mathbf{k}}^+ + \Lambda_{\mathbf{k}}^-\,\Theta(|k - k_F| - \Lambda_{\mathrm{q}}) \end{pmatrix} \delta_{K,Q}^{(4)} \ .
\tag{2.18b}
$$

Here,

$$\Lambda^e_{\mathbf{k}} \equiv \frac{1}{2E_{\mathbf{k}}} \left[E_{\mathbf{k}} + e\gamma_0 \left(\boldsymbol{\gamma} \cdot \mathbf{k} + m \right) \right] , \tag{2.19}$$

are projection operators onto states with positive ($e = +$) or negative ($e = -$) energy, where $E_{\mathbf{k}} = \sqrt{\mathbf{k}^2 + m^2}$ is the relativistic single-particle energy. The momentum cut-off Λ_q controls how many quark modes (with positive energy) are integrated out. Thus, all quark modes within a layer of width $2\Lambda_q$ around the Fermi surface are considered as relevant, while all antiquark modes and quark modes outside this layer are considered as irrelevant. Note that, for the Nambu-Gor'kov components corresponding to charge-conjugate particles, the role of the projectors onto positive and negative energy states is reversed with respect to the Nambu-Gor'kov components corresponding to particles. The reason is that, loosely speaking, a particle is actually a charge-conjugate antiparticle. For a more rigorous proof compute, for instance, $\psi_{C,1}(K) \equiv C \bar{\psi}_1^T(-K)$ using $\bar{\psi}_1(-K) = \bar{\psi}(-K) \gamma_0 \Lambda^+_{-\mathbf{k}} \gamma_0$ (for $|k - k_F| \leq \Lambda_q$) and $\gamma_0 C [\Lambda^+_{-\mathbf{k}}]^T C^{-1} \gamma_0 = \Lambda^-_{\mathbf{k}}$. In Sec. 2.2 I shall discuss other choices for the projectors $\mathcal{P}_{1,2}$, pertaining to other effective theories of hot and/or dense quark matter. The following discussion in this section, however, will be completely general and is not restricted to any particular choice for these projectors.

Employing Eq. (2.17), the partition function (2.14) becomes

$$\mathcal{Z}_q[A] = \int \prod_{n=1,2} \mathcal{D}\bar{\Psi}_n \, \mathcal{D}\Psi_n \, \exp\left(\frac{1}{2} \sum_{n,m=1,2} \bar{\Psi}_n \, \mathcal{G}^{-1}_{nm} \, \Psi_m \right) . \tag{2.20}$$

From now on, $\bar{\Psi}_{1,2}$, $\Psi_{1,2}$ are considered as vectors restricted to the $N_{1,2}$-dimensional subspace of relevant/irrelevant 3-momentum modes. The matrices $\mathcal{G}^{-1}_{nn}$, $n = 1, 2$, are defined as

$$\mathcal{G}^{-1}_{nn}(K,Q) = \mathcal{G}^{-1}_{0,nn}(K,Q) + g\mathcal{A}_{nn}(K,Q) , \tag{2.21}$$

where the indices indicate that, for a given pair of quark energies k_0, q_0, the 3-momenta $\mathbf{k}$, $\mathbf{q}$ belong to the subspace of relevant ($n = 1$) or irrelevant ($n = 2$) quark modes, i.e., $\mathcal{G}^{-1}_{nn}$ is an ($N_n \times N_n$)-dimensional matrix in 3-momentum space. The matrices $\mathcal{G}^{-1}_{nm}$, $n \neq m$, reduce to

$$\mathcal{G}^{-1}_{nm}(K,Q) = g \, \mathcal{A}_{nm}(K,Q) , \tag{2.22}$$

since $\mathcal{G}^{-1}_0$ is diagonal in 3-momentum space, i.e. $\mathcal{G}^{-1}_{0,nm} \equiv 0$ for $n \neq m$. For a given pair of quark energies k_0, q_0, $\mathcal{G}^{-1}_{nm}$ is a ($N_n \times N_m$)-dimensional matrix in 3-momentum space.

The Grassmann integration over the irrelevant quark fields $\bar{\Psi}_2$, Ψ_2 can be done exactly, if one redefines them such that the mixed terms $\sim \mathcal{G}^{-1}_{nm}$, $n \neq m$, are eliminated. To this end, substitute

$$\Upsilon \equiv \Psi_2 + \mathcal{G}_{22} \, \mathcal{G}^{-1}_{21} \, \Psi_1 , \quad \bar{\Upsilon} \equiv \bar{\Psi}_2 + \bar{\Psi}_1 \, \mathcal{G}^{-1}_{12} \, \mathcal{G}_{22} , \tag{2.23}$$

where $\mathcal{G}_{22}$ is the inverse of $\mathcal{G}^{-1}_{22}$, defined on the subspace of irrelevant quark modes. The result is

$$\mathcal{Z}_q[A] = \int \mathcal{D}\bar{\Psi}_1 \, \mathcal{D}\Psi_1 \, \exp\left[\frac{1}{2} \bar{\Psi}_1 \left(\mathcal{G}^{-1}_{11} - \mathcal{G}^{-1}_{12} \, \mathcal{G}_{22} \, \mathcal{G}^{-1}_{21} \right) \Psi_1 + \frac{1}{2} \mathrm{Tr}_q \ln \mathcal{G}^{-1}_{22} \right] . \tag{2.24}$$

The trace in the last term runs over all irrelevant quark momenta K, and not only over pairs $(K, -K)$, as prescribed by the integration measure, Eq. (2.13). This requires an additional

factor $1/2$ in front of the trace. A more intuitive way of saying this is that this factor accounts for the doubling of the quark degrees of freedom in the Nambu-Gor'kov basis. Of course, the trace runs not only over 4-momenta, but also over other quark indices, such as Nambu-Gor'kov, fundamental color, flavor, and Dirac indices. I indicated this by the subscript "q".

For a diagrammatic interpretation it is advantageous to rewrite

$$\mathcal{G}_{11}^{-1} - \mathcal{G}_{12}^{-1} \mathcal{G}_{22} \mathcal{G}_{21}^{-1} \equiv \mathcal{G}_{0,11}^{-1} + g\mathcal{B} , \tag{2.25}$$

where

$$g\mathcal{B} \equiv g\mathcal{A}_{11} - g\mathcal{A}_{12} \mathcal{G}_{22} g\mathcal{A}_{21} . \tag{2.26}$$

The propagator for irrelevant quark modes, $\mathcal{G}_{22}$, has an expansion in powers of g times the gluon field,

$$\mathcal{G}_{22} = \mathcal{G}_{0,22} \sum_{n=0}^{\infty} (-1)^n g^n \left[\mathcal{A}_{22} \mathcal{G}_{0,22}\right]^n . \tag{2.27}$$

This expansion is graphically depicted in Fig. 2.1.
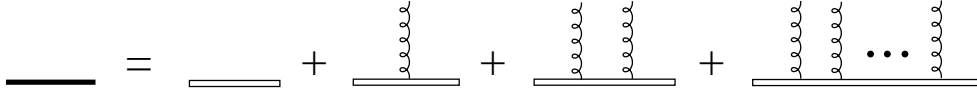
Figure 2.1: The full propagator for irrelevant quarks. The right-hand side symbolizes the expansion (2.27). The free irrelevant quark propagators $\mathcal{G}_{0,22}$ are denoted by double lines, the gluon fields $\mathcal{A}_{22}$ by curly lines.
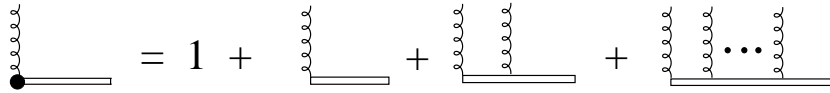
Figure 2.2: The diagrammatic symbol for the factor $(1 + g\mathcal{A} \mathcal{G}_{0,22})^{-1}$.
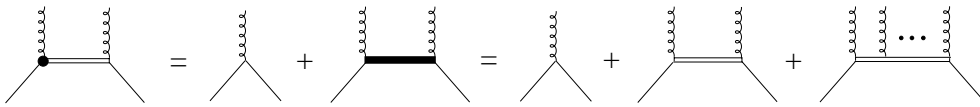
Figure 2.3: The term $\bar{\Psi}_1 g\mathcal{B} \Psi_1$. A relevant quark field is denoted by a single solid line.

Using this expansion, and suppressing the indices on $\mathcal{A}$, Eq. (2.26) can be symbolically written as

$$g\mathcal{B} = (1 + g\mathcal{A} \mathcal{G}_{0,22})^{-1} g\mathcal{A} , \tag{2.28}$$

which suggests the interpretation of the field $\mathcal{B}$ as a "modified" (non-local) gluon field. In the diagrams to be discussed below, the factor $(1 + g\mathcal{A} \mathcal{G}_{0,22})^{-1}$ will be denoted by the diagrammatical symbol shown in Fig. 2.2. With this symbol, the expression $\bar{\Psi}_1 g\mathcal{B} \Psi_1$ can be graphically depicted as shown in Fig. 2.3.
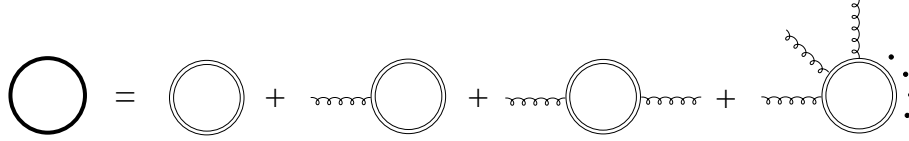
Figure 2.4: The graphical representation of the term $\mathrm{Tr}_q \ln \mathcal{G}_{22}^{-1}$ in Eq. (2.24).

Since

$$\ln \mathcal{G}_{22}^{-1} = \ln \mathcal{G}_{0,22}^{-1} - \sum_{n=1}^{\infty} \frac{(-1)^n}{n} \, g^n \, [\mathcal{G}_{0,22} \, \mathcal{A}_{22}]^n \; , \tag{2.29}$$

the last term in the exponent in Eq. (2.24) also has a graphical interpretation, shown in Fig. 2.4.

This concludes the integration over irrelevant quark modes. Note that the present treatment is (i) exact in the sense that no approximations have been made and (ii) completely general, since it is independent of the specific choice (2.18) for the projection operators. The next step is to integrate out hard gluon modes.

2.1.3 Integrating out hard gluon modes

Combining Eqs. (2.1), (2.24), and (2.26), the partition function of QCD for relevant quark modes and gluons reads

$$\mathcal{Z} \;\; = \;\; \int \mathcal{D}\bar{\Psi}_1 \, \mathcal{D}\Psi_1 \, \mathcal{D}A \, \exp\left\{ S[A, \bar{\Psi}_1, \Psi_1] \right\} \tag{2.30a}$$

$$S[A, \bar{\Psi}_1, \Psi_1] \;\; \equiv \;\; S_A[A] + \frac{1}{2} \, \bar{\Psi}_1 \left\{ \mathcal{G}_{0,11}^{-1} + g\mathcal{B}[A] \right\} \Psi_1 + \frac{1}{2} \, \mathrm{Tr}_q \ln \mathcal{G}_{22}^{-1}[A] \; , \tag{2.30b}$$

where $\mathcal{D}A \equiv \prod_P dA(P)$. For the sake of clarity, I restored the functional dependence of the "modified" gluon field $\mathcal{B}$ and the inverse irrelevant quark propagator $\mathcal{G}_{22}^{-1}$ on the gluon field A.

The gluon action in momentum space is

$$
\begin{aligned}
S_A[A] \;\; = \;\; & -\frac{1}{2} \sum_{P_1, P_2} A_\mu^a(P_1) \left[\Delta_0^{-1}\right]_{ab}^{\mu\nu}(P_1, P_2) A_\nu^b(P_2) \\
& -\frac{1}{3!} \frac{g}{\sqrt{VT^3}} \sum_{P_1, P_2, P_3} \delta^{(4)}_{P_1+P_2+P_3,0} \, \mathcal{V}^{abc}_{\alpha\beta\gamma}(P_1, P_2, P_3) \, A_a^\alpha(P_1) A_b^\beta(P_2) A_c^\gamma(P_3) \\
& -\frac{1}{4!} \left(\frac{g}{\sqrt{VT^3}} \right)^2 \sum_{P_1, \cdots, P_4} \delta^{(4)}_{P_1+P_2+P_3+P_4,0} \, \mathcal{V}^{abcd}_{\alpha\beta\gamma\delta} \, A_a^\alpha(P_1) A_b^\beta(P_2) A_c^\gamma(P_3) A_d^\delta(P_4) \\
& +\mathrm{Tr}_{gh} \ln \mathcal{W}^{-1} \; .
\end{aligned}
\tag{2.31}
$$

Here, $\Delta_0^{-1}(P_1, P_2)$ is the gauge-fixed inverse free gluon propagator. To be specific, in general Coulomb gauge it reads

$$\left[\Delta_0^{-1}\right]_{ab}^{\mu\nu}(P_1, P_2) \;\; \equiv \;\; \frac{1}{T^2} \left[\Delta_0^{-1}\right]_{ab}^{\mu\nu}(P_1) \, \delta^{(4)}_{P_1,-P_2} \; , \tag{2.32a}$$

$$\left[\Delta_0^{-1}\right]_{ab}^{\mu\nu}(P) \;\; = \;\; \delta_{ab} \left(P^2 g^{\mu\nu} - P^\mu P^\nu + \frac{1}{\xi_C} \tilde{P}^\mu \tilde{P}^\nu \right) \; , \tag{2.32b}$$

where ξ_C is the Coulomb gauge parameter and $\tilde{P}^\mu \equiv (0, \mathbf{p})$. The vertex functions are

$$\mathcal{V}^{abc}_{\alpha\beta\gamma}(P_1, P_2, P_3) \equiv \frac{i}{T} f^{abc} \left[(P_1 - P_2)_\gamma \, g_{\alpha\beta} + (P_2 - P_3)_\alpha \, g_{\beta\gamma} + (P_3 - P_1)_\beta \, g_{\alpha\gamma} \right] , \quad (2.33a)$$

$$\mathcal{V}^{abcd}_{\alpha\beta\gamma\delta} \equiv f^{abe} f^{ecd} \left(g_{\alpha\gamma} g_{\beta\delta} - g_{\alpha\delta} g_{\beta\gamma} \right) + f^{ace} f^{ebd} \left(g_{\alpha\beta} g_{\gamma\delta} - g_{\alpha\delta} g_{\beta\gamma} \right)$$
$$+ f^{ade} f^{ebc} \left(g_{\alpha\beta} g_{\gamma\delta} - g_{\alpha\gamma} g_{\beta\delta} \right) . \quad (2.33b)$$

The last term in Eq. (2.31) is the trace of the logarithm of the Faddeev-Popov determinant, with the full inverse ghost propagator $\mathcal{W}^{-1}$. The trace runs over ghost 4-momenta and adjoint color indices.

Similar to the treatment of fermions in Sec. 2.1.2 I now define projectors $\mathcal{Q}_1$, $\mathcal{Q}_2$ for soft and hard gluon modes, respectively,

$$A_1 \equiv \mathcal{Q}_1 A , \quad A_2 \equiv \mathcal{Q}_2 A , \quad (2.34)$$

where

$$\mathcal{Q}_1(P_1, P_2) \equiv \Theta(\Lambda_{\mathrm{gl}} - p_1) \, \delta^{(4)}_{P_1, P_2} , \quad (2.35a)$$

$$\mathcal{Q}_2(P_1, P_2) \equiv \Theta(p_1 - \Lambda_{\mathrm{gl}}) \, \delta^{(4)}_{P_1, P_2} . \quad (2.35b)$$

The gluon cut-off momentum Λ_{gl} defines which gluons are considered to be soft or hard, respectively.

I now insert $A \equiv A_1 + A_2$ into Eq. (2.30). The integration measure simply factorizes, $\mathcal{D}A \equiv \mathcal{D}A_1 \, \mathcal{D}A_2$. The action $S[A, \bar{\Psi}_1, \Psi_1]$ can be sorted with respect to powers of the hard gluon field,

$$S[A, \bar{\Psi}_1, \Psi_1] = S[A_1, \bar{\Psi}_1, \Psi_1] + A_2 \mathcal{J}[A_1, \bar{\Psi}_1, \Psi_1] - \frac{1}{2} A_2 \, \Delta_{22}^{-1}[A_1, \bar{\Psi}_1, \Psi_1] \, A_2 + S_I[A_1, A_2, \bar{\Psi}_1, \Psi_1] .$$
$$(2.36)$$

The first term in this expansion, containing no hard gluon fields at all, is simply the action (2.30b), with A replaced by the relevant gluon field A_1. The second term, $A_2 \mathcal{J}$, contains a single power of the hard gluon field, where

$$\mathcal{J}[A_1, \bar{\Psi}_1, \Psi_1] \equiv \left. \frac{\delta S[A, \bar{\Psi}_1, \Psi_1]}{\delta A_2} \right|_{A_2=0} \equiv \mathcal{J}_{\mathcal{B}}[A_1, \bar{\Psi}_1, \Psi_1] + \mathcal{J}_{\mathrm{loop}}[A_1] + \mathcal{J}_{\mathcal{V}}[A_1] . \quad (2.37)$$

The first contribution,

$$\mathcal{J}_{\mathcal{B}}[A_1, \bar{\Psi}_1, \Psi_1] = \frac{1}{2} \bar{\Psi}_1 \left(g \frac{\delta \mathcal{B}}{\delta A_2} \right)_{A_2=0} \Psi_1 , \quad (2.38)$$

arises from the coupling of the relevant fermions to the "modified" gluon field $\mathcal{B}$, i.e., from the second term in Eq. (2.30b). With the notation of Fig. 2.2, all diagrams corresponding to $A_2 \mathcal{J}_{\mathcal{B}}$ can be summarized into a single one, cf. Fig. 2.5. It contains precisely two relevant fermion fields, $\bar{\Psi}_1$ and Ψ_1. The second contribution, $\mathcal{J}_{\mathrm{loop}}$, arises from the terms $\mathrm{Tr}_q \ln \mathcal{G}_{22}^{-1}$ and $\mathrm{Tr}_{gh} \ln \mathcal{W}^{-1}$ in Eqs. (2.30b), (2.31). The loop consisting of irrelevant quark modes as internal lines, coupled to a single hard and arbitrarily many soft gluons, is shown in Fig. 2.6. Finally, the third contribution, $\mathcal{J}_{\mathcal{V}}$, arises from the non-Abelian vertices, cf. Fig. 2.7.
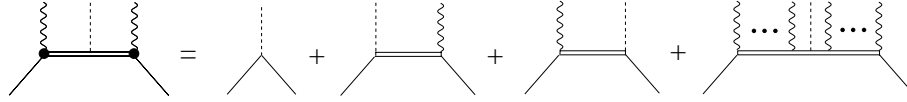
Figure 2.5: The term $A_2 \mathcal{J}_\mathcal{B}$. The hard gluon field is denoted by a dashed line, the soft gluon fields by wavy lines.
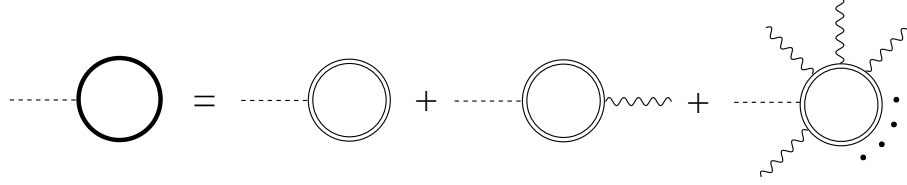
Figure 2.6: The fermionic contribution to the term $A_2 \mathcal{J}_\text{loop}$. There is an additional contribution from ghosts with similar topology.

The third term in Eq. (2.36) is quadratic in A_2, where

$$\Delta_{22}^{-1}[A_1, \bar{\Psi}_1, \Psi_1] \equiv -\left.\frac{\delta^2 S[A, \bar{\Psi}_1, \Psi_1]}{\delta A_2 \,\delta A_2}\right|_{A_2=0} \equiv \Delta_{0,22}^{-1} + \Pi_{22}[A_1, \bar{\Psi}_1, \Psi_1] \ . \tag{2.39}$$

Here, $\Delta_{0,22}^{-1}$ is the free inverse propagator for hard gluons. Similar to the "current" $\mathcal{J}$, cf. Eq. (2.37), the "self-energy" Π_{22} of hard gluons consists of three different contributions,

$$\Pi_{22}[A_1, \bar{\Psi}_1, \Psi_1] = \Pi_\mathcal{B}[A_1, \bar{\Psi}_1, \Psi_1] + \Pi_\text{loop}[A_1] + \Pi_\mathcal{V}[A_1] \ , \tag{2.40}$$

which has a diagrammatic representation as shown in Fig. 2.8. The first two contributions on the right-hand side of Eq. (2.40) can be expanded as shown in Figs. 2.9 and 2.10. Figure 2.11 depicts the three- and four-gluon vertices contained in the last term in Eq. (2.40). For further use, I explicitly give the first term,

$$\Pi_\mathcal{B}[A_1, \bar{\Psi}_1, \Psi_1] = -\frac{1}{2}\, \bar{\Psi}_1 \left(g\, \frac{\delta^2 \mathcal{B}}{\delta A_2 \delta A_2}\right)_{A_2=0} \Psi_1 \ . \tag{2.41}$$

Finally, I collect all terms with more than two hard gluon fields A_2 in Eq. (2.36) in the "interaction action" for hard gluons, $S_I[A_1, A_2, \bar{\Psi}_1, \Psi_1]$. I then perform the functional integration over the hard gluon fields A_2. Since functional integrals must be of Gaussian type in order to be exactly solvable, I resort to a method well known from perturbation theory. I add the source term $A_2 J_2$ to the action (2.30b) and may then replace the fields A_2 in S_I by functional differentiation with respect to J_2, at $J_2 = 0$. I then move the factor $\exp\{S_I[A_1, \delta/\delta J_2, \bar{\Psi}_1, \Psi_1]\}$ in front of the functional A_2-integral. Then, this functional integral is Gaussian and can be readily performed (after a suitable shift of A_2), with the result

$$\begin{aligned}
\mathcal{Z} &= \int \mathcal{D}\bar{\Psi}_1\, \mathcal{D}\Psi_1 \mathcal{D}A_1\, \exp\left\{S[A_1, \bar{\Psi}_1, \Psi_1] - \frac{1}{2}\operatorname{Tr}_g \ln \Delta_{22}^{-1}\right\} \\
&\quad \times \exp\left\{S_I\left[A_1, \frac{\delta}{\delta J_2}, \bar{\Psi}_1, \Psi_1\right]\right\} \exp\left[\frac{1}{2}\left(\mathcal{J} + J_2\right)\Delta_{22}\left(\mathcal{J} + J_2\right)\right]\bigg|_{J_2=0} \ . \tag{2.42}
\end{aligned}$$
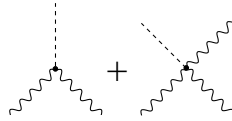
Figure 2.7: The term $A_2 \mathcal{J}_\mathcal{V}$.
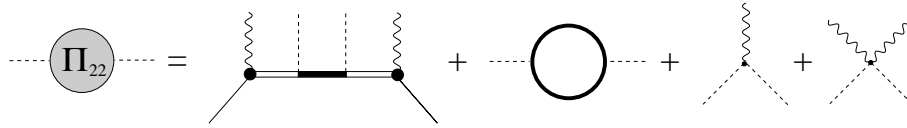
Figure 2.8: The term $A_2 \Pi_{22} A_2$ according to Eq. (2.40). The first diagram on the right-hand side corresponds to the term $A_2 \Pi_\mathcal{B} A_2$. The second diagram is the fermion-loop contribution to $A_2 \Pi_\text{loop} A_2$; there is an analogous one from a ghost loop. The last two diagrams correspond to $A_2 \Pi_\mathcal{V} A_2$.

The trace over $\ln \Delta_{22}^{-1}$ runs over gluon 4-momenta, as well as adjoint color and Lorentz indices. I indicate this with a subscript "g". Note that this result is still exact and completely general, since so far the manipulations of the partition function were independent of the specific choice (2.35) for the projection operators $\mathcal{Q}_{1,2}$. The next step is to derive the tree-level action for the effective theory of relevant quark modes and soft gluons.

2.1.4 Tree-level effective action

In order to derive the tree-level effective action, I shall employ two approximations. The first is based on the principal assumption in the construction of any effective theory, namely that soft and hard modes are well separated in momentum space. Consequently, momentum conservation does not allow a hard gluon to couple to any (finite) number of soft gluons. Under this assumption, the diagrams generated by $A_2(\mathcal{J}_\text{loop} + \mathcal{J}_\mathcal{V})$, cf. Fig. 2.6, 2.7, will not occur in the effective theory. In the following, I shall therefore omit these terms, so that $\mathcal{J} \equiv \mathcal{J}_\mathcal{B}$. Note that similar arguments cannot be applied to the diagrams generated by $A_2(\Pi_\text{loop} + \Pi_\mathcal{V})A_2$, cf. Fig. 2.10, 2.11, since now there are two hard gluon legs which take care of momentum conservation.

My second approximation is that in the "perturbative" expansion of the partition function (2.42) with respect to powers of the interaction action S_I, I only take the first term, i.e., I approximate $e^{S_I} \simeq 1$. At this point, this is simply a matter of convenience, since I do not need the higher-order terms in the expansion of e^{S_I} for the effective theories to be discussed in Sec. 2.2 or for the calculation of the gap parameter in Sec. 3.1. However, one can easily reinstall them if required by the particular problem at hand. I note in passing that the approximation $e^{S_I} \simeq 1$ becomes exact in the derivation of the exact renormalization group [117], where one only integrates out modes in a shell of infinitesimal thickness.

Diagrams generated by the higher-order terms in the expansion of e^{S_I} are those with more than one *resummed* hard gluon line. Even with the approximation $e^{S_I} \simeq 1$, Eq. (2.42) still contains diagrams with arbitrarily many *bare* hard gluon lines, arising from the expansion of

$$\ln \Delta_{22}^{-1} = \ln \Delta_{0,22}^{-1} - \sum_{n=1}^{\infty} \frac{(-1)^n}{n} \left(\Delta_{0,22} \, \Pi_{22} \right)^n \,, \tag{2.43}$$
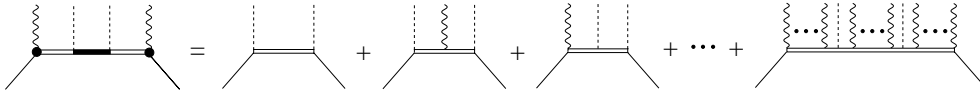
Figure 2.9: The term $A_2 \Pi_{\mathcal{B}} A_2$.
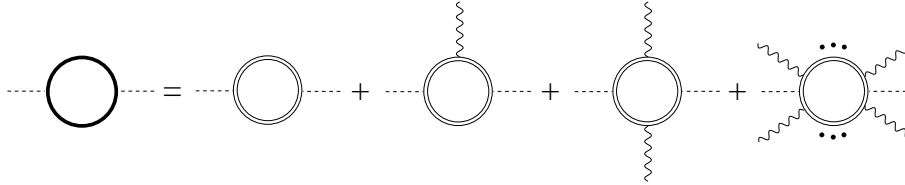
Figure 2.10: The fermionic contribution to the term $A_2 \Pi_{\text{loop}} A_2$.

and from the term $\mathcal{J}_{\mathcal{B}} \Delta_{22} \mathcal{J}_{\mathcal{B}}$ in Eq. (2.42), when expanding

$$\Delta_{22} = \Delta_{0,22} \sum_{n=0}^{\infty} (-1)^n \left(\Pi_{22} \Delta_{0,22} \right)^n . \tag{2.44}$$

With these approximations, the partition function reads

$$\mathcal{Z} = \int \mathcal{D}\bar{\Psi}_1 \, \mathcal{D}\Psi_1 \mathcal{D}A_1 \, \exp\{ S_{\text{eff}}[A_1, \bar{\Psi}_1, \Psi_1] \} , \tag{2.45}$$

where the effective action is defined as

$$
\begin{aligned}
S_{\text{eff}}[A_1, \bar{\Psi}_1, \Psi_1] \;\; \equiv \;\; & S_A[A_1] + \frac{1}{2} \bar{\Psi}_1 \left\{ \mathcal{G}_{0,11}^{-1} + g\mathcal{B}[A_1] \right\} \Psi_1 + \frac{1}{2} \operatorname{Tr}_q \ln \mathcal{G}_{22}^{-1}[A_1] \\
& - \frac{1}{2} \operatorname{Tr}_g \ln \Delta_{22}^{-1}[A_1, \bar{\Psi}_1, \Psi_1] \\
& + \frac{1}{2} \mathcal{J}_{\mathcal{B}}[A_1, \bar{\Psi}_1, \Psi_1] \, \Delta_{22}[A_1, \bar{\Psi}_1, \Psi_1] \, \mathcal{J}_{\mathcal{B}}[A_1, \bar{\Psi}_1, \Psi_1] .
\end{aligned}
\tag{2.46}
$$

This is the desired action for the effective theory describing the interaction of relevant quark modes, $\bar{\Psi}_1, \Psi_1$, and soft gluons, A_1. The functional dependence of the various terms on the right-hand side on the fields $A_1, \bar{\Psi}_1, \Psi_1$ has been restored in order to facilitate the following discussion of all possible interaction vertices occurring in this effective theory.

The diagrams corresponding to these vertices are shown in Figs. 2.12-2.16. The three- and four-gluon vertices contained in $S_A[A_1]$ are displayed in Fig. 2.12. In addition, $S_A[A_1]$ contains ghost loops with an arbitrary number of attached soft gluon legs. The topology is equivalent to that of the quark loops in Fig. 2.14 and is therefore not shown explicitly. The interaction between two relevant quarks and the "modified" soft gluon field, corresponding to $\bar{\Psi}_1 \, g\mathcal{B}[A_1] \, \Psi_1$, is depicted in Fig. 2.13. This is similar to Fig. 2.3, except that now all gluon legs are soft. Diagrams where an arbitrary number of soft gluon legs is attached to an irrelevant quark loop are generated by $\operatorname{Tr}_q \ln \mathcal{G}_{22}^{-1}$, cf. Fig. 2.14. This is similar to Fig. 2.4, but now only soft gluon legs are attached to the fermion loop. The diagrams generated by the loop of a full hard gluon propagator, $\operatorname{Tr}_g \ln \Delta_{22}^{-1}$, are shown in Fig. 2.15. The first line in this figure features the generic
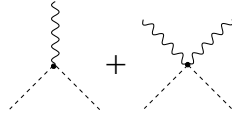
Figure 2.11: The term $A_2 \Pi_\mathcal{V} A_2$.
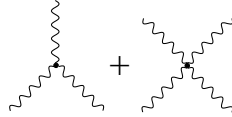
Figure 2.12: The three- and four-gluon vertices in $S_A[A_1]$, describing the self-interaction of soft gluons in Eq. (2.46).

expansion of this term according to Eq. (2.43), where the hard gluon "self-energy" insertion Π_{22}, cf. Eq. (2.40), is shown in Fig. 2.8. The second line shows examples of diagrams generated by explicitly inserting Π_{22} in the generic expansion. Besides an arbitrary number of soft gluon legs, these diagrams also feature an arbitrary number of relevant quark legs. If there are only two relevant quark legs, but no soft gluon leg, one obtains the one-loop self-energy for relevant quarks, cf. the second diagram in the second line of Fig. 2.15. The next two diagrams are obtained by adding a soft gluon leg, resulting in vertex corrections for the bare vertex between relevant quarks and soft gluons. The first of these two diagrams arises from the $n = 1$ term in Eq. (2.43), while the second originates from the $n = 2$ term. Four relevant quark legs and no soft gluon leg give rise to the scattering of two relevant quarks via exchange of two hard gluons, contained in the $n = 2$ term in Eq. (2.43), cf. the last diagram in Fig. 2.15. This diagram was also discussed in the context of the effective theory presented in Refs. [100, 101], cf. discussion in Sec. 2.2.2. Finally, the "current-current" interaction mediated by a full hard gluon propagator, $\mathcal{J}_\mathcal{B} \Delta_{22} \mathcal{J}_\mathcal{B}$, Fig. 2.16, contains also a multitude of quark-gluon vertices. The simplest one is the first on the right-hand side in Fig. 2.16, corresponding to scattering of two relevant fermions via exchange of a single hard gluon.

An important question is whether the introduction of the momentum cut-offs Λ_q, Λ_{gl} could possibly spoil the gauge invariance of the effective action (2.46). This is not the case, since gauge invariance is already explicitly broken *from the very beginning* by the choice of gauge in the gauge-fixed gluon action (2.2). I do not perceive this to be a disadvantage of my approach, since the computation of a physical quantity requires to fix the gauge anyway. The final result should, of course, neither depend on the choice of gauge, nor on Λ_q and Λ_{gl}. Note that, up to this point, I was not required to specify the gauge in the effective action (2.46).

The effective action (2.46) is formally of the form (1.40). The difference is that Eq. (2.46) contains more than one relevant field: besides relevant quarks there are also soft gluons. It is obvious that in this case there are many more possibilities to construct operators $\mathcal{O}_i$ which occur in the expansion (1.40). As pointed out in the introduction, it is therefore advantageous to derive the effective action (2.46) by explicitly integrating out irrelevant quark and hard gluon modes, and not by simply guessing the form of the operators $\mathcal{O}_i$, since then one is certain that one has constructed *all* possible operators occurring in the expansion (1.40).

As mentioned in the introduction, the standard approach to derive an effective theory, namely
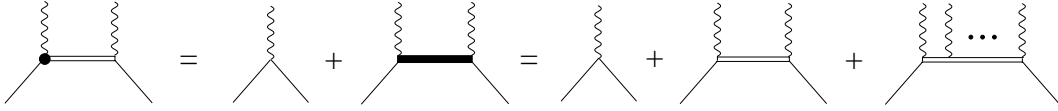
Figure 2.13: The term $\bar{\Psi}_1 \, g\mathcal{B}[A_1] \, \Psi_1$ in the effective action (2.46).
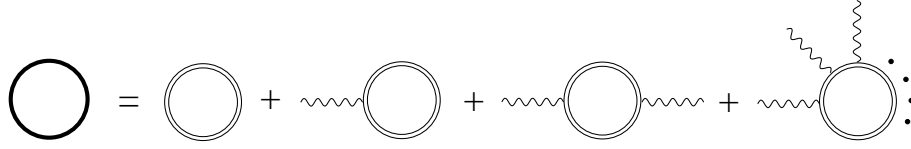
Figure 2.14: The term $\mathrm{Tr}_q \ln \mathcal{G}_{22}^{-1}[A_1]$ in the effective action (2.46).

guessing the form of the operators $\mathcal{O}_i$ and performing a naive dimensional scaling analysis to estimate their order of magnitude, fails precisely when (a) there are non-local operators, or when (b) there is more than one momentum scale. Both (a) and (b) apply here. As I shall show below, the HTL/HDL effective action is one limiting case of Eq. (2.46), and it is well known that this action is non-local. Moreover, as is obvious from the above derivation, there are indeed several momentum scales occurring in Eq. (2.46). Let us focus on the case of zero temperature, $T = 0$, and, for the sake of simplicity, assume massless quarks, $m = 0$, $\mu = k_F$. To be explicit, I employ the choice (2.18) for the projectors $\mathcal{P}_{1,2}$. In this case, the first momentum scale is defined by the Fermi energy μ. The propagator of antiquarks is $\sim 1/(k_0 + \mu + k)$. If $\Lambda_\mathrm{q}, \Lambda_\mathrm{gl} \lesssim \mu$, the exchange of an antiquark can be approximated by a contact interaction with strength $\sim 1/\mu$, on the scale of the relevant quarks, $L_\mathrm{q} \gg 1/\Lambda_\mathrm{q} \gtrsim 1/\mu$, or of the soft gluons, $L_\mathrm{gl} \gg 1/\Lambda_\mathrm{gl} \gtrsim 1/\mu$.

The second momentum scale is defined by the quark cut-off momentum Λ_q. The propagator of irrelevant quark modes is $\sim 1/(k_0 + \mu - k)$. On the scale L_q of the relevant quarks, not only the exchange of an antiquark, but also that of an irrelevant quark with momentum $\mathbf{k}$ satisfying $|k - \mu| \geq \Lambda_\mathrm{q}$ is local, with strength $\sim 1/\Lambda_\mathrm{q}$. However, suppose that the quark cut-off scale happens to be much smaller than the chemical potential, $\Lambda_\mathrm{q} \ll \mu$. In this case, antiquark exchange is "much more localized" than the exchange of an irrelevant quark, $1/\mu \ll 1/\Lambda_\mathrm{q}$.

The third momentum scale is defined by the gluon cut-off momentum Λ_gl. The propagator of a hard gluon is $\sim 1/P^2$. On the scale L_gl of a soft gluon, the exchange of a hard gluon with momentum $p \geq \Lambda_\mathrm{gl}$ can be considered local, with strength $\sim 1/\Lambda_\mathrm{gl}^2$. As I shall show below, in order to derive the value of the QCD gap parameter in weak coupling and to subleading order, the ordering of the scales turns out to be $\Lambda_\mathrm{q} \lesssim g\mu \ll \Lambda_\mathrm{gl} \lesssim \mu$. Thus, antiquark exchange happens on a length scale of the same order as hard gluon exchange, which in turn happens on a much smaller length scale than the exchange of an irrelevant quark, $1/\mu \lesssim 1/\Lambda_\mathrm{gl} \ll 1/\Lambda_\mathrm{q}$.
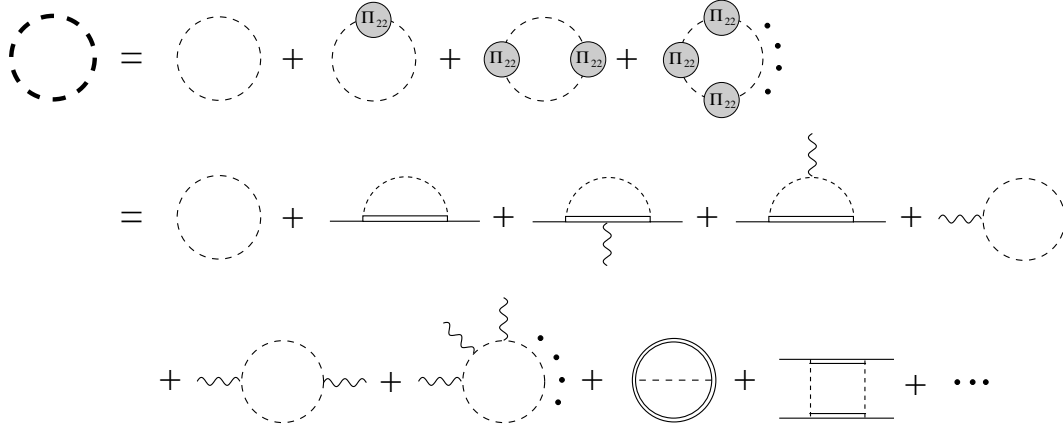
Figure 2.15: The term $\mathrm{Tr}_g \ln \Delta_{22}^{-1}[A_1, \bar\Psi_1, \Psi_1]$ in the effective action (2.46). The first line corresponds to the generic expansion (2.43), with "self-energy" insertions Π_{22}, as shown in Fig. 2.8. The second line contains some examples for diagrams generated when explicitly inserting the expression for Π_{22}.
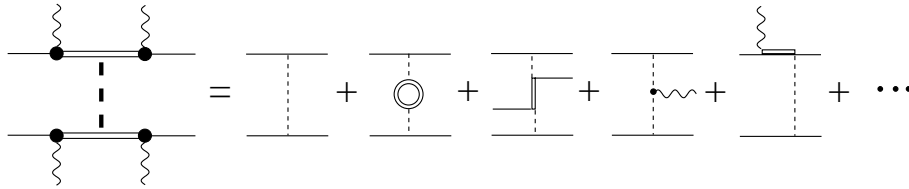
Figure 2.16: The term $\mathcal{J}_{\mathcal{B}}\Delta_{22}\mathcal{J}_{\mathcal{B}}$ in the effective action (2.46). The thick dashed line is a full hard gluon propagator, i.e., it has the expansion (2.43). The first diagram on the right-hand side of this figure results from the $n = 0$ term of this expansion, while the next three diagrams originate from the $n = 1$ term. Even a single insertion of a hard gluon "self-energy" Π_{22} gives rise to a variety of diagrams. Here, I only show the contributions corresponding to the first diagrams in Figs. 2.9, 2.10, and the three-gluon vertex. The last diagram arises from the second term of the expansion shown in Fig. 2.2.

2.2   Recovery of known effective theories

In this section I show that, for particular choices of the projectors $\mathcal{P}_{1,2}$ in Eq. (2.17), several well-known and at first sight unrelated effective theories for hot and/or dense quark matter are in fact nothing but special cases of the general effective theory defined by the action (2.46). These are the HTL/HDL effective action for quarks and gluons, and the high-density effective theory for cold, dense quark matter.

2.2.1   HTL/HDL effective action

Let us first focus on the HTL/HDL effective action. This action defines an effective theory for massless quarks and gluons with small momenta in a system at high temperature T (HTL), or large chemical potential μ (HDL). Consequently, the projectors $\mathcal{P}_{1,2}$ for quarks are given by

$$
\begin{aligned}
\mathcal{P}_1(K,Q) &= \Theta(\Lambda_{\mathrm{q}} - k)\,\delta^{(4)}_{K,Q}\,, & \text{(2.47a)} \\
\mathcal{P}_2(K,Q) &= \Theta(k - \Lambda_{\mathrm{q}})\,\delta^{(4)}_{K,Q}\,, & \text{(2.47b)}
\end{aligned}
$$

while the projectors for gluons are given by Eq. (2.35). (Note that, strictly speaking, the quarks and gluons of the HTL/HDL effective action should also have small energies in real time. Since the present effective action is defined in imaginary time, one should constrain the energy only at the end of a calculation, after analytically continuing the result to Minkowski space.)

The essential assumption to derive the HTL/HDL effective action is that there is a single momentum scale, $\Lambda_{\mathrm{q}} = \Lambda_{\mathrm{gl}} \equiv \Lambda$, which separates hard modes with momenta $\sim T$, or $\sim \mu$, from soft modes with momenta $\sim gT$, or $\sim g\mu$. In the presence of an additional energy scale T, or μ, naive perturbation theory in terms of powers of the coupling constant fails. It was shown by Braaten and Pisarski [7] that, for the n-gluon scattering amplitude the one-loop term, where n soft gluon legs are attached to a quark or gluon loop, is as important as the tree-level diagram. The same holds for the scattering of $n-2$ gluons and 2 quarks. At high T and small μ, the momenta of the quarks and gluons in the loop are of the order of the hard scale, $\sim T$. This gives rise to the name "Hard Thermal Loop" effective action, and allows to simplify the calculation of the respective diagrams. At large μ and small T, i.e., for the HDL effective action, the situation is somewhat more involved. As gluons do not have a Fermi surface, the only physical scale which determines the order of magnitude of a loop consisting exclusively of gluon propagators is the temperature. Therefore, at small T and large μ, such pure gluon loops are negligible. On the other hand, the momenta of quarks in the loop are $\sim \mu$. Thus, only loops with at least one quark line need to be considered in the HDL effective action.

In order to show that the HTL/HDL effective action is contained in the effective action (2.46), first note that a soft particle cannot become hard by interacting with another soft particle. This has the consequence that a soft quark cannot turn into a hard one by soft-gluon scattering. Therefore,

$$
g\mathcal{B}[A_1] \equiv g\mathcal{A}_{11}\,. \tag{2.48}
$$

Another consequence is that the last term in Eq. (2.46), $\mathcal{J}_{\mathcal{B}}\Delta_{22}\mathcal{J}_{\mathcal{B}}$, vanishes since $\mathcal{J}_{\mathcal{B}}$ is identical to a vertex between a soft quark and a hard gluon, which is kinematically forbidden. The

resulting action then reads

$$
\begin{aligned}
S_{\text{large}\,T/\mu}[A_1, \bar{\Psi}_1, \Psi_1] &\equiv S_A[A_1] + \frac{1}{2}\bar{\Psi}_1\left(\mathcal{G}_{0,11}^{-1} + g\mathcal{A}_{11}\right)\Psi_1 + \frac{1}{2}\operatorname{Tr}_q \ln \mathcal{G}_{22}^{-1}[A_1] \\
&\quad - \frac{1}{2}\operatorname{Tr}_g \ln \Delta_{22}^{-1}[A_1, \bar{\Psi}_1, \Psi_1] \ .
\end{aligned}
\tag{2.49}
$$

Using the expansion (2.29) one realizes that the term $\operatorname{Tr}_q \ln \mathcal{G}_{22}^{-1}$ generates all one-loop diagrams, where n soft gluon legs are attached to a hard quark loop. This is precisely the quark-loop contribution to the HTL/HDL effective action.

For hard gluons with momentum $\sim T$ or $\sim \mu$, the free inverse gluon propagator is $\Delta_{0,22}^{-1} \sim T^2$ or $\sim \mu^2$, while the contribution Π_{loop} to the hard gluon "self-energy" (2.40) is at most of the order $\sim g^2 T^2$ or $\sim g^2 \mu^2$. Consequently, Π_{loop} can be neglected and Π_{22} only contains tree-level diagrams, $\Pi_{22} \equiv \Pi_{\mathcal{B}} + \Pi_{\mathcal{V}}$. Using the expansion (2.43) of $\operatorname{Tr}_g \ln \Delta_{22}^{-1}$, the terms which contain only insertions of $\Pi_{\mathcal{V}}$ correspond to one-loop diagrams where n soft gluon legs are attached to a hard gluon loop. As was shown in Ref. [7], with the exception of the two-gluon amplitude, the loops with four-gluon vertices are suppressed. Neglecting these, one is precisely left with the pure gluon loop contribution to the HTL effective action. As discussed above, for the HDL effective action, this contribution is negligible.

The "self-energy" $\Pi_{\mathcal{B}}$ contains only two soft quark legs attached to a hard quark propagator (via emission and absorption of hard gluons). Consequently, in the expansion (2.43) of $\operatorname{Tr}_g \ln \Delta_{22}^{-1}$, the terms which contain insertions of $\Pi_{\mathcal{V}}$ and $\Pi_{\mathcal{B}}$ correspond to one-loop diagrams where an arbitrary number of soft quark and gluon legs is attached to the loop. It was shown in Ref. [7] that among these diagrams, only the ones with two soft quark legs and no four-gluon vertices are kinematically important and thus contribute to the HTL/HDL effective action. I have thus shown that this effective action, $S_{\text{HTL/HDL}}$, is contained in the effective action (2.49), and constitutes its leading contribution,

$$
S_{\text{large}\,T/\mu} = S_{\text{HTL/HDL}} + \text{higher orders} \ .
\tag{2.50}
$$

For the sake of completeness, let us briefly comment on possible ghost contributions. Ghost loops arise from the term $\operatorname{Tr}_{gh} \ln \mathcal{W}^{-1}$ in $S_A[A_1]$. Their topology and consequently their properties are completely analogous to those of the pure gluon loops discussed above.

I conclude with a remark regarding the HDL effective action. According to Eq. (2.47), at zero temperature and large chemical potential, a soft quark or antiquark has a momentum $k \sim g\mu$, i.e., it lies at the bottom of the Fermi sea, or at the top of the Dirac sea, respectively. These modes are, however, not that important in degenerate Fermi systems, because it requires a large amount of energy $k_0 \sim \mu$ to excite them. The truly relevant modes are quark modes with large momenta, $k \sim \mu$, close to the Fermi surface, because it costs little energy to excite them. A physically reasonable effective theory for cold, dense quark matter should therefore feature no antiquark modes at all, and only quark modes near the Fermi surface. Such a theory will be discussed in Sec. 2.2.2.

2.2.2 High-density effective theory

An effective theory for high-density quark matter was first proposed by Hong [100] and was further refined by Schäfer and others [102, 103, 104, 105]. In the construction of this effective

theory, one first proceeds similarly to the discussion in Sec. 2.1 and integrates out antiquark modes. (From a technical point of view, this is not done as in Sec. 2.1 by functional integration, but by employing the equations of motion for antiquarks. The result is equivalent.) On the other hand, at first all quark modes in the Fermi sea are considered as relevant. Consequently, in the notation of Sec. 2.1, the choice for the projectors $\mathcal{P}_{1,2}$ would be

$$\mathcal{P}_1(K,Q) = \begin{pmatrix} \Lambda_{\mathbf{k}}^+ & 0 \\ 0 & \Lambda_{\mathbf{k}}^- \end{pmatrix} \delta_{K,Q}^{(4)} \, , \tag{2.51a}$$

$$\mathcal{P}_2(K,Q) = \begin{pmatrix} \Lambda_{\mathbf{k}}^- & 0 \\ 0 & \Lambda_{\mathbf{k}}^+ \end{pmatrix} \delta_{K,Q}^{(4)} \, . \tag{2.51b}$$

Also, at first gluons are not separated into soft and hard modes either. After this step, the partition function of the theory assumes the form (2.1) with $\mathcal{Z}_q$ given by Eq. (2.24).

In the next step, one departs from the rigorous approach of integrating out modes, as done in Sec. 2.1, and follows the standard way of constructing an effective theory, as explained in the introduction. One focusses exclusively on quark modes close to the Fermi surface as well as on soft gluons. However, since quark modes far from the Fermi surface and hard gluons are not explicitly integrated out, the effective action does not automatically contain the terms which reflect the influence of these modes on the relevant quark and soft gluon degrees of freedom. Instead, the corresponding terms have to be written down "by hand" and the effective vertices have to be determined via matching to the underlying microscopic theory, i.e., QCD.

In order to further organize the terms occurring in the effective action, one covers the Fermi surface with "patches". Each patch is labelled according to the local Fermi velocity, $\mathbf{v}_F \equiv \hat{\mathbf{k}} \, k_F/\mu$ at its center. A patch is supposed to have a typical size $\Lambda_\parallel$ in radial ($\hat{\mathbf{k}}$) direction, and a size $\Lambda_\perp$ tangential to the Fermi surface. The momentum of quark modes inside a patch is decomposed into a large component in the direction of $\mathbf{v}_F$, the particular Fermi velocity labelling the patch under consideration, and a small residual component, $\mathbf{l}$, residing exclusively inside the patch,

$$\mathbf{k} = \mu \, \mathbf{v}_F + \mathbf{l} \, . \tag{2.52}$$

The residual component is further decomposed into a component pointing in radial direction, $\mathbf{l}_\parallel \equiv \mathbf{v}_F (\mathbf{v}_F \cdot \mathbf{l})$, and the orthogonal one, tangential to the Fermi surface, $\mathbf{l}_\perp \equiv \mathbf{l} - \mathbf{l}_\parallel$. The actual covering of the Fermi surface with such patches is not unique. One should, however, make sure that neighbouring patches do not overlap, in order to avoid double-counting of modes near the Fermi surface. In this case the total number of patches on the Fermi surface is $\sim \mu^2/\Lambda_\perp^2$.

In the following, I shall show that the action of the high-density effective theory as discussed in Refs. [100, 101, 102, 103, 104, 105] is contained in the effective action (2.46). To this end, however, I shall employ the choice (2.18) and (2.35) for the projectors for quark and gluon modes, and not Eq. (2.51) for the quark projectors. As in Refs. [100, 101, 102, 103, 104, 105], the quark mass will be set to zero, $m = 0$. One also has to clarify how the patches covering the Fermi surfaces introduced in Refs. [100, 101, 102, 103, 104, 105] arise within the effective action Eq. (2.46). It is obvious that the radial dimension $\Lambda_\parallel$ of a patch is related to the quark cut-off Λ_q. One simply chooses $\Lambda_\parallel \equiv \Lambda_q$. Similarly, since soft-gluon exchange is not supposed to move a fermion from a particular patch to another, the dimension $\Lambda_\perp$ tangential to the Fermi surface

must be related to the gluon cut-off Λ_{gl}. Again, one adheres to the most simple choice $\Lambda_\perp \equiv \Lambda_{\text{gl}}$. Since $\Lambda_{\text{gl}} \lesssim \mu$, this is consistent with the matching procedure discussed in Ref. [102], where the matching scale is chosen as $\Lambda_\perp = \sqrt{2}\mu$ (which is only slightly larger than μ). The different scales Λ_{q}, Λ_{gl}, and μ are illustrated in Fig. 2.17. The modulus of the residual momentum $\mathbf{l}$ in Eq. (2.52) is constrained to $l \leq \max(\Lambda_{\text{q}}, \Lambda_{\text{gl}})$.
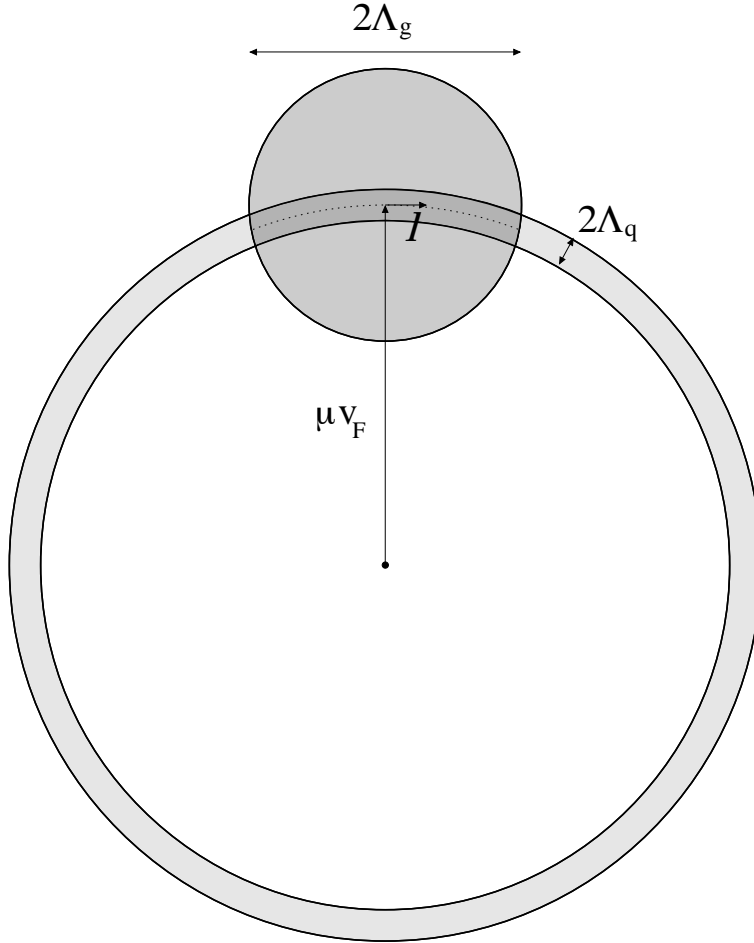
Figure 2.17: A particular patch covering the Fermi surface. The tangential dimension, $\Lambda_\perp$, is given by the maximum momentum transferred via a soft gluon, Λ_{gl}, while the radial dimension, $\Lambda_\parallel$ is defined by the maximum distance of relevant quark modes from the Fermi surface, Λ_{q}. Also shown is a typical momentum transfer $\mathbf{l}$ via a soft gluon.

In Nambu-Gor'kov space, the leading, kinetic term in the Lagrangian of the high-density effective theory reads

$$\mathcal{L}_{\text{kin}} = \frac{1}{2} \sum_{\mathbf{v}_F} \bar{\Psi}_1(X, \mathbf{v}_F) \gamma_0 \begin{pmatrix} iV \cdot D & 0 \\ 0 & i\bar{V} \cdot D_C \end{pmatrix} \Psi_1(X, \mathbf{v}_F) , \tag{2.53}$$

cf. for instance Eq. (1) of Ref. [103]. Here, the 4-vectors

$$V^\mu \equiv (1, \mathbf{v}_F) \quad , \quad \bar{V}^\mu \equiv (1, -\mathbf{v}_F) \tag{2.54}$$

are introduced. The covariant derivative for charge-conjugate fields is defined as $D_C^\mu \equiv \partial^\mu + igA_a^\mu T_a^T$. The contribution (2.53) arises from the term $\bar{\Psi}_1 \left(\mathcal{G}_{0,11}^{-1} + g\mathcal{A}_{11} \right) \Psi_1$ in Eq. (2.46). In order to see this, use $\mathcal{P}_1^2 \equiv \mathcal{P}_1$ to write

$$
\begin{aligned}
\frac{1}{2} \bar{\Psi}_1 \mathcal{G}_{0,11}^{-1} \Psi_1 &= \frac{1}{2} \bar{\Psi}_1 \gamma_0 \mathcal{P}_1 \gamma_0 \mathcal{G}_{0,11}^{-1} \mathcal{P}_1 \Psi_1 \\
&= \frac{1}{2} \sum_{K,Q} \bar{\Psi}_1(K)\gamma_0 \frac{1}{T} \begin{pmatrix} k_0 + \mu - k & 0 \\ 0 & k_0 - \mu + k \end{pmatrix} \delta_{K,Q}^{(4)} \Psi_1(Q) \\
&\simeq \frac{1}{2} \sum_{\mathbf{v}_F,L} \bar{\Psi}_1(L,\mathbf{v}_F)\gamma_0 \frac{1}{T} \begin{pmatrix} V \cdot L & 0 \\ 0 & \bar{V} \cdot L \end{pmatrix} \Psi_1(L,\mathbf{v}_F) .
\end{aligned}
\tag{2.55}
$$

In the last step, I have approximated $k \simeq \mu + \mathbf{v}_F \cdot \mathbf{l}$, which holds up to terms of order $O(l^2/\mu)$, cf. Eq. (2.52). This is a good approximation if the modulus of a typical residual quark momentum in the effective theory is $l \ll \max(\Lambda_q, \Lambda_{gl}) \lesssim \mu$. I have also introduced the 4-vector $L^\mu \equiv (k_0, \mathbf{l})$ and, applying the decomposition (2.52), I have written the sum over $\mathbf{k}$ as a double sum over $\mathbf{v}_F$ and $\mathbf{l}$. The latter sum runs over all residual momenta $\mathbf{l}$ inside a given patch, while the former runs over all patches. With this decomposition, the spinors $\bar{\Psi}_1$, Ψ_1 are defined locally on a given patch (labelled by the Fermi velocity $\mathbf{v}_F$), and depend on the 4-momentum L. Note that a Fourier transformation to coordinate space converts $V \cdot L \to iV \cdot \partial$.

Now consider the term $\bar{\Psi}_1 g\mathcal{A}_{11}\Psi_1$. Since $\mathcal{A}_{11}$ is not diagonal in momentum space, cf. Eq. (2.16), in principle the two quark spinors $\bar{\Psi}_1$, Ψ_1 can belong to different patches. However, I have chosen the tangential dimension of a patch such that a (typical) soft gluon can by definition never move a fermion across the border of a particular patch, $|\mathbf{k} - \mathbf{q}| \ll \Lambda_{gl}$. Therefore, both spinors reside in the same patch and, to leading order, $\hat{\mathbf{k}} \simeq \hat{\mathbf{q}} \simeq \mathbf{v}_F$. With these assumptions one may write $\Lambda_{\mathbf{k}}^- \slashed{A}_a(K-Q)\Lambda_{\mathbf{q}}^+ \simeq V \cdot A_a(K-Q)\gamma_0 \Lambda_{\mathbf{k}}^+$, $\Lambda_{\mathbf{k}}^+ \slashed{A}_a(K-Q)\Lambda_{\mathbf{q}}^- \simeq \bar{V} \cdot A_a(K-Q)\gamma_0 \Lambda_{\mathbf{k}}^-$. Then, introducing the residual momentum $\mathbf{l}'$ corresponding to the quark 3-momentum $\mathbf{q}$ and defining $L'^\mu \equiv (q_0, \mathbf{l}')$, the respective term in the effective action becomes

$$
\begin{aligned}
&\frac{1}{2} \bar{\Psi}_1 g\mathcal{A}_{11}\Psi_1 \simeq \\
&\frac{1}{2} \frac{g}{\sqrt{VT^3}} \sum_{\mathbf{v}_F,L,L'} \bar{\Psi}_1(L,\mathbf{v}_F)\gamma_0 \begin{pmatrix} V \cdot A_a(L-L')T_a & 0 \\ 0 & -\bar{V} \cdot A_a(L-L')T_a^T \end{pmatrix} \Psi_1(L',\mathbf{v}_F) .
\end{aligned}
\tag{2.56}
$$

In coordinate space, the sum of Eqs. (2.55) and (2.56) becomes Eq. (2.53).

Subleading terms of order $O(1/\mu)$ in the high-density effective theory are of the form

$$
\begin{aligned}
&\mathcal{L}_{O(1/\mu)} = \\
&-\frac{1}{2} \sum_{\mathbf{v}_F} \bar{\Psi}_1(X,\mathbf{v}_F)\gamma_0 \frac{1}{2\mu} \begin{pmatrix} D_\perp^2 - \frac{g}{2}\sigma^{\mu\nu}F_{\perp\mu\nu}^a T_a & 0 \\ 0 & -D_{C\perp}^2 - \frac{g}{2}\sigma^{\mu\nu}F_{\perp\mu\nu}^a T_a^T \end{pmatrix} \Psi_1(X,\mathbf{v}_F) ,
\end{aligned}
\tag{2.57}
$$

cf. Eq. (2) of Ref. [103]. Here, $D_\perp^\mu \equiv \{0, (\mathbf{1}-\mathbf{v}_F\mathbf{v}_F)\cdot\mathbf{D}\}$, and similarly for $D_{C\perp}^\mu$. The commutator of two gamma matrices is defined as usual, $\sigma^{\mu\nu} \equiv (i/2)[\gamma^\mu, \gamma^\nu]$, and $F_{\perp\mu\nu}^a T_a \equiv (i/g)[D_{\perp\mu}, D_{\perp\nu}]$.

As one will see in the following, this contribution arises from the term $-g^2\,\bar{\Psi}_1\,\mathcal{A}_{12}\,\mathcal{G}_{22}\,\mathcal{A}_{21}\,\Psi_1$ in Eq. (2.46).

First, note that, with the projectors (2.18), the irrelevant quark propagator $\mathcal{G}_{22}$ contains quark as well as antiquark modes. In order to derive Eq. (2.57), however, one has to discard the quark and keep only the antiquark modes. In essence, this is a consequence of the simpler choice (2.51) for the projectors $\mathcal{P}_{1,2}$ in the high-density effective theory of Refs. [100, 101, 102, 103, 104, 105]. In this case the propagator $\mathcal{G}_{22}$ may be simplified. A calculation quite similar to that of Eqs. (2.55) and (2.56) now leads (in coordinate space) to

$$\mathcal{G}_{22}^{-1} \equiv \mathcal{G}_{0,22}^{-1} + g\mathcal{A}_{22} \simeq \gamma_0\,\tau_3 \begin{pmatrix} 2\mu + i\bar{V}\cdot D & 0 \\ 0 & 2\mu - iV\cdot D_C \end{pmatrix}, \tag{2.58}$$

where τ_3 acts in Nambu-Gor'kov space. This result may be readily inverted to yield

$$\mathcal{G}_{22} \simeq \gamma_0\,\tau_3\,\frac{1}{2\mu}\sum_{n=0}^{\infty}\frac{1}{(2\mu)^n}\begin{pmatrix} -i\bar{V}\cdot D & 0 \\ 0 & iV\cdot D_C \end{pmatrix}^n. \tag{2.59}$$

Utilizing the projectors (2.51), one may also derive a simpler form for $g\mathcal{A}_{12}$ and $g\mathcal{A}_{21}$. Consider, for instance, the term $\bar{\Psi}_1\,g\mathcal{A}_{12}\,\Psi_2$. One follows the same steps that led to Eqs. (2.55), i.e., one assumes that the spinors $\bar{\Psi}_1$ and Ψ_2 reside in the same patch, such that $\hat{\mathbf{k}} \simeq \hat{\mathbf{q}} \simeq \mathbf{v}_F$. This allows to derive the identity $\Lambda_{\mathbf{k}}^{\mp}\,\slashed{A}^a(K-Q)\Lambda_{\mathbf{q}}^{\mp} \simeq \Lambda_{\mathbf{k}}^{\mp}\slashed{A}_{\perp}^a(K-Q)$, where $A_{\perp}^{\mu a} \equiv \{0,(\mathbf{1}-\mathbf{v}_F\mathbf{v}_F)\cdot\mathbf{A}^a\}$. Now introduce the 4-vectors L^μ, L'^μ, as in Eq. (2.56), which leads to

$$\frac{1}{2}\,\bar{\Psi}_1\,g\mathcal{A}_{12}\,\Psi_2 \simeq \frac{1}{2}\,\frac{g}{\sqrt{VT^3}}\sum_{\mathbf{v}_F,L,L'}\bar{\Psi}_1(L,\mathbf{v}_F)\begin{pmatrix} \slashed{A}_{\perp}^a(L-L')\,T_a & 0 \\ 0 & -\slashed{A}_{\perp}^a(L-L')\,T_a^T \end{pmatrix}\Psi_2(L',\mathbf{v}_F)\,. \tag{2.60}$$

One may add a term $\slashed{L}_\perp$ to the diagonal Nambu-Gor'kov components, which trivially vanishes between spinors $\bar{\Psi}_1$ and Ψ_2. This has the advantage that, in coordinate space,

$$g\mathcal{A}_{12} \simeq \begin{pmatrix} i\slashed{D}_\perp & 0 \\ 0 & i\slashed{D}_{C\perp} \end{pmatrix}, \tag{2.61}$$

i.e., this term transforms covariantly under gauge transformations, and no longer as a gauge field. A similar calculation for $g\mathcal{A}_{21}$ gives the result $g\mathcal{A}_{21} \equiv g\mathcal{A}_{12}$. Combining Eqs. (2.59) and (2.61), the term $-g^2\,\bar{\Psi}_1\,\mathcal{A}_{12}\,\mathcal{G}_{22}\,\mathcal{A}_{21}\,\Psi_1$ corresponds to the following contribution in the Lagrangian,

$$-\frac{1}{2}\sum_{\mathbf{v}_F}\bar{\Psi}_1(X,\mathbf{v}_F)\gamma_0\begin{pmatrix} \slashed{D}_\perp & 0 \\ 0 & -\slashed{D}_{C\perp} \end{pmatrix}\frac{1}{2\mu}\sum_{n=0}^{\infty}\frac{1}{(2\mu)^n}\begin{pmatrix} -i\bar{V}\cdot D & 0 \\ 0 & iV\cdot D_C \end{pmatrix}^n\begin{pmatrix} \slashed{D}_\perp & 0 \\ 0 & \slashed{D}_{C\perp} \end{pmatrix}$$
$$\times\Psi_1(X,\mathbf{v}_F)\,. \tag{2.62}$$

Taking only the $n=0$ term, and utilizing $\gamma^\mu\gamma^\nu \equiv g^{\mu\nu} - i\sigma^{\mu\nu}$, one arrives at Eq. (2.57). Note that my definition for transverse quantities, e.g. $A_\perp^\mu \equiv \{0,(\mathbf{1}-\mathbf{v}_F\mathbf{v}_F)\cdot\mathbf{A}\}$, slightly differs from that of Refs. [100, 101], where $A_\perp^\mu \equiv A^\mu - V^\mu V\cdot A$. However, both definitions agree when sandwiched between spinors $\bar{\Psi}_{1,2}$ and $\Psi_{2,1}$.

At order $O(1/\mu^2)$, besides the $n = 1$ term in Eq. (2.62), there are also four-fermion interaction terms, cf. Eqs. (3-5) of Ref. [103]. In the effective action (2.46), these contributions arise from the term $\mathcal{J}_\mathcal{B} \Delta_{22} \mathcal{J}_\mathcal{B}$ which originates from integrating out hard gluons. (Since this is not done explicitly in the construction of the high-density effective theory in Refs. [100, 101, 102, 103, 104, 105], this term is not automatically generated, but has to be added "by hand".) To leading order, this term corresponds to the exchange of a hard gluon between two quarks, cf. the first diagram on the right-hand side of Fig. 2.16. If the quarks are close to the Fermi surface, the energy in the hard gluon propagator can be neglected, and $\Delta_{0,22} \lesssim 1/\Lambda_{\rm gl}^2$. Since $1/\Lambda_{\rm gl}^2 \gtrsim 1/\mu^2$, the contribution from hard-gluon exchange is of order $O(1/\mu^2)$. Four-fermion interactions also receive corrections at one-loop order, cf. Fig. 5 of Ref. [101]. In Eq. (2.46), they are contained in the term $\mathrm{Tr}\ln \Delta_{22}^{-1}$, see the last diagram in Fig. 2.15.

Besides the quark terms in the Lagrangian of the high-density effective theory [100, 101, 102, 103, 104, 105], there are also contributions from gluons. The first is the standard Yang-Mills Lagrangian $-(1/4)F_{\mu\nu}^a F_a^{\mu\nu}$, cf. Eq. (1) of Ref. [103]. This part is contained in the term $S_A[A_1]$ in Eq. (2.46), cf. Eq. (2.2). The second contribution is a mass term for magnetic gluons,

$$\mathcal{L}_{m_g} = -\frac{m_g^2}{2}\,\mathbf{A}^a \cdot \mathbf{A}^a\,, \tag{2.63}$$

cf. Eq. (19) of Ref. [118], Eq. (18) of Ref. [101], or Eq. (27) of Ref. [102], where m_g is the gluon mass parameter (1.39). This term has to be added "by hand" in order to obtain the correct value for the HDL gluon polarization tensor within the high-density effective theory. In Eq. (2.46) this contribution arises from the $n = 2$ term of the expansion (2.29) of $\mathrm{Tr}\ln \mathcal{G}_{22}^{-1}$. The gluon polarization tensor has contributions from particle-hole and particle-antiparticle excitations. The latter give rise to $\mathcal{L}_{m_g}$. While this term arises naturally within my derivation of the effective theory, it does not in the high-density effective theory of Refs. [100, 101, 102, 103, 104, 105] because only antiquarks, but not irrelevant quark modes, are explicitly integrated out. Irrelevant quark modes can then only be taken into account by adding the appropriate counter terms.

Sometimes, the full HDL action is added to the Lagrangian of the high-density effective theory, cf. Eq. (8) of Ref. [103]. This procedure requires a word of caution. For instance, an important contribution to the HDL polarization tensor arises from particle-hole excitations around the Fermi surface. Such excitations are still relevant degrees of freedom in the effective theory. However, in order for them to appear in the gluon polarization tensor they would first have to be integrated out. Therefore, strictly speaking such contributions cannot occur in the tree-level effective action. Of course, in an effective theory one is free to add whatever contributions one deems necessary. However, one has to be careful to avoid double counting. As will be shown in Sec. 3.1, the full HDL polarization tensor will appear quite naturally in an approximate solution to the Dyson-Schwinger equation for the gluon propagator, however, not at tree-, but only at (one-)loop level.

It was claimed in Refs. [101, 102, 103] that a consistent power-counting scheme within the high-density effective theory requires $\Lambda_\perp = \Lambda_\parallel$. In contrast, I shall show in Sec. 3.1 that a computation of the gap parameter to subleading order requires $\Lambda_{\rm q} \equiv \Lambda_\parallel \ll \Lambda_\perp \equiv \Lambda_{\rm gl}$. This means that irrelevant quark modes become local on a scale $l_q \gg 1/\Lambda_{\rm q}$, while antiquark modes become local already on a much smaller scale, $l_{\bar{q}} \gg 1/\mu$, cf. discussion at the end of Sec. 2.1. As mentioned in the introduction, for two different scales power counting of terms in the

effective action becomes a non-trivial problem. While the high-density effective theory of Refs. [100, 101, 102, 103, 104, 105] contains effects from integrating out antiquarks, i.e., from the scale $1/\mu$, the effective action (2.46) in addition keeps track of the influence of irrelevant quark modes, i.e., from physics on the scale $1/\Lambda_{\mathrm{q}} \gg 1/\mu$. Since all terms in the effective action (2.46) are kept, one can be certain not to miss any important contribution just because the naive dimensional power-counting scheme is invalidated by the occurrence of two vastly different length scales.

2.3   Towards a general effective *Theory*

As explained in Sec. 1.3, the calculation of any physical quantity within the framework of an effective theory requires the knowledge of the orders of magnitude of the operators in the action of the effective theory. Only after having determined all operators needed for the desired accuracy the actual calculation can be performed [107, 108, 109]. Therefore, in principle, *all* operators in the general effective action (2.42) yet await to be power-counted. This complete analysis is beyond the scope of this work and remains a formidable future project.

In the following, however, I take a first step towards this goal and begin with the class of quark loops that appear in the effective action after integrating out irrelevant quarks in the case of large μ and small T, cf. Eq. (2.46) and Fig. 2.14.

2.3.1   Power counting quark loops at large μ and small T

In [7] the power-counting rules for HTL/HDL were generally derived. Following this analysis, analogous rules are set up for loops of irrelevant quark modes at large μ and small T. However, I choose the projection operators (2.18) instead to the HTL/HDL projection operators (2.47). Consequently, the internal *irrelevant* quark modes in the considered loops are antiquarks and quarks far from the Fermi surface with $|k - \mu| \geq \Lambda_{\mathrm{q}}$. The typical momenta of *relevant* quark modes are located much closer to the Fermi surface, $|k - \mu| \sim \Lambda_{\mathrm{q}}^{n} \ll \Lambda_{\mathrm{q}} \ll \mu$, where the upper index n abbreviates *near* to the Fermi surface. These *near* modes can be considered as the natural choice for the relevant degrees of freedom of a low-energy effective theory at large μ and small T (in contrast to the low-momentum modes of the HDL theory, cf. the short discussion at the end of Sec. 2.2.1). Therefore, a careful analysis of such loops seems worthwhile.

The cutoff for *hard* gluons may be choosen as $\Lambda_{\mathrm{gl}} \lesssim \mu$, while the *soft* gluon modes in the effective action have typical momenta of order $\Lambda_{\mathrm{gl}}^{s} \ll \Lambda_{\mathrm{gl}}$, cf. Fig. 2.17. It is clear from the outset that for $\Lambda_{\mathrm{gl}}^{s} \lesssim g\,\mu$ and $\Lambda_{\mathrm{q}} \to 0$ the considered loops must reproduce the corresponding HDLs discussed in Sec. 2.2.1. Then, however, all quarks are integrated out and one ends up with a pure gauge theory for gluons. It would be more intriguing to keep a thin layer of quark modes around the Fermi surface as explicit degrees of freedom. If one chooses Λ_{q} sufficiently smaller than Λ_{gl} the difference between the considered loops and the HDLs will become arbitrarily small.

An interesting ordering for all these scales could be

$$\phi \sim \Lambda_{\mathrm{q}}^{n} \ll \Lambda_{\mathrm{q}} = \phi^{y} M^{1-y} \ll \Lambda_{\mathrm{gl}}^{s} \ll \Lambda_{\mathrm{gl}} \lesssim \mu \, , \tag{2.64}$$

where $1 \gtrsim y \gg g$ and $M^2 \equiv (3\pi/4)\, m_g^2$, cf. Sec. 3.2.2. Soft gluons being exchanged among relevant quarks would then have energies of order ϕ. For the momentum scale $\Lambda_{\mathrm{gl}}^{s} = \phi^{1/3} M^{2/3}$

these gluons would feel the effect of Landau damping [7, 9]. For the choice $y = 2/3$ the condition $\Lambda_q \ll \Lambda_g^s$ is fulfilled. Then the considered loops of irrelevant quark modes would contain Landau damping already on the tree-level of the effective action. On the other hand, the effect of the Meissner masses would be suppressed by a factor $\phi/p \sim (\phi/M)^{2/3} \ll 1$ compared to the non-colorsuperconducting contributions in the loops (at least in the case of two external gluons) [63, 110].

For $T \gtrsim T_c$ one could use this theory for the investigation of precursory effects before the actual onset of Cooper pairing. In the strong coupling regime at $\mu \lesssim 500$ MeV numerical calculations based on the NJL-model (all gluons integrated out) showed the occurrence of low-energy collective modes in the form of strong diquark fluctuations with momenta close to the Fermi surface [111, 112]. This is in agreement with the weak coupling analysis in [113] where, after extrapolating down to $\mu \lesssim 500$ MeV, it was argued that color superconductivity could be a type-II superconductor with a second-order phase transition and strong pair fluctuations at intermediate baryonic densities. On the other hand, at asymptotically large densities in weak coupling gauge field fluctuations are found to dominate and drive the CSC transition first-order [35, 114, 115, 116]. The effective theory with the two different cutoffs proposed above might be useful in describing these fluctuations and estimating the relative order of magnitude of the diquark and the gauge field fluctuations.

The effect of the gap in the loops of irrelevant quarks certainly would have to be incorporated for $\Lambda_{gl}^s \sim \phi$. This would require the introduction of a bilocal source term for irrelevant quark modes, cf. Sec. 3.1.1, leading to non-trivial off-diagonal entries in Nambu-Gor'kov space and mixing quarks with charge-conjugate quarks. In the following, however, charge-conjugated quarks will not be used for simplicity.

The quark propagator in the mixed representation

The free propagator of massless quarks at chemical potential μ and temperature T is given by [124]

$$\tilde{G}_0(K) = \sum_{e=\pm} \Lambda_{\mathbf{k}}^e \gamma_0 \frac{k_0 - (\mu - ek)}{k_0^2 - [\epsilon_{\mathbf{k}}^e]^2} \tag{2.65}$$

where $\epsilon_{\mathbf{k}}^e \equiv |\mu - ek|$ and the projectors on positive ($e = +$) and negative ($e = -$) energy states defined as $\Lambda_{\mathbf{k}}^e \equiv \frac{1}{2}\left(1 + e\gamma_0\boldsymbol{\gamma}\cdot\hat{\mathbf{k}}\right)$. Furthermore, $k_0 \equiv -i\omega_n$ with the fermionic Matsubara frequency $\omega_n = (2n + 1)\pi T$. For the evaluation of the Matsubara sum in the loop it is advantageous [119] to use the propagators in their mixed representation

$$\tilde{G}_0(\tau, \mathbf{k}) \equiv T\sum_{k_0} e^{-k_0\tau}\tilde{G}_0(K) \,. \tag{2.66}$$

After performing the Matsubara sum in Eq. (2.66) in terms of a contour integral in the complex k_0-plane, one obtains for the range $0 \leq \tau \leq \beta$ [124]

$$\tilde{G}_0(\tau, \mathbf{k}) = -\sum_{e=\pm} \Lambda_{\mathbf{k}}^e \gamma_0 \left\{\Theta(ek - \mu)\left[1 - N(\epsilon_{\mathbf{k}}^e)\right]e^{-\epsilon_{\mathbf{k}}^e\tau} + \Theta(\mu - ek)N(\epsilon_{\mathbf{k}}^e)e^{\epsilon_{\mathbf{k}}^e\tau}\right\} \tag{2.67}$$

$$= -\sum_{e,s=\pm} \Lambda_{\mathbf{k}}^e \gamma_0 \Theta(s[ek - \mu])\tilde{f}_s(\epsilon_{\mathbf{k}}^e)e^{-s\epsilon_{\mathbf{k}}^e\tau} \,, \tag{2.68}$$

where $N(x) \equiv (e^{x/T} + 1)^{-1}$ is the thermal distribution function for fermions. For the actual power counting the replacement

$$\Theta(s[k - \mu]) \;\to\; \Theta(s[k - \mu] - \Lambda_q) \equiv \Theta_s^{\Lambda_q} \tag{2.69}$$

will be necessary. Before that, however, the form given by Eq. (2.68) may be kept to simplify the comparison with known results. Moreover, for the following calculations it is very convenient to introduce

$$\tilde{f}_s(\epsilon_{\mathbf{k}}^e) \equiv \Theta(s) - sN(\epsilon_{\mathbf{k}}^e) , \qquad s = \pm . \tag{2.70}$$

In the following, the more compact notations

$$\tilde{f}_s^e \;\equiv\; \tilde{f}_s(\epsilon_{\mathbf{k}}^e) , \tag{2.71a}$$
$$\epsilon_i \;\equiv\; \epsilon_{\mathbf{k}_i}^{e_i} = |\mu - e_i k_i| \tag{2.71b}$$
$$\Theta_s^e \;\equiv\; \Theta(s[ek - \mu]) \tag{2.71c}$$

are used. The $\tilde{f}_s^e$'s obey the following relations

$$\tilde{f}_s^e + \tilde{f}_{-s}^e \;=\; 1 , \tag{2.72}$$
$$\tilde{f}_{-s}^e \;=\; \tilde{f}_s^e \, e^{-s\epsilon_{\mathbf{k}}^e \beta} , \tag{2.73}$$
$$\tilde{f}_{-s_1}^{e_1} \tilde{f}_{s_2}^{e_2} - \tilde{f}_{s_1}^{e_1} \tilde{f}_{-s_2}^{e_2} \;=\; \frac{s_2 - s_1}{2} + s_1 N(\epsilon_1) - s_2 N(\epsilon_2) . \tag{2.74}$$

While e discriminates positive from negative energy states (quarks from antiquarks), the sign s defines the direction of the evolution in imaginary time τ (appearing in the exponent $e^{-s\epsilon_{\mathbf{k}}^e \tau}$ in the propagator): $s = +$ denotes propagation forward and $s = -$ backwards in imaginary time. Simultaneously, for modes with positive energies ($e = +$), s also splits the momentum space in one part above ($s = +$) and one below ($s = -$) the Fermi surface via $\Theta_s^+ = \Theta(s[k - \mu])$. Hence, positive energy modes above the Fermi surface always propagate forward in imaginary time, whereas those below always propagate backwards. For antiquarks, however, one finds

$$\Theta_s^- \equiv \Theta(-s) , \tag{2.75}$$

which means that negative energy modes always propagate backwards in imaginary time independently of their momentum.

Furthermore, $\tilde{f}_-^+ = N(\epsilon_{\mathbf{k}}^+)$ is the *minimum* of the thermal distribution functions of quarks and quark-holes, whereas $\tilde{f}_+^+ = \exp(|k - \mu|\beta)\, N(\epsilon_{\mathbf{k}}^+)$ corresponds to their *maximum*. Moreover, $\tilde{f}_-^- = N(\epsilon_{\mathbf{k}}^-) \simeq \exp[-(k + \mu)\beta]$ is the thermal distribution of antiquarks (exponentially suppressed) and $\tilde{f}_+^- = \exp[-(k + \mu)\beta] N(\epsilon_{\mathbf{k}}^-) \simeq 1$ that of anti-quarkholes (abundant), respectively. Eq. (2.72) reflects the normalisation of $\tilde{f}_{\pm}^e$, i.e. every state with positive (negative) energy and momentum k is occupied, either by a(n) (anti-)quark or a(n) (anti-)quarkhole.

In the range $-\beta \leq \tau \leq 0$ one obtains similarly

$$\tilde{G}_0(\tau, \mathbf{k}) \;=\; \sum_{e,s=\pm} \Lambda_{\mathbf{k}}^e \gamma_0 \Theta_s^e \tilde{f}_{-s}^e e^{-s\epsilon_{\mathbf{k}}^e \tau} , \tag{2.76}$$

and therefore, for the whole range $-\beta \leq \tau \leq \beta$

$$\tilde{G}_0(\tau, \mathbf{k}) = -\text{sign}(\tau) \sum_{e,s=\pm} \Lambda_{\mathbf{k}}^e \gamma_0 \Theta_s^e \tilde{f}_{\text{sign}(\tau)s}^e e^{-s\epsilon_{\mathbf{k}}^e \tau} . \tag{2.77}$$

If $-\beta \leq \tau \leq \beta$ and $-\beta \leq \tau \pm \beta \leq \beta$ are fulfilled, it follows with $\text{sign}(\tau \pm \beta) = \pm = -\text{sign}(\tau)$

$$\begin{aligned}
\tilde{G}_0(\tau \pm \beta, \mathbf{k}) &= \text{sign}(\tau \pm \beta) \sum_{e,s=\pm} \Lambda_{\mathbf{k}}^e \gamma_0 \Theta_s^e \tilde{f}_{\text{sign}(\tau \pm \beta)s}^e e^{-s\epsilon_{\mathbf{k}}^e(\tau \pm \beta)} \\
&= -\text{sign}(\tau) \sum_{e,s=\pm} \Lambda_{\mathbf{k}}^e \gamma_0 \Theta_s^e \tilde{f}_{-\text{sign}(\tau)s}^e e^{\text{sign}(\tau)\epsilon_{\mathbf{k}}^e \beta} e^{-s\epsilon_{\mathbf{k}}^e \tau} \\
&= -\text{sign}(\tau) \sum_{e,s=\pm} \Lambda_{\mathbf{k}}^e \gamma_0 \Theta_s^e \tilde{f}_{\text{sign}(\tau)s}^e e^{-s\epsilon_{\mathbf{k}}^e \tau} \\
&= -\tilde{G}_0(\tau, \mathbf{k}) .
\end{aligned} \tag{2.78}$$

Hence, as generally required, the mixed quark propagator $\tilde{G}_0(\tau, \mathbf{k})$ is antiperiodic with period β within its range of definition.

The 4-momentum dependent part of the considered quark loops has the general form

$$\begin{aligned}
\mathcal{J}^{\boldsymbol{\mu}}(P_1, \cdots, P_N) &= (-1)^{N+1} \frac{T}{V} \sum_K \text{Tr}_s \gamma^{\mu_1} \tilde{G}_0(K_1) \gamma^{\mu_2} \tilde{G}_0(K_2) \cdots \gamma^{\mu_N} \tilde{G}_0(K_N) \\
&= (-1)^{N+1} \int \frac{d^3\mathbf{k}}{(2\pi)^3} T \sum_{k^0} \text{Tr}_s \prod_{i=1}^N \gamma^{\mu_i} \tilde{G}_0(K_i) ,
\end{aligned} \tag{2.79}$$

where $\boldsymbol{\mu} \equiv (\mu_1, \cdots \mu_N)$ and $K_i \equiv K + P_i$. The prefactor $(-1)^{N+1}$ comes from the Feynman rule to take $-\tilde{G}_0$ as the internal quark propagator and to write an overall (-1) in front of each quark loop. The momenta of the external gluons are given by $P_{i+1} - P_i$ with $P_{N+1} = P_1$. With the inverse form of Eq. (2.66)

$$\tilde{G}_0(K) = \int_0^\beta d\tau e^{k^0 \tau} \tilde{G}_0(\tau, k) \tag{2.80}$$

it follows

$$\begin{aligned}
\mathcal{J}^{\boldsymbol{\mu}}(P_1, \cdots, P_N) &= (-1)^{N+1} \int \frac{d^3\mathbf{k}}{(2\pi)^3} T \sum_{k^0} \text{Tr}_s \prod_{i=1}^N \gamma^{\mu_i} \int_0^\beta d\tau_i e^{k_i^0 \tau_i} \tilde{G}_0(\tau_i, k_i) \\
&= (-1)^{N+1} \int \frac{d^3\mathbf{k}}{(2\pi)^3} \text{Tr}_s \prod_{i=1}^N \gamma^{\mu_i} \int_0^\beta d\tau_i e^{p_i^0 \tau_i} \tilde{G}_0(\tau_i, k_i) T \sum_{k^0} e^{k^0 \sum_{j=1}^N \tau_j} .
\end{aligned} \tag{2.81}$$

With the relation [9]

$$T \sum_{k^0} \exp\left(k^0 \sum_{i=1}^N \tau_i\right) = \sum_{m=-\infty}^\infty (-1)^m \delta\left(m\beta - \sum_{i=1}^N \tau_i\right) \tag{2.82}$$

one can perform the integral over one of the τ's trivially, say over τ_N. The fact that in the integrals $0 \leq \tau_i \leq \beta$ leads to

$$0 \leq \tau_N = m\beta - \sum_{i=1}^{N-1} \tau_i \leq \beta \tag{2.83}$$

and consequently the sum over m runs from 1 to $N-1$ only. Using $e^{p_i m\beta} = 1$ the integration over τ_N yields

$$
\begin{aligned}
\mathcal{J}^{\boldsymbol{\mu}}(P_1, \cdots, P_N) &= \\
&= (-1)^{N+1} \int \frac{d^3\mathbf{k}}{(2\pi)^3} \mathrm{Tr}_s \prod_{i=1}^{N-1} \left[\gamma^{\mu_i} \int_0^\beta d\tau_i e^{(p_i^0 - p_N^0)\tau_i} \tilde{G}_0(\tau_i, \mathbf{k}_i) \right] \gamma^{\mu_N} \\
&\quad \times \sum_{m=1}^{N-1} (-1)^m \tilde{G}_0 \left(m\beta - \sum_{j=1}^{N-1} \tau_j, \mathbf{k}_N \right) \Theta\left(m\beta - \sum_{j=1}^{N-1} \tau_j \right) \Theta\left(\sum_{j=1}^{N-1} \tau_j - (m-1)\beta \right) \\
&= -\int \frac{d^3\mathbf{k}}{(2\pi)^3} \sum_{\mathbf{e},\boldsymbol{s}} \mathcal{T}_{\mathbf{e}}^{\boldsymbol{\mu}} \Theta_{\boldsymbol{s}}^{\mathbf{e}} \sum_{m=1}^{N-1} (-1)^m \prod_{i=1}^{N-1} \left[\int_0^\beta d\tau_i \tilde{f}_{s_i}^{e_i} e^{(p_i^0 - p_N^0 - s_i\epsilon_i)\tau_i} \right] \times \\
&\quad \times \tilde{f}_{s_N}^{e_N} e^{-s_N \epsilon_N \left(m\beta - \sum_{j=1}^{N-1} \tau_j \right)} \Theta\left(m\beta - \sum_{j=1}^{N-1} \tau_j \right) \Theta\left(\sum_{j=1}^{N-1} \tau_j - (m-1)\beta \right) \\
&= -\int \frac{d^3\mathbf{k}}{(2\pi)^3} \sum_{\mathbf{e},\boldsymbol{s}} \mathcal{T}_{\mathbf{e}}^{\boldsymbol{\mu}} \Theta_{\boldsymbol{s}}^{\mathbf{e}} \sum_{m=1}^{N-1} (-1)^m \prod_{i=1}^{N-1} \left[\int_0^\beta d\tau_i \tilde{f}_{s_i}^{e_i} e^{\Omega_i \tau_i} \right] \times \\
&\quad \times \tilde{f}_{s_N}^{e_N} e^{-s_N \epsilon_N m\beta} \Theta\left(m\beta - \sum_{j=1}^{N-1} \tau_j \right) \Theta\left(\sum_{j=1}^{N-1} \tau_j - (m-1)\beta \right) ,
\end{aligned} \tag{2.84}
$$

where $\boldsymbol{s} \equiv (s_1, \cdots, s_N)$ and $\mathbf{e} \equiv (e_1, \cdots, e_N)$, as well as

$$\mathcal{T}_{\mathbf{e}}^{\mu_1 \cdots \mu_N} \equiv \mathrm{Tr}_s \left[\prod_{j=1}^N \gamma^{\mu_j} \Lambda_{\mathbf{k}_j}^{e_j} \gamma_0 \right] , \tag{2.85}$$

$$\Omega_i \equiv p_i^0 - p_N^0 - s_i\epsilon_i + s_N\epsilon_N , \tag{2.86}$$

$$\Theta_{\boldsymbol{s}}^{\mathbf{e}} \equiv \prod_{i=1}^N \Theta_{s_i}^{e_i} \tag{2.87}$$

are introduced. In the simplest case of two external gluons one has only $m = 1$ and therefore

$$
\begin{aligned}
\mathcal{J}^{\mu_1\mu_2}(P_1, P_2) &= \int \frac{d^3\mathbf{k}}{(2\pi)^3} \sum_{\mathbf{e},\boldsymbol{s}} \mathcal{T}_{\mathbf{e}}^{\mu_1\mu_2} \Theta_{\boldsymbol{s}}^{\mathbf{e}} \int_0^\beta d\tau_1 \tilde{f}_{s_1}^{e_1} e^{\Omega_1 \tau_1} \tilde{f}_{s_2}^{e_2} e^{-s_2\epsilon_2\beta} \\
&= \int \frac{d^3\mathbf{k}}{(2\pi)^3} \sum_{\mathbf{e},\boldsymbol{s}} \mathcal{T}_{\mathbf{e}}^{\mu_1\mu_2} \Theta_{\boldsymbol{s}}^{\mathbf{e}} \int_0^\beta d\tau_1 \tilde{f}_{s_1}^{e_1} \tilde{f}_{-s_2}^{e_2} e^{\Omega_1 \tau_1}
\end{aligned}
$$

$$
= \int \frac{d^3\mathbf{k}}{(2\pi)^3} \sum_{\mathbf{e},\mathbf{s}} \mathcal{T}_{\mathbf{e}}^{\mu_1\mu_2} \Theta_{\mathbf{s}}^{\mathbf{e}} \frac{\tilde{f}_{-s_1}^{e_1} \tilde{f}_{s_2}^{e_2} - \tilde{f}_{s_1}^{e_1} \tilde{f}_{-s_2}^{e_2}}{\Omega_1}
$$

$$
= \int \frac{d^3\mathbf{k}}{(2\pi)^3} \sum_{\mathbf{e},\mathbf{s}} \mathcal{T}_{\mathbf{e}}^{\mu_1\mu_2} \Theta_{\mathbf{s}}^{\mathbf{e}} \frac{\frac{s_2-s_1}{2} + s_1 N(\epsilon_1) - s_2 N(\epsilon_2)}{p_1^0 - p_2^0 - s_1\epsilon_1 + s_2\epsilon_2} , \tag{2.88}
$$

The above Eq. (2.88) is in accordance with the standard result for two external gluon fields Eq.(40) in [124]. In order to simplify power counting arguments the energy with respect to the Fermi surface is introduced

$$
E^e \equiv k - e\mu \tag{2.89}
$$

Since $\Theta_s^e \equiv \Theta(s[ek - \mu]) = \Theta(seE^e)$ one has $s = \text{sign}(eE^e)$. Furthermore, $\epsilon_{\mathbf{k}}^e \equiv |\mu - ek| = |eE^e|$ and therefore $s\epsilon = eE^e = ek - \mu$. So, in the denominators one can substitute

$$
-s_1\epsilon_1 + s_2\epsilon_2 = -e_1 k_1 + e_2 k_2 \tag{2.90}
$$

and obtains a form, which is suitable for a power-counting analysis

$$
\mathcal{J}^{\mu_1\mu_2}(P_1, P_2) = \int \frac{d^3\mathbf{k}}{(2\pi)^3} \sum_{\mathbf{e},\mathbf{s}} \mathcal{T}_{\mathbf{e}}^{\mu_1\mu_2} \Theta_{\mathbf{s}}^{\mathbf{e}} \frac{\frac{s_2-s_1}{2} + s_1 N(\epsilon_1) - s_2 N(\epsilon_2)}{p_1^0 - p_2^0 - e_1 k_1 + e_2 k_2} . \tag{2.91}
$$

To recover a more familiar form one rewrites the numerators as

$$
\frac{s_2 - s_1}{2} + s_1 N(\epsilon_1) - s_2 N(\epsilon_2) = \frac{e_2 - e_1}{2} + e_1 N(E^{e_1}) - e_2 N(E^{e_2}) \tag{2.92}
$$

and finds after performing the sum over $\mathbf{s}$

$$
\mathcal{J}^{\mu_1\mu_2}(P_1, P_2) = \int \frac{d^3\mathbf{k}}{(2\pi)^3} \sum_{\mathbf{e}} \mathcal{T}_{\mathbf{e}}^{\mu_1\mu_2} \frac{\frac{e_2-e_1}{2} + e_1 N(E^{e_1}) - e_2 N(E^{e_2})}{p_1^0 - p_2^0 - e_1 k_1 + e_2 k_2} , \tag{2.93}
$$

which is in accordance with the standard result Eq.(44) in [124]. It is also in agreement with Eq.(5.77) in [9]. Moreover, in the limit $\mu \to 0$ it reproduces the corresponding formular (A.11) in [7] using

$$
\lim_{\mu\to 0} \Theta_{\mathbf{s}}^{\mathbf{e}} = \delta_{\mathbf{s},\mathbf{e}} = \prod_{i=1}^{N} \delta_{s_i,e_i} . \tag{2.94}
$$

In the cases of $N = 3$ and 4 one obtains after rather lengthy calculations, cf. Sec. A, Eqs. (A.4) and (A.8)

$$
\mathcal{J}^{\mu_1\mu_2\mu_3}(P_1, P_2, P_3) = -\int \frac{d^3\mathbf{k}}{(2\pi)^3} \sum_{\mathbf{e},\mathbf{s}} \mathcal{T}_{\mathbf{e}}^{\mu_1\mu_2\mu_3} \Theta_{\mathbf{s}}^{\mathbf{e}} \frac{1}{p_2^0 - p_3^0 - e_2 k_2 + e_3 k_3} \times
$$

$$
\times \left[\frac{\frac{s_3-s_1}{2} + s_1 N(\epsilon_1) - s_3 N(\epsilon_3)}{p_1^0 - p_3^0 - e_1 k_1 + s_3 k_3} - \frac{\frac{s_2-s_1}{2} + s_1 N(\epsilon_1) - s_2 N(\epsilon_2)}{p_1^0 - p_2^0 - e_1 k_1 + e_2 k_2} \right]
$$

$$
\tag{2.95}
$$

and

$$
\begin{aligned}
&\mathcal{J}^{\mu_1\cdots\mu_4}(P_1,\cdots,P_4) = \\
&= -\int \frac{d^3\mathbf{k}}{(2\pi)^3}\sum_{\mathbf{e},\mathbf{s}}\mathcal{T}_{\mathbf{e}}^{\mu_1\cdots\mu_4}\Theta_{\mathbf{s}}^{\mathbf{e}}\frac{1}{p_3^0-p_4^0-e_3k_3+e_4k_4}\times \\
&\quad \left\{\frac{1}{p_2^0-p_4^0-e_2k_2+e_4k_4}\left[\frac{\frac{s_2-s_1}{2}+s_1N(\epsilon_1)-s_2N(\epsilon_2)}{p_1^0-p_2^0-e_1k_1+e_2k_2}-\frac{\frac{s_4-s_1}{2}+s_1N(\epsilon_1)-s_4N(\epsilon_4)}{p_1^0-p_4^0-e_1k_1+e_4k_4}\right]+ \right. \\
&\quad \left. +\frac{1}{p_2^0-p_3^0-s_2\epsilon_2+s_3\epsilon_3}\left[\frac{\frac{s_3-s_1}{2}+s_1N(\epsilon_1)-s_3N(\epsilon_3)}{p_1^0-p_3^0-e_1k_1+e_3k_3}-\frac{\frac{s_2-s_1}{2}+s_1N(\epsilon_1)-s_2N(\epsilon_2)}{p_1^0-p_2^0-e_1k_1+e_2k_2}\right]\right\} .
\end{aligned}
\tag{2.96}
$$

Power counting of quark loops at large μ and small T

In the case of two external gluons one has Eq. (2.91)

$$
\mathcal{J}^{\mu_1\mu_2}(Q) = \int \frac{d^3\mathbf{k}}{(2\pi)^3}\sum_{\mathbf{e},\mathbf{s}}\mathcal{T}_{\mathbf{e}}^{\mu_1\mu_2}\Theta_{\mathbf{s}}^{\mathbf{e}}\frac{\frac{s_2-s_1}{2}+s_1N(\epsilon_1)-s_2N(\epsilon_2)}{-q^0-e_1k_1+e_2k_2} ,
\tag{2.97}
$$

where $\Theta_{\mathbf{e}}^{\mathbf{s}}=\Theta_{s_1}^{e_1}\Theta_{s_2}^{e_2}$ and $\mathcal{T}_{\mathbf{e}}^{\mu_1\mu_2}=\mathrm{Tr}_s\left[\gamma^{\mu_1}\Lambda_{\mathbf{k}_1}^{e_1}\gamma_0\gamma^{\mu_2}\Lambda_{\mathbf{k}_2}^{e_2}\gamma_0\right]$, which is

$$
\begin{aligned}
\mathcal{T}_{\mathbf{e}}^{00} &= 1+e_1e_2\,\hat{\mathbf{k}}_1\cdot\hat{\mathbf{k}}_2 , & \text{(2.98a)} \\
\mathcal{T}_{\mathbf{e}}^{0i} &= \mathcal{T}_{\mathbf{e}}^{i0}=e_1\hat{k}_1^i+e_2\hat{k}_2^i , \quad i=x,y,z , & \text{(2.98b)} \\
\mathcal{T}_{\mathbf{e}}^{ij} &= \delta^{ij}\left(1-e_1e_2\,\hat{\mathbf{k}}_1\cdot\hat{\mathbf{k}}_2\right)+e_1e_2\left(\hat{k}_1^i\hat{k}_2^j+\hat{k}_1^j\hat{k}_2^i\right) , \quad i,j=x,y,z . & \text{(2.98c)}
\end{aligned}
$$

First note that after the replacement given in Eq. (2.69) with $T\ll\Lambda_{\mathrm{q}}\ll\mu$ one can estimate an upper boundary for the thermal distribution functions $N(\epsilon_i)$. In the case $e_i=+$ one has $N(\epsilon_i)<\exp(-\Lambda_{\mathrm{q}}/T)$ and for $e_i=-$ it is $N(\epsilon_i)<\exp(-\mu/T)$. Hence, all terms proportional to $N(\epsilon_i)$ are *exponentially* suppressed compared to those proportional to s_i, and will therefore be neglected. Then, only terms with $s_1=-s_2$ contribute, where one mode in the loop propagates forward and one backwards in imaginary time. Making use of Eq. (2.75) one finds that all possible combinations are

- $e_1=-\Rightarrow s_1=-\Rightarrow s_2=+\Rightarrow e_2=+$ $(\bar{q}/q^+)$

- $e_1=+,\ s_1=+\Rightarrow s_2=-\Rightarrow e_2=+$ (q^-/q^+) or $e_2=-$ $(\bar{q}/q^+)$

- $e_1=+,\ s_1=-\Rightarrow s_2=+\Rightarrow e_2=+$ (q^-/q^+) ,

where $\bar{q}$ denotes an antiquark and q^s a quark above $(s=+)$ or below $(s=-)$ the Fermi surface. After having neglected thermal excitations for irrelevant quarks, the latter two can be identified with quark and quarkhole modes, respectively. Hence, one has

$$
\mathcal{J}^{\mu_1\mu_2}(Q) =
$$

$$
\begin{aligned}
&= \int \frac{d^3\mathbf{k}}{(2\pi)^3} \left\{ \mathcal{T}^{\mu_1\mu_2}_{+-} \frac{\Theta(k_1 - \mu - \Lambda_{\mathrm{q}})}{q^0 + k_1 + k_2} + \mathcal{T}^{\mu_1\mu_2}_{-+} \frac{\Theta(k_2 - \mu - \Lambda_{\mathrm{q}})}{-q^0 + k_1 + k_2} \right. \\
&\quad \left. + \mathcal{T}^{\mu_1\mu_2}_{++} \frac{\Theta(k_2 - \mu - \Lambda_{\mathrm{q}})\Theta(\mu - \Lambda_{\mathrm{q}} - k_1) - \Theta(k_1 - \mu - \Lambda_{\mathrm{q}})\Theta(\mu - \Lambda_{\mathrm{q}} - k_2)}{-q^0 - k_1 + k_2} \right\} \\
&= \int \frac{d^3\mathbf{k}}{(2\pi)^3} \left\{ \mathcal{T}^{\mu_1\mu_2}_{+-} \frac{\Theta(k - \mu - \Lambda_{\mathrm{q}})}{q^0 + k + |\mathbf{k} + \mathbf{q}|} + \mathcal{T}^{\mu_1\mu_2}_{-+} \frac{\Theta(k - \mu - \Lambda_{\mathrm{q}})}{-q^0 + k + |\mathbf{k} - \mathbf{q}|} \right. \\
&\quad \left. + \mathcal{T}^{\mu_1\mu_2}_{++} \frac{\Theta(|\mathbf{k} + \mathbf{q}| - \mu - \Lambda_{\mathrm{q}})\Theta(\mu - \Lambda_{\mathrm{q}} - k) - \Theta(k - \mu - \Lambda_{\mathrm{q}})\Theta(\mu - \Lambda_{\mathrm{q}} - |\mathbf{k} + \mathbf{q}|)}{-q^0 - k + |\mathbf{k} + \mathbf{q}|} \right\} .
\end{aligned}
\tag{2.99}
$$

The first two terms correspond to the quark/antiquark loop. After writing $\Theta(k_2 - \mu - \Lambda_{\mathrm{q}}) = 1 - \Theta(\mu - \Lambda_{\mathrm{q}} - k_2)$ the 1 is identified as the ultraviolet-divergent vacuum contribution and has to be removed by renormalization. Since $\Lambda_{\mathrm{q}} \ll \mu$ one has $\Theta(\mu - \Lambda_{\mathrm{q}} - k_i) \simeq \Theta(\mu - k_i)$, which effectively restricts the integration region to the Fermi sphere with the volume μ^3. In the considered case of soft external gluons, $q^0, q \sim \Lambda^s_{\mathrm{gl}} \ll \mu$, one can approximate $1/(\pm q^0 + k + |\mathbf{k} + \mathbf{q}|) \approx 1/2k$. Furthermore, one may expand $\mathcal{T}^{\mu_1\mu_2}_{\mathbf{e}}$ in powers of $\frac{q}{k}$ yielding

$$
\mathcal{T}^{00}_{\mathbf{e}} = 2\delta_{e_1 e_2} + \mathcal{O}\left(\frac{q^2}{k^2}\right) ,
\tag{2.100}
$$

$$
\mathcal{T}^{0i}_{\mathbf{e}} = \mathcal{T}^{i0}_{\mathbf{e}} = 2\delta_{e_1 e_2}\hat{k}^i + 2e_1\delta_{e_1,-e_2}(\delta^{ij} - \hat{k}^i\hat{k}^j)\frac{q^j}{2k} + \mathcal{O}\left(\frac{q^2}{k^2}\right) , \quad i = x, y, z ,
\tag{2.101}
$$

$$
\mathcal{T}^{ij}_{\mathbf{e}} = 2\delta^{ij}\delta_{e_1,-e_2} + e_1 e_2 \hat{k}^i\hat{k}^j + \mathcal{O}\left(\frac{q^2}{k^2}\right) , \quad i, j = x, y, z .
\tag{2.102}
$$

For $e_1 = -e_2$ the dominant contribution arises from $\mathcal{T}^{ij}_{+-} = \mathcal{T}^{ij}_{-+} \approx 2(\delta^{ij} - \hat{k}^i\hat{k}^j)$, whereas all others are suppressed by at least one power of q/k. Then the considered integral is of order $\mu^3/\mu \sim \mu^2$. After multiplication with g^2 from the vertices it is $\sim g^2\mu^2$. Choosing $\Lambda^s_{\mathrm{gl}} \sim g\mu \ll \mu$ this would be of the order of the tree-level propagator, which is $Q^2 \sim (\Lambda^s_{\mathrm{gl}})^2$. For smaller values of Λ^s_{gl}, however, the considered term would be above tree-level, since its magnitude is independent of the cutoff Λ^s_{gl}. E.g. for $\Lambda^s_{\mathrm{gl}} \sim g^2\mu$ this term would be one power of $1/g$ above tree-level.

The third term in Eq. (2.99) contains the particle/particle-hole excitations. Considering again the choice of cutoffs given in Eq. (2.64) with $\Lambda_{\mathrm{q}} \ll \Lambda^s_{\mathrm{gl}}$ one may approximate

$$
|\mathbf{k} + \mathbf{q}| - k \approx \mathbf{q} \cdot \hat{\mathbf{k}} ,
\tag{2.103}
$$

$$
\begin{aligned}
\Theta(|\mathbf{k} + \mathbf{q}| - \mu - \Lambda_{\mathrm{q}})\Theta(\mu - \Lambda_{\mathrm{q}} - k) & \\
- \Theta(k - \mu - \Lambda_{\mathrm{q}})\Theta(\mu - \Lambda_{\mathrm{q}} - |\mathbf{k} + \mathbf{q}|) &\approx \delta(k - \mu)\, \mathbf{q} \cdot \hat{\mathbf{k}} .
\end{aligned}
\tag{2.104}
$$

To obtain this estimate note that the two quark modes in the loop must be located on opposite sides of the Fermi surface (above and below the Fermi surface) and they must be situated within a shell of width Λ^s_{gl} around the Fermi surface since their relative momentum is given by the soft gluon momentum. Hence, $k \sim \mu \gg q \sim \Lambda^s_{\mathrm{gl}}$. In Eq. (2.104) additionally use was made of tha fact that due to $\Lambda^s_{\mathrm{gl}} \gg \Lambda_{\mathrm{q}}$ the cutoff Λ_{q} in the Θ-functions on the l.h.s. can be neglected,
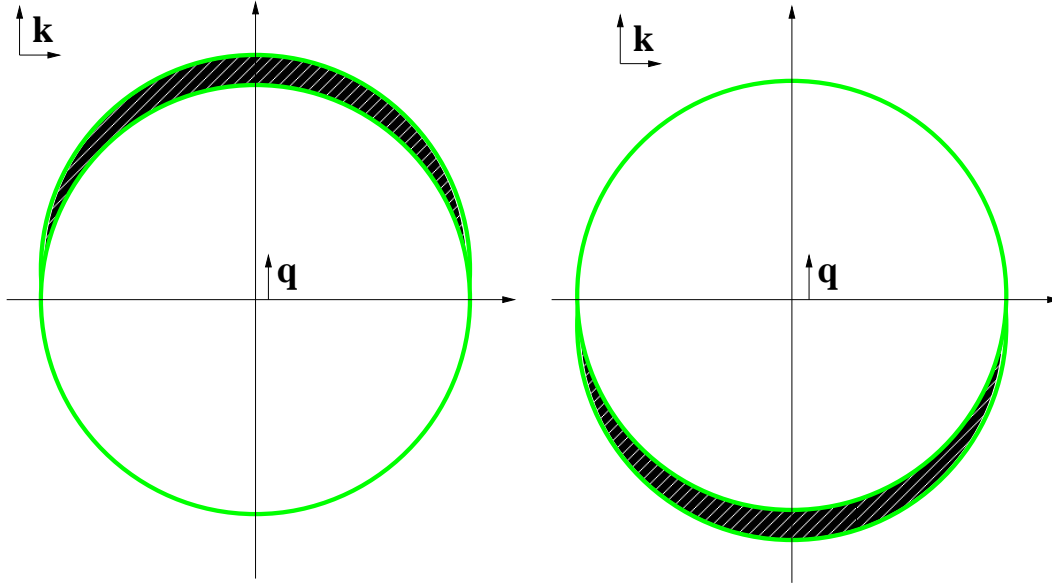
Figure 2.18: The integration region in the quark-quarkhole contribution in Eq. (2.99) is the dark shaded area for $\mu \gg q \sim \Lambda_{\mathrm{gl}}^s \gg \Lambda_{\mathrm{q}}$. The approximation in Eq. (2.104) is equivalent to including the light shaded areas corresponding to relevant quark modes with $|k - \mu| < \Lambda_{\mathrm{q}}$.

cf. Fig. 2.18. Note that in this way one will not recover the full result because the distribution functions $N(\epsilon_i)$ as well as the gap ϕ have been dropped from the outset. Furthermore, for the choice $\Lambda_{\mathrm{gl}}^s \gtrsim \Lambda_{\mathrm{q}}$ the approximation in Eq. (2.104) would become invalid and the calculation of the quark-quarkhole loop more complicated (but still feasible). Using Eqs. (2.103,2.104) the quark/quarkhole excitation in Eq. (2.99) reads

$$\mu^2 \int \frac{d\Omega}{(2\pi)^3} \mathcal{T}_{++}^{\mu_1\mu_2} \frac{\mathbf{q} \cdot \hat{\mathbf{k}}}{q^0 - \mathbf{q} \cdot \hat{\mathbf{k}}} \; , \tag{2.105}$$

which is of order μ^2 for all μ_1, μ_2. i.e. it is at the same order as the quark-antiquark loop and as the tree-level gluon propagator. In fact, Eq. (2.64) has turned out to be the right choice for the cutoffs to reproduce the HDL gluon self-energy, for details cf. [124]. For the choice $\mu \gg \Lambda_{\mathrm{gl}}^s \sim g\mu \gtrsim \Lambda_{\mathrm{q}}$ the result would nontrivially depend on the fraction $x \equiv \Lambda_{\mathrm{q}}/\Lambda_{\mathrm{gl}}^s$ and converge to the HDL result in the limit $x \to 0$.

Turning to the cases of three and four external gluons one first notes that, if not all internal lines correspond to particle and particle-hole modes the loop will be beyond tree-level. To show this one investigates the corresponding formulae Eqs. (2.95) and (2.96). As in the two-gluon case the thermal distribution functions may be neglected. Assume that the line with label 1 is an antiparticle ($s_1 = -$) and all other lines are particles ($s_j = +$, $j > 1$). Then, using the approximation Eq. (2.103) all energy denominators are of order Λ_{gl}^s except for those inside the angular brackets, which are of order μ. Combining the latter, the energy denominators standing directly in front of the angular brackets are canceled. Then in the case of three external gluons the integral multiplied by g^3 is of order $g^3 \mu^3/\mu^2 \sim g^2 \Lambda_{\mathrm{gl}}^s$, which is suppressed by g compared

to the tree-level, which is $g\Lambda_{\mathrm{gl}}^s$. In the case of 4 external gluons the integral multiplied by g^4 is of order $g^4\mu^3/(\mu^2\Lambda_{\mathrm{gl}}^s) \sim g^3$ and thus is also suppressed by g compared to tree-level, which is g^2. Analogously one verifies that also *all* other integrals containing antiparticles are suppressed by at least one power of g in comparison to tree-level. So, even though the integral region is of order μ^3 in the case that one mode corresponds to an antiparticle and all others are quarks above the Fermi surface no HDLs are produced.

In this context it seems worth mentioning that in [7] it was claimed that loops with N external gluons are HTLs if all but one of the $N-1$ occurring energy denominators carry energies with opposite sign (and therefore are of order $\Lambda_{\mathrm{g}}^s \sim gT$). It was argued there that in this special case the distribution functions appear as a sum which is of order 1 in comparison to the difference of two distribution functions, which is only of order g, appearing when all energy denominators are of order gT. This does indeed compensate the one energy denominator which is of the order of the hard scale T. If one, however, sums up *all* terms of this type systematically as it has been done above in the present treatment, one finds that these terms will cancel, up to a remaining part which is suppressed by a factor of g compared to tree-level. Hence, also in the regime of high temperatures *all* energy denominators must be of order of the soft scale Λ_{gl}^s in order to produce a HTL.

The loops containing only quark and quarkhole modes can simplified in virtue of approximations Eqs. (2.103) and (2.104) to

$$\mathcal{J}^{\mu_1\mu_2\mu_3}(Q_1,Q_2) \approx$$
$$\approx -\mu^2 \int \frac{d\Omega}{(2\pi)^3} \mathcal{T}_{+++}^{\mu_1\mu_2\mu_3} \frac{1}{(q_1^0+q_2^0)-(\mathbf{q}_1+\mathbf{q}_2)\cdot\hat{\mathbf{k}}} \left[\frac{\mathbf{q}_2\cdot\hat{\mathbf{k}}}{q_2^0-\mathbf{q}_2\cdot\hat{\mathbf{k}}} - \frac{\mathbf{q}_1\cdot\hat{\mathbf{k}}}{q_1^0-\mathbf{q}_1\cdot\hat{\mathbf{k}}} \right] \quad (2.106)$$

and

$$\mathcal{J}^{\mu_1\cdots\mu_4}(Q_1,Q_2,Q_3) \approx$$
$$\approx -\mu^2 \int \frac{d\Omega}{(2\pi)^3} \mathcal{T}_{++++}^{\mu_1\cdots\mu_4} \frac{1}{q_1^0+q_2^0+q_3^0-(\mathbf{q}_1+\mathbf{q}_2+\mathbf{q}_3)\cdot\hat{\mathbf{k}}} \times$$
$$\times \left\{ \frac{1}{q_1^0+q_2^0-(\mathbf{q}_1+\mathbf{q}_2)\cdot\hat{\mathbf{k}}} \left[\frac{\mathbf{q}_1\cdot\hat{\mathbf{k}}}{q_1^0-\mathbf{q}_1\cdot\hat{\mathbf{k}}} - \frac{\mathbf{q}_2\cdot\hat{\mathbf{k}}}{q_2^0-\mathbf{q}_2\cdot\hat{\mathbf{k}}} \right] + \right.$$
$$\left. + \frac{1}{q_3^0-\mathbf{q}_3\cdot\hat{\mathbf{k}}} \left[\frac{(\mathbf{q}_2+\mathbf{q}_3)\cdot\hat{\mathbf{k}}}{q_2^0+q_3^0-(\mathbf{q}_2+\mathbf{q}_3)\cdot\hat{\mathbf{k}}} - \frac{\mathbf{q}_2\cdot\hat{\mathbf{k}}}{q_2^0-\mathbf{q}_2\cdot\hat{\mathbf{k}}} \right] \right\} \quad (2.107)$$

After multiplying the expression for the loop of three external gluons with g^3 it is of order $g^3\mu^2/\Lambda_{\mathrm{gl}}^s \sim g\Lambda_{\mathrm{gl}}^s$, which is of the order of the corresponding tree-level diagram. Although in the angular brackets differences appear, no cancellations happen that effectively reduce the overall order of magnitude. E.g. the difference in the brackets in Eq. (2.106) vanishes for $Q_2 \to -Q_1$. In that case the energy denominator in front of the brackets disappears as well as preserving the overall order of magnitude of the loop.

Analogously, one finds for the loop with 4 external gluons $g^4\mu^2/(\Lambda_{\mathrm{gl}}^s)^2 \sim g^2$, i.e. it contributes also at tree-level. Again the various terms cannot cancel each other for any configuration of external gluon momenta $(Q_1,\cdots,Q_4)$. If, e.g., again $Q_2 \to -Q_1$, the term in front of the first angular bracket will keep the order of magnitude of the term.

One may conjecture as in [7] how the above discussions of quark loops with 3 and 4 external gluons can be generalized to loops with any number $N \geq 3$ of external gluons. Quark loops with N external gluon legs with all internal lines corresponding to particle or particle-hole modes get support from a thin layer around the Fermi surface with volume proportional of $\mu^2 \Lambda_{\mathrm{gl}}^s$. The integrand consists of $N - 1$ energy denominators which are all of order $1/\Lambda_{\mathrm{gl}}^s$ and the trace over Dirac space $\mathcal{T}_{\mathbf{e}}^{\boldsymbol{\mu}}$ which is dimensionless. Multiplying the loop with g^N it is of order

$$g^N \frac{\Lambda_{\mathrm{gl}}^s \mu^2}{(\Lambda_{\mathrm{gl}}^s)^{N-1}} = g^{N-2}(\Lambda_{\mathrm{gl}}^s)^{4-N} \left(\frac{g\mu}{\Lambda_{\mathrm{gl}}^s}\right)^2 = \text{tree-level} \times \left(\frac{g\mu}{\Lambda_{\mathrm{gl}}^s}\right)^2 . \tag{2.108}$$

Hence, if $\Lambda_{\mathrm{gl}}^s \sim g\mu$ the loop is at the order of the corresponding tree-level diagrams, $g^{N-2}(\Lambda_{\mathrm{gl}}^s)^{4-N}$, and therefore has to be resummed into the free gluon propagator or into a gluon vertex, respectively. Therefore, at this scale the free gluon propagation and the propagation via particle/hole and particle/antiparticle excitations are of equal importance. At scales $\Lambda_{\mathrm{gl}}^s < g\mu$ these loop diagrams even dominate the corresponding tree diagrams by a factor $\sim \left(g\mu/\Lambda_{\mathrm{gl}}^s\right)^2$. Gluons at scales $\Lambda_{\mathrm{gl}}^s < g\mu$ prefer to propagate as quark/antiquark or as quark/quarkhole pair rather than to propagate freely. In other words, decreasing the scale Λ_{gl}^s *sufficiently below* $g\mu$ the free propagation becomes a *small correction* to the "loop propagation" and the tree-level gluon vertices become a small correction to the dominant 3 and 4 gluon loops. This is important when considering the static limit $P \to 0$ for gluons, for example. These loops of irrelevant quark modes are therefore *relevant* operators in the effective action, cf. Sec. 1.3.

At harder scales $\Lambda_{\mathrm{gl}}^s > g\mu$ quark loops are small corrections to the free propagation and the 3 and 4 gluon vertices as in vacuum perturbation theory. Note that in the case of hot quark matter with negligible chemical potential one has analogously $\mathrm{HTL} \sim \text{tree-level} \times \left(gT/\Lambda_{\mathrm{gl}}^s\right)^2$.

All other types of quark loops will be suppressed by powers of $\Lambda_{\mathrm{gl}}^s/\mu$. If $\Lambda_{\mathrm{gl}}^s \geq g\mu$ they are below tree-level and therefore part of the perturbative expansion. For $\Lambda_{\mathrm{gl}}^s < g\mu$, however, those terms which are suppressed by $\Lambda_{\mathrm{gl}}^s/\mu$ still dominate the corresponding tree diagram by a factor of order $g\mu/\Lambda_{\mathrm{gl}}^s$. They are therefore still *relevant*. Those terms which are suppressed by $(\Lambda_{\mathrm{gl}}^s/\mu)^2$ scale as tree-level and consequently are *marginal*. Diagrams, which are suppressed by $(\Lambda_{\mathrm{gl}}^s/\mu)^3$ are always beyond tree-level and therefore perturbative.

Before applying the effective action Eq. (2.46) to some perturbative quantity one first has to extend this analysis to all the remaining diagrams contained in the effective action. In the following Chapter 3, however, it will be demonstrated how the effective action can be combined with the CJT-formalism [106] in order to facilitate the calculation of the non-perturbative color-superconducting gap-parameter.

Chapter 3

Application to
Color superconductivity

3.1 Calculation of the QCD gap parameter

In this section, I demonstrate how the effective action Eq. (2.46) derived in Sec. 2.1 can be applied to compute the gap parameter of color-superconducting quark matter to subleading order. To this end this effective action is combined with the CJT-formalism, which will be introduced below. The resulting subleading order gap equation, Eq. (3.64) is well-known. However, as will be explicitly shown, the derivation given here is substantially more rigorous as the known derivations in full QCD. One of the most important advantages is that the self-consistency is required only for *relevant* fields and propagators. Furthermore, the expansion of the various terms in the gap equation in powers of $\Lambda_{\mathrm{q}}/\Lambda_{\mathrm{gl}} \sim g$ emerges as a powerful tool to rigorously identify leading, subleading and sub-subleading order contributions to the gap parameter.

3.1.1 CJT formalism for the effective theory

The gap parameter in superconducting systems is not accessible by means of perturbation theory; one has to apply non-perturbative, self-consistent, many-body resummation techniques to calculate it. For this purpose it is convenient to employ the CJT formalism [106]. The first step is to add source terms to the effective action (2.46),

$$S_{\mathrm{eff}}[A_1, \bar{\Psi}_1, \Psi_1] \longrightarrow S_{\mathrm{eff}}[A_1, \bar{\Psi}_1, \Psi_1] + J_1 A_1 + \frac{1}{2} A_1 K_1 A_1 + \frac{1}{2} \left(\bar{\Psi}_1 H_1 + \bar{H}_1 \Psi_1 + \bar{\Psi}_1 \mathcal{K}_1 \Psi_1 \right) \ , \ (3.1)$$

where I employed the compact matrix notation defined in Eq. (2.15). J_1, $\bar{H}_1$, and H_1 are local source terms for the soft gluon and relevant quark fields, respectively, while K_1 and $\mathcal{K}_1$ are bilocal source terms. The bilocal source $\mathcal{K}_1$ for quarks is also a matrix in Nambu-Gor'kov space. Its diagonal components are source terms which couple quarks to antiquarks, while its off-diagonal components couple quarks to quarks. The latter have to be introduced for systems which can become superconducting, i.e., where the ground state has a non-vanishing diquark expectation value, $\langle \psi_1 \psi_1 \rangle \neq 0$.

One then performs a Legendre transformation with respect to all sources and arrives at the CJT effective action [106, 120]

$$
\begin{aligned}
\Gamma\left[A, \bar{\Psi}, \Psi, \Delta, \mathcal{G}\right] &= S_{\text{eff}}\left[A, \bar{\Psi}, \Psi\right] - \frac{1}{2}\operatorname{Tr}_g \ln \Delta^{-1} - \frac{1}{2}\operatorname{Tr}_g\left(D^{-1}\Delta - 1\right) \\
&+ \frac{1}{2}\operatorname{Tr}_q \ln \mathcal{G}^{-1} + \frac{1}{2}\operatorname{Tr}_q\left(G^{-1}\mathcal{G} - 1\right) + \Gamma_2\left[A, \bar{\Psi}, \Psi, \Delta, \mathcal{G}\right] .
\end{aligned} \tag{3.2}
$$

Here, $S_{\text{eff}}[A, \bar{\Psi}, \Psi]$ is the tree-level action defined in Eq. (2.46), which now depends on the *expectation values* $A \equiv \langle A_1 \rangle$, $\bar{\Psi} \equiv \langle \bar{\Psi}_1 \rangle$, and $\Psi \equiv \langle \Psi_1 \rangle$ for the one-point functions of soft gluon and relevant quark fields. In a slight abuse of notation, I use the same symbols for the expectation values as for the original fields, prior to integrating out modes. This should not lead to confusion, as the original fields no longer occur in any of the following expressions.

The quantities D^{-1} and G^{-1} in Eq. (3.2) are the inverse *tree-level* propagators for soft gluons and relevant quarks, respectively, which are determined from the effective action S_{eff}, see below. The quantities Δ and $\mathcal{G}$ are the expectation values for the two-point functions, i.e., the *full* propagators, of soft gluons and relevant quarks. The functional Γ_2 is the sum of all two-particle irreducible (2PI) diagrams. These diagrams are vacuum diagrams, i.e., they have no external legs. They are constructed from the vertices defined by the interaction part of S_{eff}, linked by full propagators Δ, $\mathcal{G}$. The expectation values for the one- and two-point functions of the theory are determined from the stationarity conditions

$$
0 = \frac{\delta\Gamma}{\delta A} = \frac{\delta\Gamma}{\delta\bar{\Psi}} = \frac{\delta\Gamma}{\delta\Psi} = \frac{\delta\Gamma}{\delta\Delta} = \frac{\delta\Gamma}{\delta\mathcal{G}} . \tag{3.3}
$$

The first condition yields the Yang-Mills equation for the expectation value A of the soft gluon field. The second and third condition correspond to the Dirac equation for Ψ and $\bar{\Psi}$, respectively. The effective action (2.46) contains a multitude of terms which depend on $A, \bar{\Psi}, \Psi$, and thus the Yang-Mills and Dirac equations are rather complex, wherefore I refrain from explicitly presenting them here. Nevertheless, for the Dirac equation the solution is trivial, since $\bar{\Psi}_1$, Ψ_1 are Grassmann-valued fields, and their expectation values must vanish identically, $\bar{\Psi} = \langle\bar{\Psi}_1\rangle = \Psi = \langle\Psi_1\rangle \equiv 0$. On the other hand, for the Yang-Mills equation, the solution A is in general non-zero but, at least for the two-flavor color superconductor considered here, it was shown [121, 122] to be parametrically small, $A \sim \phi^2/(g^2\mu)$, where ϕ is the color-superconducting gap parameter. Therefore, to subleading order in the gap equation it can be neglected.

The fourth and fifth condition (3.3) are Dyson-Schwinger equations for the soft gluon and relevant quark propagator, respectively,

$$
\begin{aligned}
\Delta^{-1} &= D^{-1} + \Pi , \tag{3.4a} \\
\mathcal{G}^{-1} &= G^{-1} + \Sigma , \tag{3.4b}
\end{aligned}
$$

where

$$
\begin{aligned}
\Pi &\equiv -2\frac{\delta\Gamma_2}{\delta\Delta^T} , \tag{3.5a} \\
\Sigma &\equiv 2\frac{\delta\Gamma_2}{\delta\mathcal{G}^T} \tag{3.5b}
\end{aligned}
$$

are the gluon and quark self-energies, respectively. The Dyson-Schwinger equation for the relevant quark propagator is a 2×2 matrix equation in Nambu-Gor'kov space,

$$\mathcal{G}^{-1} = \begin{pmatrix} [G^+]^{-1} & 0 \\ 0 & [G^-]^{-1} \end{pmatrix} + \begin{pmatrix} \Sigma^+ & \Phi^- \\ \Phi^+ & \Sigma^- \end{pmatrix} , \tag{3.6}$$

where Σ^+ is the regular self-energy for quarks and Σ^- the corresponding one for charge-conjugate quarks. The off-diagonal self-energies $\Phi^\pm$, the so-called *gap matrices*, connect regular with charge-conjugate quark degrees of freedom. A non-zero $\Phi^\pm$ corresponds to the condensation of quark Cooper pairs. Only two of the four components of this matrix equation are independent, say $[G^+]^{-1}+\Sigma^+$ and Φ^+, the other two can be obtained via $[G^-]^{-1}+\Sigma^- = C\{[G^+]^{-1}+\Sigma^+\}^T C^{-1}$, $\Phi^- \equiv \gamma_0[\Phi^+]^\dagger\gamma_0$. Equation (3.6) can be formally solved for $\mathcal{G}$ [123],

$$\mathcal{G} \equiv \begin{pmatrix} \mathcal{G}^+ & \Xi^- \\ \Xi^+ & \mathcal{G}^- \end{pmatrix} , \tag{3.7}$$

where

$$\mathcal{G}^\pm \equiv \left\{ [G^\pm]^{-1} + \Sigma^\pm - \Phi^\mp \left([G^\mp]^{-1} + \Sigma^\mp \right)^{-1} \Phi^\pm \right\}^{-1} \tag{3.8}$$

is the propagator describing normal propagation of quasiparticles and their charge-conjugate counterpart, while

$$\Xi^\pm \equiv - \left([G^\mp]^{-1} + \Sigma^\mp \right)^{-1} \Phi^\pm \mathcal{G}^\pm \tag{3.9}$$

describes anomalous propagation of quasiparticles, which is possible if the ground state is a color-superconducting quark-quark condensate, for details, see Ref. [13].

The tree-level gluon propagator is defined as

$$D^{-1} \equiv - \frac{\delta^2 S_{\text{eff}}[A, \bar{\Psi}, \Psi]}{\delta A \, \delta A} . \tag{3.10}$$

Since I ultimately evaluate the tree-level propagator at the stationary point of Γ, Eq. (3.3), where $\bar{\Psi} = \Psi = 0$, I may omit all terms in S_{eff}, Eq. (2.46), which are proportional to the quark fields. The only terms which contribute to the tree-level gluon propagator are therefore

$$D^{-1} \equiv - \frac{\delta^2}{\delta A \, \delta A} \left(S_A + \frac{1}{2} \text{Tr}_q \ln \mathcal{G}_{22}^{-1} - \frac{1}{2} \text{Tr}_g \ln \Delta_{22}^{-1} \right) . \tag{3.11}$$

Using the expansions (2.27), (2.29), (2.43), and (2.44), and exploiting the cyclic property of the trace, one finds

$$D^{-1} = - \frac{\delta^2 S_A}{\delta A \, \delta A} - \frac{g}{2} \text{Tr}_q \left(\frac{\delta \mathcal{G}_{22}}{\delta A} \frac{\delta \mathcal{A}_{22}}{\delta A} \right) + \frac{1}{2} \text{Tr}_g \left(\frac{\delta \Delta_{22}}{\delta A} \frac{\delta \Pi_{22}}{\delta A} + \Delta_{22} \frac{\delta^2 \Pi_{22}}{\delta A \, \delta A} \right) . \tag{3.12}$$

In order to proceed, note that the Dyson-Schwinger equations (3.4) are evaluated at the stationary point of the effective action, where $\bar{\Psi} = \Psi = 0$, $A \simeq 0$. For $A = 0$, the first term yields the free inverse propagator for soft gluons, $\Delta_{0,11}^{-1}$, cf. Eq. (2.31), plus a contribution from the

Faddeev-Popov determinant, $(\delta^2 \mathrm{Tr}_{gh} \ln \mathcal{W}^{-1}/\delta A \delta A)_{A=0}$. The contributions from the three- and four-gluon vertex vanish for $A = 0$. Furthermore, according to Eq. (2.16),

$$\frac{\delta \mathcal{A}_{22}(K,Q)}{\delta A(P)} = \frac{1}{\sqrt{VT^3}} \hat{\Gamma} \, \delta^{(4)}_{K,Q+P} \equiv \tilde{\Gamma}(K,Q;P) \; . \tag{3.13}$$

This is a matrix in fundamental color, flavor, and Nambu-Gor'kov space, as well as in the space of quark 4-momenta K, Q. It is a vector in Minkowski and adjoint color space ($\hat{\Gamma}$ carries a Lorentz-vector and a gluon color index), as well as in the space of gluon 4-momenta P. One evaluates $(\delta \mathcal{G}_{22}/\delta A)_{A=0}$ using the expansion (2.27). Only the term for $n = 1$ survives when taking $A = 0$. For $\bar{\Psi} = \Psi = 0$, I have $\Pi_{\mathcal{B}} = 0$, cf. Fig. 2.9, and I only need to consider $\Pi_{22} = \Pi_{\mathrm{loop}} + \Pi_{\mathcal{V}}$. Then, the term $\mathcal{V}^{(3)} \equiv (\delta \Pi_{\mathcal{V}}/\delta A)_{A=0}$ corresponds to a triple-gluon vertex, cf. Fig. 2.11, where two hard gluons couple to one soft gluon. The term $(\delta \Pi_{\mathrm{loop}}/\delta A)_{A=0}$ is a correction to this vertex: it couples two hard gluons to a soft one through an (irrelevant) quark loop, cf. Fig. 2.10. According to arguments well known from the HTL/HDL effective theory, this vertex correction can never be of the same order as the tree-level vertex $\mathcal{V}^{(3)}$, since the two incoming gluons are hard. I therefore neglect $(\delta \Pi_{\mathrm{loop}}/\delta A)_{A=0}$ in the following. Similarly, $\mathcal{V}^{(4)} \equiv (\delta^2 \Pi_{\mathcal{V}}/\delta A \delta A)_{A=0}$ is a four-gluon vertex, cf. Fig. 2.11, where two hard gluons couple to two soft ones, and $(\delta^2 \Pi_{\mathrm{loop}}/\delta A \delta A)_{A=0}$ is the one-(quark-)loop correction to this vertex, cf. Fig. 2.10. Applying the same arguments as above I only keep $\mathcal{V}^{(4)}$. Arguments from the HTL/HDL effective theory also show that to leading order one may approximate $\Delta_{22} \simeq \Delta_{0,22}$. Finally, utilizing the same arguments I approximate $\delta \Delta_{22}/\delta A \simeq -\Delta_{0,22} \mathcal{V}^{(3)} \Delta_{0,22}$. Then, the inverse tree-level gluon propagator of Eq. (3.12) becomes

$$\begin{aligned}
D^{-1} &= \Delta_{0,11}^{-1} + \frac{g^2}{2} \mathrm{Tr}_q \left(\mathcal{G}_{0,22} \tilde{\Gamma} \, \mathcal{G}_{0,22} \tilde{\Gamma} \right) - \frac{1}{2} \mathrm{Tr}_g \left(\Delta_{0,22} \, \mathcal{V}^{(3)} \, \Delta_{0,22} \, \mathcal{V}^{(3)} \right) + \frac{1}{2} \mathrm{Tr}_g \left(\Delta_{0,22} \, \mathcal{V}^{(4)} \right) \\
&\quad - \left. \frac{\delta^2 \mathrm{Tr}_{gh} \ln \mathcal{W}^{-1}}{\delta A \, \delta A} \right|_{A=0} .
\end{aligned} \tag{3.14}$$

The second term represents an (irrelevant) quark-loop, while the third term is a hard gluon loop. The fourth term is a hard gluon tadpole. Finally, the last term in Eq. (3.14) corresponds to a ghost loop necessary to cancel loop contributions from unphysical gluon degrees of freedom. Note that in the effective theory loop contributions involving irrelevant quarks and hard gluons occur already in the tree-level action (2.46). Therefore, such loops also arise in the inverse tree-level propagator (3.14) for the soft gluons of the effective theory. For the projection operators (2.35) and (2.47) the inverse tree-level propagator (3.14) is precisely the HTL/HDL-resummed inverse gluon propagator. For small temperatures, $T \ll \mu$, the contribution from the gluon and ghost loops is negligible as compared to that from the quark loop,

$$D^{-1} \simeq \Delta_{0,11}^{-1} + \frac{g^2}{2} \mathrm{Tr}_q \left(\mathcal{G}_{0,22} \tilde{\Gamma} \, \mathcal{G}_{0,22} \tilde{\Gamma} \right) \; . \tag{3.15}$$

The inverse tree-level quark propagator is defined as

$$G^{-1} \equiv -2 \frac{\delta^2 S_{\mathrm{eff}}[A, \bar{\Psi}, \Psi]}{\delta \bar{\Psi} \, \delta \Psi} \; . \tag{3.16}$$

For $\bar{\Psi} = \Psi = 0$, the last term in Eq. (2.46) does not contribute to G^{-1} because it has at least four external quark legs, and the two functional derivatives $\delta/\delta\bar{\Psi}$, $\delta/\delta\Psi$ amputate only two of them. The first and the third term in Eq. (2.46) do not depend on $\bar{\Psi}, \Psi$ at all, therefore

$$G^{-1} = \mathcal{G}_{0,11}^{-1} + g\mathcal{B}[A] + \frac{\delta^2 \mathrm{Tr}_g \ln \Delta_{22}^{-1}}{\delta\bar{\Psi}\,\delta\Psi} \ . \tag{3.17}$$

Using the expansion formulae (2.43) and (2.44) and the fact that Π_{22} depends on $\bar{\Psi}, \Psi$ only through $\Pi_{\mathcal{B}}$, I obtain

$$\frac{\delta^2 \mathrm{Tr}_g \ln \Delta_{22}^{-1}}{\delta\bar{\Psi}\,\delta\Psi} = \mathrm{Tr}_g \left(\Delta_{22} \frac{\delta^2 \Pi_{\mathcal{B}}}{\delta\bar{\Psi}\,\delta\Psi} \right) \ . \tag{3.18}$$

I have exploited the fact that this expression is evaluated at $\bar{\Psi} = \Psi = 0$, i.e., terms with external quark legs will eventually vanish. The trace runs only over adjoint colors, Lorentz indices, and (hard) gluon 4-momenta. Since Δ_{22} is a hard gluon propagator, the contribution from Π_{22} to Δ_{22} may be neglected to the order I am computing, and I may set $\Delta_{22} \simeq \Delta_{0,22}$. Furthermore, $(\delta^2 \Pi_{\mathcal{B}}/\delta\bar{\Psi}\delta\Psi)_{A=0} \equiv -g^2\, \tilde{\Gamma}\, \mathcal{G}_{0,22}\, \tilde{\Gamma}$, cf. Fig. 2.9. At $\bar{\Psi} = \Psi = 0$, $A \simeq 0$ I am left with

$$G^{-1} = \mathcal{G}_{0,11}^{-1} - g^2 \, \mathrm{Tr}_g \left(\Delta_{0,22}\, \tilde{\Gamma}\, \mathcal{G}_{0,22}\, \tilde{\Gamma} \right) \ . \tag{3.19}$$

As was the case for the tree-level gluon propagator, also the tree-level quark propagator receives a loop contribution; here it arises from a loop involving an irrelevant quark and a hard gluon line. The term $\tilde{\Gamma}\mathcal{G}_{0,22}\tilde{\Gamma}$ under the gluon trace remains a matrix in the quark indices, i.e., fundamental color, flavor, Dirac, and quark 4-momenta.

I now proceed to solve the Dyson-Schwinger equations (3.4) for the soft gluon and relevant quark propagator. To this end I have to determine Γ_2. Of course it is not feasible to consider *all* possible 2PI diagrams. The advantage of the CJT formalism is that *any* truncation of Γ_2 defines a meaningful, self-consistent many-body approximation for which one can solve the Dyson-Schwinger equations (3.4). In the truncation of Γ_2 I only take into account 2-loop diagrams which are 2PI with respect to the soft gluon and relevant quark propagators $\Delta, \mathcal{G}$,

$$\Gamma_2 = -\frac{g^2}{4} \mathrm{Tr}_{q,g} \left(\mathcal{G}\, \tilde{\Gamma}\, \mathcal{G}\, \tilde{\Gamma}\, \Delta \right) - \frac{g^2}{2} \mathrm{Tr}_{q,g} \left(\mathcal{G}\, \tilde{\Gamma}\, \mathcal{G}_{0,22}\, \tilde{\Gamma}\, \Delta \right) - \frac{g^2}{4} \mathrm{Tr}_{q,g} \left(\mathcal{G}\, \tilde{\Gamma}\, \mathcal{G}\, \tilde{\Gamma}\, \Delta_{0,22} \right) \ . \tag{3.20}$$

The traces now run over quark as well as over gluon indices. Consider, for instance, the term $\mathcal{G}\,\tilde{\Gamma}\,\mathcal{G}\,\tilde{\Gamma}$. It is a matrix in the space of fundamental color, flavor, Dirac and quark 4-momenta, of which the trace is taken through Tr_q. In addition, due to the two factors $\tilde{\Gamma}$ it carries two Lorentz-vector, adjoint-color, and gluon-4-momenta indices. The trace Tr_g contracts these indices with the corresponding ones from the gluon propagator Δ.

Figure 3.1: Diagrammatic representation of Γ_2, Eq. (3.20).

The diagrams corresponding to Eq. (3.20) are shown in Fig. 3.1. The first two terms are constructed from the quark-gluon coupling $\sim \bar{\Psi}\, g\mathcal{B}\, \Psi$. Using Eq. (2.26), one may either obtain an ordinary quark-gluon vertex $\sim g\, \bar{\Psi}\, \mathcal{A}\, \Psi$, involving one soft gluon and two relevant quark legs, or a vertex $\sim g^2\, \bar{\Psi}\, \mathcal{A}\, \mathcal{G}_{22}\, \mathcal{A}\, \Psi$, with (at least) two soft gluon legs and two relevant quark legs. To lowest order, I approximate $\mathcal{G}_{22} \simeq \mathcal{G}_{0,22}$, which neglects vertices with more than two soft gluon legs. Taking two ordinary quark-gluon vertices and tying them together to obtain a 2PI 2-loop diagram, I arrive at the first term in Eq. (3.20), or the first diagram in Fig. 3.1. Taking one of the two-gluon-two-quark vertices and tying the legs together, one obtains the second term in Eq. (3.20), or the second diagram in Fig. 3.1, respectively. Finally, the third term/diagram arises from the last term in Eq. (2.46). To lowest order, this corresponds to a four-quark vertex $\sim g^2\, \bar{\Psi}\, \tilde{\Gamma}\, \Psi\, \Delta_{0,22}\bar{\Psi}\, \tilde{\Gamma}\, \Psi$. Tying the quark legs together to form a 2PI diagram, one obtains the corresponding term/diagram in Eq. (3.20)/Fig. 3.1.

The combinatorial factors in front of the various terms in Eq. (3.20) are explained as follows. In the first diagram, there are two ordinary quark-gluon vertices. According to Eq. (2.46), each diagram comes with a factor $1/2$. Moreover, since there are two vertices, the diagram is, in the perturbative sense, a diagram of second order, which causes an additional factor $1/2$ [15]. Finally, there are two possibilities to connect the quark lines between the two vertices. In total, I then have a prefactor $-(1/2)^2 \times 1/2 \times 2 = -1/4$, where the minus sign arises from the fermion loop. The second diagram arises from the two-quark-two-gluon vertex, which already comes with a prefactor $-1/2$ in Eq. (2.46). It is perturbatively of first order, and there is only one possibility to tie the quark and gluon lines together, so there is no additional combinatorial factor (and no additional minus sign) for this diagram. Finally, the third diagram arises from the four-quark vertex, $(1/2)\mathcal{J}_{\mathcal{B}}\Delta_{0,22}\mathcal{J}_{\mathcal{B}}$, in Eq. (2.46). This vertex comes with a factor $1/2$ and is perturbatively of first order. However, there are two additional factors $1/2$ residing in $\mathcal{J}_{\mathcal{B}}$, since $\mathcal{J}_{\mathcal{B}} \sim (1/2)\bar{\Psi}\, \hat{\Gamma}\, \Psi$, cf. Eq. (2.38). Again, there are two possibilities to tie the quark lines together, so that, in total, I have a prefactor $-1/2 \times (1/2)^2 \times 2 = -1/4$, where the minus sign again stands for the quark loop.

Figure 3.2: Diagrammatic representation of Γ_2^{QCD}, after decomposing quark lines into relevant and irrelevant, as well as gluon propagators into soft and hard contributions.

At this point, it is instructive to compare Γ_2, Eq. (3.20), in the effective theory with Γ_2^{QCD} which one would have written down in QCD at the same loop level. Γ_2^{QCD} would be equivalent to the first diagram of Fig. 3.1, but now the quark and gluon lines represent the full propagators for *all* momentum modes, relevant *and* irrelevant as well as soft *and* hard. In order to compare with Γ_2 of the effective theory, I decompose the quark propagators into relevant and irrelevant modes, and the gluon propagator into soft and hard modes. One obtains the six diagrams shown in Fig. 3.2. The first three are precisely the same that occur in Γ_2 of the effective theory, including the combinatorial prefactors. The last three diagrams do not occur in Γ_2 of the effective theory, because they are not 2PI with respect to the relevant quark propagator $\mathcal{G}$ and the soft gluon

propagator Δ. Nevertheless, they are still included in the CJT effective action of the effective theory, Eq. (3.2): opening the relevant quark line of the fourth diagram, I recognize the loop contribution to the tree-level quark propagator G^{-1}, cf. Eq. (3.19). Now consider the fifth term in Eq. (3.2): here, this loop contribution to G^{-1} is multiplied by $\mathcal{G}$ and traced over, which yields the fourth diagram in Γ_2^{QCD}. Similarly, opening the soft gluon line of the fifth diagram, I identify this diagram as the irrelevant quark-loop contribution to the tree-level gluon propagator D^{-1}, cf. Eq. (3.15). The third term in Eq. (3.2), where this contribution is multiplied by Δ and traced over, then yields the fifth diagram of Γ_2^{QCD}. Finally, the sixth diagram resides in the term $\sim \mathrm{Tr}_g \ln \Delta_{22}^{-1}$ of the tree-level effective action S_{eff}, cf. Fig. 2.15. Therefore, in principle, the CJT effective action (3.2) for the effective theory contains the same information as the corresponding one for QCD. However, while in QCD self-consistency is maintained for *all* momentum modes via the solution of the stationarity condition (3.3), in the effective theory self-consistency is only required for the *relevant* quark and *soft* gluon modes. These are the *only* dynamical degrees of freedom in the CJT effective action; the irrelevant fermion and hard gluon modes, which were integrated out, only appear in the vertices of the tree-level action (2.46). In this sense the effective theory provides a simplification of the full problem.

3.1.2 Dyson-Schwinger equations for relevant quarks and soft gluons

After having specified Γ_2 in Eq. (3.20) I am now in the position to write down the Dyson-Schwinger equations (3.4) explicitly. For the full inverse propagator of soft gluons I obtain with Eqs. (3.4a), (3.5a), (3.15), and (3.20)

$$\Delta^{-1} = \Delta_{0,11}^{-1} + \frac{g^2}{2} \left[\mathrm{Tr}_q \left(\mathcal{G}_{0,22} \, \tilde{\Gamma} \, \mathcal{G}_{0,22} \, \tilde{\Gamma} \right) + 2 \, \mathrm{Tr}_q \left(\mathcal{G} \, \tilde{\Gamma} \, \mathcal{G}_{0,22} \, \tilde{\Gamma} \right) + \mathrm{Tr}_q \left(\mathcal{G} \, \tilde{\Gamma} \, \mathcal{G} \, \tilde{\Gamma} \right) \right] . \qquad (3.21)$$

The first term in square brackets takes into account the effect of quark-antiquark excitations as well as quark-hole excitations far from the Fermi surface. The second term is the contribution from excitations where one quark is close to the Fermi surface (a relevant quark) while the second is far from the Fermi surface or an antiquark (an irrelevant quark). The relevant quark propagator $\mathcal{G}$ can have diagonal elements in Nambu-Gor'kov space, corresponding to normal propagation of quasiparticles, as well as off-diagonal elements, corresponding to anomalous propagation of quasiparticles, cf. Eq. (3.7). However, in the second term in square brackets the latter contribution is absent, because $\mathcal{G}_{0,22}$ is purely diagonal in Nambu-Gor'kov space, cf. Eq. (2.12). This is different for the last term in square brackets, which corresponds to quark-hole excitations close to the Fermi surface. Both quark propagators have to be determined self-consistently and may have off-diagonal elements in Nambu-Gor'kov space. Consequently, the trace over Nambu-Gor'kov space gives two contributions, a loop where both quarks propagate normally, and another one where they propagate anomalously. Diagrams of this type have been evaluated in Ref. [124] and lead to the Meissner effect for gluons in a color superconductor.

For the full inverse propagator of relevant quarks I obtain with Eqs. (3.4b), (3.5b), (3.19), and (3.20)

$$\mathcal{G}^{-1} = \mathcal{G}_{0,11}^{-1} - g^2 \left[\mathrm{Tr}_g \left(\Delta_{0,22} \, \tilde{\Gamma} \, \mathcal{G}_{0,22} \, \tilde{\Gamma} \right) + \mathrm{Tr}_g \left(\Delta \, \tilde{\Gamma} \, \mathcal{G}_{0,22} \, \tilde{\Gamma} \right) + \mathrm{Tr}_g \left(\Delta_{0,22} \, \tilde{\Gamma} \, \mathcal{G} \, \tilde{\Gamma} \right) + \mathrm{Tr}_g \left(\Delta \, \tilde{\Gamma} \, \mathcal{G} \, \tilde{\Gamma} \right) \right] . $$
$$(3.22)$$

The first two terms in square brackets do not have off-diagonal components in Nambu-Gor'kov space. They contribute only to the regular quark self-energy. The other two terms in square brackets have both diagonal and off-diagonal components in Nambu-Gor'kov space. The diagonal components contribute to the regular quark self-energy, in particular, the fourth term leads to the quark wave-function renormalization factor computed first in Ref. [125]. It gives rise to non-Fermi liquid behavior [97]. The off-diagonal components enter the gap equation for the color-superconducting gap parameter.

The system of Eqs. (3.21) and (3.22) has to be solved self-consistently for the full propagators of quarks and gluons. However, as was shown in Ref. [126], in order to extract the color-superconducting gap parameter to subleading order it is sufficient to consider the gluon propagator in HDL approximation; corrections arising from the color-superconducting gap in the quasiparticle spectrum are of sub-subleading order in the gap equation. For the present purpose this means that it is not necessary to self-consistently solve Eq. (3.21) together with Eq. (3.22); one may approximate $\mathcal{G}$ on the right-hand side of Eq. (3.21) by $\mathcal{G}_{0,11}$. In essence, this is equivalent to considering only the first term on the right-hand side of Eq. (3.22) when solving Eq. (3.21). Of course, under this approximation the effect of the regular quark self-energy (leading to wave-function renormalization) and of the anomalous quark self-energy (which accounts for the gap in the quasiparticle excitation spectrum) are neglected.

With this approximation, and using $\mathcal{G}_0 \equiv \mathcal{G}_{0,11} \oplus \mathcal{G}_{0,22}$, one may combine the terms in Eq. (3.21) to give

$$\Delta^{-1} \simeq \Delta_{0,11}^{-1} + \frac{g^2}{2} \operatorname{Tr}_q \left(\mathcal{G}_0 \, \tilde{\Gamma} \, \mathcal{G}_0 \, \tilde{\Gamma} \right) \; . \tag{3.23}$$

Taking the gluon cut-off scale $\Lambda_{\rm gl}$ to fulfill $g\mu \ll \Lambda_{\rm gl} \lesssim \mu$, soft gluons are defined to have momenta of order $g\mu$. I compute the fermion loop in Eq. (3.23) under this assumption (taking the soft gluon energy to be of the same order of magnitude as the gluon momentum). I then realize that the soft gluon propagator determined by Eq. (3.23) is just the gluon propagator in HDL approximation. I indicate this fact in the following by a subscript, $\Delta \equiv \Delta_{\rm HDL}$. Armed with this (approximate) solution of the Dyson-Schwinger equation (3.21) I now proceed to solve Eq. (3.22). I consider the two independent components $[G^+]^{-1} + \Sigma^+$ and Φ^+ in Nambu-Gor'kov space separately. Due to translational invariance it is convenient to define $[G^+]^{-1}(K,Q) \equiv (1/T)[G^+]^{-1}(K)\,\delta_{K,Q}^{(4)}$, $\Sigma^+(K,Q) \equiv (1/T)\Sigma^+(K)\,\delta_{K,Q}^{(4)}$ and using Eqs. (2.10), (2.12), (2.32), (3.13), I obtain the Dyson-Schwinger equation for $[G^+]^{-1} + \Sigma^+$,

$$
\begin{aligned}
&[G^+]^{-1}(K) + \Sigma^+(K) = \\
&[G_{0,11}^+]^{-1}(K) - g^2 \frac{T}{V} \sum_Q \left\{ [\Delta_{0,22}]_{ab}^{\mu\nu}(K-Q) + [\Delta_{\rm HDL}]_{ab}^{\mu\nu}(K-Q) \right\} \gamma_\mu T^a \, G_{0,22}(Q) \, \gamma_\nu T^b \\
&-g^2 \frac{T}{V} \sum_Q \left\{ [\Delta_{0,22}]_{ab}^{\mu\nu}(K-Q) + [\Delta_{\rm HDL}]_{ab}^{\mu\nu}(K-Q) \right\} \gamma_\mu T^a \, \mathcal{G}^+(Q) \, \gamma_\nu T^b \; . \tag{3.24}
\end{aligned}
$$

Note that the first sum over Q runs over irrelevant quark momenta, $0 \leq q < \mu - \Lambda_{\rm q}$ and $\mu + \Lambda_{\rm q} < q < \infty$, while the second sum runs over relevant quark momenta, $\mu - \Lambda_{\rm q} \leq q \leq \mu + \Lambda_{\rm q}$. There is no double counting of gluon exchange contributions, since the hard gluon propagator $\Delta_{0,22}$ has support only for gluon momenta $|\mathbf{k} - \mathbf{q}| > \Lambda_{\rm gl}$, while the HDL propagator is restricted

to gluon momenta $|\mathbf{k} - \mathbf{q}| \leq \Lambda_{\mathrm{gl}}$. To subleading order in the gap equation, I do not have to solve this Dyson-Schwinger equation self-consistently. It is sufficient to use the approximation $\mathcal{G}^+ \simeq G_{0,11}^+$ on the right-hand side of Eq. (3.24) and to keep only the last term which, as discussed above, is responsible for non-Fermi liquid behavior in cold, dense quark matter. The net result is then simply a wave-function renormalization for the free quark propagator $G_{0,11}^+$ [125],

$$[G^+]^{-1}(K) + \Sigma^+(K) \simeq [G_{0,11}^+]^{-1}(K) + \bar{g}^2 \, k_0 \, \gamma_0 \, \ln \frac{M^2}{k_0^2} \equiv \left[Z^{-1}(k_0) \, k_0 + \mu \right] \gamma_0 - \boldsymbol{\gamma} \cdot \mathbf{k} \,, \quad (3.25)$$

where $\bar{g} \equiv g/(3\sqrt{2}\pi)$ and $M^2 = (3\pi/4)m_g^2$, with the gluon mass parameter m_g defined in Eq. (1.39). Neglecting effects from the finite life-time of quasi-particles [123], which are of sub-subleading order in the gap equation, the wave-function renormalization factor is

$$Z(k_0) = \left(1 + \bar{g}^2 \, \ln \frac{M^2}{k_0^2} \right)^{-1} . \tag{3.26}$$

Due to translational invariance, it is convenient to define $\Phi^+(K,Q) \equiv (1/T) \, \Phi^+(K) \, \delta_{K,Q}^{(4)}$ and $\Xi^+(K,Q) \equiv T \, \Xi^+(K) \, \delta_{K,Q}^{(4)}$, and the Dyson-Schwinger equation for $\Phi^+(K)$ becomes

$$\Phi^+(K) = g^2 \frac{T}{V} \sum_Q \left\{ [\Delta_{0,22}]_{ab}^{\mu\nu} (K - Q) + [\Delta_{\mathrm{HDL}}]_{ab}^{\mu\nu} (K - Q) \right\} \gamma_\mu (T^a)^T \, \Xi^+(Q) \, \gamma_\nu T^b \,. \quad (3.27)$$

Here, the sum runs only over relevant quark momenta, $\mu - \Lambda_{\mathrm{q}} \leq q \leq \mu + \Lambda_{\mathrm{q}}$. This is the gap equation for the color-superconducting gap parameter within my effective theory. There is no contribution from irrelevant fermions, since their propagator is diagonal in Nambu-Gor'kov space.

While the gluon cut-off was taken to be $\Lambda_{\mathrm{gl}} \lesssim \mu$, so that soft gluons have typical momenta of order $g\mu$, so far I have not specified the magnitude of Λ_{q}. In weak coupling, the color-superconducting gap function is strongly peaked around the Fermi surface [53, 55, 54]. For a subleading-order calculation of the gap parameter, it is therefore sufficient to consider as relevant quark modes those within a thin layer of width $2\Lambda_{\mathrm{q}}$ around the Fermi surface. For the following, my principal assumption is $\Lambda_{\mathrm{q}} \lesssim g\mu \ll \Lambda_{\mathrm{gl}} \lesssim \mu$. As I shall see below, this assumption is crucial to identify sub-subleading corrections to the gap equation (3.27), which arise, for instance, from the pole of the gluon propagator. Note that this assumption is different from that of Refs. [101, 103], where it is assumed that $\Lambda_{\mathrm{q}} \simeq \Lambda_{\mathrm{gl}}$.

For a two-flavor color superconductor, the color-flavor-spin structure of the gap matrix is [13]

$$\Phi^+(K) = J_3 \tau_2 \gamma_5 \, \Lambda_{\mathbf{k}}^+ \, \Theta(\Lambda_{\mathrm{q}} - |k - \mu|) \, \phi(K) \,, \tag{3.28}$$

where $(J_3)_{ij} \equiv -i\epsilon_{ij3}$ and $(\tau_2)_{fg} \equiv -i\epsilon_{fg}$ represent the fact that quark pairs condense in the color-antitriplet, flavor-singlet channel. The Dirac matrix γ_5 restricts quark pairing to the even-parity channel (which is the preferred one due to the $U(1)_A$ anomaly of QCD). In the effective action (2.46), antiquark and irrelevant quark degrees of freedom are integrated out. The condensation of antiquark or irrelevant quark pairs, while in principle possible, is thus not taken into account; the bilocal source terms in Eq. (3.1) only allow for the condensation of

relevant quark degrees of freedom. The condensation of antiquarks or irrelevant quarks could also be accounted for, if one introduces bilocal source terms already in Eq. (2.6), i.e., *prior* to integrating out any of the quark degrees of freedom. While there is in principle no obstacle in following this course of action, it is, however, not really necessary if one is interested in a calculation of the color-superconducting gap parameter to subleading order in weak coupling: antiquarks contribute to the gap equation beyond subleading order [127], and the gap function for quarks falls off rapidly away from the Fermi surface, i.e., in the region of irrelevant quark modes, and thus also contributes at most to sub-subleading order to the gap equation. Consequently, the Dirac structure of the gap matrix (3.27) contains only the projector $\Lambda_{\mathbf{k}}^+$ onto positive energy states. The theta function accounts for the fact that the gap function $\phi(K)$ pertains only to relevant quark modes.

Inserting Eq. (3.25) and the corresponding one for $[G^-]^{-1} + \Sigma^-$, as well as Eq. (3.28), into the definition (3.9) for the anomalous quark propagator, one obtains

$$\Xi^+(Q) = J_3\tau_2\gamma_5\,\Lambda_{\mathbf{q}}^-\,\Theta(\Lambda_{\mathrm{q}} - |q - \mu|)\,\frac{\phi(Q)}{[q_0/Z(q_0)]^2 - \epsilon_q^2}\,. \tag{3.29}$$

One now plugs this expression into the gap equation (3.27), multiplies both sides with $J_3\tau_2\gamma_5\Lambda_{\mathbf{k}}^+$, and traces over color, flavor, and Dirac degrees of freedom. These traces simplify considerably since both hard and HDL gluon propagators are diagonal in adjoint color space, $[\Delta_{0,22}]_{ab}^{\mu\nu} \equiv \delta_{ab}\,\Delta_{0,22}^{\mu\nu}$, $[\Delta_{\mathrm{HDL}}]_{ab}^{\mu\nu} \equiv \delta_{ab}\,\Delta_{\mathrm{HDL}}^{\mu\nu}$. The result is an integral equation for the gap function $\phi(K)$,

$$\phi(K) = \frac{g^2}{3}\frac{T}{V}\sum_Q \left[\Delta_{0,22}^{\mu\nu}(K - Q) + \Delta_{\mathrm{HDL}}^{\mu\nu}(K - Q)\right] \mathrm{Tr}_s\left(\Lambda_{\mathbf{k}}^+\gamma_\mu\Lambda_{\mathbf{q}}^-\gamma_\nu\right)\,\frac{\phi(Q)}{[q_0/Z(q_0)]^2 - \epsilon_q^2}\,. \tag{3.30}$$

The sum over Q runs only over relevant quark momenta, $|q - \mu| \leq \Lambda_{\mathrm{q}}$. Also, the 3-momentum $\mathbf{k}$ is relevant, $|k - \mu| \leq \Lambda_{\mathrm{q}}$.

3.1.3 Solution of the gap equation to sub-leading order

In pure Coulomb gauge, both the hard gluon and the HDL propagators have the form

$$\Delta^{00}(P) = \Delta^\ell(P) \quad,\quad \Delta^{0i}(P) = 0 \quad,\quad \Delta^{ij}(P) = (\delta^{ij} - \hat{p}^i\hat{p}^j)\,\Delta^t(P)\,, \tag{3.31}$$

where $\Delta^{\ell,t}$ are the propagators for longitudinal and transverse gluon degrees of freedom. For hard gluons

$$\Delta_{0,22}^\ell(P) = -\frac{1}{p^2}\,, \tag{3.32a}$$

$$\Delta_{0,22}^t(P) = -\frac{1}{P^2}\,, \tag{3.32b}$$

while for soft, HDL-resummed gluons

$$\Delta_{\mathrm{HDL}}^\ell(P) = -\frac{1}{p^2 - \Pi_{\mathrm{HDL}}^\ell(P)}\,, \tag{3.33a}$$

$$\Delta_{\mathrm{HDL}}^t(P) = -\frac{1}{P^2 - \Pi_{\mathrm{HDL}}^t(P)}\,, \tag{3.33b}$$

with the HDL self-energies [9]

$$\Pi^\ell_{\text{HDL}}(p_0, p) = -3\,m_g^2 \left[1 - \frac{p_0}{2p} \ln\left(\frac{p_0 + p}{p_0 - p} \right) \right] , \tag{3.34a}$$

$$\Pi^t_{\text{HDL}}(p_0, p) = \frac{3}{2}\,m_g^2 \left[\frac{p_0^2}{p^2} + \left(1 - \frac{p_0^2}{p^2} \right) \frac{p_0}{2p} \ln\left(\frac{p_0 + p}{p_0 - p} \right) \right] . \tag{3.34b}$$

The HDL propagators (3.33) have quasiparticle poles at $p_0 = \pm\omega_{\ell,t}(p)$, and a cut between $p_0 = -p$ and $p_0 = p$ [9]. The gluon energy on the quasiparticle mass-shell is always larger than the gluon mass parameter, $\omega_{\ell,t}(p) \geq m_g$, where the equality holds for zero momentum, $p = 0$.

(a) (b)
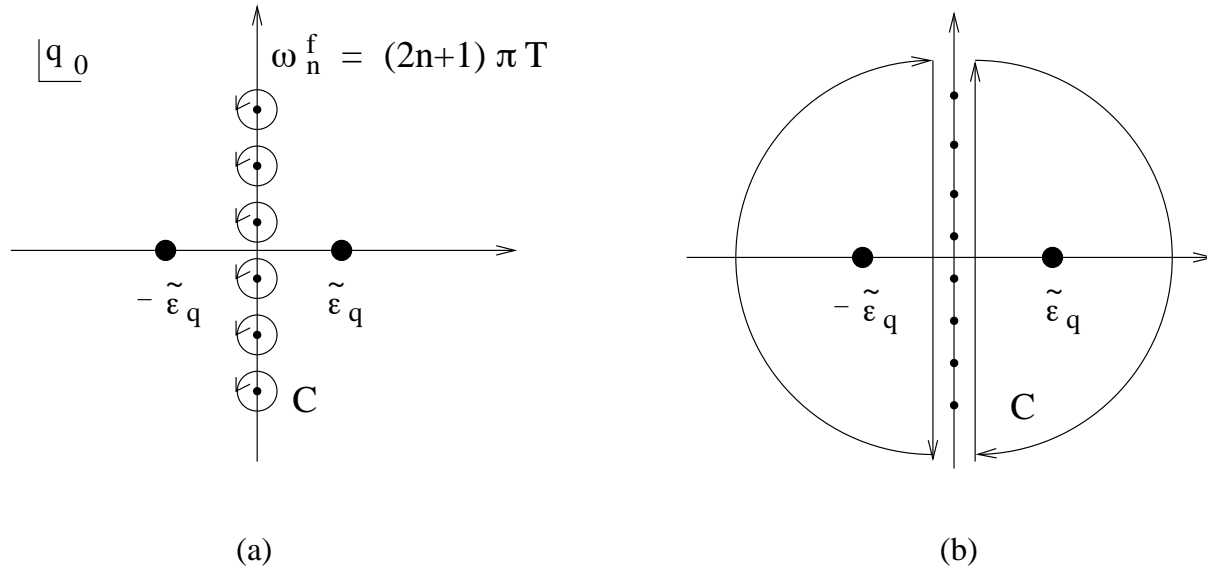
Figure 3.3: (a) The contour $\mathcal{C}$ in Eq. (3.35) encloses the poles of $\tanh[q_0/(2T)]$ on the imaginary q_0 axis. (b) Deforming the contour $\mathcal{C}$ and adding semicircles at infinity to enclose the poles of the quark propagator on the real q_0 axis.

I first perform the Matsubara sum, using the method of contour integration in the complex q_0 plane [9, 15],

$$T \sum_n f(q_0) \equiv \frac{1}{2\pi i} \oint_{\mathcal{C}} dq_0 \, \frac{1}{2} \tanh\left(\frac{q_0}{2T} \right) f(q_0) \tag{3.35}$$

where the contour $\mathcal{C}$ consists of circles running around the poles $\omega_n^{\text{f}} = (2n+1)\pi T$ of $\tanh[q_0/((2T)]$ on the imaginary q_0 axis, cf. Fig. 3.3 (a). Inserting the propagators (3.32) and (3.33) into Eq. (3.30), I have to compute four distinct terms. The first one arises from the exchange of static electric hard gluons. Since $\Delta^\ell_{0,22}(P)$ does not depend on $p_0 = k_0 - q_0$, only the quark propagator gives rise to a pole of $f(q_0)$, cf. Fig. 3.3 (b). After deforming the contour and closing it at infinity as shown in Fig. 3.3 (b), one employs the residue theorem to pick up the poles of the quark propagator,

$$T \sum_n \Delta^\ell_{0,22}(P) \frac{\phi(Q)}{[q_0/Z(q_0)]^2 - \epsilon_q^2} = \frac{1}{p^2} \tanh\left(\frac{\tilde{\epsilon}_q}{2T} \right) \frac{Z^2(\tilde{\epsilon}_q)}{4\,\tilde{\epsilon}_q} \left[\phi(\tilde{\epsilon}_q, \mathbf{q}) + \phi(-\tilde{\epsilon}_q, \mathbf{q}) \right] , \tag{3.36}$$

with $\tilde{\epsilon}_q \equiv \epsilon_q Z(\tilde{\epsilon}_q)$. Here, I have used the fact that the quark wave-function renormalization factor is an even function of its argument, $Z(q_0) \equiv Z(-q_0)$, cf. Eq. (3.26). An essential assumption in order to derive Eq. (3.36) is that the gap function $\phi(Q)$ is analytic in the complex q_0 plane. This assumption will also be made in all subsequent considerations.

Figure 3.4: Same as in Fig. 3.3, but for magnetic hard gluon exchange. Now also the gluon propagator has poles at $k_0 \pm p$ in the complex q_0 plane. These are further away from the imaginary axis than the poles $\tilde{\epsilon}_q$ of the quark propagator, because for my choice of quark and gluon cut-offs, $\Lambda_{\rm q} \ll \Lambda_{\rm gl}$, I have $\tilde{\epsilon}_q \lesssim \Lambda_{\rm q} \ll \Lambda_{\rm gl} \leq p$.

By the same method one computes the second term in Eq. (3.30), corresponding to magnetic hard gluon exchange. This is slightly more comp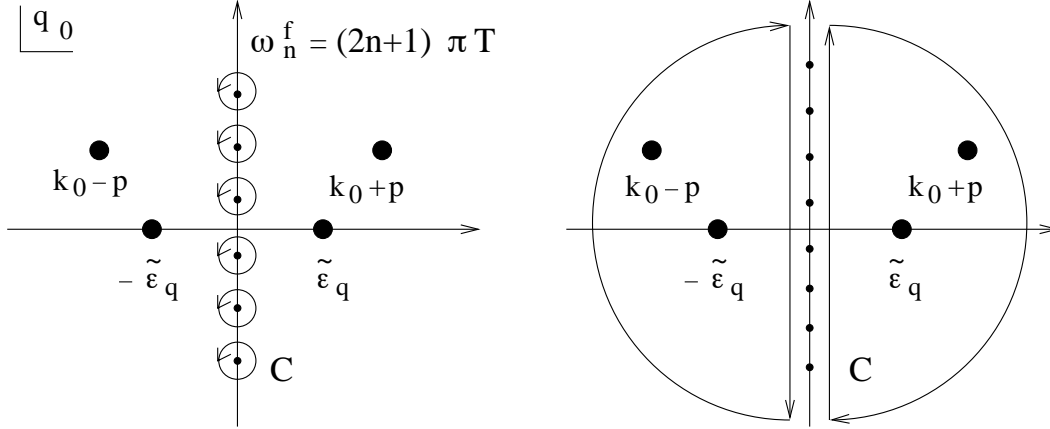licated, since not only the quark propagator but also $\Delta_{0,22}^t(P)$ has poles in the complex q_0 plane. The latter are located at $p_0 = \pm p$, i.e., $q_0 = k_0 \pm p$, cf. Fig. 3.4. The external quark energy k_0 is fixed and, prior to analytic continuation $k_0 \rightarrow \tilde{\epsilon}_k + i\eta$ to the quasiparticle mass-shell, is equal to one particular fermionic Matsubara frequency, cf. Fig. 3.4. The residue theorem now yields four contributions, two from the quark and two from the gluon poles. Using $\tanh[(k_0 \pm p)/(2T)] \equiv \pm \coth(p/2T)$ and analytically continuing $k_0 \rightarrow \tilde{\epsilon}_k + i\eta$ I find

$$T \sum_n \Delta_{0,22}^t(P) \frac{\phi(Q)}{[q_0/Z(q_0)]^2 - \epsilon_q^2} =$$

$$\tanh\left(\frac{\tilde{\epsilon}_q}{2T}\right) \frac{Z^2(\tilde{\epsilon}_q)}{4\,\tilde{\epsilon}_q} \left[\frac{\phi(\tilde{\epsilon}_q, \mathbf{q})}{(\tilde{\epsilon}_k - \tilde{\epsilon}_q + i\eta)^2 - p^2} + \frac{\phi(-\tilde{\epsilon}_q, \mathbf{q})}{(\tilde{\epsilon}_k + \tilde{\epsilon}_q + i\eta)^2 - p^2} \right]$$

$$+ \coth\left(\frac{p}{2T}\right) \frac{1}{4p} \left[\frac{Z^2(p + \tilde{\epsilon}_k)\,\phi(p + \tilde{\epsilon}_k, \mathbf{q})}{(p + \tilde{\epsilon}_k + i\eta)^2 - \epsilon_q^2 Z^2(p + \tilde{\epsilon}_k)} + \frac{Z^2(p - \tilde{\epsilon}_k)\,\phi(\tilde{\epsilon}_k - p, \mathbf{q})}{(p - \tilde{\epsilon}_k - i\eta)^2 - \epsilon_q^2 Z^2(p - \tilde{\epsilon}_k)} \right] . \quad (3.37)$$

Since the gluon momentum is hard, $p \geq \Lambda_{\rm gl}$, and thus much larger than the quasiparticle energies $\tilde{\epsilon}_k, \tilde{\epsilon}_q$ which are at most of the order of the quark cut-off $\Lambda_{\rm q} \ll \Lambda_{\rm gl}$, to order $O(\Lambda_{\rm q}/\Lambda_{\rm gl})$ one may neglect the terms $(\tilde{\epsilon}_k \pm \tilde{\epsilon}_q + i\eta)^2$ in the energy denominators of the first term. Furthermore, in the second term one may approximate $Z(p \pm \tilde{\epsilon}_k) \simeq Z(p) = 1 + O(g^2)$ and $\phi(p \pm \tilde{\epsilon}_k, \mathbf{q}) \simeq \phi(p, \mathbf{q})$. Note that the gap function is far off-shell for $p \geq \Lambda_{\rm gl} \gg \Lambda_{\rm q} \geq |\mu - q|$. Then, to order $O(\Lambda_{\rm q}/\Lambda_{\rm gl})$,

one may also neglect $\tilde{\epsilon}_k, \tilde{\epsilon}_q$ in the energy denominators of the second term. I obtain

$$
T \sum_n \Delta_{0,22}^t(P) \frac{\phi(Q)}{[q_0/Z(q_0)]^2 - \epsilon_q^2} =
$$
$$
-\frac{1}{p^2} \tanh\left(\frac{\tilde{\epsilon}_q}{2T}\right) \frac{Z^2(\tilde{\epsilon}_q)}{4\,\tilde{\epsilon}_q} \, [\phi(\tilde{\epsilon}_q, \mathbf{q}) + \phi(-\tilde{\epsilon}_q, \mathbf{q})] \left[1 + O\left(\frac{\Lambda_{\mathrm{q}}^2}{\Lambda_{\mathrm{gl}}^2}\right)\right]
$$
$$
+ \coth\left(\frac{p}{2T}\right) \frac{\phi(p, \mathbf{q})}{2\,p^3} \left[1 + O\left(\frac{\Lambda_{\mathrm{q}}^2}{\Lambda_{\mathrm{gl}}^2}\right)\right] \; . \tag{3.38}
$$

As a next step one estimates to which order the two remaining terms contribute to the gap equation (3.30). At $T = 0$, one may set the hyperbolic functions to one. I shall also ignore the difference between the on-shell and off-shell gap functions, and take $\phi(p, \mathbf{q}) \simeq \phi(\pm\tilde{\epsilon}_q, \mathbf{q}) \equiv \phi = const.$. For the purpose of power counting, one may restrict oneself to the leading contribution of the Dirac traces in Eq. (3.30), which is of order one, cf. Eqs. (3.55) below. In order to obtain the leading contribution of the first term in Eq. (3.38), one may also set $Z^2(\tilde{\epsilon}_q) \simeq 1$. The integral over the absolute magnitude of the quark momentum is $\int dq\, q^2$, while the angular integration is $\int d\cos\theta \equiv \int dp\, p/(kq)$. Then, the first term in Eq. (3.38) leads to the following contribution in the gap equation

$$
g^2 \frac{\phi}{k} \int_{\mu-\Lambda_{\mathrm{q}}}^{\mu+\Lambda_{\mathrm{q}}} dq \frac{q}{\epsilon_q} \int_{\Lambda_{\mathrm{gl}}}^{k+q} \frac{dp}{p} \simeq g^2\,\phi\, \ln\left(\frac{2\Lambda_{\mathrm{q}}}{\phi}\right) \ln\left(\frac{2\mu}{\Lambda_{\mathrm{gl}}}\right) \sim g^2\,\phi\, \frac{1}{g} = g\,\phi \; , \tag{3.39}
$$

where I approximated $k \simeq q \simeq \mu$ and employed the weak-coupling solution (1.36) to estimate $\ln(2\Lambda_{\mathrm{q}}/\phi) \sim 1/g$. Furthermore, for $\Lambda_{\mathrm{gl}} \lesssim \mu$, the angular logarithm is $\ln(2\mu/\Lambda_{\mathrm{gl}}) \sim O(1)$. According to the discussion presented in the introduction, the contribution from hard magnetic gluon exchange is thus of subleading order in the gap equation. Note that the term arising from hard electric gluon exchange, Eq. (3.36), is of the same order as the first term in Eq. (3.38), and thus also contributes to subleading order. The way I estimated the first term on the right-hand side of Eq. (3.38) is equivalent to just taking the hard magnetic gluon propagator in the static limit, $\Delta_{0,22}^t(P) \simeq 1/p^2$, which is correct up to terms of order $O(\Lambda_{\mathrm{q}}^2/\Lambda_{\mathrm{gl}}^2)$. To this order, the propagator for hard magnetic gluons is thus (up to a sign) identical to the one for hard electric gluons. Since the ratio $\Lambda_{\mathrm{q}}/\Lambda_{\mathrm{gl}} \simeq g\mu/\mu \equiv g$, this approximation introduces corrections at order $O(g^3\phi)$ in the gap equation, which is *beyond* sub-subleading order, $O(g^2\phi)$.

Similarly, I estimate the contribution of the second term in Eq. (3.38) to the gap equation (3.30),

$$
g^2 \frac{\phi}{k} \int_{\mu-\Lambda_{\mathrm{q}}}^{\mu+\Lambda_{\mathrm{q}}} dq\, q \int_{\Lambda_{\mathrm{gl}}}^{k+q} \frac{dp}{p^2} \sim g^2\,\phi\, \frac{\Lambda_{\mathrm{q}}}{\Lambda_{\mathrm{gl}}} \sim g^3\phi \; , \tag{3.40}
$$

i.e., for my choice $\Lambda_{\mathrm{q}}/\Lambda_{\mathrm{gl}} \sim g$, this term contributes beyond sub-subleading order. Note that this estimate is conservative, as I assumed the off-shell gap function to be of the same order as the gap at the Fermi surface, $\phi(p, \mathbf{q}) \sim \phi$. However, I know [55] that, for energies far from the Fermi surface, $\tilde{\epsilon}_q \sim \Lambda_{\mathrm{q}} \lesssim g\mu$, even the on-shell gap function is suppressed by one power of g compared to the value of the gap at the Fermi surface, $\phi(\Lambda_{\mathrm{q}}, \mathbf{q}) \sim g\phi$. The off-shell gap function at $q_0 = p \gtrsim \Lambda_{\mathrm{gl}} \gg \Lambda_{\mathrm{q}}$ may be even smaller. In order to decide this issue, one would

have to perform a computation of the gap function for arbitrary values of the energy q_0, and not just on the quasiparticle mass-shell, $q_0 \equiv \tilde{\epsilon}_q$. I note that for the choice $\Lambda_q \simeq \Lambda_{gl}$ for the cut-offs [101, 103], the ratio Λ_q/Λ_{gl} is of order one and cannot be used as a parameter to sort the various contributions according to their order of magnitude. The expansion of the denominators in powers of Λ_q/Λ_{gl} as seen on the right-hand side of Eq. (3.38) is then inapplicable.
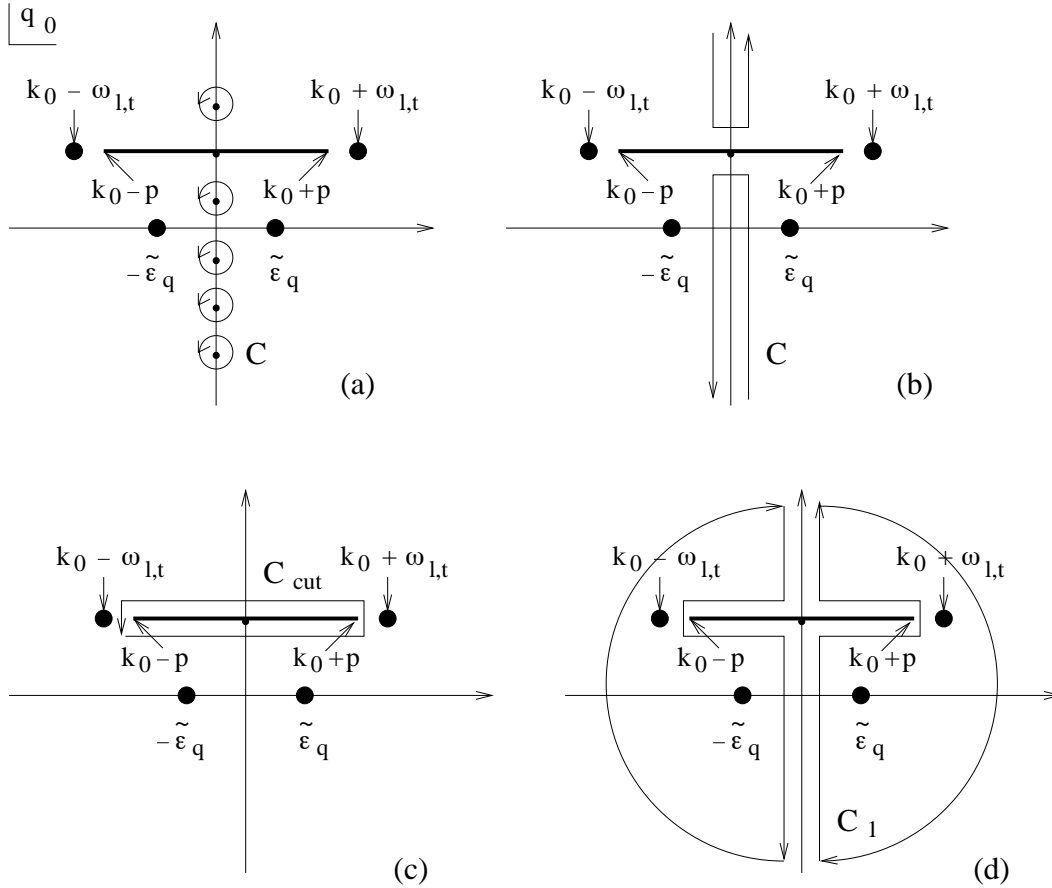
Figure 3.5: Evaluating the Matsubara sum for HDL-resummed gluon propagators. (a) The original contour $\mathcal{C}$ in Eq. (3.35). There is no circle around the point $k_0 = q_0$, where the corresponding term in the Matsubara sum has a cut arising from the HDL gluon propagator. (b) Deforming the contour $\mathcal{C}$. (c) The contour $\mathcal{C}_{\mathrm{cut}}$ running around the cut. (d) The contour $\mathcal{C}_1 = \mathcal{C} + \mathcal{C}_{\mathrm{cut}}$ which is closed at infinity.

The third and fourth terms in the gap equation (3.30) arise from soft, HDL-resummed electric and magnetic gluon exchange. Evaluating the Matsubara sum via contour integration in the complex q_0 plane is considerably more difficult than in the previous cases, because the HDL gluon propagators $\Delta_{\mathrm{HDL}}^{\ell,t}$ do not only have poles but also cuts. The analytic structure is shown in Fig. 3.5 (a). Besides the poles of the quark propagator at $q_0 = \pm\tilde{\epsilon}_q$, there are also those from the gluon propagator at $q_0 = k_0 \pm \omega_{\ell,t}(p)$. The cut of the gluon propagator between $-p \leq p_0 \leq p$ translates into a cut between $k_0 - p \leq q_0 \leq k_0 + p$. Prior to analytic continuation, the gluon poles and the cut are shifted away from the real axis and located at the (imaginary) external

Matsubara frequency k_0.

The Matsubara sum over q_0 is evaluated in the standard way, cf. Eq. (3.35), with the caveat that the contribution at $q_0 = k_0$, where the cut of the gluon propagator is located, has to be omitted. This is similar to the zero-temperature case where the Matsubara sum becomes a continuous integral along the imaginary q_0 axis and where one has to avoid integrating over the cut. Alternatively, the term $q_0 = k_0$ can be included in the Matsubara sum if one shifts the cut by some small amount $\pm i\epsilon$ along the imaginary q_0 axis. The final result will be the same, as one still has to circumvent the cut by a proper choice of the integration contour.

I now deform the contour as shown in Fig. 3.5 (b), and add and subtract a contour integral running around the cut, Fig. 3.5 (c). The integral over the contour $\mathcal{C} + \mathcal{C}_{\text{cut}}$ can be closed at infinity, yielding the contour $\mathcal{C}_1$ shown in Fig. 3.5 (d). One obtains

$$
T \sum_n \Delta^{\ell,t}_{\text{HDL}}(P) \frac{\phi(Q)}{[q_0/Z(q_0)]^2 - \epsilon_q^2} =
$$
$$
\frac{1}{2\pi i} \left[\oint_{\mathcal{C}_1} - \oint_{\mathcal{C}_{\text{cut}}} \right] dq_0 \, \frac{1}{2} \, \tanh\left(\frac{q_0}{2T}\right) \Delta^{\ell,t}_{\text{HDL}}(P) \frac{\phi(Q)}{[q_0/Z(q_0)]^2 - \epsilon_q^2} \, . \tag{3.41}
$$

Evaluating the integral over $\mathcal{C}_1$ is rather similar to the case of hard gluon exchange: one just picks up the poles of the quark and gluon propagators inside the contour $\mathcal{C}_1$. After analytic continuation $k_0 \to \tilde{\epsilon}_k + i\eta$ one obtains

$$
\frac{1}{2\pi i} \oint_{\mathcal{C}_1} dq_0 \, \frac{1}{2} \, \tanh\left(\frac{q_0}{2T}\right) \Delta^{\ell,t}_{\text{HDL}}(P) \frac{\phi(Q)}{[q_0/Z(q_0)]^2 - \epsilon_q^2} \simeq
$$
$$
- \tanh\left(\frac{\tilde{\epsilon}_q}{2T}\right) \frac{Z^2(\tilde{\epsilon}_q)}{4\,\tilde{\epsilon}_q} \left[\Delta^{\ell,t}_{\text{HDL}}(\tilde{\epsilon}_k - \tilde{\epsilon}_q + i\eta, \mathbf{p}) \, \phi(\tilde{\epsilon}_q, \mathbf{q}) + \Delta^{\ell,t}_{\text{HDL}}(\tilde{\epsilon}_k + \tilde{\epsilon}_q + i\eta, \mathbf{p}) \, \phi(-\tilde{\epsilon}_q, \mathbf{q}) \right]
$$
$$
- \coth\left(\frac{\omega_{\ell,t}}{2T}\right) \frac{1}{2\,\omega_{\ell,t}^2} \left[\phi(\omega_{\ell,t} + \tilde{\epsilon}_k, \mathbf{q}) \, Z_{\ell,t}(-\omega_{\ell,t}, p) - \phi(\tilde{\epsilon}_k - \omega_{\ell,t}, \mathbf{q}) \, Z_{\ell,t}(\omega_{\ell,t}, p) \right]
$$
$$
\times \left[1 + O\left(\frac{\epsilon_q^2}{\omega_{\ell,t}^2}\right) \right] \, . \tag{3.42}
$$

Here, I approximated the quark wave-function renormalization factor $Z(\omega_{\ell,t} \pm \tilde{\epsilon}_k) \simeq 1 + O(g^2)$. I also expanded the denominators of the quark propagator $(\tilde{\epsilon}_k \pm \omega_{\ell,t} + i\eta)^2 - \epsilon_q^2 \simeq \omega_{\ell,t}^2 [1 + O(\epsilon_q^2/\omega_{\ell,t}^2)]$. For my choice of the cut-off $\Lambda_q \lesssim g\mu \sim m_g$, I may estimate $\omega_{\ell,t} \geq m_g \gtrsim \Lambda_q \geq \epsilon_q$, i.e., the corrections of order $O(\epsilon_q^2/\omega_{\ell,t}^2)$ are small everywhere except for a small region of phase space where $p \simeq 0$ and $\epsilon_q \simeq \Lambda_q$. (In principle, in the expansion of the denominators there are also linear terms, $\sim \pm \tilde{\epsilon}_k/\omega_{\ell,t}$, but these are very small everywhere for external momenta close to the Fermi surface, $k \simeq \mu$.) Note that the gap function is again off-shell at the gluon pole, although not as far as in the case of hard gluon exchange, cf. Eq. (3.38). The residues of the HDL gluon propagators at the respective poles are [9]

$$
Z_\ell(\omega_\ell, p) = \frac{\omega_\ell(\omega_\ell^2 - p^2)}{p^2(p^2 + 3m_g^2 - \omega_\ell^2)} \, , \tag{3.43a}
$$

$$
Z_t(\omega_t, p) = \frac{\omega_t(\omega_t^2 - p^2)}{3m_g^2\omega_t^2 - (\omega_t^2 - p^2)^2} \, . \tag{3.43b}
$$

To very good approximation, one finds that $Z_t(\omega_t, p) \simeq 1/(2\omega_t)$ for all momenta p. In the longitudinal case, the residue is very well approximated by $Z_l(\omega_l, p) \simeq \omega_l/(2\,p^2)$ for small momenta $p \lesssim m_g$, while for large momenta, $m_g \ll p$, $Z_l(\omega_l, p) \sim \exp[-2p^2/(3m_g^2)]/p$, i.e., it is exponentially suppressed [128].

These approximate forms allow for a simple power counting of the gluon-pole contribution in Eq. (3.42) to the gap equation (3.30). To this end, I approximate the gap function by its value at the Fermi surface, $\phi(\pm\omega_{\ell,t} + \tilde{\epsilon}_k, \mathbf{q}) \simeq \phi$, and consider the limiting case $T = 0$ where $\coth[\omega_{\ell,t}/(2T)] = 1$. Then, the contribution from the longitudinal gluon pole is

$$g^2 \frac{\phi}{k} \int_{\mu-\Lambda_{\mathrm{q}}}^{\mu+\Lambda_{\mathrm{q}}} dq\, q \left[\int_{|k-q|}^{m_g} \frac{dp}{2\,p\,\omega_\ell} + \int_{m_g}^{\Lambda_{\mathrm{gl}}} \frac{dp}{\omega_\ell^2} \exp\left(-\frac{2p^2}{3m_g^2}\right) \right] \sim g^2\, \phi\, \frac{\Lambda_{\mathrm{q}}}{m_g} \sim g^2 \phi \ . \tag{3.44}$$

In the first p integral, which only runs up to the scale m_g, one may approximate $\omega_\ell \simeq m_g$, while in the second p integral, which runs from m_g to $\Lambda_{\mathrm{gl}} \lesssim \mu$, one may take $\omega_\ell \simeq p$. To obtain the right-hand side of Eq. (3.44) I have set $k \simeq q \simeq \mu$, and I have employed my choice $\Lambda_{\mathrm{q}} \lesssim g\mu$ for the quark cut-off. This also allowed me to approximate logarithms of Λ_{q}/m_g by numbers of order $O(1)$. With this choice for the quark cut-off, the contribution (3.44) is of sub-subleading order, $\sim O(g^2\phi)$, to the gap equation.

With a more careful evaluation of the integrals, one could extract the precise numerical prefactor of the sub-subleading contribution (3.44). Note, however, that further suppression factors may arise from the off-shellness of the gap function at $\phi(\pm\omega_{\ell,t}+\tilde{\epsilon}_k, \mathbf{q})$, which consequently would render this contribution beyond sub-subleading order. As noted previously, this issue can only be decided if $\phi(q_0, \mathbf{q})$ is known also off the quasiparticle mass-shell, and not only on-shell. I also note that the $1/p^2$ factor in the residue Z_ℓ is an artifact of the Coulomb gauge [128], and does not appear in e.g. covariant gauge. One would have to collect all other terms of sub-subleading order to make sure that the complete sub-subleading contribution is gauge invariant and the term (3.44) is not cancelled by some other terms.

Similarly, I estimate the contribution from the transverse gluon pole,

$$g^2 \frac{\phi}{k} \int_{\mu-\Lambda_{\mathrm{q}}}^{\mu+\Lambda_{\mathrm{q}}} dq\, q \int_{|k-q|}^{\Lambda_{\mathrm{gl}}} \frac{dp\, p}{2\,\omega_t^3} \sim g^2 \phi \int_0^{\Lambda_{\mathrm{q}}} d\xi \int_{m_g}^{\Lambda_{\mathrm{gl}}} \frac{d\omega_t}{\omega_t^2} \sim g^2 \phi\, \frac{\Lambda_{\mathrm{q}}}{m_g} \sim g^2 \phi \ , \tag{3.45}$$

where I defined $\xi \equiv q - \mu$. I approximated $dp\, p \simeq d\omega_t\, \omega_t$ since, for the purpose of power counting, to very good approximation one may take the dispersion relation of the transverse gluon equal to that of a relativistic particle with mass m_g, $\omega_t(p) \simeq (p^2+m_g^2)^{1/2}$. I also used $\Lambda_{\mathrm{q}} \lesssim m_g \ll \Lambda_{\mathrm{gl}}$ and $k \simeq q \simeq \mu$. In conclusion, also the transverse gluon pole possibly contributes to sub-subleading order in the gap equation, with the same caveats concerning the off-shellness of the gap function as mentioned previously.

Let us now focus on the integral around the cut of the gluon propagator in Eq. (3.41). I substitute q_0 by $p_0 = k_0 - q_0 \equiv \omega$ and use the fact that $\tanh[q_0/(2T)] \equiv -\coth[\omega/(2T)]$. Since the gluon propagator is the only part of the integrand which is discontinuous across the cut, I obtain after analytic continuation $k_0 \to \tilde{\epsilon}_k + i\eta$

$$-\frac{1}{2\pi i} \oint_{\mathcal{C}_{\mathrm{cut}}} dq_0\, \frac{1}{2} \tanh\left(\frac{q_0}{2T}\right) \Delta_{\mathrm{HDL}}^{\ell,t}(P) \frac{\phi(Q)}{[q_0/Z(q_0)]^2 - \epsilon_q^2}$$

$$= \int_{-p}^{p} d\omega\, \frac{1}{2} \coth\left(\frac{\omega}{2T}\right) \frac{Z^2(\tilde{\epsilon}_k - \omega)\, \phi(\tilde{\epsilon}_k - \omega, \mathbf{q})}{(\tilde{\epsilon}_k - \omega + i\eta)^2 - [Z(\tilde{\epsilon}_k - \omega)\, \epsilon_q]^2}\, \rho_{\mathrm{cut}}^{\ell,t}(\omega, \mathbf{p}) \ , \tag{3.46}$$

where $\rho_{\mathrm{cut}}^{\ell,t}(\omega, p) \equiv \mathrm{Im}\Delta_{\mathrm{HDL}}^{\ell,t}(\omega + i\eta, p)/\pi$ is the spectral density of the HDL propagator arising from the cut. Explicitly,

$$\rho_{\mathrm{cut}}^{\ell}(\omega, \mathbf{p}) = \frac{2M^2}{\pi} \frac{\omega}{p} \left\{ \left[p^2 + 3\, m_g^2 \left(1 - \frac{\omega}{2p} \ln \left| \frac{p+\omega}{p-\omega} \right| \right) \right]^2 + \left(2M^2 \frac{\omega}{p} \right)^2 \right\}^{-1} , \tag{3.47a}$$

$$\rho_{\mathrm{cut}}^{t}(\omega, \mathbf{p}) = \frac{M^2}{\pi} \frac{\omega}{p} \frac{p^2}{p^2 - \omega^2} \left\{ \left[p^2 + \frac{3}{2} m_g^2 \left(\frac{\omega^2}{p^2 - \omega^2} + \frac{\omega}{2p} \ln \left| \frac{p+\omega}{p-\omega} \right| \right) \right]^2 + \left(M^2 \frac{\omega}{p} \right)^2 \right\}^{-1} . \tag{3.47b}$$

In order to power count the contribution from the cut of $\Delta_{\mathrm{HDL}}^{\ell}$ to the gap equation, it is sufficient to approximate the spectral density by [55]

$$\rho_{\mathrm{cut}}^{\ell}(\omega, \mathbf{p}) \simeq \frac{2M^2}{\pi} \frac{\omega}{p} \frac{1}{(p^2 + 3\, m_g^2)^2} . \tag{3.48}$$

This form reproduces the correct behavior for $\omega \ll p$. For $\omega \lesssim p$, it overestimates the spectral density when $p \lesssim m_g$, while it slightly underestimates it for $p \gtrsim m_g$. For the gap equation, however, this region is unimportant, since the respective contribution is suppressed by the large energy denominator $(\tilde{\epsilon}_k - \omega + i\eta)^2 - [Z(\tilde{\epsilon}_k - \omega)\,\epsilon_q]^2 \simeq p^2$ in Eq. (3.46). To leading order, one may set $Z(\tilde{\epsilon}_k - \omega) \simeq 1$. I also approximate $\phi(\tilde{\epsilon}_k - \omega, \mathbf{q}) \simeq \phi$. Then, the ω integral can be performed analytically. (One may compute this integral with the principal value prescription; the contribution from the complex pole contributes to the imaginary part of the gap function, which I neglect throughout this computation to subleading order, cf. Sec. 3.2.) This produces at most logarithmic singularities, which are integrable. I therefore simply approximate the ω integral by a number of order $O(1)$. Consequently, the contribution from Eq. (3.46) to the gap equation is of order

$$g^2 \frac{\phi}{k} \int_{\mu - \Lambda_q}^{\mu + \Lambda_q} dq\, q \int_{|k-q|}^{\Lambda_{\mathrm{gl}}} dp \, \frac{m_g^2}{(p^2 + 3\, m_g^2)^2} \quad \sim \quad g^2 \phi \int_0^{\Lambda_q} d\xi \left(\int_\xi^{m_g} \frac{dp}{m_g^2} + m_g^2 \int_{m_g}^{\Lambda_{\mathrm{gl}}} \frac{dp}{p^4} \right)$$

$$\sim \quad g^2 \phi \frac{\Lambda_q}{m_g} \sim g^2 \phi , \tag{3.49}$$

where I approximated the p integral by a method similar to the one employed in Eq. (3.44). For my choice $\Lambda_q \lesssim g\mu$, Eq. (3.49) constitutes another (potential) contribution of sub-subleading order to the gap equation.

Finally, I estimate the contribution from the cut of the transverse gluon propagator. For all momenta p and energies $-p \le \omega \le p$, a very good approximation for the spectral density (3.47b) is given by the formula

$$\rho_{\mathrm{cut}}^{t}(\omega, \mathbf{p}) \simeq \frac{M^2}{\pi} \frac{\omega\, p}{p^6 + (M^2\, \omega)^2} . \tag{3.50}$$

This approximate result constitutes an upper bound for the full result (3.47b). The advantage of using this approximate form is that, interchanging the order of the p and ω integration in the gap

equation, the former may immediately be performed. Approximating $Z(\tilde{\epsilon}_k - \omega) \simeq 1$, neglecting the dependence of the gap function on the direction of $\mathbf{q}$, and defining $\lambda \equiv \max(|k - q|, \omega)$, at $T = 0$ the contribution to the gap equation is

$$
g^2 \int_{\mu-\Lambda_q}^{\mu+\Lambda_q} dq \, \frac{q}{k} \int_0^{\Lambda_{gl}} d\omega \sum_{\sigma=\pm} \frac{\phi(\tilde{\epsilon}_k - \sigma\omega, q)}{(\tilde{\epsilon}_k - \sigma\omega)^2 - \epsilon_q^2} \left[\arctan\left(\frac{\Lambda_{gl}^3}{\omega M^2}\right) - \arctan\left(\frac{\lambda^3}{\omega M^2}\right) \right]
$$
$$
\sim g^2 \int_0^{\Lambda_q} \frac{d\xi}{\epsilon_q} \int_0^M d\omega \sum_{\sigma_1,\sigma_2=\pm} \frac{\sigma_1 \, \phi(\tilde{\epsilon}_k - \sigma_2\,\omega, q)}{\tilde{\epsilon}_k - \sigma_2\omega - \sigma_1\epsilon_q} \tag{3.51}
$$

Here, I have used the fact that the particular combination of arctan's in the first line effectively cuts off the ω integral at the scale $\omega \sim M$. As usual, I have set $k \simeq q \simeq \mu$. After estimating $\phi(\tilde{\epsilon}_k \pm \omega, q) \simeq \phi$ one first performs the integral over ω

$$
g^2 \phi \int_0^{\Lambda_q} \frac{d\xi}{\epsilon_q} \int_0^M d\omega \sum_{\sigma_1,\sigma_2=\pm} \frac{\sigma_1}{\tilde{\epsilon}_k - \sigma_2\omega - \sigma_1\epsilon_q}
$$
$$
= -g^2 \phi \int_0^{\Lambda_q} \frac{d\xi}{\epsilon_q} \sum_{\sigma_1,\sigma_2=\pm} \sigma_1\sigma_2 \ln\left| \frac{\tilde{\epsilon}_k - \sigma_1\epsilon_q - \sigma_2 M}{\tilde{\epsilon}_k - \sigma_1\epsilon_q} \right| . \tag{3.52}
$$

The denominator under the logarithm in Eq. (3.52) does not contribute because of the sum over σ_2. In the region $\xi > \phi$ one may neglect $\tilde{\epsilon}_k$ in the numerator under the logarithm and obtains

$$
2g^2 \phi \int_\phi^{\Lambda_q} \frac{d\xi}{\epsilon_q} \ln\left| \frac{\epsilon_q + M}{\epsilon_q - M} \right| \sim g^2 \phi , \tag{3.53}
$$

where the estimate on the r.h.s results after expanding the logarithm in powers of ϵ_q/M. In the region $\xi < \phi$ one has

$$
g^2 \phi \int_0^\phi \frac{d\xi}{\epsilon_q} \sum_{\sigma_1,\sigma_2=\pm} \sigma_1\sigma_2 \ln\left| 1 - \sigma_2\frac{\tilde{\epsilon}_k - \sigma_1\epsilon_q}{M} \right| \sim g^2 \phi \, \frac{\phi}{M} . \tag{3.54}
$$

Consequently, the contribution (3.51) is at most of sub-subleading order.

The remaining term from the evaluation of the Matsubara sum in Eq. (3.41) is the contribution from the quark pole, i.e., the first line of Eq. (3.42). This has to be combined with the subleading-order terms from hard-gluon exchange, i.e., from Eq. (3.36) and from the first line of Eq. (3.38), in order to obtain the gap equation which contains all contributions of leading and subleading order. Before doing so, however, I also evaluate the Dirac traces in Eq. (3.30). In pure Coulomb gauge, I only require

$$
\text{Tr}_s \left(\Lambda_{\mathbf{k}}^+ \gamma_0 \Lambda_{\mathbf{q}}^- \gamma_0 \right) = \frac{(k+q)^2 - p^2}{2\,k\,q} , \tag{3.55a}
$$

$$
(\delta^{ij} - \hat{p}^i\hat{p}^j) \, \text{Tr}_s \left(\Lambda_{\mathbf{k}}^+ \gamma_i \Lambda_{\mathbf{q}}^- \gamma_j \right) = -2 - \frac{p^2}{2\,k\,q} + \frac{(k^2 - q^2)^2}{2\,k\,q\,p^2} , \tag{3.55b}
$$

where I used $p^2 \equiv (\mathbf{k} - \mathbf{q})^2 = k^2 + q^2 - 2\,k\,q\,\hat{\mathbf{k}}\cdot\hat{\mathbf{q}}$ to eliminate $\hat{\mathbf{k}}\cdot\hat{\mathbf{q}}$ in favor of p^2. Let us estimate the order of magnitude of the terms arising from the traces at the Fermi surface, $k \equiv \mu$. Setting

$q \equiv \mu + \xi$, where $-\Lambda_{\mathrm{q}} \leq \xi \leq \Lambda_{\mathrm{q}}$, one obtains

$$\mathrm{Tr}_s \left(\Lambda_{\mathbf{k}}^+ \gamma_0 \Lambda_{\mathbf{q}}^- \gamma_0 \right) \; = \; 2 - \frac{p^2}{2\,k\,q} + O\left(\frac{\xi^2}{\mu^2} \right) \, , \tag{3.56a}$$

$$(\delta^{ij} - \hat{p}^i \hat{p}^j)\,\mathrm{Tr}_s \left(\Lambda_{\mathbf{k}}^+ \gamma_i \Lambda_{\mathbf{q}}^- \gamma_j \right) \; = \; -2 - \frac{p^2}{2\,k\,q} + O\left(\frac{\xi^2}{\mu^2} \right) \, . \tag{3.56b}$$

As shown above, the contribution from hard-gluon exchange is at most of subleading order. Thus, for this contribution it is sufficient to keep only the leading terms in Eq. (3.56), i.e., one may safely neglect terms of order $O(\xi^2/\mu^2) \lesssim O(\Lambda_{\mathrm{q}}^2/\Lambda_{\mathrm{gl}}^2) \sim O(g^2)$ or higher. Note that, since for hard gluon exchange $p \sim \mu \gtrsim \Lambda_{\mathrm{gl}}$, the terms $p^2/(2kq)$ cannot be omitted. However, since the magnetic gluon propagator is effectively $\sim 1/p^2$, cf. Eq. (3.38), i.e., (up to a sign) identical to the electric propagator, these terms will ultimately cancel between the electric and the magnetic contribution. This cancellation is well known, see for instance Ref. [76], and is special to the spin-zero case. It does not occur in spin-one color superconductors where there is an additional exponential prefactor which suppresses the magnitude of the spin-one gap relative to the spin-zero case [76].

As is well known, electric soft-gluon exchange also contributes to subleading order in the gap equation. Thus, as in the case of hard-gluon exchange, one may drop the terms of order $O(\xi^2/\mu^2)$ in Eq. (3.56a). On the other hand, magnetic soft-gluon exchange constitutes the leading order contribution to the gap equation. I therefore would have to keep all terms up to *sub*leading order, i.e., $\sim O(\xi/\mu)$. Fortunately, the corrections to the result (3.56b) are of order $O(\xi^2/\mu^2) \sim O(g^2)$, i.e., they are of *sub-sub*leading order and thus can also be omitted.

I combine Eqs. (3.36), (3.38), and the first line of Eq. (3.42), and assume that the gap function is even in its energy argument, $\phi(-\tilde{\epsilon}_q, \mathbf{q}) = \phi(\tilde{\epsilon}_q, \mathbf{q})$, and isotropic, $\phi(\tilde{\epsilon}_q, \mathbf{q}) \equiv \phi(\tilde{\epsilon}_q, q) \equiv \phi_q$. Then, on the quasiparticle mass-shell $k_0 = \tilde{\epsilon}_k$ the gap equation (3.30) becomes

$$\phi_k \; = \; \frac{g^2}{24\pi^2} \int_{\mu-\Lambda_{\mathrm{q}}}^{\mu+\Lambda_{\mathrm{q}}} dq\, \frac{q}{k}\, \frac{Z^2(\tilde{\epsilon}_q)}{\tilde{\epsilon}_q}\, \tanh\left(\frac{\tilde{\epsilon}_q}{2T} \right)\, \phi_q \int_{|k-q|}^{k+q} dp\,p \left\{ \Theta(p - \Lambda_{\mathrm{gl}})\,\frac{4}{p^2} + \Theta(\Lambda_{\mathrm{gl}} - p) \right.$$
$$\left. \times \sum_{s=\pm} \left[\Delta_{\mathrm{HDL}}^{\ell}(\tilde{\epsilon}_k - s\tilde{\epsilon}_q + i\eta, p) \left(-1 + \frac{p^2}{4\,k\,q} \right) + \Delta_{\mathrm{HDL}}^{t}(\tilde{\epsilon}_k - s\tilde{\epsilon}_q + i\eta, p) \left(1 + \frac{p^2}{4\,k\,q} \right) \right] \right\} \, . \tag{3.57}$$

The next step is to divide the integration region in the $p-q$ plane into two parts, separated by the gluon "light cone" $|\tilde{\epsilon}_k - s\tilde{\epsilon}_q| = p$. For my choice $\Lambda_{\mathrm{q}} \ll \Lambda_{\mathrm{gl}}$ the region, where $|\tilde{\epsilon}_k - s\tilde{\epsilon}_q| < p$, is very large, while its complement is rather small. In order to estimate the contribution from the latter to the gap equation, one may approximate the HDL gluon propagators by their limiting forms for large gluon energies, cf. Eqs. (3.33), (3.34),

$$p_0 \gg p \, : \qquad \Delta_{\mathrm{HDL}}^{\ell}(P) \simeq \frac{p_0^2}{m_g^2\,p^2} \quad , \quad \Delta_{\mathrm{HDL}}^{t}(P) \simeq \frac{1}{m_g^2} \, . \tag{3.58}$$

Following the power-counting scheme employed previously, the contribution from the electric sector is of order

$$g^2\,\frac{\phi}{k} \int_{\mu-\Lambda_{\mathrm{q}}}^{\mu+\Lambda_{\mathrm{q}}} dq\, \frac{q}{\epsilon_q}\, \frac{(\tilde{\epsilon}_k - s\tilde{\epsilon}_q)^2}{m_g^2} \int_{|k-q|}^{|\tilde{\epsilon}_k - s\tilde{\epsilon}_q|} \frac{dp}{p} \sim g^2\,\frac{\phi}{m_g^2} \int_0^{\Lambda_{\mathrm{q}}} d\xi\, \epsilon_q \sim g^2\,\phi\,\frac{\Lambda_{\mathrm{q}}^2}{m_g^2} \sim g^2\,\phi \, . \tag{3.59}$$

This is a contribution of sub-subleading order, as long as one adheres to the choice $\Lambda_{\rm q} \lesssim g\mu$. Analogously, I estimate the contribution from the magnetic sector to be

$$
g^2 \frac{\phi}{k} \int_{\mu-\Lambda_{\rm q}}^{\mu+\Lambda_{\rm q}} dq \, \frac{q}{\epsilon_q} \int_{|k-q|}^{|\tilde\epsilon_k - s\tilde\epsilon_q|} dp \, p \, \frac{1}{m_g^2} \sim g^2 \, \frac{\phi}{m_g^2} \int_0^{\Lambda_{\rm q}} \frac{d\xi}{\epsilon_q} \, \xi^2 \sim g^2 \, \phi \, \frac{\Lambda_{\rm q}^2}{m_g^2} \sim g^2 \, \phi \; . \tag{3.60}
$$

Consequently, all contributions from the region $|\tilde\epsilon_k - s\tilde\epsilon_q| \geq p$ are of sub-subleading order, and the further analysis can be restricted to the region $|\tilde\epsilon_k - s\tilde\epsilon_q| < p$. In this region, it is permissible to use the low-energy limit of the HDL gluon propagator, which follows from Eqs. (3.33), (3.34) keeping only the leading terms in the gluon energy,

$$
p_0 \ll p \; : \qquad \Delta_{\rm HDL}^\ell(P) \simeq -\frac{1}{p^2 + 3\,m_g^2} \quad , \qquad \Delta_{\rm HDL}^t(P) \simeq \frac{p^4}{p^6 + M^4\,p_0^2} \; . \tag{3.61}
$$

Here, I only retained the real part of the transverse gluon propagator, since the imaginary part contributes to the imaginary part of the gap function, which is usually ignored. (In Ref. [55] it was argued that, at least close to the Fermi surface, the contribution of the imaginary part is of sub-subleading order in the gap equation.) With the approximation (3.61), the gap equation (3.57) becomes

$$
\begin{aligned}
\phi_k \;=\;& \frac{g^2}{24\pi^2} \int_{\mu-\Lambda_{\rm q}}^{\mu+\Lambda_{\rm q}} dq \, \frac{q}{k} \, \frac{Z^2(\tilde\epsilon_q)}{\tilde\epsilon_q} \, \tanh\left(\frac{\tilde\epsilon_q}{2T}\right) \phi_q \left\{ 4 \ln\left(\frac{k+q}{\Lambda_{\rm gl}}\right) \right. \\
&\left. + \sum_{s=\pm} \int_{|\tilde\epsilon_k - s\tilde\epsilon_q|}^{\Lambda_{\rm gl}} dp \left[\frac{p}{p^2 + 3\,m_g^2} \left(1 - \frac{p^2}{4\,k\,q}\right) + \frac{p^5}{p^6 + M^4(\tilde\epsilon_k - s\tilde\epsilon_q)^2} \left(1 + \frac{p^2}{4\,k\,q}\right) \right] \right\},
\end{aligned}
\tag{3.62}
$$

where I already performed the integration over hard gluon momenta $p \geq \Lambda_{\rm gl}$. The integration over soft gluon momenta can also be performed analytically. Formally, the terms $\sim p^2/(4kq)$ give rise to subleading-order contributions, $\sim \Lambda_{\rm gl}^2/(8kq)$, but they ultimately cancel, since they come with different signs in the electric and the magnetic part. Other contributions from these terms are at most of sub-subleading order. Exploiting the symmetry of the integrand around the Fermi surface and setting $k \simeq \mu$, I arrive at

$$
\begin{aligned}
\phi_k =& \\
\frac{g^2}{12\pi^2} \int_0^{\Lambda_{\rm q}}& d(q-\mu) \, \frac{Z^2(\tilde\epsilon_q)}{\tilde\epsilon_q} \, \tanh\left(\frac{\tilde\epsilon_q}{2T}\right) \phi_q \left[2 \ln\left(\frac{4\mu^2}{\Lambda_{\rm gl}^2}\right) + \ln\left(\frac{\Lambda_{\rm gl}^2}{3\,m_g^2}\right) + \frac{1}{3} \ln\left(\frac{\Lambda_{\rm gl}^6}{M^4|\tilde\epsilon_k^2 - \tilde\epsilon_q^2|}\right) \right].
\end{aligned}
\tag{3.63}
$$

Here, I have neglected terms $\sim \tilde\epsilon_k - s\tilde\epsilon_q$ against $3\,m_g^2$ under the logarithm arising from soft electric gluons, and terms $\sim (\tilde\epsilon_k - s\tilde\epsilon_q)^6$ against $M^4(\tilde\epsilon_k - s\tilde\epsilon_q)^2$ under the logarithm from soft magnetic gluons.

Now observe that the gluon cut-off $\Lambda_{\rm gl}$ cancels in the final result,

$$
\phi_k = \frac{g^2}{18\pi^2} \int_0^{\Lambda_{\rm q}} d(q-\mu) \, \frac{Z^2(\tilde\epsilon_q)}{\tilde\epsilon_q} \, \tanh\left(\frac{\tilde\epsilon_q}{2T}\right) \phi_q \, \frac{1}{2} \ln\left(\frac{\tilde b^2 \mu^2}{|\tilde\epsilon_k^2 - \tilde\epsilon_q^2|}\right) \; , \tag{3.64}
$$

where $\tilde{b} \equiv 256\pi^4[2/(N_f g^2)]^{5/2}$. This is Eq. (19) of Ref. [98], since $\bar{g}^2 \equiv g^2/(18\pi^2)$, with the upper limit of the $(q - \mu)$ integration, δ, replaced by the quark cut-off $\Lambda_{\rm q}$.

The solution of the gap equation (3.64) is well known, and given by Eq. (1.36). As was shown in Ref. [55], the dependence on the cut-off $\Lambda_{\rm q}$ enters only at sub-subleading order, i.e., it constitutes an $O(g)$ correction to the prefactor in Eq. (1.36). Therefore, to subleading order I do not need a matching calculation to eliminate $\Lambda_{\rm q}$.

The result (3.64) shows that the standard gap equation of QCD can be obtained from the effective action (2.46). The above, rather elaborate derivation of Eq. (3.64) demonstrates that, in order to obtain this result, it is mandatory to choose $\Lambda_{\rm q} \ll \Lambda_{\rm gl}$. This also enabled me to identify potential sub-subleading order contributions. However, I argued that, at this order, the off-shell behavior of the gap function has to be taken into account. This requires a complex ansatz for the gap function, which will be considered in the following Sec. 3.2.

3.2 The imaginary part of the gap function

The scalar gap function $\phi(K)$ contains the energy and momentum dependence of the (2SC) gap matrix $\Phi^+(K) = J_3\tau_2\gamma_5\,\Lambda_{\mathbf{k}}^+\,\Theta(\Lambda_{\mathrm{q}} - |k - \mu|)\,\phi(K)$, which solves the gap equation Eq. (3.30)

$$\Phi^+(K) = g^2\,\frac{T}{V}\sum_Q \Delta_{ab}^{\mu\nu}(K - Q)\,\gamma_\mu(T^a)^T\,\Xi^+(Q)\,\gamma_\nu T^b \ . \tag{3.65}$$

Due to the dependence of the gluon propagator $\Delta(K - Q)$ on the external energy $k_0 = -\omega_n = -i(2n+1)\pi T$ the solution $\phi(K)$ must be energy-dependent itself. Hence, solving the gap equation *self-consistently* requires an *energy dependent* ansatz for the gap function.

The function $\phi(K)$ solving Eq. (3.65) for some Matsubara frequency k_0 can be considered as the *analytic continuation* of the gap function $\phi(\omega, \mathbf{k})$ of physical and therefore real frequencies ω. Then the physical gap function $\phi(\omega, \mathbf{k})$ has to have singularities along the real ω-axis so that the analytic continuation $\phi(K)$ is, as required, *not* a constant in complex energy k_0. To see this write without loss of generality

$$\phi(K) \equiv \tilde{\phi}(K) + \phi_0(\mathbf{k}) \ , \tag{3.66}$$

where the energy dependence of $\phi(K)$ is contained in $\tilde{\phi}(K)$. It is physical to assume, and it will be confirmed when solving the gap equation, that $\phi(K)$ becomes local, i.e. independent of energy, for asymptotically large energies, i.e. that $\tilde{\phi}(K) \to 0$ and $\phi(K) \to \phi_0(\mathbf{k})$ for $k_0 \to \infty$. Cauchy's theorem gives for any k_0 off the real axis

$$
\begin{aligned}
\phi(k_0, \mathbf{k}) &= \oint_{\mathcal{C}} \frac{dz}{2\pi i}\,\frac{\phi(z, \mathbf{k})}{z - k_0} \\
&= \int_{-\infty}^{\infty} \frac{d\omega'}{2\pi i}\,\frac{\phi(\omega' + i\eta, \mathbf{k}) - \phi(\omega' - i\eta, \mathbf{k})}{\omega' - k_0} + \oint_{\mathcal{C}'} \frac{dz}{2\pi i}\,\frac{\phi(z, \mathbf{k})}{z} \ ,
\end{aligned}
\tag{3.67}
$$

where the contour $\mathcal{C}$ circumvents all non-analyticities of $\phi(K)$ on the real k_0-axis as depicted in Fig. 3.6 and $\mathcal{C}'$ is a circle whose radius tends to infinity. I define the spectral density of $\phi(K)$ by

$$\rho_\phi(\omega, \mathbf{k}) \equiv \frac{1}{2\pi i}\,[\phi(\omega + i\eta, \mathbf{k}) - \phi(\omega - i\eta, \mathbf{k})] \ , \tag{3.68}$$

which contains all non-analyticities of $\phi(\omega, \mathbf{k})$. Using $\phi(z, \mathbf{k})|_{z\in\mathcal{C}'} \equiv \phi_0(\mathbf{k})$ one obtains

$$\phi(k_0, \mathbf{k}) = \int_{-\infty}^{\infty} d\omega\,\frac{\rho_\phi(\omega, \mathbf{k})}{\omega - k_0} + \phi_0(\mathbf{k}) \ , \tag{3.69}$$

where the first term is identified as $\tilde{\phi}(K)$. Eq. (3.69) holds for all k_0 surrounded by contour $\mathcal{C}$, in particular for frequencies infinitesimally close to the real axis, $k_0 = \omega + i\epsilon$ with $\epsilon > \eta > 0$. For such frequencies one can employ the Dirac identity $1/(x - i\epsilon) \equiv \mathcal{P}(1/x) + i\pi\delta(x)$ to obtain

$$
\begin{aligned}
\phi(\omega + i\epsilon, \mathbf{k}) &= \\
&= \int_{-\infty}^{\infty} d\omega'\,\frac{\rho_\phi(\omega', \mathbf{k})}{\omega' - \omega - i\epsilon} + \phi_0(\mathbf{k}) = \mathcal{P}\int_{-\infty}^{\infty} d\omega'\,\frac{\rho_\phi(\omega', \mathbf{k})}{\omega' - \omega} + \phi_0(\mathbf{k}) + i\pi\rho_\phi(\omega, \mathbf{k}) \ .
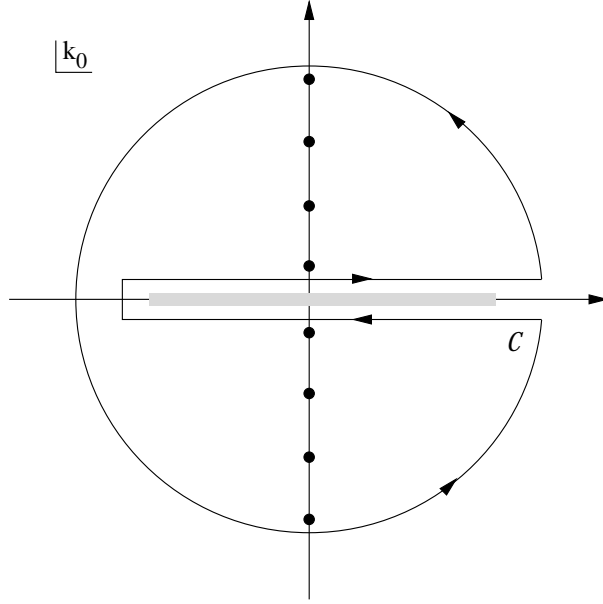\end{aligned}
\tag{3.70}
$$

Figure 3.6: The contour $\mathcal{C}$ circumvents all non-analyticities of $\phi(K)$ on the real k_0-axis in the shaded area. The dots indicate the fermionic Matsubara frequencies, $k_0 = -i(2n+1)\pi T$.

Hence, for real $\phi_0(\mathbf{k})$ and $\rho_\phi(\omega, \mathbf{k})$

$$\operatorname{Re}\phi(\omega + i\epsilon, \mathbf{k}) \;=\; \mathcal{P}\int\limits_{-\infty}^{\infty} d\omega' \, \frac{\rho_\phi(\omega', \mathbf{k})}{\omega - \omega'} + \phi_0(\mathbf{k}) \; , \tag{3.71}$$

$$\operatorname{Im}\phi(\omega + i\epsilon, \mathbf{k}) \;=\; \pi\, \rho_\phi(\omega, \mathbf{k}) \; . \tag{3.72}$$

Combining Eq. (3.68) with Eq. (3.72) yields the identity

$$\operatorname{Im}\phi(\omega + i\epsilon, \mathbf{k}) = \frac{1}{2i} \left[\phi(\omega + i\epsilon, \mathbf{k}) - \phi(\omega - i\epsilon, \mathbf{k}) \right] \; , \tag{3.73}$$

i.e. non-analyticitis along the real k_0-axis are equivalent to a nonzero imaginary part of the gap function. Furthermore, one finds the dispersion relations for $\tilde\phi(\omega + i\eta, \mathbf{k})$

$$\operatorname{Re}\tilde\phi(\omega + i\epsilon, \mathbf{k}) \;=\; \frac{1}{\pi}\mathcal{P}\int\limits_{-\infty}^{\infty} d\omega' \, \frac{\operatorname{Im}\tilde\phi(\omega' + i\epsilon, \mathbf{k})}{\omega' - \omega} \; , \tag{3.74a}$$

$$\operatorname{Im}\tilde\phi(\omega + i\epsilon, \mathbf{k}) \;=\; -\frac{1}{\pi}\mathcal{P}\int\limits_{-\infty}^{\infty} d\omega' \, \frac{\operatorname{Re}\tilde\phi(\omega' + i\epsilon, \mathbf{k})}{\omega' - \omega} \; , \tag{3.74b}$$

i.e. $\operatorname{Im}\tilde\phi(\omega + i\epsilon, \mathbf{k})$ and $\operatorname{Re}\tilde\phi(\omega + i\epsilon, \mathbf{k})$ are Hilbert transforms of each other, $\operatorname{Re}\tilde\phi = \mathcal{H}[\operatorname{Im}\tilde\phi]$. It follows that $\tilde\phi \neq 0$ only if both $\operatorname{Re}\tilde\phi$ and $\operatorname{Im}\tilde\phi$ are nonzero. Consequently, the gap function ϕ is energy-dependent only if it has a nonzero imaginary part, $\operatorname{Im}\phi \equiv \operatorname{Im}\tilde\phi \neq 0$, which in turn is generated by its non-analyticities along the real k_0 axis, cf. Eq. (3.73).

This investigation accounts for the energy dependence of the gap function by including the non-analyticities of ϕ in the solution of the gap equation. This finally leads to a *complex gap equation*, whose real and imaginary parts are coupled integral equations

$$\operatorname{Re}\phi = \operatorname{Re}\phi\left[\phi, \Delta, \Sigma\right], \tag{3.75a}$$

$$\operatorname{Im}\phi = \operatorname{Im}\phi\left[\phi, \Delta, \Sigma\right], \tag{3.75b}$$

which have to be solved self-consistently. Of course, there are analogous DSEs for Δ and Σ, which in principle would have to be solved self-consistently simultaneously with Eqs. (3.75). However, it has been shown [126] that to subleading order one may replace $\Delta = \Delta_{\text{HDL}}$ in Eq. (3.75a). (This can be refined by taking $\Delta = \Delta_{\text{HDL}}$ for soft gluon momenta and the free propagator $\Delta = \Delta_{0,22}$ for hard momenta [26].) Also Σ may be replaced by its one-loop approximation in Eq. (3.75a) to subleading order [125, 98]. Furthermore, the contribution of $\operatorname{Im}\Sigma$ to $\operatorname{Re}\phi$ in Eq. (3.75a) has been shown to be of sub-subleading order [125] and therefore will be neglected in the following. However, the contribution of $\operatorname{Im}\phi$ to $\operatorname{Re}\phi$ in Eq. (3.75a) has not been systematically accounted for, yet. In the following it will be checked if $\operatorname{Im}\phi$ contributes leading or subleading order corrections to the real part of the gap function or not, i.e. whether the common simplification of Eq. (3.75a)

$$\operatorname{Re}\phi = \operatorname{Re}\phi\left[\operatorname{Re}\phi, \Delta, \Sigma\right] \tag{3.76}$$

is justified to subleading order or not. To this end it is admissible to make the *same* approximations in Eq. (3.75b) as in Eq. (3.75a) yielding

$$\operatorname{Re}\phi = \operatorname{Re}\phi\left[\phi, \Delta_{\text{HDL}}, \Delta_{0,22}, \operatorname{Re}\Sigma_{1\,\text{loop}}\right], \tag{3.77a}$$

$$\operatorname{Im}\phi = \operatorname{Im}\phi\left[\phi, \Delta_{\text{HDL}}, \Delta_{0,22}, \operatorname{Re}\Sigma_{1\,\text{loop}}\right]. \tag{3.77b}$$

This can be justified when considering $\operatorname{Im}\phi \equiv \operatorname{Im}\tilde{\phi}$ as the Hilbert transform of $\operatorname{Re}\tilde{\phi}$ in its subleading order approximation. As such it must be insensitive to any sub-subleading order corrections to $\operatorname{Re}\tilde{\phi}$. In other words, one assumes that contributions, which do not enter $\operatorname{Re}\phi$ directly via Eq. (3.75a) do not enter $\operatorname{Re}\phi$ indirectly via Eq. (3.75b). As stated in the beginning the main contributions to $\operatorname{Im}\phi$ are expected to arise from the energy dependence of the gluon propagator $\Delta(K - Q)$.

The gap in the quasiparticle excitation spectrum is given by the modulus of the complex gap function

$$|\phi| = \sqrt{(\operatorname{Re}\phi)^2 + (\operatorname{Im}\phi)^2}\,. \tag{3.78}$$

Hence, there are two possibilities how the physical quantity $|\phi|$ is affected by $\operatorname{Im}\phi$ to subleading order. The first is that $\operatorname{Im}\phi$ enters $\operatorname{Re}\phi$ to subleading order through Eq. (3.77a) as already discussed. The second is that $\operatorname{Im}\phi$ appearing on the r.h.s. of Eq. (3.78) is of order $\operatorname{Re}\phi$. In [55] it is estimated that $\operatorname{Im}\phi = 0$ on the Fermi surface and $\operatorname{Im}\phi \sim g\operatorname{Re}\phi$ exponentially close to the Fermi surface. This will be confirmed in the following. It follows that in *these* momentum regimes $\operatorname{Im}\phi$ contributes at most at order $g^2\operatorname{Re}\phi$ to $|\phi|$, i.e. at sub-subleading order. Hence, the second of the two possibilities mentioned above can be discarded in this momentum regime.

However, at momenta $|k - \mu| \sim g\,\mu$ it is $\mathrm{Im}\,\phi \sim \mathrm{Re}\,\phi$ and both the real and the imaginary part contribute at the same order of magnitude to $|\phi|$. Also this will be confirmed in the following. The modulus appears in the complex gap equation only in the on-shell energy dispersion relation

$$\epsilon_q = \sqrt{(k - \mu)^2 + |\phi|^2}\,. \tag{3.79}$$

In the region $\zeta = |k - \mu| \sim g\,\mu$, where $\mathrm{Im}\phi \sim \mathrm{Re}\phi$, it is $\zeta \gg \phi$ and therefore $\epsilon_q \simeq \zeta$. Hence, in the gap equation it is self-consistent to subleading-order to approximate $|\phi| \simeq \mathrm{Re}\,\phi$ and write

$$\epsilon_q \simeq \sqrt{(k - \mu)^2 + (\mathrm{Re}\,\phi_q)^2}\,. \tag{3.80}$$

Consequently, in contrast to $|\phi|$ the on-shell energy ϵ_q can be affected by $\mathrm{Im}\,\phi_q$ only through $\mathrm{Re}\,\phi_q$ for all ζ.

Before actually solving the complex gap equation it is worthwhile investigate how the symmetry properties of the gap matrix $\Phi^+(K)$ affect the gap function $\phi(K)$. Remembering $\psi_C(K) = C\bar{\psi}^T(-K)$, $\bar{\psi}_C(K) = \psi^T(-K)C$, and $C = -C^{-1} = -C^T$ it follows from the antisymmetry of the quark fields that

$$
\begin{aligned}
\sum_K \bar{\psi}_C(K)\Phi^+(K)\psi(K) &\equiv -\left(\sum_K \bar{\psi}_C(K)\Phi^+(K)\psi(K)\right)^T \\
&= -\sum_K \psi^T(K)\left[\Phi^+(K)\right]^T \bar{\psi}_C^T(K) \\
&= \sum_K \bar{\psi}_C(K)\,C^{-1}\left[\Phi^+(-K)\right]^T C\,\psi(K)\,.
\end{aligned} \tag{3.81}
$$

Hence, the gap matrix must fulfill

$$C\,\Phi^+(K)\,C^{-1} = \left[\Phi^+(-K)\right]^T\,. \tag{3.82}$$

Since $C\gamma_5\Lambda_{\mathbf{k}}^+C^{-1} = [\gamma_5\Lambda_{-\mathbf{k}}^+]^T$ and in the 2SC case $[J_3\tau_2]^T = J_3\tau_2$ it follows for the gap function

$$\phi(K) \;=\; \phi(-K)\,. \tag{3.83}$$

Assuming that the gap function is symmetric under reflection of 3-momentum $\mathbf{k}$, $\phi(k_0, \mathbf{k}) = \phi(k_0, -\mathbf{k})$ one obtains with Eqs. (3.71,3.72)

$$
\begin{aligned}
\mathrm{Re}\,\phi(\omega + i\eta, \mathbf{k}) &= \mathrm{Re}\,\phi(-\omega + i\eta, \mathbf{k})\,, & \text{(3.84a)} \\
\mathrm{Im}\,\phi(\omega + i\eta, \mathbf{k}) &= -\mathrm{Im}\,\phi(-\omega + i\eta, \mathbf{k})\,, & \text{(3.84b)} \\
\rho_\phi(\omega, \mathbf{k}) &= -\rho_\phi(-\omega, \mathbf{k})\,. & \text{(3.84c)}
\end{aligned}
$$

Hence, one found that $\mathrm{Re}\,\phi$ is an even function in ω while $\mathrm{Im}\,\phi$ and ρ_ϕ are odd.

Furthermore, one introduces the spectral representations for the gluon propagators. In the case of soft, HDL-resummed electric and magnetic gluon propagators, cf. Eqs. (3.33), one has [9, 128]

$$\rho_{\ell,t}(\omega, \mathbf{p}) \;=\; \rho_{\ell,t}^{\mathrm{pole}}(\omega, \mathbf{p})\,\{\delta\left[\omega - \omega_{\ell,t}(\mathbf{p})\right] - \delta\left[\omega - \omega_{\ell,t}(\mathbf{p})\right]\} + \rho_{\ell,t}^{\mathrm{cut}}(\omega, \mathbf{p})\,\theta(p - |\omega|)\,, \tag{3.85}$$

where $\rho_{\ell,t}^{\text{cut}}$ are the contributions from the cut of the logarithm in the HDL self-energies $\Pi_{\text{HDL}}^{\ell,t}$, cf. (3.34), and already given in Eqs. (3.47). The contributions from the gluon poles at $\omega = \pm\omega_{\ell,t}$ are given by the respective residues of the propagator, $\rho_{\ell,t}^{\text{pole}}(\omega, \mathbf{p}) \equiv Z_{\ell,t}(\omega, \mathbf{p})$, cf. Eqs. (3.43). For the respective hard gluon propagators, cf. Eqs. (3.32), one has $\Delta_{0,22}^{\ell}(\omega \pm i\eta, \mathbf{p}) = -1/p^2$ and $\Delta_{0,22}^{t}(\omega \pm i\eta, \mathbf{p}) = -1/[(\omega \pm i\eta)^2 - p^2]$ and therefore with $\rho_{0,22}^{\ell,t}(\omega, \mathbf{p}) \equiv [\Delta_{0,22}^{\ell,t}(\omega + i\eta, \mathbf{p}) - \Delta_{0,22}^{\ell,t}(\omega - i\eta, \mathbf{p})]/(2\pi i)$

$$\rho_{0,22}^{\ell}(\omega, \mathbf{p}) = 0 , \tag{3.86a}$$

$$\rho_{0,22}^{t}(\omega, \mathbf{p}) = \text{sign}(\omega)\delta(\omega^2 - p^2) . \tag{3.86b}$$

With these spectral densitis, $\rho_{\text{HDL}}^{\ell,t}$ and $\rho_{0,22}^{\ell,t}$, one may express the respective gluon propagators in their spectral representations

$$\Delta^{\ell}(P) = -\frac{1}{p^2} + \int\limits_{-\infty}^{\infty} d\omega \, \frac{\rho^{\ell}(\omega, \mathbf{p})}{\omega - p_0} \quad , \quad \Delta^{t}(P) = \int\limits_{-\infty}^{\infty} d\omega \, \frac{\rho^{t}(\omega, \mathbf{p})}{\omega - p_0} . \tag{3.87}$$

3.2.1 Solving the complex gap equation

In the following solution of the complex gap equation (3.77) it will be shown that its imaginary part, Eq. (3.77b), can be decomposed as

$$\text{Im}\,\phi = \mathcal{A} + \mathcal{B} , \tag{3.88}$$

where $\mathcal{A}$ contains only contributions, where the gap function is on the quasi-particle mass-shell, and $\mathcal{B}$ contains the rest. Then all contributions in the imaginary part of the gap function, which are generated by the energy dependence, i.e. by the non-analyticities of ϕ, are collected in $\mathcal{B}$. Therefore, all terms in $\mathcal{B}$ have not been considered so far and neglecting $\mathcal{B}$ must lead to the known subleading order result for $\text{Re}\phi(\tilde{\epsilon}_q, q)$. In the following it will checked, whether this result is self-consistent. Self-consistency is fulfilled only if the contributions contained in $\mathcal{B}$ enter $\text{Re}\phi(\tilde{\epsilon}_q, q)$ beyond subeading order, i.e. at sub-subleading order. To this end it is first assumed that self-consistency is indeed fulfilled and then analyzed, if $\mathcal{B}$ really contributes beyond subleading order. This procedure comprises of the following steps.

In order to obtain $\mathcal{A}$ and $\mathcal{B}$, first the Matsubara sum over the internal frequency q_0 is perfomed, cf. Sec. 3.2.1, and then all imaginary contributions are extracted and organised according to Eq. (3.88), cf. Sec. 3.2.1. In the first part of Sec. 3.2.2 the order of magnitude of $\text{Im}\,\phi$ will be determined by inserting the known leading order result for $\text{Re}\,\phi(\tilde{\epsilon}_{\mathbf{q}}, \mathbf{q})$ into $\mathcal{A}$, while the yet unknown term $\mathcal{B}$ has to be neglected first. Of course, this estimate for $\text{Im}\,\phi$ can be self-consistent only if reinserting it into $\mathcal{B}$ in Eq. (3.88) only yields sufficiently small corrections to $\text{Im}\,\phi$, i.e. if

$$\text{Im}\,\phi \approx \mathcal{A} . \tag{3.89}$$

This will be analyzed in the second part of Sec. 3.2.2, where this estimate for $\text{Im}\,\phi$ is used to determine the order of magnitude of $\mathcal{B}$. It will be shown that Eq. (3.89) is indeed fulfilled, i.e. that $\mathcal{B}$ constitutes a small correction to $\mathcal{A}$. With these results the order of magnitude of

$\operatorname{Re}\tilde{\phi}(\epsilon_{\mathbf{k}}, \mathbf{k})$ is estimated in Sec. 3.2.3 via the dispersion relation Eq. (3.74a), i.e. by Hilbert transforming $\mathcal{A}$ and $\mathcal{B}$. It is found that $\operatorname{Re}\tilde{\phi}(\epsilon_{\mathbf{k}}, \mathbf{k}) \sim \mathcal{H}[\mathcal{A}] \sim \phi$ for momenta $\mathbf{k}$ close to the Fermi surface, while $\mathcal{H}[\mathcal{B}] \sim g^2\phi$, i.e. $\operatorname{Im}\phi$ contributes beyond subleading order to $\operatorname{Re}\tilde{\phi}(\epsilon_{\mathbf{k}}, \mathbf{k})$ or according to Eq. (3.76)

$$\operatorname{Re}\tilde{\phi} = \operatorname{Re}\tilde{\phi}\left[\operatorname{Re}\phi\right] . \tag{3.90}$$

In Sec. 3.2.3 it is shown that also $\phi_0(\mathbf{k}) \sim \phi$ and that the imaginary part of the gap function contributes to $\phi_0(\mathbf{k})$ at $g^2\phi$, i.e. beyond subleading order. Consequently,

$$\phi_0 = \phi_0[\operatorname{Re}\phi] \tag{3.91}$$

to subleading order. Hereby it is shown that to subleading order Eq. (3.77a) becomes Eq. (3.76), which means that the imaginary part of the gap function does not enter the real part at this accuracy. In other words, the real part of the gap equation is decoupled from its imaginary part. On the other hand, the imaginary part of the gap equation is not decoupled from the real part of the gap equation, cf. Eq. (3.89). It turns out that for momenta close to the Fermi surface $\operatorname{Im}\phi$ can be calculated self-consistently from $\operatorname{Re}\phi$ alone, which is performed in Sec. 3.2.5.

Performing the Matsubara sum

The complex gap equation (3.65) reads to subleading order, cf. Eq. (3.41),

$$\phi(K) = \frac{g^2}{3}\frac{T}{V}\sum_Q \operatorname{Tr}_s\left(\Lambda_{\mathbf{k}}^+\gamma_\mu\Lambda_{\mathbf{q}}^-\gamma_\nu\right)\Delta^{\mu\nu}(K-Q)\frac{\phi(Q)}{[q_0/Z(q_0)]^2 - \epsilon_q^2} , \tag{3.92}$$

where the quark wave-function renormalization factor $Z(q_0) \equiv [1 + \bar{g}^2\ln(M^2/q_0^2)]^{-1}$ contains the effect of the normal quark self-energy $\Sigma(Q)$. As explained before, only its real part contributes at subleading order and therefore will be accounted for in the following, while its imaginary part will be neglected. Physically this is equivalent to assume the (normal) quasi-particle excitations to be infinitely long-lived, i.e. ignoring their decay due to scattering processes with quarks inside the Fermi sea. Mathematically it amounts to neglecting the cut of the logarithm when performing the Matsubara sum over q_0. Consequently, at subleading order the only effect of $Z(q_0)$ in Eq. (3.92) is a shift of the poles of the propagator

$$\tilde{\Delta}(Q) \equiv \frac{Z^2(q_0)}{q_0^2 - [Z(q_0)\,\epsilon_q]^2} = \frac{1}{2\tilde{\epsilon}_{\mathbf{q}}}\sum_{\sigma=\pm}\frac{\sigma\,Z^2(q_0)}{q_0 - \sigma Z(q_0)\,\epsilon_{\mathbf{q}}} \tag{3.93}$$

to $q_0 = \pm Z(\epsilon_{\mathbf{q}})\,\epsilon_{\mathbf{q}} \equiv \pm\tilde{\epsilon}_{\mathbf{q}}$.

The Matsubara sum over q_0 in Eq. (3.65) is performed via contour integration, cf. Fig. 3.7,

$$\begin{aligned}
\mathcal{M}^{\ell,t}(k_0, \mathbf{p}, \mathbf{q}) &\equiv T\sum_{q_0\neq k_0}\Delta^{\ell,t}(Q-K)\tilde{\Delta}(Q)\phi(Q) \\
&= \int_\mathcal{C}\frac{dq_0}{2\pi i}\frac{1}{2}\tanh\left(\frac{q_0}{2T}\right)\Delta^{\ell,t}(Q-K)\tilde{\Delta}(Q)\phi(Q) \\
&\equiv \int_\mathcal{C}\frac{dq_0}{2\pi i}\mathcal{K}^{\ell,t}(q_0) .
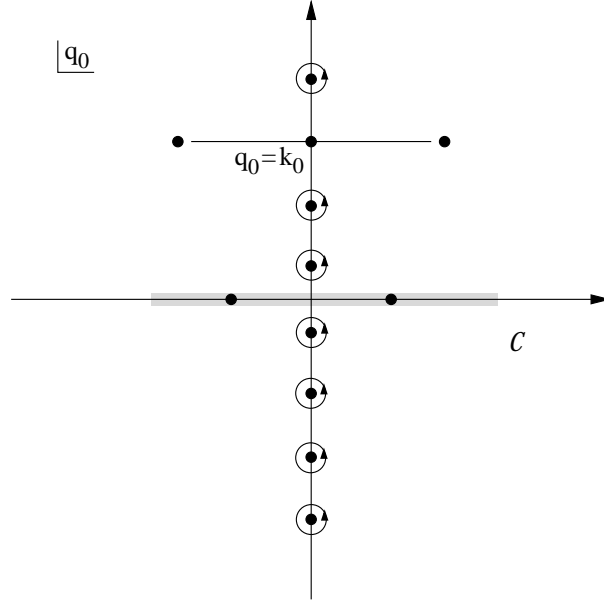\end{aligned} \tag{3.94}$$

Figure 3.7: The contour $\mathcal{C}$ in Eq. (3.94) encloses the poles of $\tanh[q_0/(2T)]$ on the imaginary q_0 axis. The additional poles and the cut at $q_0 = k_0$ arise from the the gluon propagator, while the two poles on the real axis are due to the quasiquarks. The undetermined singularities of the gap function on the real q_0-axis are indicated by the shaded area.

In order to introduce the spectral densities of the gap function and of the magnetic and longitudinal gluon propagators, the contour $\mathcal{C}$ in Eq. (3.94) is deformed as shown in Fig. 3.8, yielding

$$
\begin{aligned}
\mathcal{M}^{\ell,t}(k_0, \mathbf{p}, \mathbf{q}) &= \int\limits_{\mathcal{C}_\infty} \frac{dq_0}{2\pi i} \, \mathcal{K}^{\ell,t}(q_0) + \int\limits_{-\infty}^{\infty} \frac{dq_0}{2\pi i} \left[\mathcal{K}^{\ell,t}(q_0 + i\eta) - \mathcal{K}^{\ell,t}(q_0 - i\eta) \right] \\
&\quad + \int\limits_{-\infty}^{\infty} \frac{dq_0}{2\pi i} \left[\mathcal{K}^{\ell,t}(q_0 + k_0 + i\eta) - \mathcal{K}^{\ell,t}(q_0 + k_0 - i\eta) \right] \\
&\equiv I_\infty + I_0 + I_{k_0} \, .
\end{aligned} \tag{3.95}
$$

The explicit form of the integral I_∞ reads

$$
I_\infty \equiv \int\limits_{\mathcal{C}_\infty} \frac{dq_0}{2\pi i} \frac{1}{2} \tanh\left(\frac{q_0}{2T}\right) \Delta^{\ell,t}(Q - K)\tilde{\Delta}(Q)\phi(Q) \, . \tag{3.96}
$$

For the integration along the contour $\mathcal{C}_\infty$ one parametrizes $dq_0 = i|q_0|e^{i\theta}d\theta$ and find for $|q_0| \longrightarrow \infty$

$$
\left| \tanh\left(\frac{q_0}{2T}\right) \right| \to 1 \, , \; \tilde{\Delta}(Q) \to \frac{1}{q_0^2} \, , \; \phi(Q) \to \phi_0(\mathbf{q}) \, ,
$$

$$
\Delta^{\ell}(Q - K) \to -\frac{1}{|\mathbf{q} - \mathbf{k}|^2} \, , \; \Delta^t(Q - K) \to -\frac{1}{q_0^2} \, . \tag{3.97}
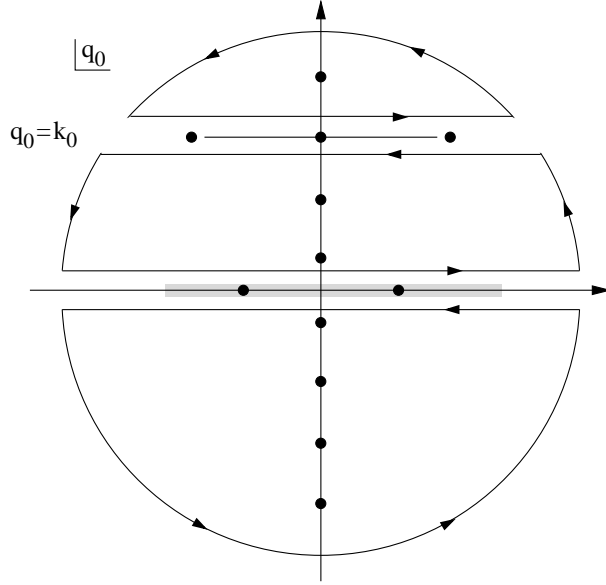$$

Figure 3.8: Deforming the contour $\mathcal{C}$ to introduce the spectral densities of $\Delta^{\ell,t}$ and ϕ, cf. Eq. (3.95).

Consequently,

$$dq_0 \, \mathcal{K}^\ell(q_0) \sim \frac{1}{q_0} \,, \;\; dq_0 \, \mathcal{K}^\ell(q_0) \sim \frac{1}{q_0^3} \tag{3.98}$$

and I_∞ vanishes, $I_\infty = 0$. Using Eq. (3.93) the integral I_0 can be decomposed

$$
\begin{aligned}
I_0 \;=\;& \int\limits_{-\infty}^{\infty} \frac{dq_0}{2\pi i} \frac{1}{2} \tanh\left(\frac{q_0}{2T}\right) \Delta^{\ell,t}(Q-K) Z^2(q_0) \\
& \times \left[\tilde{\Delta}(q_0 + i\eta, \mathbf{q})\phi(q_0 + i\eta, \mathbf{q}) - \tilde{\Delta}(q_0 - i\eta, \mathbf{q})\phi(q_0 - i\eta, \mathbf{q}) \right] \\
=\;& \frac{1}{2\tilde{\epsilon}_{\mathbf{q}}} \sum_{\sigma=\pm} \sigma \mathcal{P}_{\sigma\tilde{\epsilon}_{\mathbf{q}}} \int\limits_{-\infty}^{\infty} \frac{dq_0}{2\pi i} \frac{1}{2} \tanh\left(\frac{q_0}{2T}\right) \Delta^{\ell,t}(Q-K) Z^2(q_0) \frac{\phi(q_0 + i\eta, \mathbf{q}) - \phi(q_0 - i\eta, \mathbf{q})}{q_0 - \sigma\tilde{\epsilon}_{\mathbf{q}}} \\
& + \frac{1}{2\tilde{\epsilon}_{\mathbf{q}}} \sum_{\sigma=\pm} \sigma \int\limits_{\sigma\tilde{\epsilon}_{\mathbf{q}}-\eta}^{\sigma\tilde{\epsilon}_{\mathbf{q}}+\eta} \frac{dq_0}{2\pi i} \frac{1}{2} \tanh\left(\frac{q_0}{2T}\right) \Delta^{\ell,t}(Q-K) Z^2(q_0) \frac{\phi(q_0 + i\eta, \mathbf{q})}{q_0 - \sigma\tilde{\epsilon}_{\mathbf{q}} + i\eta} \\
& + \frac{1}{2\tilde{\epsilon}_{\mathbf{q}}} \sum_{\sigma=\pm} \sigma \int\limits_{\sigma\tilde{\epsilon}_{\mathbf{q}}+\eta}^{\sigma\tilde{\epsilon}_{\mathbf{q}}-\eta} \frac{dq_0}{2\pi i} \frac{1}{2} \tanh\left(\frac{q_0}{2T}\right) \Delta^{\ell,t}(Q-K) Z^2(q_0) \frac{\phi(q_0 - i\eta, \mathbf{q})}{q_0 - \sigma\tilde{\epsilon}_{\mathbf{q}} - i\eta} \,,
\end{aligned}
\tag{3.99}
$$

where the notation $\mathcal{P}_{\pm\tilde{\epsilon}_{\mathbf{q}}}$ refers to the principal value prescription for the quark pole at $q_0 = \pm\tilde{\epsilon}_{\mathbf{q}}$. In the first term on the r.h.s. of Eq. (3.99) the difference of the retarded and advanced gap function may be replaced by the spectral density of the gap function, cf. Eq. (3.68). In the second term one may substitute $q_0' \equiv q_0 - \sigma\tilde{\epsilon}_{\mathbf{q}}$ and deform the contour of integration into an

infinitesimally small semicircle around the quark pole at $q_0' = 0$. With $dq_0' = i\,\eta\,e^{i\theta}d\theta$ this term becomes

$$
\frac{1}{2\tilde{\epsilon}_{\mathbf{q}}} \sum_{\sigma=\pm} \sigma \int_{\pi}^{0} \frac{i\,\eta\,e^{i\theta}d\theta}{2\pi i} \frac{1}{\eta\,e^{i\theta}} \frac{1}{2} \tanh\left(\frac{\sigma\tilde{\epsilon}_{\mathbf{q}}}{2T}\right) \Delta^{\ell,t}(\sigma\tilde{\epsilon}_{\mathbf{q}} - k_0, \mathbf{p}) Z^2(\tilde{\epsilon}_{\mathbf{q}})\,\phi(\sigma\tilde{\epsilon}_{\mathbf{q}} + i\eta, \mathbf{q})
$$

$$
= \quad -\frac{1}{4\tilde{\epsilon}_{\mathbf{q}}} \sum_{\sigma=\pm} \sigma \frac{1}{2} \tanh\left(\frac{\sigma\tilde{\epsilon}_{\mathbf{q}}}{2T}\right) \Delta^{\ell,t}(\sigma\tilde{\epsilon}_{\mathbf{q}} - k_0, \mathbf{p}) Z^2(\tilde{\epsilon}_{\mathbf{q}})\,\phi(\sigma\tilde{\epsilon}_{\mathbf{q}} + i\eta, \mathbf{q}) \ . \tag{3.100}
$$

The third term in Eq. (3.99) can be evaluated analogously to the second. The result will differ from the second term only by containing the advanced instead of the retarded gap function. Collecting all three terms one obtains using $\phi(\omega + i\eta) + \phi(\omega - i\eta) = 2\mathrm{Re}\,\phi(\omega + i\eta)$

$$
I_0 \quad = \quad \frac{1}{2\tilde{\epsilon}_{\mathbf{q}}} \sum_{\sigma=\pm} \sigma\mathcal{P}_{\sigma\tilde{\epsilon}_{\mathbf{q}}} \int_{-\infty}^{\infty} dq_0 \frac{1}{2} \tanh\left(\frac{q_0}{2T}\right) \Delta^{\ell,t}(q_0 - k_0, \mathbf{p}) Z^2(q_0) \frac{\rho_\phi(q_0, \mathbf{q})}{q_0 - \sigma\tilde{\epsilon}_{\mathbf{q}}}
$$

$$
- \frac{1}{2\tilde{\epsilon}_{\mathbf{q}}} \frac{1}{2} \tanh\left(\frac{\tilde{\epsilon}_{\mathbf{q}}}{2T}\right) Z^2(\tilde{\epsilon}_{\mathbf{q}})\,\mathrm{Re}\,\phi(\tilde{\epsilon}_{\mathbf{q}}, \mathbf{q}) \sum_{\sigma=\pm} \Delta^{\ell,t}(\sigma\tilde{\epsilon}_{\mathbf{q}} - k_0, \mathbf{p}) \ . \tag{3.101}
$$

The first term arises from the non-analyticities of the gap function, $\phi(Q)$, and the second from the poles of the quark propagator $\tilde{\Delta}(Q)$, cf. Eq. (3.93), at $q_0 = \pm\tilde{\epsilon}_{\mathbf{q}}$. The last integral I_{k_0} reads

$$
I_{k_0} =
$$

$$
\mathcal{P}_0 \int_{-\infty}^{\infty} \frac{dq_0}{2\pi i} \frac{1}{2} \coth\left(\frac{q_0}{2T}\right) \tilde{\Delta}(q_0 + k_0, \mathbf{q})\phi(q_0 + k_0, \mathbf{q}) \left[\Delta^{\ell,t}(q_0 + i\eta, \mathbf{p}) - \Delta^{\ell,t}(q_0 - i\eta, \mathbf{p})\right]
$$

$$
+ \int_{-\eta}^{\eta} \frac{dq_0}{2\pi i} \frac{1}{2} \coth\left(\frac{q_0 + i\eta}{2T}\right) \Delta^{\ell,t}(q_0 + i\eta, \mathbf{p})\tilde{\Delta}(q_0 + k_0, \mathbf{q})\phi(q_0 + k_0, \mathbf{q})
$$

$$
+ \int_{\eta}^{-\eta} \frac{dq_0}{2\pi i} \frac{1}{2} \coth\left(\frac{q_0 - i\eta}{2T}\right) \Delta^{\ell,t}(q_0 - i\eta, \mathbf{p})\tilde{\Delta}(q_0 + k_0, \mathbf{q})\phi(q_0 + k_0, \mathbf{q}) \ . \tag{3.102}
$$

In the first term the difference of the retarded and advanced gluon propagator, $\Delta^{\ell,t}(q_0 \pm i\eta, \mathbf{p})$, may be replaced by the gluon spectral density. In the second and third term the integrals over q_0 can be performed after taking the limit $\coth(q_0/2T)/2 \to T/q_0$ for $\eta \to 0$ and parametrize the contour as $dq_0 = i\,\eta\,e^{i\theta}d\theta$. One obtains for the second term

$$
T \int_{\pi}^{0} \frac{i\,\eta\,e^{i\theta}d\theta}{2\pi i} \frac{1}{\eta\,e^{i\theta}} \Delta^{\ell,t}(0 + i\eta, \mathbf{p})\tilde{\Delta}(k_0, \mathbf{q})\phi(k_0, \mathbf{q}) = -\frac{T}{2}\Delta^{\ell,t}(0 + i\eta, \mathbf{p})\tilde{\Delta}(k_0, \mathbf{q})\phi(k_0, \mathbf{q}) \ .
$$

$$
\tag{3.103}
$$

For the third term the result differs only in the occurence of the advanced gluon propagator instead of the retarded. Combining all three terms in Eq. (3.102) yields

$$
I_{k_0} \quad = \quad \frac{1}{2\tilde{\epsilon}_{\mathbf{q}}} \sum_{\sigma=\pm} \sigma\mathcal{P}_0 \int_{-\infty}^{\infty} dq_0 \frac{1}{2} \coth\left(\frac{q_0}{2T}\right) \phi(q_0 + k_0, \mathbf{q}) Z^2(q_0 + k_0) \frac{\rho^{\ell,t}(q_0, \mathbf{p})}{q_0 - \sigma\tilde{\epsilon}_{\mathbf{q}} + k_0}
$$

$$-T \operatorname{Re} \Delta^{\ell,t}(0+i\eta,\mathbf{p})\,\tilde{\Delta}(k_0,\mathbf{q})\,\phi(k_0,\mathbf{q})\;. \tag{3.104}$$

The first term is due to the non-analyticities of the longitudinal and magnetic gluon propagators, $\Delta^{\ell,t}$. The second arises from the pole of $\coth(q_0/2T)$ at $q_0 = 0$ corresponding to the large occupation number density of gluons in the classical limit, $q_0 \ll T$. The latter contribution has been shown to be beyond subleading order [55] and will be discarded in the following.

The imaginary part of the gap equation

After having performed the Matsubara sum one considers energies k_0 close to the real axis, $k_0 = \omega + i\eta$ in order to employ the Dirac identity to split the complex gap equation (3.92) into its real and imaginary part. To this end one extracts the imaginary parts of the contributions I_0 and I_{k_0}, cf. Eqs. (3.101,3.104). For the imaginary part of Eq. (3.92) one finds using that $\operatorname{Re}\phi$ and Z^2 are even in q_0

$$\operatorname{Im}\phi(\omega+i\eta,\mathbf{k}) =$$
$$\frac{g^2}{3}\int\frac{d^3q}{(2\pi)^3}\left[\operatorname{Tr}_s^\ell(k,p,q)\operatorname{Im}\mathcal{M}^\ell(\omega+i\eta,\mathbf{p},\mathbf{q})+\operatorname{Tr}_s^t(k,p,q)\operatorname{Im}\mathcal{M}^t(\omega+i\eta,\mathbf{p},\mathbf{q})\right]\;, \tag{3.105}$$

where

$$\operatorname{Im}\mathcal{M}^{\ell,t}(\omega+i\eta,\mathbf{p},\mathbf{q}) =$$
$$\frac{\pi}{4\tilde{\epsilon}_\mathbf{q}}\sum_{\sigma=\pm}\sigma\mathcal{P}\int\limits_{-\infty}^{\infty}dq_0\frac{\rho^{\ell,t}(\omega-q_0,\mathbf{p})\rho_\phi(q_0,\mathbf{q})}{q_0-\sigma\tilde{\epsilon}_\mathbf{q}}Z^2(q_0)\left[\tanh\left(\frac{q_0}{2T}\right)+\coth\left(\frac{\omega-q_0}{2T}\right)\right]$$
$$-\frac{\pi}{4\tilde{\epsilon}_\mathbf{q}}\operatorname{Re}\phi(\tilde{\epsilon}_\mathbf{q},\mathbf{q})\,Z^2(\tilde{\epsilon}_\mathbf{q})\sum_{\sigma=\pm}\sigma\rho^{\ell,t}(\omega-\sigma\tilde{\epsilon}_\mathbf{q},\mathbf{p})\left[\tanh\left(\frac{\sigma\tilde{\epsilon}_\mathbf{q}}{2T}\right)+\coth\left(\frac{\omega-\sigma\tilde{\epsilon}_\mathbf{q}}{2T}\right)\right]$$
$$\equiv \operatorname{Im}\mathcal{M}_\mathcal{B}^{\ell,t}(\omega+i\eta,\mathbf{p},\mathbf{q})+\operatorname{Im}\mathcal{M}_\mathcal{A}^{\ell,t}(\omega+i\eta,\mathbf{p},\mathbf{q})\;. \tag{3.106}$$

Note, that in the above Eq. (3.105) $\omega + i\eta$ appears with a minus sign in the argument of the gluon propagators. The traces over Dirac space $\operatorname{Tr}_s^{\ell,t}(k,p,q)$ are introduced in Eqs. (3.55) The first term on the r.h.s of Eq. (3.106), $\operatorname{Im}\mathcal{M}_\mathcal{B}^{\ell,t}$, is due to the non-analyticities of $\phi(K)$ and has been neglected in all previous treatments. Inserted into Eq. (3.105) it constitutes the term $\mathcal{B}[\operatorname{Im}\phi]$ introduced in Eq. (3.88). The second term, $\operatorname{Im}\mathcal{M}_\mathcal{A}^{\ell,t}$, contains all contributions to $\phi(K)$ that have been considered so far to subleading order. Inserted into Eq. (3.105) it constitutes the term $\mathcal{A}[\operatorname{Re}\phi]$. As already announced it contains the real part of the gap function always on the quasiparticle mass-shell. It is instructive to shortly analyze this issue before proceeding further. The anomalous propagator $\Xi(Q) \equiv Z^2(q_0)\,\phi(Q)/(q_0^2-\tilde{\epsilon}_q^2)$ has the spectral density

$$\rho_\Xi(\omega,\mathbf{q}) \equiv \frac{1}{2\pi i}\left[\Xi(\omega+i\eta,\mathbf{q})-\Xi(\omega-i\eta,\mathbf{q})\right]$$
$$= \frac{1}{2\pi i}\left[\frac{Z^2(\omega+i\eta)\,\tilde{\phi}(\omega+i\eta,\mathbf{q})}{\omega^2-[Z(\omega)\epsilon_\mathbf{q}]^2+\operatorname{sign}(\omega)i\eta}-\frac{Z^2(\omega-i\eta)\,\tilde{\phi}(\omega-i\eta,\mathbf{q})}{\omega^2-[Z(\omega)\epsilon_\mathbf{q}]^2-\operatorname{sign}(\omega)i\eta}\right]$$
$$\simeq \frac{1}{2\pi i}\left\{Z^2(\omega)\mathcal{P}\frac{\tilde{\phi}(\omega+i\eta,\mathbf{q})-\tilde{\phi}(\omega-i\eta,\mathbf{q})}{\omega^2-[Z(\omega)\epsilon_\mathbf{q}]^2}\right.$$

$$-i\pi\text{sign}(\omega)\,Z^2(\tilde{\epsilon}_{\mathbf{q}})\,\delta\left(\omega^2 - \tilde{\epsilon}_{\mathbf{q}}^2\right)\left[\phi(\omega + i\eta, \mathbf{q}) + \phi(\omega - i\eta, \mathbf{q})\right]\Big\}$$

$$= -Z^2(\omega)\mathcal{P}\,\frac{\rho_\phi(\omega, \mathbf{q})}{\omega^2 - [Z(\omega)\epsilon_{\mathbf{q}}]^2} - \text{sign}(\omega)\,Z^2(\tilde{\epsilon}_{\mathbf{q}})\,\text{Re}\,\phi(\omega + i\eta, \mathbf{q})\,\delta\left(\omega^2 - \tilde{\epsilon}_{\mathbf{q}}^2\right),$$

$$(3.107)$$

where the cut of $Z(\omega)$ has been neglected. It follows that $\rho_\phi(\omega, \mathbf{q}) \neq 0$ leads to additional support of $\rho_\Xi(\omega, \mathbf{q})$ around the quasiparticle pole $\omega \equiv \tilde{\epsilon}_q$. Furthermore, neglecting $\text{Im}\,\phi$ is equivalent to approximating

$$\rho_\Xi(\omega, \mathbf{q}) \simeq -\text{sign}(\omega)\,\text{Re}\,\phi(\tilde{\epsilon}_{\mathbf{q}} + i\eta, \mathbf{q})\,Z^2(\tilde{\epsilon}_{\mathbf{q}})\,\delta\left(\omega^2 - \tilde{\epsilon}_{\mathbf{q}}^2\right) \qquad (3.108)$$

as it has been done in [55], cf. Eq. (41). As a consequence, the gap function on the r.h.s. of the gap equation is always forced onto the quasiparticle mass-shell and the gap equation takes the standard form, cf. Eq. (3.64). The occurrence of the external energy $\tilde{\epsilon}_k$ on the r.h.s. due to the energy-dependent gluon propagators indicates that the solution still would possess some energy dependence although not provided in the ansatz Eq. (3.108). This demonstrates explicitly the inherent inconsistency of this ansatz.

It is interesting to note that in Eq. (3.107) $\text{Im}\,\phi \neq 0$ does not shift the quasiparticle pole into complex q_0- plane, since $\epsilon_q \equiv \sqrt{(q - \mu)^2 + |\phi|^2}$. Therefore, no damping of Ξ is caused. In order to restore the effect of damping due to $\text{Im}\,\phi$ one would have to include $\text{Im}\,\Sigma$, which is beyond the scope of this work.

In the limit of small temperatures, $T \to 0$, the hyperbolic functions in Eq. (3.106) simplify, yielding for $\omega > 0$

$$\text{Im}\mathcal{M}_{T=0}^{\ell,t}(\omega + i\eta, \mathbf{p}, \mathbf{q}) = \frac{\pi}{2\tilde{\epsilon}_{\mathbf{q}}}\left[\sum_{\sigma=\pm}\sigma\,\mathcal{P}\int_0^\omega dq_0\,\frac{\rho^{\ell,t}(\omega - q_0, \mathbf{p})\rho_\phi(q_0, \mathbf{q})}{q_0 - \sigma\tilde{\epsilon}_{\mathbf{q}}}\,Z^2(q_0)\right.$$

$$\left. - Z^2(\tilde{\epsilon}_{\mathbf{q}})\,\text{Re}\,\phi(\tilde{\epsilon}_{\mathbf{q}}, \mathbf{q})\,\rho^{\ell,t}(\omega - \tilde{\epsilon}_{\mathbf{q}}, \mathbf{p})\,\theta(\omega - \tilde{\epsilon}_{\mathbf{q}})\right]$$

$$\equiv \text{Im}\mathcal{M}_{\mathcal{B},T=0}^{\ell,t}(\omega + i\eta, \mathbf{p}, \mathbf{q}) + \text{Im}\mathcal{M}_{\mathcal{A},T=0}^{\ell,t}(\omega + i\eta, \mathbf{p}, \mathbf{q})\,.$$

$$(3.109)$$

Here, use was made of the oddness of ρ_ϕ in ω, cf. Eq. (3.84c).

3.2.2 Estimating the order of magnitude of $\mathcal{A}$ and $\mathcal{B}$

Following the strategy explained in Sec. 3.2.1 it is necessary to know the order of magnitude of the real part of the on-shell gap function $\text{Re}\,\phi(\tilde{\epsilon}_{\mathbf{q}}, \mathbf{q})$ in order to estimate the magnitude of the parts $\mathcal{A}$ and $\mathcal{B}$ of $\text{Im}\,\phi$, cf. Eq. (3.88). It is known that $\phi_k \equiv \text{Re}\,\phi(\epsilon_{\mathbf{k}}, \mathbf{k})$ is momentum dependent [13]

$$\phi(x) \equiv \phi_0^{\text{2SC}}\,F(x)\,, \qquad (3.110)$$

where ϕ_0^{2SC} is the value of the gap for momenta on the Fermi surface

$$\phi_0^{\text{2SC}} = 2\,\tilde{b}\,b_0'\,\mu\,\exp\left(-\frac{\pi}{2\,\bar{g}}\right) \qquad (3.111)$$

with $\bar{g} \equiv g/(3\sqrt{2}\pi)$ and the constants (subleading and therefore in principle irrelevant for the present purposes)

$$\tilde{b} \equiv 256\,\pi^4 \left(\frac{2}{N_f g^2}\right)^{5/2} \, , \qquad b_0' \equiv \exp\left(-\frac{\pi^2+4}{8}\right) \, . \tag{3.112}$$

The variable x is a exponential measure for the distance of $\mathbf{k}$ from the Fermi surface

$$x \equiv \bar{g}\,\ln\left(\frac{2\tilde{b}\mu}{k-\mu+\epsilon_{\mathbf{k}}}\right) \, . \tag{3.113}$$

For $|k-\mu| \sim \phi$ one finds $x = \pi/2 + O(\bar{g})$, while for $|k-\mu| \sim M$ it is $x \sim O(\bar{g})$. The function $F(x)$ is to leading order given by $F(x) = \sin(x)$. Hence, for momenta exponentially close to the Fermi surface, $|k-\mu| \sim \phi$, the on-shell gap function is $\phi(\epsilon_{\mathbf{k}},\mathbf{k}) = \phi_0^{2SC}[1+O(\bar{g}^2)]$, i.e. constant to leading order. For momenta $|k-\mu| \sim M$, one has $\phi(\epsilon_{\mathbf{k}},k) = \bar{g}\,\phi_0^{2SC}$. Hence, the real part of the on-shell gap function is sharply peaked around the Fermi surface. This exponential decay off the Fermi surface becomes apparent when considering *intermediate* distances from the Fermi surface (between ϕ and M) defined by the variable scale

$$\Lambda_y \equiv \phi^y M^{1-y} \tag{3.114}$$

with $0 < y < 1$. For $|k-\mu| \sim \Lambda_y$ one has $x = y\,\pi/2 + O(\bar{g})$ and $F(y) \simeq \sin(y\,\pi/2) \simeq y$. Hence, decreasing y (i.e. exponentially admixing the scale M to Λ_y and exponentially receding from the Fermi surface) decreases the magnitude of the gap approximately linearly. For $y \sim \bar{g}$ the gap function has decreased to $\bar{g}\,\phi_0^{2SC}$. The intermediate scales may be also used to investigate the generation of the so-called BCS-log. Denoting $\Lambda_1 = \phi$ and $\Lambda_0 = M$ and exploiting $\Lambda_1 \ll \Lambda_{\bar{g}} \lesssim \Lambda_0$ one may write

$$
\begin{aligned}
g^2 \int_0^M \frac{d\xi}{\epsilon_{\mathbf{q}}}\,\phi_q &\equiv g^2 \int_0^{\Lambda_1} \frac{d\xi}{\epsilon_{\mathbf{q}}}\,\phi_q + g^2 \int_{\Lambda_1}^{\Lambda_{\bar{g}}} \frac{d\xi}{\epsilon_{\mathbf{q}}}\,\phi_q + g^2 \int_{\Lambda_{\bar{g}}}^{\Lambda_0} \frac{d\xi}{\epsilon_{\mathbf{q}}}\,\phi_q \\
&\simeq g^2 \ln(\sqrt{2}+1)\,\phi_0 + g^2 \left[\ln\left(\frac{2\Lambda_{\bar{g}}}{\Lambda_1}\right) - \ln(\sqrt{2}+1)\right]\phi_0 + g^2 \ln\left(\frac{\Lambda_0}{\Lambda_{\bar{g}}}\right)g\phi_0 \\
&\simeq g^2 \ln\left(\frac{2M^{1-\bar{g}}}{\phi^{1-\bar{g}}}\right)\phi_0 + g^3 \ln\left(\frac{M^{\bar{g}}}{\phi^{\bar{g}}}\right)\phi_0 \\
&\sim g\phi_0 \, ,
\end{aligned}
\tag{3.115}
$$

where use was made of Eq. (3.111) yielding the BCS-log, $\ln(M/\phi) \sim 1/g$. It is shown that the BCS-log arises from integrating over intermediate scales, $\Lambda_1 < \xi < \Lambda_{\bar{g}}$. In the region $\Lambda_{\bar{g}} < \xi < M$ the BCS-log does not occur due to the exponential $\bar{g}$ under the logarithm. In addition the contribution from this region is suppressed by an extra factor $\bar{g}$ from $\phi_q \sim \bar{g}\phi_0$. In the QCD gap-equation the gluon propagator has to be added to the integrand. (Then the region $\Lambda_1 < \xi < \Lambda_{\bar{g}}$ is enhanced by an additional large logarithm due to almost static, Landau-damped magnetic gluons.) However, the above observation that the BCS-log is generated by intermediate scales $\Lambda_{1>y>\bar{g}}$ remains valid in the full gap equation.

Landau-damped gluons contributing to $\mathcal{A}$

For the purpose of power counting the various terms in Eq. (3.105) one may restrict oneself to the leading contribution of the Dirac traces Eqs. (3.55), which is of order one. The integral over the absolute magnitude of the quark momentum is $\int dq\, q^2$, while the angular integration is $\int d\cos\theta \equiv \int dp\, p/(kq)$. Furthermore, only the zero-temperature limit, $T = 0$ is considered, allowing for the estimate $Z^2(\tilde{\epsilon}_{\mathbf{q}}) \sim 1$. The contribution of $\mathcal{M}^{\ell,t}_{\mathcal{A},T=0}$ in Eq. (3.109) arising from $\rho^{\ell,t}_{\mathrm{cut}}(\omega - \epsilon_{\mathbf{q}}, \mathbf{p})$ to $\mathcal{A}$ is

$$\mathcal{A}^{\ell,t}_{\mathrm{cut}}(\omega, \mathbf{k}) \quad \sim \quad g^2 \int\limits_0^\delta \frac{d\xi}{\epsilon_{\mathbf{q}}} \, \mathrm{Re}\, \phi(\epsilon_{\mathbf{q}}, \mathbf{q}) \int\limits_\lambda^{\Lambda_{\mathrm{gl}}} dp\, p\, \rho^{\ell,t}_{\mathrm{cut}}(\omega^*, \mathbf{p}) \,, \tag{3.116}$$

where $\omega^* \equiv \omega - \epsilon_{\mathbf{q}} < \omega$, $\delta \equiv \min(\omega, \Lambda_{\mathrm{q}})$ and $\lambda \equiv \max(|\xi - \zeta|, \omega^*)$ with $\zeta \equiv |k - \mu|$. Due to the condition $\lambda < p < \Lambda_{\mathrm{gl}}$ it immediately follows that $\mathcal{A}^{\ell,t}_{\mathrm{cut}} = 0$ for $\omega > \Lambda_{\mathrm{gl}} + \Lambda_{\mathrm{q}} \sim \mu$. Inserting the approximative forms

$$\rho^t_{\mathrm{cut}}(\omega^*, \mathbf{p}) \simeq \frac{M^2}{\pi} \frac{\omega^* p}{p^6 + (M^2\,\omega^*)^2} \,, \quad \rho^\ell_{\mathrm{cut}}(\omega^*, \mathbf{p}) \simeq \frac{2M^2}{\pi} \frac{\omega^*}{p} \frac{1}{(p^2 + 3\,m_g^2)^2} \tag{3.117}$$

the integration over p can be performed analytically. For energies $\omega < \Lambda_{\mathrm{gl}}$ one finds for the transverse part

$$\mathcal{A}^t_{\mathrm{cut}}(\omega, \mathbf{k}) \quad \sim \quad g^2 \int\limits_0^\omega \frac{d\xi}{\epsilon_{\mathbf{q}}} \mathrm{Re}\, \phi(\epsilon_{\mathbf{q}}, \mathbf{q}) \left[\arctan\left(\frac{\Lambda^3_{\mathrm{gl}}}{M^2\omega^*} \right) - \arctan\left(\frac{\lambda^3}{M^2\omega^*} \right) \right] \,. \tag{3.118}$$

For all $\zeta \leq \Lambda_{\mathrm{q}}$ and $\omega < \Lambda_{\mathrm{gl}}$ it is $\Lambda^3_{\mathrm{gl}}/M^2\omega^* \gg 1$ and the first arctan in the squared brackets may be set equal to $\pi/2$. Considering $\zeta, \omega \ll M$ the argument of the second arctan is $\lambda^3/M^2\omega^* \ll 1$ and the combination of both arctans is ~ 1. Increasing the energy to $\omega \sim M$ one finds $\lambda^3/M^2\omega^* \sim M/(M - \xi)$, which becomes large only for $\xi \to M$. However, since the integration over ξ stops here anyway this case does not have to be analyzed further. Consequently, also for $\omega \sim M$ one may estimate the arctans to be ~ 1. For $\omega \gg M$ one has $\lambda^3/M^2\omega^* \gg 1$ and the arctans finally cancel. Considering $\zeta \lesssim M$ one finds for $\omega \ll M$ that $\lambda^3/M^2\omega^* \sim M/\omega^* \gg 1$ and the arctans cancel. The same is true for $\omega \gg M$ since then $\lambda^3/M^2\omega^* \sim (\omega/M)^2 \gg 1$. Only in the region $\omega \sim M$ it is $\lambda^3/M^2\omega^* \sim M/\omega^* \sim 1$ and the arctans do not cancel.

One first considers $\zeta \ll M$ and $\omega \sim \phi$. Because in this special case the integral over ξ does not yield the BCS-log one finds

$$\mathcal{A}^t_{\mathrm{cut}}(\phi, \mathbf{k}) \quad \sim \quad g^2\phi \,. \tag{3.119}$$

For larger energies $\omega \sim \Lambda_y$ with $0 < y < 1$ and $\zeta \ll M$ one substitutes $\xi(y') \equiv \Lambda_{y'}$, $d\xi/\xi = \ln(\phi/M)\, dy'$, one finds with Eq. (3.110)

$$\mathcal{A}^t_{\mathrm{cut}}(\omega, \mathbf{k}) \quad \sim \quad g^2 \ln\left(\frac{\phi}{M} \right) \phi \int\limits_1^y dy\, \sin\left(\frac{\pi y}{2} \right) \sim g\,\phi\, \cos\left(\frac{\pi y}{2} \right) \,. \tag{3.120}$$

Following the discussion after Eq. (3.118) the limit $y \to 0$ of Eq. (3.120) is valid also for $\zeta \sim M$. Hence for $\omega \sim M$ and all $\zeta < \Lambda_{\mathrm{q}}$ it is $\mathcal{A}_{\mathrm{cut}}^t(\omega, \mathbf{k}) \sim g \phi$. For all other values of ω and ζ the contribution $\mathcal{A}_{\mathrm{cut}}^t(\omega, \mathbf{k})$ is strongly suppressed.

In the longitudinal sector one finds for the integral over the gluon momentum p

$$
\begin{aligned}
\mathcal{I}(\lambda) &\equiv M^2 \int_\lambda^{\Lambda_{\mathrm{gl}}} \frac{dp}{(p^2 + X^2)^2} \sim \frac{1}{X} \left[\arctan\left(\frac{\Lambda_{\mathrm{gl}}}{X}\right) - \arctan\left(\frac{\lambda}{X}\right) \right] - \frac{\lambda}{X^2 + \lambda^2} \\
&\sim \begin{cases} 1/X, & \text{for } \lambda \leq X \\ 1/\lambda, & \text{for } \lambda \gg X \end{cases},
\end{aligned}
\tag{3.121}
$$

where it is abbreviated $X^2 \equiv 3m_g^2$. Since $\zeta \leq \Lambda_{\mathrm{q}} \sim X$, solely the magnitude of ω decides whether $\lambda \leq X$ or $\lambda \gg X$ is realized. It follows that in contrast to the transversal case the order of magnitude of $\mathcal{A}_{\mathrm{cut}}^\ell$ is not dependent on the choice of ζ. Energies $\omega \sim \Lambda_y$ with $0 \leq y < 1$ correspond to $\lambda \leq X$, where the r.h.s. of Eq. (3.121) is $\sim 1/X$. Beginning with the special case $\omega \sim \Lambda_1$ one finds

$$
\mathcal{A}_{\mathrm{cut}}^\ell(\omega, \mathbf{k}) \sim g^2 \int_0^\omega \frac{d\xi}{\epsilon_{\mathbf{q}}} \operatorname{Re} \phi(\epsilon_{\mathbf{q}}, \mathbf{q}) \frac{\omega^*}{M} \sim g^2 \phi \frac{\phi}{M} .
\tag{3.122}
$$

For $\omega \sim \Lambda_y$ with $0 < y < 1$ one has similarly

$$
\begin{aligned}
\mathcal{A}_{\mathrm{cut}}^\ell(\omega, \mathbf{k}) &\sim g \phi \int_1^y dy' \sin\left(\frac{\pi y'}{2}\right) \frac{\omega^*}{M} \sim g \phi \int_1^y dy' \sin\left(\frac{\pi y'}{2}\right) \left[\left(\frac{\phi}{M}\right)^y - \left(\frac{\phi}{M}\right)^{y'} \right] \\
&\sim g \phi \cos\left(\frac{\pi y}{2}\right) \left(\frac{\phi}{M}\right)^y .
\end{aligned}
\tag{3.123}
$$

Hence, in the considered energy regime $\mathcal{A}_{\mathrm{cut}}^\ell$ is suppressed by the factor $(\phi/M)^y$ as compared to $\mathcal{A}_{\mathrm{cut}}^t$, i.e. $\mathcal{A}_{\mathrm{cut}}^\ell \ll \mathcal{A}_{\mathrm{cut}}^t$. For energies $\omega \sim M$ the longitudinal and the transversal cut contribute at the same order, $\mathcal{A}_{\mathrm{cut}}^\ell \sim \mathcal{A}_{\mathrm{cut}}^t \sim g \phi$. For much larger energies, $M \ll \omega < \mu$, (ζ is bounded by Λ_{q}) it is $\lambda = \omega^* \simeq \omega \gg X$ and the r.h.s. of Eq. (3.121) is $\sim 1/\lambda \sim 1/\omega$. It follows with $\delta = \Lambda_{\mathrm{q}} \sim \Lambda_0$

$$
\mathcal{A}_{\mathrm{cut}}^\ell(\omega, \mathbf{k}) \sim g \phi \int_1^0 dy \sin\left(\frac{\pi y}{2}\right) \frac{\omega^*}{\omega} \sim g \phi \int_1^0 dy \sin\left(\frac{\pi y}{2}\right) \sim g \phi
\tag{3.124}
$$

and one found that $\mathcal{A}_{\mathrm{cut}}^\ell \gg \mathcal{A}_{\mathrm{cut}}^t$ in this large-energy regime. The results for $\mathcal{A}_{\mathrm{cut}}^{\ell,t}$ are summarized in Tables 3.1 and 3.2.

Undamped gluons contributing to $\mathcal{A}$

The contributions from the undamped gluon excitations to $\mathcal{A}$ read analogously to Eq. (3.116)

$$
\mathcal{A}_{\mathrm{pole}}^{\ell,t}(\omega, \mathbf{k}) \sim g^2 \int_0^\delta \frac{d\xi}{\epsilon_{\mathbf{q}}} \operatorname{Re} \phi(\epsilon_{\mathbf{q}}, \mathbf{q}) \int_{|\xi-\zeta|}^{2\mu} dp \, p \, \rho_{\mathrm{pole}}^{\ell,t}(\omega^*, \mathbf{p}) \, \delta[\omega^* - \omega_{\ell,t}(\mathbf{p})] .
\tag{3.125}
$$

ω	ϕ	$\Lambda_{1>y>0}$	M	$M \ll \omega < \mu$
$\mathcal{A}_{\text{cut}}^{t}$	$g^2 \phi$	$g\,\phi\,\cos\left(\frac{\pi y}{2}\right)$	$g\,\phi$	0
$\mathcal{A}_{\text{cut}}^{\ell}$	$g^2\phi\,\frac{\phi}{M}$	$g\,\phi\left(\frac{\phi}{M}\right)^y \cos\left(\frac{\pi y}{2}\right)$	$g\,\phi$	$g\,\phi$
$\mathcal{A}_{\text{cut}}$	$g^2\phi$	$g\,\phi\,\cos\left(\frac{\pi y}{2}\right)$	$g\,\phi$	$g\,\phi$

Table 3.1: Estimates for $\mathcal{A}_{\text{cut}}^{\ell,t}$ and $\mathcal{A}_{\text{cut}} = \mathcal{A}_{\text{cut}}^{\ell} + \mathcal{A}_{\text{cut}}^{t}$ at different energy scales and $\zeta \ll M$.

ω	ϕ	$\Lambda_{1>y>0}$	M	$M \ll \omega < \mu$
$\mathcal{A}_{\text{cut}}^{t}$	0	0	$g\,\phi$	0
$\mathcal{A}_{\text{cut}}^{\ell}$	$g^2\phi\,\frac{\phi}{M}$	$g\,\phi\left(\frac{\phi}{M}\right)^y \cos\left(\frac{\pi y}{2}\right)$	$g\,\phi$	$g\,\phi$
$\mathcal{A}_{\text{cut}}$	$g^2\phi\,\frac{\phi}{M}$	$g\,\phi\left(\frac{\phi}{M}\right)^y \cos\left(\frac{\pi y}{2}\right)$	$g\,\phi$	$g\,\phi$

Table 3.2: Estimates for $\mathcal{A}_{\text{cut}}^{\ell,t}$ and $\mathcal{A}_{\text{cut}} = \mathcal{A}_{\text{cut}}^{\ell} + \mathcal{A}_{\text{cut}}^{t}$ at different energy scales and $\zeta \lesssim M$.

Due to the δ−function and $\omega_{\ell,t}(\mathbf{p}) \geq m_g$ this contribution will be nonzero only for energies $\omega > m_g \sim M$. The upper boundary $\sim 2\mu$ in the integral over p is due to the constraint on relevant quark momenta near the Fermi surface in the effective theory, $\xi \leq \Lambda_{\text{q}}$, where $\Lambda_{\text{q}} \sim g\mu$ is the quark cutoff, cf. Fig. 3.9. Due to this kinematic limitation it immediately follows that $\mathcal{A}_{\text{pole}}^{\ell,t} = 0$ for $\omega > 2\mu + \Lambda_{\text{q}} \simeq 2\mu$, since then $\omega^* \equiv \omega - \xi > \omega_{\ell,t}$ always and the δ−function on the r.h.s. of Eq. (3.125) is identically zero.

For the transverse sector one may approximate for all momenta p

$$\rho_{\text{pole}}^{t}(\omega_t(\mathbf{p}), \mathbf{p}) \simeq -\frac{1}{2\omega_t(\mathbf{p})} \, , \tag{3.126}$$

and $\omega_t(\mathbf{p}) \simeq \sqrt{p^2 + m_g^2}$. One finds after substituting $dp\,p \simeq d\omega_t\,\omega_t$ and assuming $\zeta \ll M$

$$
\begin{aligned}
\mathcal{A}_{\text{pole}}^{t}(\omega, \mathbf{k}) \;\sim\; & g^2 \int_0^{\Lambda_{\text{q}}} \frac{d\xi}{\epsilon_{\mathbf{q}}} \operatorname{Re}\phi(\epsilon_{\mathbf{q}}, \mathbf{q}) \int_{\sqrt{m_g^2 + \xi^2}}^{2\mu} d\omega_t\, \delta[\omega^* - \omega_t] \\
\;\sim\; & g^2 \int_0^{\xi_{\max}} \frac{d\xi}{\epsilon_{\mathbf{q}}} \operatorname{Re}\phi(\epsilon_{\mathbf{q}}, \mathbf{q}) \sim g\,\phi \, , \tag{3.127}
\end{aligned}
$$

where $\xi_{\max} \equiv \min[(\omega^2 - m_g^2)/(2\omega), \Lambda_{\text{q}}]$. In Fig. 3.10 the integration regions for ξ and ω_t are visualized. For $\xi > \xi_{\max}$ it is $\omega^* = \omega - \xi < \sqrt{m_g^2 + \xi^2} < \omega_t$ and the δ−function under the integral over ω_t is always zero. The last estimate on the r.h.s. of Eq. (3.127) is valid for energies, which are at least $\omega > m_g + \Lambda_y$ with $y < 1$, because then $\xi_{\max}$ is at least Λ_y and the BCS-log is generated cancelling one power of g. For $\zeta \lesssim M$ one has $p > |\xi - \zeta|$ and therefore $\omega_t > \sqrt{m_g^2 + |\xi - \zeta|^2}$. For $\Lambda_1 < \xi < \Lambda_{\bar{g}}$ it is $\omega_t \simeq \sqrt{m_g^2 + \zeta^2} \gtrsim \sqrt{2}m_g$, while for $\Lambda_{\bar{g}} < \xi < \Lambda_0$ it is $\omega_t > m_g$ (independent of the signs of ξ and ζ). It turns out that for ω exponentially close to m_g, i.e. for energies of the form $\omega \sim m_g + \Lambda_y$ with $y > 0$, $\omega^* \equiv \omega - \xi = \omega_t$ cannot be fulfilled
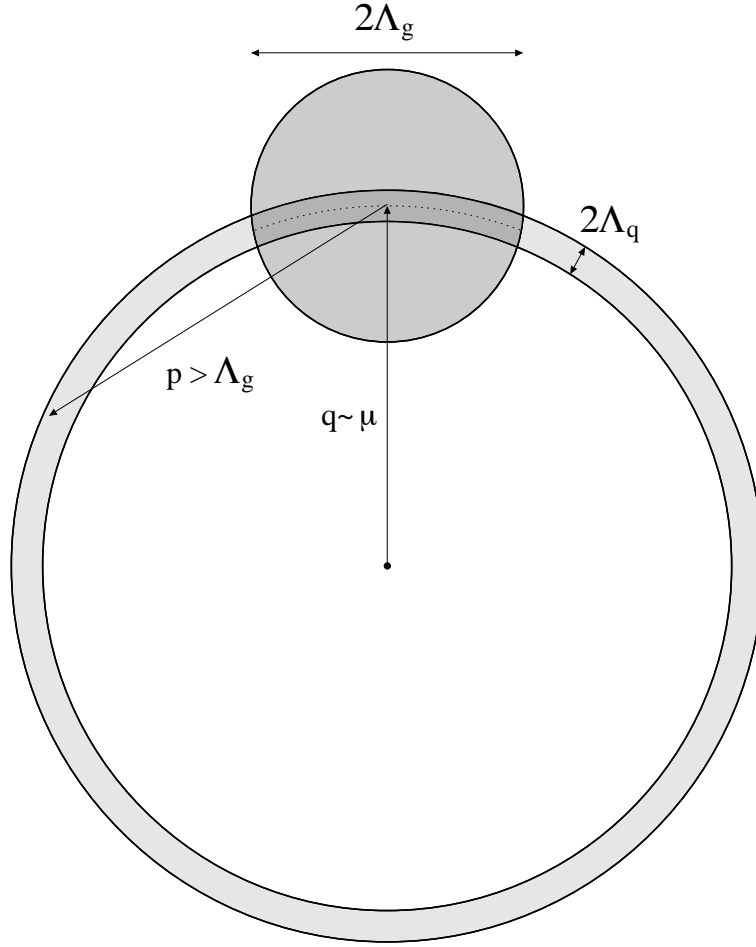
Figure 3.9: Hard gluon exchange with momentum $p > \Lambda_{\mathrm{gl}} \sim \mu$. The quark has to remain within the layer of width $2\Lambda_{\mathrm{q}} \sim g\mu$ around the Fermi-surface. This effectively restricts the hard gluon momentum, $p \lesssim \mu + 2\Lambda_{\mathrm{q}}$.

in the whole integration region $\Lambda_1 < \xi < \Lambda_0$. Consequently, $\mathcal{A}^t_{\mathrm{pole}} = 0$ in this energy domain. Only for energies $\omega > \sqrt{m_g^2 + \zeta^2} \gtrsim \sqrt{2}m_g$ one finds again $\mathcal{A}^t_{\mathrm{pole}} \sim g\,\phi$, which remains valid up to $\omega \lesssim 2\mu$.

In the longitudinal gluon sector one may approximate for gluon momenta $p < m_g$

$$\rho^\ell_{\mathrm{pole}}(\omega_\ell(\mathbf{p}), \mathbf{p}) \simeq -\frac{\omega_\ell(\mathbf{p})}{2p^2} \tag{3.128}$$

and $\omega_\ell(\mathbf{p}) \simeq \sqrt{p^2 + m_g^2}$. For $\omega = m_g + \Lambda_y$ with $0 < y < 1$ one finds after substituting $dp\,p \simeq$
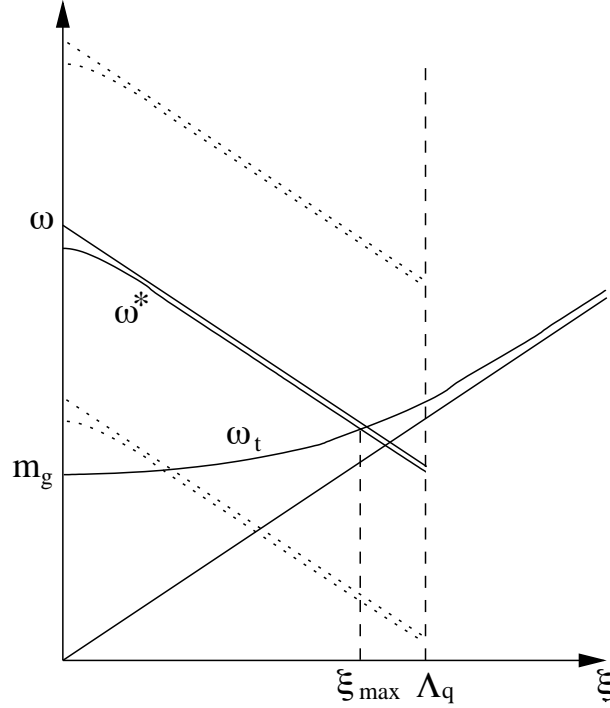
Figure 3.10: The integration regions of ξ and ω_t in Eq. (3.127). Only those values of ξ contribute, for which the integral along ω_t, starting at $\omega_t = \sqrt{m_g^2 + \xi^2}$ and ending at $\omega_t \simeq 2\mu$, has a point of intersection with $\omega^* = \omega - \xi$, $\omega_t = \omega^*$. Only for $\omega > m_g + \Lambda_y$ with $y < 1$ the integration region is sufficiently large to generate the BCS-log. The dotted lines correspond to different values of ω.

$d\omega_\ell \, \omega_\ell$ and assuming $\zeta \ll M$

$$
\begin{aligned}
\mathcal{A}^\ell_{\text{pole}}(\omega, \mathbf{k}) \quad &\sim \quad g^2 \int\limits_0^{\Lambda_q} \frac{d\xi}{\epsilon_{\mathbf{q}}} \operatorname{Re} \phi(\epsilon_{\mathbf{q}}, \mathbf{q}) \int\limits_{\sqrt{m_g^2 + \xi^2}}^{\sqrt{2}\,m_g} d\omega_\ell \, \frac{\omega_\ell^2}{\omega_\ell^2 - m_g^2} \, \delta[\omega^* - \omega_\ell] \\
&\sim \quad g^2 \int\limits_0^{\xi_{\text{max}}} \frac{d\xi}{\epsilon_{\mathbf{q}}} \operatorname{Re} \phi(\epsilon_{\mathbf{q}}, \mathbf{q}) \frac{(\omega - \epsilon_{\mathbf{q}})^2}{(\omega - \epsilon_{\mathbf{q}})^2 - m_g^2} \ ,
\end{aligned}
\tag{3.129}
$$

where the upper limit $\xi_{\text{max}} \equiv (\omega^2 - m_g^2)/(2\omega) \sim \Lambda_y$ is obtained analogously to the transversal case. Since $\xi_{\text{max}} \ll \omega$ and $\omega \gtrsim m_g$ one may approximate the energy fraction under the integral by $\omega^2/(\omega^2 - m_g^2) \sim \omega/(\omega - m_g)$. Then the integral over ξ may be readily performed yielding

$$
\mathcal{A}^\ell_{\text{pole}}(\omega, \mathbf{k}) \sim g \, \phi \, \frac{\omega}{\omega - m_g} \sim g \, \phi \left(\frac{M}{\phi} \right)^y \ ,
\tag{3.130}
$$

where the BCS-log has cancelled one power of g. Analogously to the transversal case, for $\zeta \lesssim M$ one finds $\mathcal{A}^\ell_{\text{pole}} = 0$ if ω is exponentially close to m_g. For $\omega > \sqrt{m_g^2 + \zeta^2} \gtrsim \sqrt{2} m_g$ it

ω	$< m_g + \Lambda_1$	$\sim m_g + \Lambda_{1>y>0}$	$\gtrsim \sqrt{2}m_g$	$m_g \ll \omega < 2\mu$
$\mathcal{A}^t_{\text{pole}}$	0	$g\,\phi$	$g\,\phi$	$g\,\phi$
$\mathcal{A}^\ell_{\text{pole}}$	0	$g\,\phi\left(\frac{M}{\phi}\right)^g$	$g\,\phi$	$g\,\phi\,\exp\left(-\frac{2\omega^2}{3m_g^2}\right)$
$\mathcal{A}_{\text{pole}}$	0	$g\,\phi\left(\frac{M}{\phi}\right)^g$	$g\,\phi$	$g\,\phi$

Table 3.3: Estimates for $\mathcal{A}^{\ell,t}_{\text{pole}}$ and $\mathcal{A}_{\text{pole}} = \mathcal{A}^\ell_{\text{pole}} + \mathcal{A}^t_{\text{pole}}$ at different energy scales and $\zeta \ll M$.

ω	$< m_g + \Lambda_1$	$\sim m_g + \Lambda_{1>y>0}$	$\gtrsim \sqrt{2}m_g$	$m_g \ll \omega < 2\mu$
$\mathcal{A}^t_{\text{pole}}$	0	0	$g\,\phi$	$g\,\phi$
$\mathcal{A}^\ell_{\text{pole}}$	0	0	$g\,\phi$	$g\,\phi\,\exp\left(-\frac{2\omega^2}{3m_g^2}\right)$
$\mathcal{A}_{\text{pole}}$	0	0	$g\,\phi$	$g\,\phi$

Table 3.4: Estimates for $\mathcal{A}^{\ell,t}_{\text{pole}}$ and $\mathcal{A}_{\text{pole}} = \mathcal{A}^\ell_{\text{pole}} + \mathcal{A}^t_{\text{pole}}$ at different energy scales and $\zeta \lesssim M$.

follows $\mathcal{A}^\ell_{\text{pole}} \sim g\,\phi$ again. For much larger energies, $\omega \gg m_g$, gluon momenta $p \gg m_g$ have to be considered in the estimate of $\mathcal{A}^\ell_{\text{pole}}$, cf. upper dotted lines in Fig. 3.10. For those the longitudinal gluon spectral density becomes exponentially suppressed

$$\rho^\ell_{\text{pole}}(\omega_l(\mathbf{p}), \mathbf{p}) \sim \frac{\exp\left(-\frac{2p^2}{3m_g^2}\right)}{p} \tag{3.131}$$

and one has for $m_g \ll \omega < 2\mu$ with $\omega_l(\mathbf{p}) \simeq p$

$$\mathcal{A}^\ell_{\text{pole}}(\omega, \mathbf{k}) \sim g^2 \int_0^{\Lambda_q} \frac{d\xi}{\epsilon_{\mathbf{q}}} \operatorname{Re}\phi(\epsilon_{\mathbf{q}}, \mathbf{q}) \int_{\sqrt{2}m_g}^{2\mu} d\omega_\ell \exp\left(-\frac{2\omega_\ell^2}{3m_g^2}\right) \delta[\omega^* - \omega_\ell]$$

$$\sim g^2\phi \int_{\Lambda_1}^{\Lambda_{\bar{g}}} \frac{d\xi}{\xi} \exp\left[-\frac{2(\omega-\xi)^2}{3m_g^2}\right] \sim g\,\phi\,\exp\left(-\frac{2\omega^2}{3m_g^2}\right) , \tag{3.132}$$

which is the continuation of the estimate given in Eq. (3.130) to large energies $\omega \gg m_g$ and is valid for all $\zeta \leq \Lambda_q$. The results for $\mathcal{A}^{\ell,t}_{\text{pole}}$ are summarized in Tables 3.3 and 3.4.

Landau-damped gluons contributing to $\mathcal{B}$

In the Landau-damped gluon sector $\mathcal{M}^{\ell,t}_{\mathcal{B},T=0}$ in Eq. (3.109) contributes to $\mathcal{B}$ as

$$\mathcal{B}^{\ell,t}_{\text{cut}}(\omega, \mathbf{k}) \sim g^2 \int_0^{\Lambda_q} \frac{d\xi}{\epsilon_{\mathbf{q}}} \int_0^\omega dq_0 \sum_{\sigma=\pm} \frac{\sigma}{q_0 - \sigma\epsilon_{\mathbf{q}}} \rho_\phi(q_0, \mathbf{q}) \int_\lambda^{\Lambda_{\text{gl}}} dp\, p\, \rho^{\ell,t}_{\text{cut}}(\omega', \mathbf{p}) , \tag{3.133}$$

where $\omega' \equiv \omega - q_0 < \omega$ and $\lambda \equiv \max(|\xi - \zeta|, \omega')$. Substituting the estimates of $\mathcal{A}(q_0, \mathbf{q})$ for $\rho_\phi(q_0, \mathbf{q})$ one estimates $\mathcal{B}^{\ell,t}_{\text{cut}}(\omega, \mathbf{k})$ for different domains of ω and ζ. Due to the condition $\lambda < \Lambda_{\text{gl}}$

in Eq. (3.133) and $\mathcal{A}(q_0, \mathbf{q}) = 0$ for $q_0 > 2\mu$ it immediately follows that $\mathcal{B}_{\text{cut}}^{\ell,t}(\omega, \mathbf{k}) = 0$ for $\omega > \Lambda_{\text{gl}} + 2\mu \sim 3\mu$. Inserting the approximative forms (3.117) for $\rho_{\text{cut}}^{\ell,t}$ into Eq. (3.133) the integration over p can be performed analogously to Eqs. (3.118,3.121). In the transverse case one finds

$$\mathcal{B}_{\text{cut}}^t(\omega, \mathbf{k}) \sim g^2 \int\limits_0^{\Lambda_{\text{q}}} \frac{d\xi}{\epsilon_{\mathbf{q}}} \int\limits_0^{\omega} dq_0 \sum_{\sigma=\pm} \frac{\sigma \, \mathcal{A}(q_0, \mathbf{q})}{q_0 - \sigma\epsilon_{\mathbf{q}}} \left[\arctan\left(\frac{\Lambda_{\text{gl}}^3}{M^2\omega'}\right) - \arctan\left(\frac{\lambda^3}{M^2\omega'}\right) \right] . \qquad (3.134)$$

The analysis of the domains of ω, ζ and ξ where the arctans in the squared brackets in Eq. (3.134) do not cancel is analogous the one after Eq. (3.118). For all ξ, $\zeta \leq \Lambda_{\text{q}}$ and $\omega < 3\mu$ it is $\Lambda_{\text{gl}}^3/M^2\omega' \gg 1$ and the first arctan in the squared brackets may be set equal to $\pi/2$. Considering $\zeta, \omega \ll M$ the argument of the second arctan is $\lambda^3/M^2\omega' \sim \xi^3/M^2\omega'$. As long as $\xi < (M^2\omega')^{1/3}$, this is not $\gg 1$ and the combination of both arctans is ~ 1. Increasing the energy to $\omega \sim M$ one finds that $\lambda^3/M^2\omega'$ becomes large only for $q_0 \to \omega$, because then $\lambda^3/M^2\omega' \sim \xi^3/M^2(\omega - q_0) \gg 1$. However, since the integration over q_0 stops here anyway this case does not have to be analyzed further. Consequently, also for $\omega \sim M$ one may estimate the arctans to be ~ 1. For $\omega \gg M$ one has $\lambda^3/M^2\omega' \sim [(\omega - q_0)/M]^2$ which is $\lesssim 1$ only for $\omega - M \lesssim q_0 \lesssim \omega$. For values of ω outside this range, the arctans cancel. Considering $\zeta \lesssim M$ one finds for $\omega \ll M$ that $\lambda^3/M^2\omega' \sim M/\omega' \gg 1$ and the arctans cancel. (In the region where $|\xi - \zeta|$ is sufficienty small the arctans do not cancel. However, since this requires $\xi \lesssim M$, the BCS-log cannot be generated. Therefore, this special case can always be neglected.) In the region $\omega \sim M$ it is $\lambda^3/M^2\omega' \sim M/\omega' \sim 1$ and the arctans do not cancel. For $\omega \gg M$ the respective analysis as made for $\zeta \ll M$ applies.

Before proceeding further one proves that the generation of the BCS-log can be prevented if additional logarithmic dependences appear under the integral over ξ in the following form

$$\int\limits_{\Lambda_1}^{\Lambda_0} \frac{d\xi}{\xi} \ln\left|\frac{\xi + \Lambda_y}{\xi - \Lambda_y}\right| = \int\limits_{\Lambda_1}^{\Lambda_y} \frac{d\xi}{\xi} \ln\left(\frac{\xi + \Lambda_y}{\Lambda_y - \xi}\right) + \int\limits_{\Lambda_y}^{\Lambda_0} \frac{d\xi}{\xi} \ln\left(\frac{\xi + \Lambda_y}{\xi - \Lambda_y}\right) , \qquad (3.135)$$

where $0 \leq y \leq 1$. Introducing the dilogarithm [129]

$$\text{Li}_2(x) \equiv \int\limits_x^0 \frac{d\xi}{\xi} \ln(1 - \xi) , \qquad (3.136)$$

which has the values $-\frac{1}{12}\pi^2 \equiv \text{Li}_2(-1) \leq \text{Li}_2(x) \leq \text{Li}_2(1) \equiv \frac{1}{6}\pi^2$ for $-1 \leq x \leq 1$, one may express the first term on the r.h.s. of Eq. (3.135) as

$$\int\limits_{\Lambda_1}^{\Lambda_y} \frac{d\xi}{\xi} \ln\left(\frac{\xi + \Lambda_y}{\Lambda_y - \xi}\right) = \int\limits_{\Lambda_1/\Lambda_y}^1 \frac{d\xi}{\xi} \ln\left(\frac{1 + \xi}{1 - \xi}\right) = \text{Li}_2(1) - \text{Li}_2(-1) + \text{Li}_2\left(-\frac{\Lambda_1}{\Lambda_y}\right) - \text{Li}_2\left(\frac{\Lambda_1}{\Lambda_y}\right)$$

$$= \frac{\pi^2}{4} + \text{Li}_2\left(-\frac{\Lambda_1}{\Lambda_y}\right) - \text{Li}_2\left(\frac{\Lambda_1}{\Lambda_y}\right) . \qquad (3.137)$$

Since $0 < \Lambda_1/\Lambda_y \leq 1$ this term is of order 1 and no BCS-log has been generated in this term. The second term on the r.h.s. of Eq. (3.135) is

$$
\int_{\Lambda_y}^{\Lambda_0} \frac{d\xi}{\xi} \ln\left(\frac{\xi + \Lambda_y}{\xi - \Lambda_y}\right) = \int_1^{\Lambda_0/\Lambda_y} \frac{d\xi}{\xi} \ln\left(\frac{1+\xi}{\xi-1}\right) = -\int_1^{\Lambda_y/\Lambda_0} \frac{d\chi}{\chi} \ln\left(\frac{1+1/\chi}{1/\chi-1}\right)
$$

$$
= \int_{\Lambda_y/\Lambda_0}^1 \frac{d\chi}{\chi} \ln\left(\frac{1+\chi}{1-\chi}\right) = \mathrm{Li}_2(1) - \mathrm{Li}_2(-1) + \mathrm{Li}_2\left(-\frac{\Lambda_y}{\Lambda_0}\right) - \mathrm{Li}_2\left(\frac{\Lambda_y}{\Lambda_0}\right)
$$

$$
= \frac{\pi^2}{4} + \mathrm{Li}_2\left(-\frac{\Lambda_y}{\Lambda_0}\right) - \mathrm{Li}_2\left(\frac{\Lambda_y}{\Lambda_0}\right) \; . \tag{3.138}
$$

In the second step one substituted $\chi \equiv 1/\xi$ with $d\chi/\chi = -d\xi/\xi$. Similarly to Eq. (3.137) it is $0 < \Lambda_y/\Lambda_0 \leq 1$. Hence, also this term is of order 1 and no BCS-log has been generated here, either, proving the above statement.

Beginning with energies $\omega \sim \phi$ one may use Eq. (3.119) to estimate $\mathcal{A} \sim \mathcal{A}_{\mathrm{cut}}^t \sim g^2\phi$. Assuming $\zeta \ll M$ one has

$$
\mathcal{B}_{\mathrm{cut}}^t(\phi, \mathbf{k}) \sim g^4\phi \int_0^{\Lambda_q} \frac{d\xi}{\epsilon_\mathbf{q}} \int_0^\phi dq_0 \sum_{\sigma=\pm} \frac{\sigma}{q_0 - \sigma\epsilon_\mathbf{q}} \left[\arctan\left(\frac{\Lambda_{\mathrm{gl}}^3}{M^2\omega'}\right) - \arctan\left(\frac{\lambda^3}{M^2\omega'}\right)\right]
$$

$$
\sim g^4\phi \int_0^{\Lambda_{1/3}} \frac{d\xi}{\epsilon_\mathbf{q}} \ln\left|\frac{\epsilon_\mathbf{q} - \phi}{\epsilon_\mathbf{q} + \phi}\right| \sim g^4\phi \; . \tag{3.139}
$$

The arctans in the squared brackets cancel for $\lambda^3 \gg M^2\phi$, which leads to the upper boundary $\Lambda_{1/3}$ in the inegral over ξ. As discussed before the generation of the BCS-log was prevented by the additional logarithm under the integral. For $\zeta \lesssim M$ the arctans in Eq. (3.139) would have cancelled yielding $\mathcal{B}_{\mathrm{cut}}^t(\phi, \mathbf{k}) \simeq 0$.

For $\omega \sim \Lambda_y$ with $0 \leq y < 1$ one conservatively estimates $\mathcal{A} \sim \mathcal{A}_{\mathrm{cut}}^t \sim g\phi$, cf. Eq. (3.120), and obtain similarly to Eq. (3.139), assuming $\zeta \ll M$

$$
\mathcal{B}_{\mathrm{cut}}^t(\Lambda_y, \mathbf{k}) \sim g^3\phi \int_0^{\Lambda_q} \frac{d\xi}{\epsilon_\mathbf{q}} \int_0^{\Lambda_y} dq_0 \sum_{\sigma=\pm} \frac{\sigma}{q_0 - \sigma\epsilon_\mathbf{q}} \left[\arctan\left(\frac{\Lambda_{\mathrm{gl}}^3}{M^2\omega'}\right) - \arctan\left(\frac{\lambda^3}{M^2\omega'}\right)\right]
$$

$$
\sim g^3\phi \int_0^{\Lambda_{y/3}} \frac{d\xi}{\epsilon_\mathbf{q}} \ln\left|\frac{\epsilon_\mathbf{q} - \Lambda_y}{\epsilon_\mathbf{q} + \Lambda_y}\right| \sim g^3\phi \; , \tag{3.140}
$$

where again no BCS-log was generated. Here, the arctans cancel for $\lambda \gg M^2\Lambda_y$, leading to the constraint $\xi < \Lambda_{y/3}$. Again, for $\zeta \lesssim M$ the arctans in Eq. (3.139) would have cancelled yielding $\mathcal{B}_{\mathrm{cut}}^t(\Lambda_y, \mathbf{k}) \simeq 0$.

For energies $\omega \sim m_g + \Lambda_y$ with $0 \leq y < 1$ the combination of the arctangents in Eq. (3.134)

is ~ 1 for all $\zeta \leq \Lambda_\mathrm{q}$. Integrating over q_0 from 0 to m_g one finds similarly to Eq. (3.140)

$$g^3 \phi \int\limits_0^{\Lambda_\mathrm{q}} \frac{d\xi}{\epsilon_\mathbf{q}} \, \ln \left| \frac{\epsilon_\mathbf{q} - \Lambda_0}{\epsilon_\mathbf{q} + \Lambda_0} \right| \sim g^3 \phi \, . \tag{3.141}$$

The dominant contribution, however, is generated when integrating over q_0 from m_g to $m_g + \Lambda_y$ where one has $\mathcal{A} \sim \mathcal{A}^\ell_\mathrm{pole} \sim g \, \phi \, (M/\phi)^y$, cf. Eq. (3.130),

$$
\begin{aligned}
\mathcal{B}^t_\mathrm{cut}(m_g + \Lambda_y, \mathbf{k}) \quad &\sim \quad g^3 \phi \int\limits_0^{\Lambda_\mathrm{q}} \frac{d\xi}{\epsilon_\mathbf{q}} \int\limits_{m_g+\Lambda_1}^{m_g+\Lambda_y} dq_0 \sum_{\sigma=\pm} \frac{\sigma}{q_0 - \sigma\epsilon_\mathbf{q}} \frac{q_0}{q_0 - m_g} \\
&\sim \quad g^2 \phi \int\limits_0^{\Lambda_\mathrm{q}} \frac{d\xi}{\epsilon_\mathbf{q}} \sum_{\sigma=\pm} \frac{\sigma \, m_g}{\sigma\epsilon_\mathbf{q} - m_g} \int\limits_1^y dy' \sim g^2 \phi \int\limits_0^{\Lambda_\mathrm{q}} d\xi \, \frac{m_g}{\xi^2 - m_g^2} \\
&\sim \quad g^2 \, \phi \, . \tag{3.142}
\end{aligned}
$$

For energies $\omega \gtrsim m_g$ but not exponentially close to m_q, the integration over q_0 from $2m_g$ to ω may be performed after estimating $\mathcal{A} \sim g \, \phi$, cf. Eqs. (3.124,3.129), yielding

$$
\begin{aligned}
g^3 \phi \int\limits_0^{\Lambda_\mathrm{q}} \frac{d\xi}{\epsilon_\mathbf{q}} \int\limits_{2m_g}^\omega dq_0 \sum_{\sigma=\pm} \frac{\sigma}{q_0 - \sigma\epsilon_\mathbf{q}} \quad &\sim \quad g^3 \phi \int\limits_0^{\Lambda_\mathrm{q}} \frac{d\xi}{\epsilon_\mathbf{q}} \left[\ln \left(\frac{\omega - \epsilon_q}{\epsilon_q + \omega} \right) - \ln \left(\frac{\omega - M + \epsilon_q}{\omega - M - \epsilon_q} \right) \right] \\
&\sim \quad g^3 \phi \, . \tag{3.143}
\end{aligned}
$$

Hence, one found that generally for energies $\omega \gtrsim m_g$ it is

$$\mathcal{B}^t_\mathrm{cut}(\omega, \mathbf{k}) \quad \sim \quad g^2 \phi \, . \tag{3.144}$$

In the limit of very large energies, $\omega \gg M$, it is $\lambda^3/(M^2 \omega') \equiv (\omega - q_0)^2/M^2 \lesssim 1$ only for $\omega - M \lesssim q_0 \lesssim \omega$. For values of q_0 outside this range the arctans in Eq. (3.134) cancel. Inside this range one may estimate $\mathcal{A} \sim g \, \phi$ and find $\mathcal{B}^t_\mathrm{cut}$ to be strongly suppressed

$$\mathcal{B}^t_\mathrm{cut}(\omega, \mathbf{k}) \sim g^3 \phi \int\limits_0^{\Lambda_\mathrm{q}} \frac{d\xi}{\epsilon_\mathbf{q}} \int\limits_{\omega-M}^\omega dq_0 \sum_{\sigma=\pm} \frac{\sigma}{q_0 - \sigma\epsilon_\mathbf{q}} \sim g^3 \phi \int\limits_{\Lambda_1}^{\Lambda_0} d\xi \int\limits_{\omega-M}^\omega \frac{dq_0}{q_0^2} \sim g^3 \phi \left(\frac{M}{\omega} \right)^2 . \tag{3.145}$$

In the case of longitudinal gluons one obtains

$$\mathcal{B}^\ell_\mathrm{cut}(\omega, \mathbf{k}) \quad \sim \quad g^2 \int\limits_0^{\Lambda_\mathrm{q}} \frac{d\xi}{\epsilon_\mathbf{q}} \int\limits_0^\omega dq_0 \sum_{\sigma=\pm} \frac{\sigma \, \mathcal{A}(q_0, \mathbf{q})}{q_0 - \sigma\epsilon_\mathbf{q}} \, \omega' \, \mathcal{I}(\lambda) \, , \tag{3.146}$$

where $\mathcal{I}(\lambda)$ is defined in Eq. (3.121). Analogously to the analysis of $\mathcal{A}^\ell_\mathrm{cut}$ one finds for $\omega \sim \phi$

$$
\begin{aligned}
\mathcal{B}^\ell_\mathrm{cut}(\phi, \mathbf{k}) \quad &\sim \quad g^4 \phi \int\limits_0^{\Lambda_\mathrm{q}} \frac{d\xi}{\epsilon_\mathbf{q}} \int\limits_0^\phi dq_0 \sum_{\sigma=\pm} \frac{\sigma}{q_0 - \sigma\epsilon_\mathbf{q}} \frac{\phi}{M} \sim g^4 \phi \frac{\phi}{M} \int\limits_0^{\Lambda_\mathrm{q}} \frac{d\xi}{\epsilon_\mathbf{q}} \, \ln \left| \frac{\epsilon_\mathbf{q} - \phi}{\epsilon_\mathbf{q} + \phi} \right| \\
&\sim \quad g^4 \phi \, \frac{\phi}{M} \tag{3.147}
\end{aligned}
$$

ω	ϕ	$\Lambda_{1>y>0}$	$\gtrsim m_g$	$m_g \ll \omega < 3\mu$
$\mathcal{B}_{\mathrm{cut}}^{t}$	$g^4\phi$	$g^3\phi$	$g^2\phi$	$g^3\phi\left(\frac{M}{\omega}\right)^2$
$\mathcal{B}_{\mathrm{cut}}^{\ell}$	$g^4\phi\,\frac{\phi}{M}$	$g^3\phi\left(\frac{\phi}{M}\right)^y$	$g^2\phi$	$g^3\phi\left(\frac{M}{\omega}\right)$
$\mathcal{B}_{\mathrm{cut}}$	$g^4\phi$	$g^3\phi$	$g^2\phi$	$g^3\phi\left(\frac{M}{\omega}\right)$

Table 3.5: Estimates for $\mathcal{B}_{\mathrm{cut}}^{\ell,t}$ and $\mathcal{B}_{\mathrm{cut}} = \mathcal{B}_{\mathrm{cut}}^{\ell} + \mathcal{B}_{\mathrm{cut}}^{t}$ at different energy scales and $\zeta \ll M$.

ω	ϕ	$\Lambda_{1>y>0}$	$\gtrsim m_g$	$m_g \ll \omega < 3\mu$
$\mathcal{B}_{\mathrm{cut}}^{t}$	0	0	$g^2\phi$	$g^3\phi\left(\frac{M}{\omega}\right)^2$
$\mathcal{B}_{\mathrm{cut}}^{\ell}$	$g^4\phi\,\frac{\phi}{M}$	$g^3\phi\left(\frac{\phi}{M}\right)^y$	$g^2\phi$	$g^3\phi\left(\frac{M}{\omega}\right)$
$\mathcal{B}_{\mathrm{cut}}$	$g^4\phi\,\frac{\phi}{M}$	$g^3\phi\left(\frac{\phi}{M}\right)^y$	$g^2\phi$	$g^3\phi\left(\frac{M}{\omega}\right)$

Table 3.6: Estimates for $\mathcal{B}_{\mathrm{cut}}^{\ell,t}$ and $\mathcal{B}_{\mathrm{cut}} = \mathcal{B}_{\mathrm{cut}}^{\ell} + \mathcal{B}_{\mathrm{cut}}^{t}$ at different energy scales and $\zeta \lesssim M$.

and similarly for $\omega \sim \Lambda_y$ with $0 \le y < 1$

$$
\begin{aligned}
\mathcal{B}_{\mathrm{cut}}^{\ell}(\Lambda_y, \mathbf{k}) \;\sim\;& g^3\phi \int_0^{\Lambda_{\mathrm{q}}} \frac{d\xi}{\epsilon_{\mathbf{q}}} \int_0^{\Lambda_y} dq_0 \sum_{\sigma=\pm} \frac{\sigma}{q_0 - \sigma\epsilon_{\mathbf{q}}} \frac{\Lambda_y}{M} \sim g^3\phi \frac{\Lambda_y}{M} \int_0^{\Lambda_{\mathrm{q}}} \frac{d\xi}{\epsilon_{\mathbf{q}}} \, \ln\left|\frac{\epsilon_{\mathbf{q}} - \Lambda_y}{\epsilon_{\mathbf{q}} + \Lambda_y}\right| \\
\sim\;& g^3\phi \left(\frac{\phi}{M}\right)^y .
\end{aligned}
\tag{3.148}
$$

For $\omega \sim m_g + \Lambda_y$ with $0 \le y < 1$ it is $\omega' \mathcal{I}(\lambda) \sim 1$ and one finds as in Eq. (3.142)

$$
\mathcal{B}_{\mathrm{cut}}^{\ell}(m_g + \Lambda_y, \mathbf{k}) \;\sim\; g^2\phi .
\tag{3.149}
$$

Also for energies $\omega \gtrsim M$ the analysis is very similar to the transversal case since $\omega' \mathcal{I}(\lambda) \sim 1$, and one finds again

$$
\mathcal{B}_{\mathrm{cut}}^{\ell}(\omega, \mathbf{k}) \sim g^2\phi .
\tag{3.150}
$$

In the limit of very large energies, $\omega \gg \Lambda_{\mathrm{gl}} \sim \mu$, only the range $\omega - \Lambda_{\mathrm{gl}} < q_0 < \omega$ contributes, cf. Eq. (3.133). As soon as $\omega - \Lambda_{\mathrm{gl}} > 2m_g$ one may estimate $\mathcal{A} \sim g\phi$ and obtain with $\omega' \mathcal{I}(\lambda) \sim 1$

$$
\begin{aligned}
\mathcal{B}_{\mathrm{cut}}^{\ell}(\omega, \mathbf{k}) \;\sim\;& g^3\phi \int_0^{\Lambda_{\mathrm{q}}} \frac{d\xi}{\epsilon_{\mathbf{q}}} \int_{\omega - \Lambda_{\mathrm{gl}}}^{\omega} dq_0 \sum_{\sigma=\pm} \frac{\sigma}{q_0 - \sigma\epsilon_{\mathbf{q}}} \sim g^3\phi \int_0^{\Lambda_{\mathrm{q}}} d\xi \int_{\omega - \Lambda_{\mathrm{gl}}}^{\omega} \frac{dq_0}{q_0^2} \\
\sim\;& g^3\phi \frac{M\Lambda_{\mathrm{gl}}}{\omega^2} \sim g^3\phi \frac{M}{\omega} .
\end{aligned}
\tag{3.151}
$$

Hence, also $\mathcal{B}_{\mathrm{cut}}^{\ell}$ becomes small in the limit of large energies, cf. Eq. (3.145).

Undamped gluons contributing to $\mathcal{B}$

In the undamped gluon sector the term $\mathcal{M}_{\mathcal{B},T=0}^{\ell,t}$ in Eq. (3.109) gives the contribution

$$\mathcal{B}_{\text{pole}}^{\ell,t}(\omega,\mathbf{k}) \sim g^2 \int\limits_0^{\Lambda_q} \frac{d\xi}{\epsilon_\mathbf{q}} \int\limits_0^\omega dq_0 \sum_{\sigma=\pm} \frac{\sigma\,\rho_\phi(q_0,\mathbf{q})}{q_0 - \sigma\epsilon_\mathbf{q}} \int\limits_{|\zeta-\xi|}^{2\mu} dp\,p\,\rho_{\text{pole}}^{\ell,t}(\omega',\mathbf{p})\,\delta[\omega' - \omega_{\ell,t}(\mathbf{p})]\,, \quad (3.152)$$

which is nonzero only for energies $\omega > m_g$. Due to the restriction $p < 2\mu$ in Eq. (3.152) it follows with similar arguments as for $\mathcal{B}_{\text{cut}}^{\ell,t}$ that $\mathcal{B}_{\text{pole}}^{\ell,t}(\omega,\mathbf{k}) = 0$ for $\omega > 4\mu$. For transversal gluons one finds using the same approximations as for $\mathcal{A}_{\text{pole}}^t$ beginning with energies $\omega \sim m_g + \Lambda_{1<y\le 0}$ and assuming $\zeta \ll M$

$$
\begin{aligned}
\mathcal{B}_{\text{pole}}^t(\omega,\mathbf{k}) &\sim g^2 \int\limits_{\Lambda_1}^{\Lambda_0} \frac{d\xi}{\xi} \int\limits_0^\omega dq_0 \sum_{\sigma=\pm} \frac{\sigma\,\mathcal{A}(q_0,\mathbf{q})}{q_0 - \sigma\epsilon_\mathbf{q}} \int\limits_{\sqrt{\xi^2+m_g^2}}^{2\mu} d\omega_t\,\delta[\omega' - \omega_t] \\
&\sim g^3\phi \int\limits_{\Lambda_1}^{\Lambda_{y/2}} \frac{d\xi}{\xi} \int\limits_0^{\omega-\sqrt{m_g^2+\xi^2}} dq_0 \sum_{\sigma=\pm} \frac{\sigma}{\sigma\xi - q_0} \sim g^3\phi \int\limits_{\Lambda_1}^{\Lambda_{y/2}} \frac{d\xi}{\xi}\,\ln\left|\frac{\omega - \sqrt{m_g^2+\xi^2} - \xi}{\omega - \sqrt{m_g^2+\xi^2} + \xi}\right| \\
&\sim g^3\phi\,,
\end{aligned}
\tag{3.153}
$$

where to guarantee $\omega - \sqrt{\xi^2 + m_g^2} > 0$ the upper boundary of the integral over ξ is reduced from $\Lambda_q \sim \Lambda_0$ to the scale $\sqrt{m_g\Lambda_y} \sim \Lambda_{y/2}$. Furthermore, one estimated $\mathcal{A} \sim g\,\phi$, which is valid since $q_0 < \Lambda_y \le m_g$ for the considered energies. For $\omega > 2m_g$ the integral over q_0 also runs over values $q_0 > m_g$ receiving contributions from $\mathcal{A}_{\text{pole}}^\ell$, cf. Eq. (3.130). As a consequence one finds

$$\mathcal{B}_{\text{pole}}^t(\omega,\mathbf{k}) \sim g^2\phi \tag{3.154}$$

analogously to Eq. (3.142). For $\omega \gg m_g$ the additional contributions from $2m_q < q_0 < \omega$ are only $\sim g^3\phi$ as can be seen in the same way as in Eq. (3.143) and $\mathcal{B}_{\text{pole}}^t \sim g^2\phi$. However, for $\omega \gtrsim 2\mu + 2m_g$ the condition $\omega' = \omega_\ell$ can be fulfilled only for $q_0 > \omega - 2\mu \gtrsim 2m_g$, where $\mathcal{A} \sim g\,\phi$, and one may estimate

$$
\begin{aligned}
\mathcal{B}_{\text{pole}}^t(\omega,\mathbf{k}) &\sim g^3\phi \int\limits_{\Lambda_1}^{\Lambda_0} \frac{d\xi}{\xi} \int\limits_{\omega-2\mu}^\omega dq_0 \sum_{\sigma=\pm} \frac{\sigma}{q_0 - \sigma\epsilon_\mathbf{q}} \sim g^3\phi \int\limits_{\Lambda_1}^{\Lambda_0} d\xi \int\limits_{\omega-2\mu}^\omega \frac{dq_0}{q_0^2} \\
&\sim g^3\phi\,\frac{M\,2\mu}{\omega^2} \sim g^3\phi\,\frac{M}{\omega}\,.
\end{aligned}
\tag{3.155}
$$

For $\zeta \lesssim M$ and $\omega \sim m_g + \Lambda_{1<y<0}$ the condition $\omega - \sqrt{m_g^2 + |\xi - \zeta|^2} > 0$ leads to $|\zeta| - \Lambda_{y/2} < \xi < |\zeta| + \Lambda_{y/2}$. Then the integral over ξ finally yields $\mathcal{B}_{\text{pole}}^t \sim g^3\phi\,(\Lambda_{y/2}/M) \sim g^3\phi\,(\phi/M)^{y/2}$. For $\omega > 2m_g$ and $\omega \gg m_g$ the same analyses as in the case of $\zeta \ll M$ apply.

In the longitudinal sector starting with energies $\omega = m_g + \Lambda_y$ with $0 < y < 1$ and momenta $p \lesssim m_g$ one may employ Eq. (3.128). Assuming $\zeta \ll M$ one obtains

$$
\mathcal{B}^\ell_{\mathrm{pole}}(\omega, \mathbf{k}) \quad \sim \quad g^2 \int_{\Lambda_1}^{\Lambda_0} \frac{d\xi}{\xi} \int_0^\omega dq_0 \sum_{\sigma=\pm} \frac{\sigma \, \mathcal{A}(q_0, \mathbf{q})}{q_0 - \sigma\epsilon_\mathbf{q}} \int_{\sqrt{\xi^2+m_g^2}}^\omega d\omega_\ell \frac{\omega_\ell^2}{\omega_\ell^2 - m_g^2} \, \delta[\omega' - \omega_\ell]
$$

$$
\sim \quad g^2 \int_{\Lambda_1}^{\Lambda_{y/2}} \frac{d\xi}{\xi} \int_0^{\omega-\sqrt{\xi^2+m_g^2}} dq_0 \sum_{\sigma=\pm} \frac{\sigma \, \mathcal{A}(q_0, \mathbf{q})}{q_0 - \sigma\epsilon_\mathbf{q}} \frac{(\omega-q_0)^2}{(\omega-q_0)^2 - m_g^2} \, , \tag{3.156}
$$

where upper boundaries of the integrals over ξ and q_0 are analogous to the transversal case, cf. Eq. (3.153). Since $q_0 \leq \omega - \sqrt{\xi^2 + m_g^2}$ is much smaller than $\omega \sim m_g + \Lambda_y$, one may neglect q_0 against ω on the r.h.s of Eq. (3.156). Therefore, one may estimate $\mathcal{A} \sim g\,\phi$ and finally obtain

$$
\mathcal{B}^\ell_{\mathrm{pole}}(\omega, \mathbf{k}) \quad \sim \quad g^3 \phi \frac{\omega^2}{\omega^2 - m_g^2} \int_{\Lambda_1}^{\Lambda_{y/2}} \frac{d\xi}{\xi} \ln \left| \frac{\omega - \sqrt{m_g^2 + \xi^2} - \xi}{\omega - \sqrt{m_g^2 + \xi^2} + \xi} \right|
$$

$$
\sim \quad g^3 \phi \frac{\omega}{\omega - m_g} \sim g^3 \phi \left(\frac{M}{\phi} \right)^y \, . \tag{3.157}
$$

For larger energies $\omega \gtrsim 2m_g$ the upper boundary of the integral over q_0 will just exceed m_g, where it is $\mathcal{A} \sim \mathcal{A}^\ell_{\mathrm{pole}}$, cf. Eq. (3.130). One finds analogously to $\mathcal{B}^t_{\mathrm{pole}}$ that this gives the main contribution

$$
\mathcal{B}^\ell_{\mathrm{pole}}(\omega, \mathbf{k}) \quad \sim \quad g^2 \int_{\Lambda_1}^{\Lambda_0} \frac{d\xi}{\xi} \int_{m_g}^\omega dq_0 \sum_{\sigma=\pm} \frac{\sigma \, \mathcal{A}(q_0, \mathbf{q})}{q_0 - \sigma\epsilon_\mathbf{q}} \int_{\sqrt{\xi^2+m_g^2}}^\omega d\omega_\ell \frac{\omega_\ell^2}{\omega_\ell^2 - m_g^2} \, \delta[\omega' - \omega_\ell]
$$

$$
\sim \quad g^3 \phi \int_{\Lambda_1}^{\Lambda_0} \frac{d\xi}{\xi} \int_{m_g}^{\omega-\sqrt{\xi^2+m_g^2}} dq_0 \sum_{\sigma=\pm} \frac{\sigma}{q_0 - \sigma\epsilon_\mathbf{q}} \frac{q_0}{q_0 - m_g} \frac{(\omega-q_0)^2}{(\omega-q_0)^2 - m_g^2}
$$

$$
\sim \quad g^2 \phi \, , \tag{3.158}
$$

where one exploited $(\omega - q_0)^2 / [(\omega - q_0)^2 - m_g^2] \sim 1$ (since always $\omega - q_0 \sim m_g$) and estimated the integral over q_0 as in Eq. (3.142). For energies $\omega \gg 2m_g$ one finds analogously to Eq. (3.132) for the contribution from the integration region $2m_g < q_0 < \omega$, where one may approximate $\mathcal{A} \sim g^2 \phi$,

$$
g^3 \phi \int_0^{\Lambda_\mathrm{q}} \frac{d\xi}{\epsilon_\mathbf{q}} \int_{2m_g}^\omega dq_0 \sum_{\sigma=\pm} \frac{\sigma}{q_0 - \sigma\epsilon_\mathbf{q}} \int_{m_g}^{2\mu} d\omega_\ell \exp\left(-\frac{2\omega_\ell^2}{3m_g^2} \right) \delta[\omega' - \omega_\ell]
$$

$$
\sim \quad g^3 \phi \int_{\Lambda_1}^{\Lambda_0} \frac{d\xi}{\xi} \int_{2m_g}^\omega dq_0 \sum_{\sigma=\pm} \frac{\sigma}{q_0 - \sigma\epsilon_\mathbf{q}} \exp\left[-\frac{2(\omega-q_0)^2}{3m_g^2} \right]
$$

ω	$< m_g + \Lambda_1$	$\sim m_g + \Lambda_{1 > y \geq 0}$	$\gtrsim 2m_g$	$m_g \ll \omega < 4\mu$
$\mathcal{B}^t_{\text{pole}}$	0	$g^3\phi$	$g^2\phi$	$g^3\phi\frac{M}{\omega}$
$\mathcal{B}^\ell_{\text{pole}}$	0	$g^3\phi\left(\frac{M}{\phi}\right)^y$	$g^2\phi$	$g^3\phi\left(\frac{M}{\omega}\right)^2$
$\mathcal{B}_{\text{pole}}$	0	$g^3\phi\left(\frac{M}{\phi}\right)^y$	$g^2\phi$	$g^3\phi\frac{M}{\omega}$

Table 3.7: Estimates for $\mathcal{B}^{\ell,t}_{\text{pole}}$ and $\mathcal{B}_{\text{pole}}$ at different energy scales and $\zeta \ll M$.

ω	$< m_g + \Lambda_1$	$\sim m_g + \Lambda_{1 > y \geq 0}$	$\gtrsim 2m_g$	$m_g \ll \omega < 4\mu$
$\mathcal{B}^t_{\text{pole}}$	0	$g^3\phi\left(\frac{\phi}{M}\right)^{y/2}$	$g^2\phi$	$g^3\phi\frac{M}{\omega}$
$\mathcal{B}^\ell_{\text{pole}}$	0	$g^3\phi\left(\frac{M}{\phi}\right)^{y/2}$	$g^2\phi$	$g^3\phi\left(\frac{M}{\omega}\right)^2$
$\mathcal{B}_{\text{pole}}$	0	$g^3\phi\left(\frac{M}{\phi}\right)^{y/2}$	$g^2\phi$	$g^3\phi\frac{M}{\omega}$

Table 3.8: Estimates for $\mathcal{B}^{\ell,t}_{\text{pole}}$ and $\mathcal{B}_{\text{pole}} = \mathcal{B}^\ell_{\text{pole}} + \mathcal{B}^t_{\text{pole}}$ at different energy scales and $\zeta \lesssim M$.

$$\sim\ g^3\phi \int\limits_0^{\Lambda_q} d\xi \int\limits_{2m_g}^\omega \frac{dq_0}{q_0^2} \exp\left(-\frac{2\omega_\ell^2}{3m_g^2}\right) \sim g^3\phi\left(\frac{M}{\omega}\right)^2 . \tag{3.159}$$

Hence, in the considered large energy regime, $\omega \gg 2m_g$ the main contribution to $\mathcal{B}^\ell_{\text{pole}}$ comes from Eq. (3.158), and it is $\mathcal{B}^\ell_{\text{pole}} \sim g^2\phi$. Similarly to the transversal case, this holds up to energies $\omega > 2\mu + 2m_g$ since then it is always $q_0 > 2m_g$ leading to

$$\text{B}^\ell_{\text{pole}}(\omega, \mathbf{k}) \sim g^3\,\phi\left(\frac{M}{\omega}\right)^2 . \tag{3.160}$$

Analogously to the transversal case one finds that for $\zeta \lesssim M$ and $\omega \sim m_g + \Lambda_{1 < y < 0}$ the condition $\omega - \sqrt{m_g^2 + |\xi - \zeta|^2} > 0$ leads to $|\zeta| - \Lambda_{y/2} < \xi < |\zeta| + \Lambda_{y/2}$. Then the integral over ξ finally yields $\mathcal{B}^\ell_{\text{pole}} \sim g^3\phi\,(M/\phi)^y\,(\Lambda_{y/2}/M) \sim g^3\phi\,(M/\phi)^{y/2}$. For $\omega > 2m_g$ and $\omega \gg m_g$ the same analyses as in the case of $\zeta \ll M$ apply. The results of this subsection are summarized in Tables 3.7 and 3.8.

3.2.3   Estimating $\mathcal{H}[\mathcal{A}]$ and $\mathcal{H}[\mathcal{B}]$ and ϕ_0

Hilbert transforming $\mathcal{A}$ and $\mathcal{B}$

Having determined the order of magnitude of $\text{Im}\,\phi$ at various characteristic energy scales one is now in the position to (qualitatively) Hilbert-transform $\text{Im}\,\phi$ for $\zeta \ll M$ and to find the order of magnitude of $\text{Re}\,\tilde{\phi}$ and the corrections due to $\mathcal{B}$. To this end one splits the integral over ω in

the dispersion relation Eq. (3.74a) as

$$
\begin{aligned}
\operatorname{Re}\tilde{\phi}(\epsilon_{\mathbf{k}},\mathbf{k}) &= \mathcal{P}\int_{-\infty}^{\infty}d\omega\,\frac{\rho_{\phi}(\omega,\mathbf{k})}{\omega-\epsilon_{\mathbf{k}}} = \mathcal{P}\int_{0}^{\infty}d\omega\sum_{\sigma=\pm}\frac{\rho_{\phi}(\omega,\mathbf{k})}{\omega-\sigma\epsilon_{\mathbf{k}}} \\
&= \mathcal{P}\left[\int_{0}^{\Lambda_1}+\int_{\Lambda_1}^{\Lambda_{\bar{g}}}+\int_{\Lambda_{\bar{g}}}^{\Lambda_0}+\int_{m_g+\Lambda_1}^{2m_g}+\int_{2m_g}^{2\mu}+\int_{2\mu}^{4\mu}\right]d\omega\sum_{\sigma=\pm}\frac{\rho_{\phi}(\omega,\mathbf{k})}{\omega-\sigma\epsilon_{\mathbf{k}}}\,.
\end{aligned}
\tag{3.161}
$$

Since the integral is additive, one may choose for each region the leading contribution. At the first scale $0\le\omega\le\Lambda_1$ it is $\rho_{\phi}\sim\mathcal{A}_{\mathrm{cut}}^{t}\sim g^2\phi$, cf. Eq. (3.119), and one has the contribution

$$
\mathcal{P}\int_{0}^{\Lambda_1}d\omega\sum_{\sigma=\pm}\frac{\mathcal{A}_{\mathrm{cut}}^{t}(\omega,\mathbf{k})}{\omega-\sigma\epsilon_{\mathbf{k}}}\sim g^2\phi\,\ln\left(\frac{\phi}{\epsilon_{\mathbf{k}}}\right)\sim g^2\,\phi\,.
\tag{3.162}
$$

At the scale $\Lambda_1\le\omega\le\Lambda_{\bar{g}}$ one has $\rho_{\phi}\sim\mathcal{A}_{\mathrm{cut}}^{t}\sim g\,\phi$, cf. Eq. (3.120). With the substitution $d\omega/\omega=\ln(\phi/M)\,dy$ one finds

$$
\mathcal{P}\int_{\Lambda_1}^{\Lambda_{\bar{g}}}d\omega\sum_{\sigma=\pm}\frac{\mathcal{A}_{\mathrm{cut}}^{t}(\omega,\mathbf{k})}{\omega-\sigma\epsilon_{\mathbf{k}}}\sim g\,\phi\int_{\Lambda_1}^{\Lambda_{\bar{g}}}\frac{d\omega}{\omega}\sim g\,\phi\ln\left(\frac{\phi}{M}\right)\int_{1}^{\bar{g}}dy\sim\phi\,.
\tag{3.163}
$$

The contribution from $\mathcal{A}_{\mathrm{cut}}^{\ell}\sim g\,\phi\,(\phi/M)^{y}$ at the same scale, cf. Eq. (3.123), can be shown to be much smaller. One has

$$
\mathcal{P}\int_{\Lambda_1}^{\Lambda_{\bar{g}}}d\omega\sum_{\sigma=\pm}\frac{\mathcal{A}_{\mathrm{cut}}^{\ell}(\omega,\mathbf{k})}{\omega-\sigma\epsilon_{\mathbf{k}}}\sim g\,\phi\,\ln\left(\frac{\phi}{M}\right)\int_{1}^{\bar{g}}dy\left(\frac{\phi}{M}\right)^{y}\sim g\,\phi\,\frac{\phi}{M}\,.
\tag{3.164}
$$

At the scale $\Lambda_{\bar{g}}\le\omega\le\Lambda_0$ one has $\rho_{\phi}\sim\mathcal{A}_{\mathrm{cut}}^{t}\sim\mathcal{A}_{\mathrm{cut}}^{\ell}\sim g\,\phi$, cf. Eq. (3.120, 3.123), and finds

$$
\mathcal{P}\int_{\Lambda_{\bar{g}}}^{\Lambda_0}d\omega\sum_{\sigma=\pm}\frac{\mathcal{A}_{\mathrm{cut}}(\omega,\mathbf{k})}{\omega-\sigma\epsilon_{\mathbf{k}}}\sim g\,\phi\int_{\Lambda_{\bar{g}}}^{\Lambda_0}\frac{d\omega}{\omega}\sim\phi\int_{\bar{g}}^{0}dy\sim g\,\phi\,.
\tag{3.165}
$$

For energies $\omega\gtrsim m_g+\Lambda_y$ with $0\le y<1$ one has $\rho_{\phi}\sim\mathcal{A}_{\mathrm{pole}}^{\ell}\sim g\,\phi\,(M/\phi)^{y}$, cf. Eq. (3.130), and finds with $d\omega=\ln(\phi/M)\,\Lambda_y\,dy$

$$
\mathcal{P}\int_{m_g+\Lambda_1}^{m_g+\Lambda_0}d\omega\sum_{\sigma=\pm}\frac{\mathcal{A}_{\mathrm{pole}}^{\ell}(\omega,\mathbf{k})}{\omega-\sigma\epsilon_{\mathbf{k}}}\sim\frac{g\,\phi}{M}\ln\left(\frac{\phi}{M}\right)\int_{1}^{0}dy\,\Lambda_y\left(\frac{M}{\phi}\right)^{y}\sim\frac{\phi}{M}\int_{1}^{0}dy\,M\sim\phi\,.
\tag{3.166}
$$

Integrating over $2m_g<\omega<2\mu$ with $\rho_{\phi}\sim\mathcal{A}_{\mathrm{pole}}^{t}\sim g\,\phi$, cf. Eq. (3.127), one obtains

$$
\mathcal{P}\int_{2m_g}^{2\mu}d\omega\sum_{\sigma=\pm}\frac{\mathcal{A}_{\mathrm{pole}}^{t}(\omega,\mathbf{k})}{\omega-\sigma\epsilon_{\mathbf{k}}}\sim g\,\phi\int_{2m_g}^{2\mu}\frac{d\omega}{\omega}\sim g\,\phi\ln\left(\frac{\mu}{M}\right)\sim g\,\phi\,.
\tag{3.167}
$$

Finally, integrating over $2\mu < \omega < 4\mu$ with $\rho_\phi \sim \mathcal{B}^t_{\mathrm{pole}} \sim g^3\phi\,(M/\omega)$, cf. Eqs. (3.151,3.155), one obtains

$$\mathcal{P}\int\limits_{2\mu}^{4\mu} d\omega \sum_{\sigma=\pm} \frac{\mathcal{B}^t_{\mathrm{pole}}(\omega,\mathbf{k})}{\omega - \sigma\epsilon_{\mathbf{k}}} \sim g^3\phi\,M\int\limits_{2\mu}^{4\mu}\frac{d\omega}{\omega^2} \sim g^3\phi\,\frac{M}{\mu} \sim g^4\phi\;. \tag{3.168}$$

As expected, $\mathrm{Re}\,\tilde{\phi} \sim \phi$. Furthermore, I find several potential sources for sub-subleading order correction from to $\mathcal{H}[\mathcal{B}]$ to $\mathrm{Re}\,\phi$. The first comes from $\mathcal{B}^t_{\mathrm{cut}}$, which is $\sim g^2\mathcal{A}^t_{\mathrm{cut}}$ for $\omega \sim \Lambda_y$ with $0 < y < 1$, cf. Eq. (3.140). After Hilbert transformation it yields a contribution of order $g^2\phi$ to $\mathrm{Re}\,\tilde{\phi}$, cf. Eq. (3.163), and is therefore of sub-subleading order. At this point, also from $\mathcal{B}^\ell_{\mathrm{pole}} \sim g^2\mathcal{A}^\ell_{\mathrm{pole}}$ a sub-subleading order contribution seems possible, since the corresponding contribution from $\mathcal{A}^\ell_{\mathrm{pole}}$ is $\sim \phi$, cf. (3.166). As the latter, however, combines with ϕ_0 to a subleading order term, cf. Sec. 3.2.4, it would be interesting to investigate if also $\mathcal{B}^\ell_{\mathrm{pole}}$ finds an analogous partner to cancel similarly. If not, it would contribute at sub-subleading order to $\mathrm{Re}\,\tilde{\phi}$. Furthermore, one found that $\mathcal{B} \sim g\mathcal{A} \sim g^2\phi$ for $\omega \gtrsim M$, cf. Eqs. (3.144,3.150,3.154,3.158). From the estimate in Eq. (3.167) one deduces that the corresponding contribution of $\mathcal{H}[\mathcal{B}]$ to $\mathrm{Re}\,\phi$ is of sub-subleading order. In the next section it will be analyzed at which order $\mathrm{Im}\,\phi$ contributes to the local part of the gab function, ϕ_0.

The contribution of $\mathrm{Im}\,\phi$ to ϕ_0

The gap equation for $\phi_0(\mathbf{k})$ is obtained by considering the integrals I_0 and I_{k_0}, cf. Eqs. (3.101,3.104), in the limit $k_0 \to \infty$. Since $p \lesssim 2\mu$ the gluon spectral densities $\rho^{\ell,t}(q_0,\mathbf{p})$ are nonzero only for $q_0 \lesssim 2\mu$. Consequently, the integral over q_0 in Eq. (3.104) is effectively bounded by $\pm 2\mu$. Then, due to the energy denominator under the integral, I_{k_0} tends to zero as $k_0 \to \infty$. In the second term on the r.h.s. of Eq. (3.101) one has $\tilde{\epsilon}_{\mathbf{q}} < \Lambda_q \sim g\mu$. Therefore, one may neglect the imaginary part of the gluon propagator $\Delta^{\ell,t}(\pm\tilde{\epsilon}_{\mathbf{q}} - k_0,\mathbf{p})$, cf. Eqs. (3.33), for $k_0 \gg 2\mu > p$. In the transverse case the gluon propagator becomes $\Delta^t \sim 1/k_0^2$ and the respective contribution vanishes in the limit $k_0 \to \infty$. In the longitudinal sector one has $\Delta^\ell \to -1/p^2$. Hence, the longitudinal contribution of the considered term does not vanish. In the first term on the r.h.s. of Eq. (3.101) the integral over q_0 only runs to values $q_0 \sim \mu$ due to the presence of ρ_ϕ. In the limit $k_0 \to \infty$ again only the contribution from the static electric gluon propagator $\Delta^\ell \to -1/p^2$ remains. Consequently, one finds for $\phi_0(\mathbf{k})$ to subleading order

$$
\begin{aligned}
\phi_0(\mathbf{k}) \;=\; & -\frac{g^2}{3(2\pi)^2}\int\limits_{\Lambda_1}^{\Lambda_0}\frac{d\xi}{\xi}\int\limits_{\xi}^{2\mu}\frac{dp}{p}\,\mathrm{Tr}^\ell_s(k,p,q)\left\{\left[\phi_0(\mathbf{q}) + \mathrm{Re}\,\tilde{\phi}(\tilde{\epsilon}_{\mathbf{q}} + i\eta,\mathbf{q})\right] Z^2(\tilde{\epsilon}_{\mathbf{q}})\tanh\left(\frac{\tilde{\epsilon}_{\mathbf{q}}}{2T}\right)\right. \\
& \left. -\mathcal{P}\int\limits_{-\infty}^{\infty} d\omega\,\frac{\rho_\phi(\omega,\mathbf{q})}{\tilde{\epsilon}_{\mathbf{q}} - \omega}\,Z^2(\omega)\tanh\left(\frac{\omega}{2T}\right)\right\}\;.
\end{aligned}
\tag{3.169}
$$

In the limit $T \to 0$ the hyperbolic functions simplify, yielding after performing the integral over p and with $\mathrm{Tr}_s^\ell(k,p,q) \sim 1$

$$
\phi_0(\mathbf{k}) \quad \sim \quad g^2 \int_{\Lambda_1}^{\Lambda_0} \frac{d\xi}{\xi} \ln\left(\frac{2\mu}{\xi}\right) \left\{ \left[\phi_0(\mathbf{q}) + \mathrm{Re}\,\tilde{\phi}(\tilde{\epsilon}_\mathbf{q} + i\eta, \mathbf{q}) \right] \right.
$$
$$
\left. -\mathcal{P} \int_0^\infty d\omega \sum_{\sigma=\pm} \rho_\phi(\omega, \mathbf{q}) \frac{\sigma}{\sigma\tilde{\epsilon}_\mathbf{q} - \omega} \right\} \;. \tag{3.170}
$$

Using $\mathrm{Re}\,\tilde{\phi}(\tilde{\epsilon}_\mathbf{q} + i\eta, \mathbf{q}) \sim \phi$ one finds for the respective contribution in Eq. (3.170)

$$
g^2 \phi \int_{\Lambda_1}^{\Lambda_0} \frac{d\xi}{\xi} \ln\left(\frac{2\mu}{\xi}\right) \sim \phi \;, \tag{3.171}
$$

and hence $\phi_0(\mathbf{k}) \sim \phi$. Consequently, the integration over the first term in the squared brackets, $\phi_0(\mathbf{q})$, also gives a contribution of order ϕ to $\phi_0(\mathbf{k})$. The remaining term is the contribution from ρ_ϕ and is identical to Eq. (3.161) up to an extra sign σ arising from the hyperbolic tangent. One can conservatively estimate this term by appoximating $\rho_\phi \sim g\,\phi$ for $0 < \omega < 4\mu$ and all $\Lambda_1 \le \xi \le \Lambda_0$ and adding $\rho_\phi \sim g\,\phi\,(M/\phi)^y$ in the range $\omega \sim m_g + \Lambda_y$, $1 > y > 0$ and $\Lambda_1 < \xi < \Lambda_{\bar{g}}$. One obtains

$$
g^3 \phi \int_{\Lambda_1}^{\Lambda_0} \frac{d\xi}{\xi} \ln\left(\frac{2\mu}{\xi}\right) \mathcal{P} \int_0^{4\mu} d\omega \sum_{\sigma=\pm} \frac{\sigma}{\omega - \sigma\xi} \sim g^3 \phi \int_{\Lambda_1}^{\Lambda_0} \frac{d\xi}{\xi} \ln\left(\frac{2\mu}{\xi}\right) \ln\left(\frac{\xi + 4\mu}{\xi - 4\mu}\right)
$$
$$
\sim g^3 \phi \frac{1}{\mu} \int_{\Lambda_1}^{\Lambda_0} d\xi \ln\left(\frac{2\mu}{\xi}\right) \sim g^3 \phi \frac{M}{\mu} \sim g^4 \phi \tag{3.172}
$$

and

$$
g^2 \int_{\Lambda_1}^{\Lambda_{\bar{g}}} \frac{d\xi}{\xi} \ln\left(\frac{2\mu}{\xi}\right) \mathcal{P} \int_{m_g+\Lambda_1}^{m_g+\Lambda_0} d\omega \sum_{\sigma=\pm} \frac{\sigma\,\rho_\phi(\omega, \mathbf{q})}{\omega - \sigma\xi} \sim g^2 \frac{\phi}{M^2} \int_{\Lambda_1}^{\Lambda_{\bar{g}}} d\xi \ln\left(\frac{2\mu}{\xi}\right) \int_1^0 dy\, \Lambda_y \left(\frac{M}{\phi}\right)^y
$$
$$
\sim g^2 \frac{\phi}{M} \int_{\Lambda_1}^{\Lambda_{\bar{g}}} d\xi \ln\left(\frac{2\mu}{\xi}\right) \sim g^2 \phi \;, \tag{3.173}
$$

where one has estimated $\sum_\sigma \sigma/(\omega - \sigma\xi) \sim \xi/M$, since $\xi \ll \omega \sim M$. It follows that the contributions from ρ_ϕ to ϕ_0 are of order $g^2\phi$ and hence of sub-subleading order, cf. discussion after Eq. (3.168).

Finally, one has found that the contribution of $\mathrm{Im}\,\phi$ to $\mathrm{Re}\,\phi(\epsilon_\mathbf{k}, \mathbf{k}) = \mathrm{Re}\,\tilde{\phi}(\epsilon_\mathbf{k}, \mathbf{k}) + \phi_0(\mathbf{k})$ are in total beyond subleading order.

3.2.4 Reproducing $\operatorname{Re}\phi(\epsilon_{\mathbf{k}} + i\eta, \mathbf{k})$ to subleading order

Although $\rho_\phi(\omega, \mathbf{k})$ and $\phi_0(\mathbf{k})$ have not been calculated (in principle possible) but only estimated in magnitude, the main goal of this analysis has been achieved. The imaginary part of the gap function is shown to be at most of order $g\operatorname{Re}\phi(\epsilon_{\mathbf{k}}, \mathbf{k})$ for $\epsilon_{\mathbf{k}} < \Lambda_{\mathbf{q}} \sim g\mu$ (then it is $|\phi| = \operatorname{Re}\phi$, cf. Eq. (3.78)) and it enters $\operatorname{Re}\phi(\epsilon_{\mathbf{k}}, \mathbf{k})$ beyond subleading order.

Neglecting all terms that have been identified to originate from ρ_ϕ, namely $\operatorname{Im}\mathcal{M}_{\mathcal{B}}(\omega + i\eta, \mathbf{q}, \mathbf{p})$ in Eq. (3.106), and Hilbert transforming the remaining term $\operatorname{Im}\mathcal{M}_{\mathcal{A}}(\omega + i\eta, \mathbf{q}, \mathbf{p})$ gives the gap equation for $\operatorname{Re}\tilde{\phi}(\epsilon_{\mathbf{k}}, \mathbf{k})$ to subleading order

$$
\begin{aligned}
\operatorname{Re}\tilde{\phi}(\epsilon_{\mathbf{k}} + i\eta, \mathbf{k}) \;=\; & -\frac{g^2}{3}\int\frac{d^3\mathbf{q}}{(2\pi)^3}\frac{Z^2(\tilde{\epsilon}_{\mathbf{q}})}{2\tilde{\epsilon}_{\mathbf{q}}}\operatorname{Re}\phi(\tilde{\epsilon}_{\mathbf{q}} + i\eta, \mathbf{q}) \\
& \times \mathcal{P}\int_{-\infty}^{\infty} d\omega \sum_{\sigma=\pm}\frac{\sigma\left[\operatorname{Tr}_s^\ell(k,p,q)\rho^\ell(\omega,\mathbf{p}) + \operatorname{Tr}_s^t(k,p,q)\rho^t(\omega,\mathbf{p})\right]}{\omega - \epsilon_{\mathbf{k}} + \sigma\tilde{\epsilon}_{\mathbf{q}}} \\
& \times \frac{1}{2}\left[\tanh\left(\frac{\sigma\tilde{\epsilon}_{\mathbf{q}}}{2T}\right) + \coth\left(\frac{\omega}{2T}\right)\right] .
\end{aligned}
\tag{3.174}
$$

Adding

$$
\phi_0(\mathbf{k}) = -\frac{g^2}{3}\int\frac{d^3\mathbf{q}}{(2\pi)^3}\frac{Z^2(\tilde{\epsilon}_{\mathbf{q}})}{2\tilde{\epsilon}_{\mathbf{q}}}\operatorname{Tr}_s^\ell(k,p,q)\left(-\frac{2}{p^2}\right)\operatorname{Re}\phi(\tilde{\epsilon}_{\mathbf{q}} + i\eta, \mathbf{q})\frac{1}{2}\tanh\left(\frac{\tilde{\epsilon}_{\mathbf{q}}}{2T}\right)
\tag{3.175}
$$

to Eq. (3.174) one reproduces the well known gap equation for $\operatorname{Re}\phi(\epsilon_{\mathbf{k}}, \mathbf{k})$ to subleading order, cf. [55]. To see explicitly how $\phi_0 \sim \phi$ and $\mathcal{H}[\mathcal{A}_{\text{pole}}^\ell] \sim \phi$ combine to a subleading order contribution, one first notes that all terms $\sim \coth$ are at most of sub-subleading order, cf. Sec. 3.2.1. Then Eq. (3.174) simplifies to

$$
\begin{aligned}
\operatorname{Re}\tilde{\phi}(\epsilon_{\mathbf{k}} + i\eta, \mathbf{k}) \;=\; & -\frac{g^2}{3}\int\frac{d^3\mathbf{q}}{(2\pi)^3}\frac{Z^2(\tilde{\epsilon}_{\mathbf{q}})}{2\tilde{\epsilon}_{\mathbf{q}}}\operatorname{Re}\phi(\tilde{\epsilon}_{\mathbf{q}} + i\eta, \mathbf{q})\frac{1}{2}\tanh\left(\frac{\tilde{\epsilon}_{\mathbf{q}}}{2T}\right) \\
& \times \mathcal{P}\int_{-\infty}^{\infty} d\omega \sum_{\sigma=\pm}\frac{\operatorname{Tr}_s^\ell(k,p,q)\rho^\ell(\omega,\mathbf{p}) + \operatorname{Tr}_s^t(k,p,q)\rho^t(\omega,\mathbf{p})}{\omega - \epsilon_{\mathbf{k}} + \sigma\tilde{\epsilon}_{\mathbf{q}}}
\end{aligned}
$$

$$
\begin{aligned}
=\; & -\frac{g^2}{3(2\pi)^2}\int_0^{\Lambda_{\mathbf{q}}} d\xi\,\frac{Z^2(\tilde{\epsilon}_{\mathbf{q}})}{2\tilde{\epsilon}_{\mathbf{q}}}\operatorname{Re}\phi(\tilde{\epsilon}_{\mathbf{q}} + i\eta, \mathbf{q})\,\tanh\left(\frac{\tilde{\epsilon}_{\mathbf{q}}}{2T}\right) \\
& \times \sum_{\sigma=\pm}\left[\int_{|\xi-\zeta|}^{\Lambda_{\text{gl}}} dp\,p\left\{\operatorname{Tr}_s^\ell(k,p,q)\left[\frac{1}{p^2} + \Delta_{\text{HDL}}^\ell(\epsilon_{\mathbf{k}} - \sigma\tilde{\epsilon}_{\mathbf{q}}, \mathbf{p})\right] + \operatorname{Tr}_s^t(k,p,q)\Delta_{\text{HDL}}^t(\epsilon_{\mathbf{k}} - \sigma\tilde{\epsilon}_{\mathbf{q}}, \mathbf{p})\right\} \right. \\
& \left. + \int_{\Lambda_{\text{gl}}}^{2\mu} dp\,p\,\operatorname{Tr}_s^t(k,p,q)\,\Delta_{0,22}^t(\epsilon_{\mathbf{k}} - \sigma\tilde{\epsilon}_{\mathbf{q}}, \mathbf{p})\right],
\end{aligned}
\tag{3.176}
$$

where one used $\rho^\ell(\omega, \mathbf{p}) \equiv 0$ for $p > \Lambda_{\text{gl}}$ in the effective theory, cf. Eq. (3.86a). Adding Eqs. (3.175,3.176), the $1/p^2$-term from the soft electric gluon propagator in Eq. (3.176) effectively

restricts the p-integral in ϕ_0 from Λ_{gl} to 2μ. After aproximating the hard magnetic gluon propagator as $\Delta^t_{0,22}(\epsilon_{\mathbf{k}} - \sigma\tilde{\epsilon}_{\mathbf{q}}, \mathbf{p}) = 1/p^2 + O(\Lambda_{\mathrm{q}}/\Lambda_{\mathrm{gl}})$, one can combine it with the remaining contribution from ϕ_0. Using $\mathrm{Tr}^\ell_s(k, p, q) - \mathrm{Tr}^t_s(k, p, q) = 4 + O(\Lambda_{\mathrm{q}}/\Lambda_{\mathrm{gl}})$, one finally arrives at Eq. (124) of [98]. Hence, indeed $\phi_0 + \mathcal{H}[\mathcal{A}^\ell_{\mathrm{pole}}] \sim g\,\phi$, i.e. contribute at subleading order to $\mathrm{Re}\,\phi$.

3.2.5 Calculating $\mathrm{Im}\,\phi(\epsilon_{\mathbf{k}} + i\eta, \mathbf{k})$ near the Fermi surface

In Sec. 3.2.2 the contributions $\mathcal{A}$ and $\mathcal{B}$ to $\mathrm{Im}\,\phi$ have been estimated for different regimes of ω and ζ, cf. Tab. 3.1-3.8. In the case that both ω and ζ are $\sim \Lambda_y$ with some y satisfying $0 < y \leq 1$ one found $\mathcal{A}^t_{\mathrm{cut}}$ to be the dominant contribution to $\mathrm{Im}\,\phi$, while in all other regimes of ω and ζ different gluon sectors contribute at the respective leading order and therefore mix. Furthermore, for $\omega < 2m_g$ also the contributions from $\mathcal{B}$ have to be considered, since there $\mathcal{B}$ is suppressed relative to $\mathcal{A}$ only by one power of g.

In the following the imaginary part of the on-shell gap function $\mathrm{Im}\,\phi(\epsilon_{\mathbf{k}} + i\eta, \mathbf{k})$ near the Fermi surface, $\zeta \sim \Lambda_y$ with $1 < y < 0$, at zero temperature, $T = 0$, is calculated. It follows

$$
\begin{aligned}
\mathrm{Im}\,\phi(\epsilon_{\mathbf{k}} + i\eta, \mathbf{k}) \;\simeq\;& \frac{g^2\,\pi}{3(2\pi)^2} \int_{\Lambda_1}^{\epsilon_{\mathbf{k}}} \frac{d\xi}{\xi}\, Z^2(\tilde{\epsilon}_{\mathbf{q}})\, \mathrm{Re}\,\phi(\tilde{\epsilon}_{\mathbf{q}} + i\eta, \mathbf{q}) \int_\lambda^{\Lambda_{\mathrm{gl}}} dp\, p\, \rho^t_{\mathrm{cut}}(\omega^*, \mathbf{p})\, \mathrm{Tr}^t_s(k, p, q) \\[2mm]
\simeq\;& \frac{g^2\,\pi}{3(2\pi)^2} \int_{\Lambda_1}^{\epsilon_{\mathbf{k}}} \frac{d\xi}{\xi}\, Z^2(\tilde{\epsilon}_{\mathbf{q}})\, \mathrm{Re}\,\phi(\tilde{\epsilon}_{\mathbf{q}} + i\eta, \mathbf{q}) \int_\lambda^{\Lambda_{\mathrm{gl}}} dp\, \frac{2M^2\,\omega^*}{\pi}\, \frac{p^2}{p^6 + (M^2\omega^*)^2} \\[2mm]
\simeq\;& \frac{g^2\,\pi}{9(2\pi)^2} \int_{\Lambda_1}^{\epsilon_{\mathbf{k}}} \frac{d\xi}{\xi}\, Z^2(\tilde{\epsilon}_{\mathbf{q}})\, \mathrm{Re}\,\phi(\tilde{\epsilon}_{\mathbf{q}} + i\eta, \mathbf{q}) \\[2mm]
\simeq\;& \frac{g^2\,\pi}{9(2\pi)^2} \ln\left(\frac{\phi}{M}\right) \phi \int_1^y dy'\, \sin\left(\frac{\pi\,y'}{2}\right)\left(1 - \frac{\bar{g}\,\pi\,y'}{2}\right) \\[2mm]
=\;& -\frac{g^2}{18\,\pi^2} \ln\left(\frac{\phi}{M}\right) \phi\, \cos\left(\frac{\pi\,y}{2}\right) + \mathcal{O}(\bar{g}^2) \\[2mm]
=\;& \bar{g}\,\phi\, \frac{\pi}{2} \cos\left(\frac{\pi\,y}{2}\right) + \mathcal{O}(\bar{g}^2)\,,
\end{aligned}
\tag{3.177}
$$

where one substituted $\epsilon_{\mathbf{k}} = \Lambda_y$ and $d\xi/\xi = dy'\,\ln(\phi/M)$ and used $\ln(\phi/M) = -3\pi^2/(\sqrt{2}\,g)$ and $\bar{g} \equiv g/(3\sqrt{2}\pi)$. Furthermore, it was sufficient to approximate $\mathrm{Tr}^t_s(k, p, q) \simeq -2$. The corrections due to the term $-p^2/2\mu^2$ are easily shown to be suppressed by a factor $\sim (M/\mu)^2 \sim g^2$ compared to the final result in Eq. (3.177). To estimate the contributions from the term $-(k^2 - q^2)^2/(2\,k\,q\,p^2) \simeq -2(\xi - \zeta)^2/p^2$ one first conservatively sets $\zeta = 0$. At the lower boundary of the p-integral, $p \geq \lambda$, this term is ~ 1. One finds for the integral over p

$$
\int_\lambda^{\Lambda_{\mathrm{gl}}} dp\, \frac{M^2\,\omega^*\,\xi^2}{p^6 + (M^2\omega^*)^2} < \left(\frac{\Lambda_{3y/5}}{\Lambda_{y/3}}\right)^5 \sim \left(\frac{\phi}{M}\right)^{\frac{4y}{15}}.
\tag{3.178}
$$

The integral over ξ then can be estimated to be at most of order

$$\int_1^y dy' \, \sin\left(\frac{\pi y'}{2}\right) \left(\frac{\phi}{M}\right)^{\frac{4y'}{15}} < \int_1^y dy' \left(\frac{\phi}{M}\right)^{\frac{4y'}{15}} \sim \frac{\left(\frac{\phi}{M}\right)^{\frac{4}{15}} - \left(\frac{\phi}{M}\right)^{\frac{4y}{15}}}{\ln\left(\frac{\phi}{M}\right)} \lesssim g \left(\frac{\phi}{M}\right)^{\frac{4y}{15}} \, . \qquad (3.179)$$

Hence, also this contribution is suppressed by a factor of g compared to the result given in Eq. (3.177).

Chapter 4

Summary and Outlook

In this work I have presented a formal derivation of a general effective action for non-Abelian gauge theories, Eq. (2.46). This was motivated by the occurence of well-separated momentum scales in hot and/or dense quark matter. To this end I first introduced cut-offs in momentum space for quarks, Λ_{q}, and gluons, Λ_{gl}. These cut-offs separate relevant from irrelevant quark modes and soft from hard gluon modes. I then explicitly integrated out irrelevant quark and hard gluon modes. The effective action (2.46) is completely general and, as shown explicitly in Sec. 2.2.1, after appropriately choosing Λ_{q} and Λ_{gl}, it comprises well-known effective actions as special cases, for instance, the "Hard Thermal Loop" (HTL) and "Hard Dense Loop" (HDL) effective actions. I also demonstrated, cf. Sec. 2.2.2, that the high-density effective theory introduced by Hong and others [100, 101, 102, 103, 104, 105] is contained in the effective action (2.46).

In Sec. 2.3 it is argued that in order to obtain a complete effective theory, in principle, all diagrams appearing in the effective action (2.46) have to be power-counted. This remains as a future project. A first step towards this goal, however, is performed for the special case of an effective theory for cold and dense quark matter, i.e. for quarks with momenta $|k - \mu| \sim \phi$ around the Fermi surface and soft gluons with momenta of order $\Lambda_{\mathrm{gl}}^{s} \ll \mu$. To this end, one specific class of diagrams occurring in the effective action (2.46), loops of irrelevant quarks with N external soft gluon legs, is power-counted for the cutoff parameters fulfilling $\phi \ll \Lambda_{\mathrm{q}} \ll \Lambda_{\mathrm{gl}} \simeq \mu$ and the projection operators given in Eqs. (2.18) and (2.35). It is shown that for the considered momentum regime these loops are of the order of the corresponding bare vertices (bare gluon propagator and gluon vertices) times the factor $(g\mu)^2/(\Lambda_{\mathrm{gl}}^{s})^2$. They are therefore "relevant" operators in the effective action, as their magnitude increases when the soft gluon scale $\Lambda_{\mathrm{gl}}^{s}$ decreases. They contain Debye screening and Landau damping (as known from HDLs), whereas the Meissner effect for the magnetic gluons is negligible as long as $\Lambda_{\mathrm{gl}}^{s} \gg \phi$. A possible field of application could be the precursory effects to color superconductivity at temperatures above the (non-perturbative) onset of Cooper pairing, $T \gtrsim T_c \sim \phi$.

As it is known from the HTL/HDL power-counting scheme there is another important class of diagrams, i.e. those with 2 external quark and $N - 2$ external gluon legs. It would be interesting to analyze how their orders of magnitude change as the cutoffs are shifted. Especially the 1-loop corrections to the quark-gluon vertex could contribute to the gap parameter at sub-subleading

order.

In Sec. 3.1 I showed how the QCD gap equation can be derived from the effective action (2.46). The gap equation is a Dyson-Schwinger equation for the anomalous part of the quark self-energy. It has to be solved self-consistently, which is feasible only after truncating the set of all possible diagrams contributing to the Dyson-Schwinger equation. Such truncations can be derived in a systematic way within the general Cornwall-Jackiw-Tomboulis (CJT) formalism [106]. Here, I only include diagrams of the sunset-type, cf. Fig. 3.1, in the CJT effective action, which gives rise to one-loop diagrams (with self-consistently determined quark and gluon propagators) in the quark and gluon self-energies.

In principle, the CJT effective action (3.2) for the effective theory contains the same information as the corresponding one for QCD. However, while in full QCD self-consistency is maintained for *all* momentum modes via the solution of the stationarity condition (3.3), in the effective theory self-consistency is only required for the *relevant* quark and *soft* gluon modes. These are the *only* dynamical degrees of freedom in the CJT effective action; the irrelevant fermion and hard gluon modes, which were integrated out, only appear in the vertices of the tree-level action (2.46). In this sense, the effective theory provides a simplification of *any* physical problem that has to be solved self-consistently. How this facilitates the actual computation is exemplified explicitly with the solution of the color-superconducting gap equation.

Usually, the advantage of an effective theory is that the degree of importance of various operators can be estimated (via power counting) at the level of the effective action, i.e., *prior* to the actual calculation of a physical quantity. This tremendously simplifies the computation of quantities which are accessible within a perturbative framework. On the other hand, the requirement of self-consistency for the solution of the Dyson-Schwinger equation invalidates any such power-counting scheme on the level of the effective action. For instance, perturbatively, the right-hand side of the gap equation (1.35) is proportional to g^2. However, self-consistency generates additional large logarithms $\sim \ln(\mu/\phi) \sim 1/g$ which cancel powers of g.

Nevertheless, it turns out that there is still a distinct advantage in using the CJT effective action (3.2) of the effective theory for the derivation and the solution of Dyson-Schwinger equations for quantities which have to be determined self-consistently, such as the color-superconducting gap function in QCD. This advantage originates from the introduction of the cut-offs which separate various regions in momentum space. Choosing $\Lambda_{\rm q} \ll \Lambda_{\rm gl}$ they allow for a *rigorous* power counting of different contributions to the Dyson-Schwinger equation after expanding in $\Lambda_{\rm q}/\Lambda_{\rm gl} \ll 1$. I explicitly demonstrated this in Sec. 3.1, where I reviewed the calculation of the color-superconducting gap parameter to subleading order and in Sec. 3.2, where I considered the imaginary part of the gap function.

In order to obtain the standard result (1.36), it was mandatory to choose $\Lambda_{\rm q} \lesssim g\mu \ll \Lambda_{\rm gl} \lesssim \mu$, cf. Fig. 4.1. This is in contrast to previous statements in the literature [101, 102, 103] that a consistent power-counting scheme requires $\Lambda_{\rm q} \sim \Lambda_{\rm gl}$. In particular, the choice $\Lambda_{\rm q} \ll \Lambda_{\rm gl}$ has the consequence that the gluon energy in the QCD gap equation is restricted to values $p_0 \lesssim \Lambda_{\rm q}$, while the gluon momentum can be much larger, $p \lesssim \Lambda_{\rm gl}$. This naturally explains why it is permissible to use the low-energy limit (3.61) of the HDL gluon propagators in order to extract the dominant contribution to the gap equation (which arises from soft magnetic gluons). In previous calculations of the gap within the framework of an effective theory [101, 102, 103], the low-energy limit for the HDL propagators was used without further justification, even though
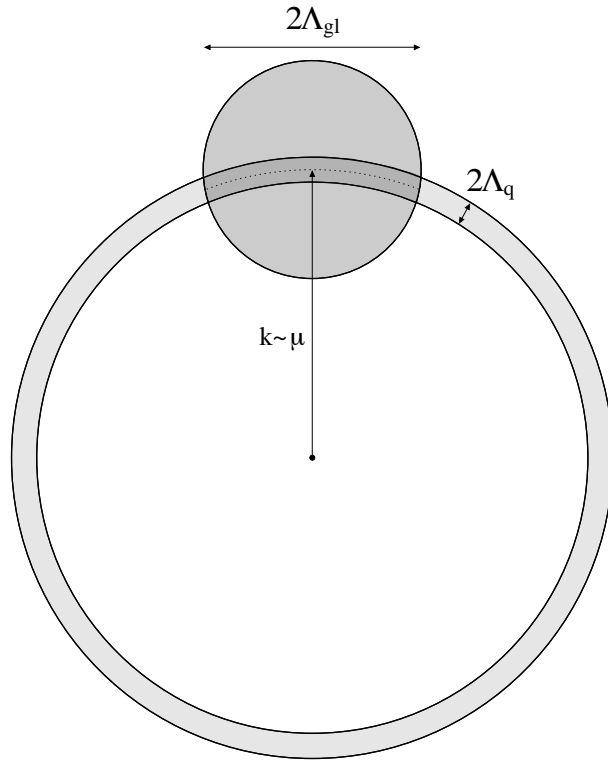
Figure 4.1: Momentum regime of quarks near the Fermi surface, $|k - \mu| \ll \Lambda_{\mathrm{q}}$, and soft gluons, $p \ll \Lambda_{\mathrm{gl}}$.

for the choice $\Lambda_{\mathrm{q}} \sim \Lambda_{\mathrm{gl}}$ the gluon energy can be of the same order as the gluon momentum. The physical picture which arises from the choice $\Lambda_{\mathrm{q}} \lesssim g\mu \ll \Lambda_{\mathrm{gl}} \lesssim \mu$ is summarized in Fig. 4.1. Relevant quarks are located within a thin layer of width $\sim \Lambda_{\mathrm{q}}$ around the Fermi surface. Soft gluon exchange mediates between quarks within a "patch" of size $\sim \Lambda_{\mathrm{gl}}$ inside this layer. The area of the patch is much larger than its thickness. Hard gluon exchange mediates between quark states inside and outside of the patch.

Obviously, this picture, as well as all power-counting arguments, are rigorously valid only at asymptotically large values of the quark chemical potential, where $g \ll 1$. In the physically relevant region, $\mu \lesssim 1$ GeV and $g \sim 1$, the scale hierarchy $\Lambda_{\mathrm{q}} \lesssim g\mu \ll \Lambda_{\mathrm{gl}} \lesssim \mu$ breaks down. When all scales are of the same order, the patch on the Fermi surface becomes a sphere of the size of the Fermi sphere.

In the course of the calculation, I was able to identify various potential contributions of sub-subleading order. However, I argued that, at this order, a self-consistent solution of the gap equation must take into account the *off-shell* behavior of the gap function. To this end, I investigated the imaginary part of the gap function, which (loosely speaking) generates the energy dependence of the gap function. Due to the energy dependent gluon propagator in the gap equation a self-consistent solution requires a energy dependent and therefore complex ansatz. Consequently, I considered a complex gap equation, which is pair of two coupled gap equations, one for the real and one for the imaginary part of the gap function.

To solve it self-consistently, I first inserted the known leading order result of the real part of the gap function into the imaginary gap equation. In this way I estimated the order of magnitude of the imaginary part of the gap function for various energy and momentum regimes, cf. Tables I-III. The self-consistency of this approach was controlled by reinserting these estimates into the imaginary gap equation, cf. Tables IV-VI. Using these results it was checked at which order the imaginary part contributes to the real part of the gap function. It was found that it enters at sub-subleading order. Furthermore, several sub-subleading order terms in the real part of the gap equation arising from the imaginary part of the gap function have been identified.

Finally, I calculated the imaginary part of the on-shell gap function for momenta exponentially close to the Fermi surface, cf. Eq. (3.177). In this regime only Landau damped transversal gluons had to be considered. Also for the complex gap equation the two momentum cutoffs Λ_q and Λ_{gl} proved to be a powerful means for the rigorous power counting of innumerable terms.

For a complete sub-subleading order calculation it also appears to be necessary to include 2PI diagrams beyond those of sunset topology in Γ_2, cf. Eq. (3.20) and Fig. 3.1. As a first step it would be interesting to include the vertex corrections into the gap equation.

The general effective action (2.46) derived in this work puts the known effective theories for hot and dense matter on a more formal basis and gives better insight and control over the different approximations made. It connects previous results and puts them on a common footing. Thereby, it has the potential to provide a framework for systematic studies of various problems in the field of hot and dense systems. Besides an improvement of the result for the color-superconducting gap parameter beyond subleading order, I believe that it can serve as a convenient starting point to investigate other interesting problems pertaining to hot and/or dense quark matter.

Appendix A

Matsubara sums in quark loops

In the following the Matsubara sum and the $\tau-$integrals in quark loops with three and four external gluon fields is performed, always starting from the general Eq. (2.84).

Three external glouns

For three external glouns ($N = 3$) one has $m = 1, 2$ and Eq. (2.84) becomes

$$
\mathcal{J}^{\mu_1\mu_2\mu_3}(P_1, P_2, P_3) =
$$

$$
= -\int \frac{d^3\mathbf{k}}{(2\pi)^3} \sum_{\mathbf{e},\boldsymbol{s}} \mathcal{T}_{\mathbf{e}}^{\mu_1\mu_2\mu_3} \Theta_{\boldsymbol{s}}^{\mathbf{e}} \sum_{m=1}^{2} (-1)^m \prod_{i=1}^{2} \left[\int_0^\beta d\tau_i \tilde{f}_{s_i}^{e_i} e^{\Omega_i \tau_i} \right] \times
$$

$$
\times \tilde{f}_{s_3}^{e_3} e^{-s_3 \epsilon_3 m\beta} \Theta\left(m\beta - \sum_{j=1}^{2} \tau_j\right) \Theta\left(\sum_{j=1}^{2} \tau_j - (m-1)\beta\right)
$$

$$
= -\int \frac{d^3\mathbf{k}}{(2\pi)^3} \sum_{\mathbf{e},\boldsymbol{s}} \mathcal{T}_{\mathbf{e}}^{\mu_1\mu_2\mu_3} \Theta_{\boldsymbol{s}}^{\mathbf{e}} \times
$$

$$
\times \left\{ \prod_{i=1}^{2} \left[\int_0^\beta d\tau_i \tilde{f}_{s_i}^{e_i} e^{\Omega_i \tau_i} \right] \tilde{f}_{s_3}^{e_3} e^{-2s_3 \epsilon_3 \beta} \Theta\left(\tau_1 + \tau_2 - \beta\right) - \right.
$$

$$
\left. - \prod_{i=1}^{2} \left[\int_0^\beta d\tau_i \tilde{f}_{s_i}^{e_i} e^{\Omega_i \tau_i} \right] \tilde{f}_{s_3}^{e_3} e^{-s_3 \epsilon_3 \beta} \Theta\left(\beta - \tau_1 - \tau_2\right) \right\} \tag{A.1}
$$

Using Eqs. (2.73) and (2.72) one finds

$$
\tilde{f}_{s_3}^{e_3} e^{-s_3 \epsilon_3 \beta} \Theta\left(\beta - \tau_1 - \tau_2\right) - \tilde{f}_{s_3}^{e_3} e^{-2s_3 \epsilon_3 \beta} \Theta\left(\tau_1 + \tau_2 - \beta\right)
$$

$$
= \tilde{f}_{-s_3}^{e_3} \Theta\left(\beta - \tau_1 - \tau_2\right) + \left[\tilde{f}_{-s_3}^{e_3} - e^{-s_3 \epsilon_3 \beta}\right] \Theta\left(\tau_1 + \tau_2 - \beta\right)
$$

$$
= \tilde{f}_{-s_3}^{e_3} - e^{-s_3 \epsilon_3 \beta} \Theta\left(\tau_1 + \tau_2 - \beta\right) , \tag{A.2}
$$

117

which leads to

$$\mathcal{J}^{\mu_1\mu_2\mu_3}(P_1, P_2, P_3) =$$
$$= -\int \frac{d^3\mathbf{k}}{(2\pi)^3} \sum_{\mathbf{e},\boldsymbol{s}} \mathcal{T}_{\mathbf{e}}^{\mu_1\mu_2\mu_3} \Theta_{\boldsymbol{s}}^{\mathbf{e}} \times$$
$$\times \left\{ e^{-s_3\epsilon_3\beta} \int_0^\beta d\tau_1 \int_{\beta-\tau_1}^\beta d\tau_2 \tilde{f}_{s_1}^{e_1} e^{\Omega_1\tau_1} \tilde{f}_{s_2}^{e_2} e^{\Omega_2\tau_2} - \prod_{i=1}^2 \left[\int_0^\beta d\tau_i \tilde{f}_{s_i}^{e_i} e^{\Omega_i\tau_i} \right] \tilde{f}_{-s_3}^{e_3} \right\}. \tag{A.3}$$

After having performed the integral over τ_2 one can combine three of the four remaining τ_1-integrals by using $\tilde{f}_{-s_2}^{e_2} \tilde{f}_{s_3}^{e_3} - \tilde{f}_{s_2}^{e_2} \tilde{f}_{-s_3}^{e_3} - \tilde{f}_{-s_2}^{e_2} = -\tilde{f}_{-s_3}^{e_3}$ and obtains

$$\mathcal{J}^{\mu_1\mu_2\mu_3}(P_1, P_2, P_3) =$$
$$= -\int \frac{d^3\mathbf{k}}{(2\pi)^3} \sum_{\mathbf{e},\boldsymbol{s}} \mathcal{T}_{\mathbf{e}}^{\mu_1\mu_2\mu_3} \Theta_{\boldsymbol{s}}^{\mathbf{e}} \times$$
$$\times \left\{ \frac{1}{\Omega_2} \int_0^\beta d\tau_1 e^{\Omega_1\tau_1} \tilde{f}_{s_1}^{e_1} \tilde{f}_{-s_3}^{e_3} - \frac{1}{\Omega_2} \int_0^\beta d\tau_1 e^{(\Omega_1-\Omega_2)\tau_1} \tilde{f}_{s_1}^{e_1} \tilde{f}_{-s_2}^{e_2} \right\}$$
$$= -\int \frac{d^3\mathbf{k}}{(2\pi)^3} \sum_{\mathbf{e},\boldsymbol{s}} \mathcal{T}_{\mathbf{e}}^{\mu_1\mu_2\mu_3} \Theta_{\boldsymbol{s}}^{\mathbf{e}} \times$$
$$\times \frac{1}{\Omega_2} \left\{ \frac{1}{\Omega_1} \left[\tilde{f}_{-s_1}^{e_1} \tilde{f}_{s_3}^{e_3} - \tilde{f}_{s_1}^{e_1} \tilde{f}_{-s_3}^{e_3} \right] - \frac{1}{\Omega_1-\Omega_2} \left[\tilde{f}_{-s_1}^{e_1} \tilde{f}_{s_2}^{e_2} - \tilde{f}_{s_1}^{e_1} \tilde{f}_{-s_2}^{e_2} \right] \right\}$$
$$= -\int \frac{d^3\mathbf{k}}{(2\pi)^3} \sum_{\mathbf{e},\boldsymbol{s}} \mathcal{T}_{\mathbf{e}}^{\mu_1\mu_2\mu_3} \Theta_{\boldsymbol{s}}^{\mathbf{e}} \frac{1}{p_2^0 - p_3^0 - s_2\epsilon_2 + s_3\epsilon_3} \times$$
$$\times \left[\frac{\frac{s_3-s_1}{2} + s_1 N(\epsilon_1) - s_3 N(\epsilon_3)}{p_1^0 - p_3^0 - s_1\epsilon_1 + s_3\epsilon_3} - \frac{\frac{s_2-s_1}{2} + s_1 N(\epsilon_1) - s_2 N(\epsilon_2)}{p_1^0 - p_2^0 - s_1\epsilon_1 + s_2\epsilon_2} \right]. \tag{A.4}$$

In the limit $\mu \to 0$ and after using Eq. (2.94) this reproduces the corresoponding formula (A.17) in [7].

Four external Gluons

In the case of four external gluons one has $m = 1, 2, 3$ and Eq. (2.84) becomes

$$\mathcal{J}^{\mu_1\cdots\mu_4}(P_1, \cdots, P_4) =$$
$$= -\int \frac{d^3\mathbf{k}}{(2\pi)^3} \sum_{\mathbf{e},\boldsymbol{s}} \mathcal{T}_{\mathbf{e}}^{\mu_1\cdots\mu_4} \Theta_{\boldsymbol{s}}^{\mathbf{e}} \sum_{m=1}^3 (-1)^m \prod_{i=1}^3 \left[\int_0^\beta d\tau_i \tilde{f}_{s_i}^{e_i} e^{\Omega_i\tau_i} \right] \times$$
$$\times \tilde{f}_{s_4}^{e_4} e^{-s_4\epsilon_4 m\beta} \Theta\left(m\beta - \sum_{j=1}^3 \tau_j \right) \Theta\left(\sum_{j=1}^3 \tau_j - (m-1)\beta \right)$$

$$= - \int \frac{d^3\mathbf{k}}{(2\pi)^3} \sum_{\mathbf{e},\mathbf{s}} \mathcal{T}_{\mathbf{e}}^{\mu_1\cdots\mu_4} \Theta_{\mathbf{s}}^{\mathbf{e}} \prod_{i=1}^{3} \left[\int_0^\beta d\tau_i \tilde{f}_{s_i}^{e_i} e^{\Omega_i\tau_i} \right] \left\{ -\tilde{f}_{s_4}^{e_4} e^{-s_4\epsilon_4\beta} \Theta \left(\beta - \sum_{j=1}^{3} \tau_j \right) + \right.$$

$$\left. + \tilde{f}_{s_4}^{e_3} e^{-2s_4\epsilon_4\beta} \Theta \left(2\beta - \sum_{j=1}^{3} \tau_j \right) \Theta \left(\sum_{j=1}^{3} \tau_j - \beta \right) - \tilde{f}_{s_4}^{e_4} e^{-3s_4\epsilon_4\beta} \Theta \left(\sum_{j=1}^{3} \tau_j - 2\beta \right) \right\} . \quad \text{(A.5)}$$

Using Eqs. (2.73) and (2.72) and respecting $0 \leq \tau_i \leq \beta$ one finds

$$-\tilde{f}_{s_4}^{e_4} e^{-s_4\epsilon_4\beta} \Theta \left(\beta - \sum_{j=1}^{3} \tau_j \right) + \tilde{f}_{s_4}^{e_4} e^{-2s_4\epsilon_4\beta} \Theta \left(2\beta - \sum_{j=1}^{3} \tau_j \right) \Theta \left(\sum_{j=1}^{3} \tau_j - \beta \right) -$$

$$-\tilde{f}_{s_4}^{e_4} e^{-3s_4\epsilon_4\beta} \Theta \left(\sum_{j=1}^{3} \tau_j - 2\beta \right) =$$

$$= -\tilde{f}_{-s_4}^{e_4} + e^{-s_4\epsilon_4\beta} \left\{ \Theta \left(\tau_1 + \tau_2 - \beta \right) + \Theta \left(\sum_{j=1}^{3} \tau_j - \beta \right) \Theta \left(\beta - \tau_1 - \tau_2 \right) \right\} -$$

$$-e^{-2s_4\epsilon_4\beta} \Theta \left(\sum_{j=1}^{3} \tau_j - 2\beta \right) . \quad \text{(A.6)}$$

Hence, we have the following τ-integrals

$$-\prod_{i=1}^{3} \left[\int_0^\beta d\tau_i \tilde{f}_{s_i}^{e_i} e^{\Omega_i\tau_i} \right] \tilde{f}_{-s_4}^{e_4} + \tilde{f}_{s_1}^{e_1} \tilde{f}_{s_2}^{e_2} \tilde{f}_{s_3}^{e_3} e^{-s_4\epsilon_4\beta} \int_0^\beta d\tau_1 \int_{\beta-\tau_1}^\beta d\tau_2 \int_0^\beta d\tau_3 e^{\Omega_1\tau_1} e^{\Omega_2\tau_2} e^{\Omega_3\tau_3} +$$

$$+\tilde{f}_{s_1}^{e_1} \tilde{f}_{s_2}^{e_2} \tilde{f}_{s_3}^{e_3} e^{-s_4\epsilon_4\beta} \int_0^\beta d\tau_1 \int_0^{\beta-\tau_1} d\tau_2 \int_{\beta-\tau_1-\tau_2}^\beta d\tau_3 e^{\Omega_1\tau_1} e^{\Omega_2\tau_2} e^{\Omega_3\tau_3} -$$

$$-\tilde{f}_{s_1}^{e_1} \tilde{f}_{s_2}^{e_2} \tilde{f}_{s_3}^{e_3} e^{-2s_4\epsilon_4\beta} \int_0^\beta d\tau_1 \int_{\beta-\tau_1}^\beta d\tau_2 \int_{2\beta-\tau_1-\tau_2}^\beta d\tau_3 e^{\Omega_1\tau_1} e^{\Omega_2\tau_2} e^{\Omega_3\tau_3} \quad \text{(A.7)}$$

Performing the τ-integrals one by one and using Eqs. (2.73) and (2.72) after each integration to combine the corresponding terms one finally obtains the result

$$\mathcal{J}^{\mu_1\cdots\mu_4}(P_1,\cdots,P_4) =$$

$$= -\int \frac{d^3\mathbf{k}}{(2\pi)^3} \sum_{\mathbf{e},\mathbf{s}} \mathcal{T}_{\mathbf{e}}^{\mu_1\cdots\mu_4} \Theta_{\mathbf{s}}^{\mathbf{e}} \times$$

$$\frac{1}{\Omega_3} \left\{ \frac{1}{\Omega_2} \left[\frac{\tilde{f}_{-s_1}^{e_1} \tilde{f}_{s_2}^{e_2} - \tilde{f}_{s_1}^{e_1} \tilde{f}_{-s_2}^{e_2}}{\Omega_1 - \Omega_2} - \frac{\tilde{f}_{-s_1}^{e_1} \tilde{f}_{s_4}^{e_4} - \tilde{f}_{s_1}^{e_1} \tilde{f}_{-s_4}^{e_4}}{\Omega_1} \right] + \right.$$

$$\left. \frac{1}{\Omega_2 - \Omega_3} \left[\frac{\tilde{f}_{-s_1}^{e_1} \tilde{f}_{s_3}^{e_3} - \tilde{f}_{s_1}^{e_1} \tilde{f}_{-s_3}^{e_3}}{\Omega_1 - \Omega_3} - \frac{\tilde{f}_{-s_1}^{e_1} \tilde{f}_{s_2}^{e_2} - \tilde{f}_{s_1}^{e_1} \tilde{f}_{-s_2}^{e_2}}{\Omega_1 - \Omega_2} \right] \right\} =$$

$$= -\int \frac{d^3\mathbf{k}}{(2\pi)^3} \sum_{\mathbf{e},\mathbf{s}} \mathcal{T}_{\mathbf{e}}^{\mu_1\cdots\mu_4} \Theta_{\mathbf{s}}^{\mathbf{e}} \frac{1}{p_3^0 - p_4^0 - s_3\epsilon_3 + s_4\epsilon_4} \times$$

$$\left\{ \frac{1}{p_2^0 - p_4^0 - s_2\epsilon_2 + s_4\epsilon_4} \left[\frac{\frac{s_2-s_1}{2} + s_1 N(\epsilon_1) - s_2 N(\epsilon_2)}{p_1^0 - p_2^0 - s_1\epsilon_1 + s_2\epsilon_2} - \frac{\frac{s_4-s_1}{2} + s_1 N(\epsilon_1) - s_4 N(\epsilon_4)}{p_1^0 - p_4^0 - s_1\epsilon_1 + s_4\epsilon_4} \right] + \right.$$

$$\left. + \frac{1}{p_2^0 - p_3^0 - s_2\epsilon_2 + s_3\epsilon_3} \left[\frac{\frac{s_3-s_1}{2} + s_1 N(\epsilon_1) - s_3 N(\epsilon_3)}{p_1^0 - p_3^0 - s_1\epsilon_1 + s_3\epsilon_3} - \frac{\frac{s_2-s_1}{2} + s_1 N(\epsilon_1) - s_2 N(\epsilon_2)}{p_1^0 - p_2^0 - s_1\epsilon_1 + s_2\epsilon_2} \right] \right\}$$

$$\text{(A.8)}$$

In the limit $\mu \to 0$ and after using Eq. (2.94) this reproduces the corresoponding formula (A.19) in [7].

Anhang B

Zusammenfassung

In dieser Arbeit wird eine allgemeine effektive Wirkung für Quarkmaterie abgeleitet und auf den Effekt der Farbsupraleitung angewendet [6]. Motiviert wird dieser Zugang durch das Auftreten wohl separierter Impulsskalen in dichter und/oder heißer Quarkmaterie. Als Ausgangspunkt dient die Theorie der starken Wechselwirkung, die Quantenchromodynamik (QCD), bei nichtverschwindenden Temperaturen T und quarkchemischen Potentialen μ [9, 10]. Die QCD ist eine nicht-Abelsche $SU(3)_c$-Eichtheorie. Die Quarks, die elementaren Grundbausteine der hadronischen Materie, gehören zur fundamentalen Darstellung der $SU(3)_c$, während die Eichbosonen, die Gluonen, der adjungierten Darstellung entsprechen. Die QCD ist eine asymptotisch freie Theorie [1], d.h. dass die Kopplungskonstante g auf großen Impulsskalen Q klein wird, $g(Q) \sim 1/\ln(Q/\Lambda_{\mathrm{QCD}})$, wobei $\Lambda_{\mathrm{QCD}} \sim 200$ MeV. In dieser Arbeit werden asymptotisch hohe Temperaturen, $T \gg \Lambda_{\mathrm{QCD}}$, und/oder asymptotisch hohe quarkchemische Potentiale, $\mu \gg \Lambda_{\mathrm{QCD}}$, angenommen, so dass immer $g \ll 1$ gilt und somit (semi-)perturbative Techniken anwendbar sind.

Im Fall kalter, dichter Quarkmaterie treten mehrere Impulsskalen auf, die weit voneinander getrennt sind. Es sind diese $\mu \gg g\mu \gg \phi$. Die erste ist realisiert durch den Fermi-Impuls der Quarks, $k_F \equiv \sqrt{\mu^2 - m_q^2} \simeq \mu$. Hier wurde der ultrarelativistische Limes angewendet, indem die Quarkmasse m_q gegenüber der Fermi-Energie $\epsilon_F = \mu$ vernachlässigt wurde. Die Skala $g\mu$ ist wegen $g \ll 1$ viel kleiner als μ und manifestiert sich als Debye-Masse der (elektrischen) Gluonen, $M_D = g\mu\sqrt{N_f}/(2\pi)$ [9]. Diese Gluonen besitzen damit nur eine endliche Reichweite der Ordnung $\sim 1/M_D$. N_f ist die Zahl der Quarkflavors, die an der Abschirmung der Gluonen beteiligt sind. Schließlich ist $\phi \sim \mu/g^5 \exp(-c/g)$ die Lücke im Energiespektrum der (Quasi-)Quarks, $\epsilon_k = \sqrt{(k-\mu)^2 + \phi^2}$, die zur Farbsupraleitung führt [53]. Sie wird hervorgerufen durch ein Kondensat von Cooper-Paaren, welches sich bei $T \lesssim \phi$ aus den Quarks nahe der Fermi-Fläche bildet. Ursache ist der attraktive $[\bar{3}]_c^a$-Kanal im Ein-Gluon-Austausch zwischen zwei Quarks [13]. Diese Cooper-Paare sind nicht farbneutral und brechen somit die lokale Eichsymmetrie $SU(3)_c$. Dies führt zu Meissner-Massen der (magnetischen) Gluonen durch den Anderson-Higgs-Mechanismus [13]. Analog treten im Fall heißer Quarkmaterie, $T \gg \Lambda_{\mathrm{QCD}}$, die zwei weit getrennten Skalen $T \gg gT$ auf [9]. Häufig bezeichnet man große Skalen als "hart" und kleine als "weich". Das Auftreten harter und weicher Skalen in heißer und/oder dichter Quarkmaterie motiviert die Konstruktion einer effektiven Theorie.

Allgemein sind effektive Theorien [107] für die Situation konzipiert, in der man an einer weichen Impulsskala Λ_1, bzw. großen Längenskala $1/\Lambda_1$ interessiert ist, die zugrundeliegende, mikroskopische Quantenfeldtheorie aber eine viel härtere Impulsskala, bzw. kleinere Längenskala $1/\Lambda_0$, beinhaltet, $\Lambda_0 \gg \Lambda_1$, bzw. $1/\Lambda_0 \ll 1/\Lambda_1$. Man nimmt an, dass die Dynamik auf der weichen Skala unabhängig von den Details der Dynamik auf der harten Skala ist, und eliminiert deswegen die harten, mikroskopischen Moden aus der Theorie. Diese sind dann nicht mehr als explizite Freiheitsgrade, sondern nur noch implizit in den Vertices der effektiven Theorie enthalten. Diese Vertices mit internen mikroskopischen Moden werden als "lokal" auf der großen Längenskala $1/\Lambda_1$ angenommen, also als unabhängig von den externen weichen Impulsen. Ihre Form versucht man meistens aufgrund von Symmetrieüberlegungen zu erraten. Ihre Größenordnung schätzt man anschließend durch Bestimmung ihrer Energiedimension ab. Wenn man sich dann auf eine bestimmte Genauigkeit in den zu berechnenden Größen beschränkt, braucht man nur Operatoren bestimmter Relevanzklassen zu berücksichtigen, was die Rechnungen wesentlich vereinfacht.

Als kurzes Beispiel betrachte man eine Theorie mit nur einem skalaren Feld ϕ und einer intrinsischen harten Skala Λ. Um die für die Physik der weichen Skala $E \ll \Lambda$ irrelevanten Details der harten Skala Λ zu eliminieren, spaltet man das Feld ϕ in einen harten und einen weichen Anteil auf, $\phi = \varphi + \psi$, vgl. Fig. B.1. Der Ansatz für eine effektive Wirkung lautet dann
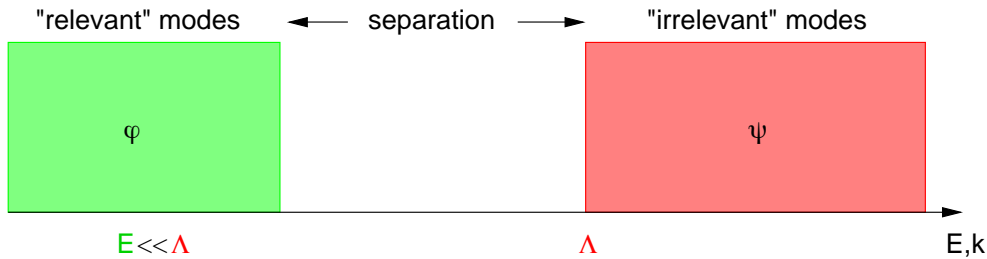

Abbildung B.1: Trennung der Skalen E und Λ.

unter Berücksichtigung aller Symmetrien der zugrundeliegenden Theorie [108]

$$S_{\text{eff}}[\varphi] = \int d^D x \sum_i g_i \mathcal{O}_i(\varphi) \,, \tag{B.1}$$

wobei die Operatoren $\mathcal{O}_i(\varphi)$ die Vertices und $g_i = g_i(\Lambda)$ die zugehörigen Kopplungskonstanten der effektiven Theorie sind. Sei δ nun die Energiedimension des Feldes φ, $\varphi \sim E^\delta$, und der i-te Operator in Eq. (B.1) zusammengesetzt gemäß $\mathcal{O}_i \sim \partial^N \varphi^M$, dann ist $\mathcal{O}_i \sim E^{N+M\delta} \equiv E^{\delta_i}$. Da die Wirkung S_{eff} dimensionslos ist, folgt $g_i(\Lambda) \sim \Lambda^{D-\delta_i}$. Somit hat man insgesamt für den i-ten Term gefunden: $\int dx^D g_i \mathcal{O}_i \sim (E/\Lambda)^{\delta_i - D}$. Für $\delta_i < D$ wird dieser Term immer größer, wenn $E \to 0$, für $\delta_i = D$ bleibt er unverändert und für $\delta_i > D$ wird er immer kleiner. Dementsprechend bezeichnet man ihn als "relevant", "marginal" oder "irrelevant". Um mit Hilfe der Wirkung (B.1) auf der Energieskala $E = s\Lambda$ eine physikalische Größe mit einer Genauigkeit s^{n+1} perturbativ auszurechnen, benötigt man nun lediglich die Operatoren $\mathcal{O}_i$ mit $\delta_i \leq D + n$. Für den Fall, dass $s \ll 1$, dass die Skalen E und Λ also weit voneinander separiert sind, sind für eine gegebene Genauigkeit nur wenige Operatoren notwendig, was letztlich die Rechnung wesentlich vereinfacht.

Diese Vorgehensweise ist allerdings im Falle heißer und/oder dichter Quarkmaterie nicht praktikabel. Erstens entstehen hier "nicht-lokale" Vertices, z.B. die sog. Hard Thermal/Dense Loops (HTL/HDL) [9]. Ihre funktionale Abhängigkeit von den externen weichen Impulsen lässt sich unmöglich erraten. Zweitens lassen sich im Fall selbstkonsistent zu berechnender Größen die Beiträge der einzelnen Vertices nicht vor der eigentlichen Rechnung abschätzen. So entstehen bspw. im Fall der Gap-Funktion ϕ der Farbsupraleitung im Verlauf der Lösung der zugehörigen Gap-Gleichung,

$$\phi = g^2 \, \phi \left[\zeta \, \ln^2 \left(\frac{\mu}{\phi} \right) + \beta \, \ln \left(\frac{\mu}{\phi} \right) + \alpha \right] , \tag{B.2}$$

große Logarithmen, $\ln(\mu/\phi) \sim 1/g \gg 1$, die man auf der Ebene der Vertices in der effektiven Wirkung nicht vorhersehen kann. Drittens sind sowohl harte Quark- wie auch Gluonmoden zu eliminieren. Zum einen führt dies zu einer viel größeren Vielfalt an möglichen Topologien der Vertices als im Fall eines einzelnen Feldes, vgl. Fign. 2.13-2.16. Zum anderen treten zwei cutoff-Parameter auf, Λ_q und Λ_g, deren Verhältnis zueinander und zu den zugrundeliegenden physikalischen Skalen $\mu \gg g\mu \gg \phi$ a priori nicht bekannt ist. Dies macht eine einfache dimensionale Größenabschätzung der einzelnen Vertices unmöglich.

Es ist daher der Ansatz dieser Arbeit, die Vertices der effektiven Wirkung nicht zu erraten, sondern exakt und möglichst allgemein abzuleiten. Als Ausgangspunkt dient die Zustandssumme der QCD im Pfadintegralformalismus, vgl. Gln. (1.1-1.3). Der Quarksektor lässt sich in kompakter Form schreiben als

$$\mathcal{Z}_q[A] = \int \mathcal{D}\bar{\Psi} \, \mathcal{D}\Psi \exp \left[\frac{1}{2} \bar{\Psi} \left(\mathcal{G}_0^{-1} + g\mathcal{A} \right) \Psi \right] , \tag{B.3}$$

wobei die Integration über die Quarkimpulse sowie Spin-, Farb- und Flavorindices der Quarkfelder Ψ und $\bar{\Psi}$ nicht ausgeschrieben sind. $\mathcal{G}_0$ ist der freie Quarkpropagator, $\mathcal{A}$ das Gluonfeld zusammengefasst mit dem Quark-Gluonvertex und g die Kopplungskonstante der QCD. Als erster Schritt wird im Impulsraum der cutoff-Parameter Λ_q eingeführt, der "relevante" von "irrelevanten" Quarkmoden trennt. Mit diesem lassen sich Projektionsoperatoren einführen, wie z.B. Gln. (2.18), mit denen man die Quarkfelder formal in relevante Moden (mit Index 1) und irrelevante Moden (mit Index 2) aufspalten kann

$$\Psi_1 \equiv \mathcal{P}_1 \, \Psi \ , \quad \Psi_2 \equiv \mathcal{P}_2 \, \Psi \ , \quad \bar{\Psi}_1 \equiv \bar{\Psi} \, \gamma_0 \mathcal{P}_1 \gamma_0 \ , \quad \bar{\Psi}_2 \equiv \bar{\Psi} \, \gamma_0 \mathcal{P}_2 \gamma_0 \ . \tag{B.4}$$

Durch Einsetzen wird die Zustandssumme zu

$$\mathcal{Z}_q[A] = \int \prod_{n=1,2} \mathcal{D}\bar{\Psi}_n \, \mathcal{D}\Psi_n \exp \left[\frac{1}{2} \sum_{n,m=1,2} \bar{\Psi}_n \left(\mathcal{G}_0^{-1} + g\mathcal{A} \right)_{nm}^{-1} \Psi_m \right] . \tag{B.5}$$

Durch geeignetes Verschieben der Felder $\bar{\Psi}_2, \Psi_2$, Gl. (2.23), lassen sich die Terme, die linear in diesen Feldern sind, eliminieren. Danach ist das Pfadintegral über diese Felder Gaußsch und somit exakt lösbar. Man erhält

$$\mathcal{Z}_q[A] = \int \mathcal{D}\bar{\Psi}_1 \, \mathcal{D}\Psi_1 \exp \left[\frac{1}{2} \bar{\Psi}_1 \left(\mathcal{G}_{0,11}^{-1} + g\mathcal{B} \right) \Psi_1 + \frac{1}{2} \operatorname{Tr}_q \ln \mathcal{G}_{22}^{-1} \right] . \tag{B.6}$$
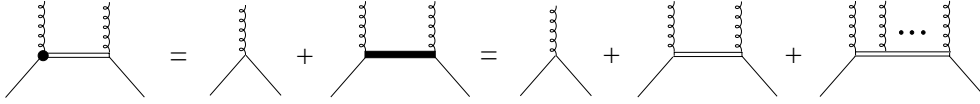
Abbildung B.2: Der Term $\bar{\Psi}_1\, g\mathcal{B}\, \Psi_1$. Ein relevantes Quarkfeld ist als einfache gerade Linie dargestellt, irrelevante Quarkmoden im Innern als doppelte Linien. Gekringelte Linien sind Gluonfelder.

Als Folge des Verschiebens der irrelevanten Quarkfelder liegt das Gluonfeld in der modifizierten Form $g\mathcal{B} = (1 + g\mathcal{A}\,\mathcal{G}_{0,22})^{-1}\, g\mathcal{A}$ vor, was sich diagrammatisch wie in Fig. B.2 darstellen lässt. Der Term $\frac{1}{2}\,\mathrm{Tr}_q \ln \mathcal{G}_{22}^{-1}$ resultiert vom Ausintegrieren und entspricht Einschleifendiagrammen mit internen irrelevanten Quarkmoden und externen Gluonbeinen, vgl. Fig. B.3. Das Resultat in Gl. (B.6) ist exakt und aufgrund der noch frei wählbaren Projektoren völlig allgemein.
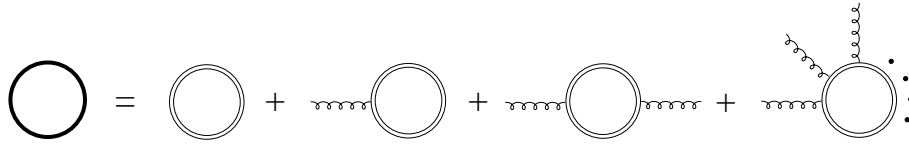
Abbildung B.3: Die graphische Darstellung des Terms $\mathrm{Tr}_q \ln \mathcal{G}_{22}^{-1}$ in Eq. (B.6).

Addiert man zum Exponenten in Gl. (B.6) die Wirkung des Gluonfeldes, vgl. Gln. (2.30, 2.31), und führt auch Gluonprojektoren ein, Gl. (2.35), so lassen sich die einzelnen Terme in der resultierenden Wirkung nach der Anzahl der harten Gluonfelder, A_2, sortieren

$$S[A, \bar{\Psi}_1, \Psi_1] = S[A_1, \bar{\Psi}_1, \Psi_1] + A_2 \mathcal{J}[A_1, \bar{\Psi}_1, \Psi_1] - \frac{1}{2}\, A_2\, \Delta_{22}^{-1}[A_1, \bar{\Psi}_1, \Psi_1]\, A_2 + S_I[A_1, A_2, \bar{\Psi}_1, \Psi_1]\,. \tag{B.7}$$

Für die Definition und diagrammatische Darstellung des "harten Gluonstromes" $\mathcal{J}[A_1, \bar{\Psi}_1, \Psi_1]$ siehe Gl. (2.37) und Fign. 2.5–2.7, für die des "harten Gluonpropagators" $\Delta_{22}^{-1}[A_1, \bar{\Psi}_1, \Psi_1]$ siehe Gl. (2.40) und Fign. 2.9–2.11. Im Unterschied zum Quarksektor treten nun auch Terme in allen höheren Ordnungen des harten Gluonfeldes auf. Sie sind im "Wechselwirkungsterm" $S_I[A_1, A_2, \bar{\Psi}_1, \Psi_1]$ zusammengefasst. Um weiter exakt vorgehen zu können, führe ich nun einen Quellterm $J_2 A_2$ für das harte Gluonfeld ein und substituiere im Wechselwirkungsterm $A_2 \to \delta/\delta J_2$. Dann lässt sich der Faktor $\exp\{S_I[A_1, \delta/\delta J_2, \bar{\Psi}_1, \Psi_1]\}$ vor das Pfadintegral über $\mathcal{D}A_2$ ziehen. Verschiebt man dann das harte Gluonfeld gemäß $A_2 \to A_2 - (\mathcal{J} + J_2)\Delta_{22}$, so nimmt das Integral eine Gaußsche Form an und lässt sich wiederum exakt lösen

$$
\begin{aligned}
\mathcal{Z} \;=\; & \int \mathcal{D}\bar{\Psi}_1\, \mathcal{D}\Psi_1 \mathcal{D}A_1 \, \exp\left\{ S[A_1, \bar{\Psi}_1, \Psi_1] - \frac{1}{2}\,\mathrm{Tr}_g \ln \Delta_{22}^{-1} \right\} \\
& \times \exp\left\{ S_I\left[A_1, \frac{\delta}{\delta J_2}, \bar{\Psi}_1, \Psi_1\right]\right\} \exp\left[\frac{1}{2}\,(\mathcal{J} + J_2)\, \Delta_{22}\, (\mathcal{J} + J_2)\right]\Big|_{J_2 = 0}\,. \tag{B.8}
\end{aligned}
$$

Dieses Resultat ist exakt, vollständig und völlig allgemein, da die Projektionsoperatoren noch nicht spezifiziert wurden. Es wurde nicht geraten, wie es in der Konstruktion einer effektiven Theorie normalerweise üblich ist. Somit sind auch alle nicht-trivialen Energie- und Impulsabhängigkeiten intakt (non-locality). Außerdem sind die Diagramme durch das explizite

Ausintegrieren zu Diagrammklassen zusammengefasst, wodurch eine systematische Behandlung ermöglicht wird.

Für das Folgende mache ich nun zwei Näherungen: Die erste basiert auf der prinzipiellen Annahme, die jeder effektiven Theorie zugrundeliegt, dass nämlich harte und weiche Impulsskalen weit voneinander separiert sind. Man nimmt also an, dass wegen der Impulserhaltung ein hartes Gluon nicht mit (endlich vielen) weichen Gluonen koppeln kann. So tragen die Diagramme Fig. 2.6, 2.7 nicht zur effektiven Wirkung (B.7) bei. Die zweite Näherung ist die Vernachlässigung des Termes S_I, $e^{S_I} \simeq 1$, in Gl. (B.8), der die Diagramme mit mehr als einer resummierten harten Gluonlinie beinhaltet. Diese Approximation ist noch nicht strikt begründet. Es wird allerdings gezeigt, dass die so erhaltene, approximative effektive Wirkung bekannte effektive Theorien beinhaltet und es außerdem erlaubt, die Gap-Funktion ϕ zur sogenannten "subleading order" auszurechnen. Falls benötigt, lässt sich der Term S_I auch leicht wieder restaurieren. Auf diese Weise ist die Zustandssumme für relevante Quark- und weiche Gluonfelder

$$\mathcal{Z} = \int \mathcal{D}\bar{\Psi}_1 \, \mathcal{D}\Psi_1 \mathcal{D}A_1 \, \exp\{S_{\text{eff}}[A_1, \bar{\Psi}_1, \Psi_1]\} \, , \tag{B.9}$$

mit der gesuchten effektiven Wirkung

$$\begin{aligned}
S_{\text{eff}}[A_1, \bar{\Psi}_1, \Psi_1] \quad \equiv \quad & S_A[A_1] + \frac{1}{2} \, \bar{\Psi}_1 \left\{ \mathcal{G}_{0,11}^{-1} + g\mathcal{B}[A_1] \right\} \Psi_1 + \frac{1}{2} \operatorname{Tr}_q \ln \mathcal{G}_{22}^{-1}[A_1] \\
& -\frac{1}{2} \operatorname{Tr}_g \ln \Delta_{22}^{-1}[A_1, \bar{\Psi}_1, \Psi_1] \\
& +\frac{1}{2} \, \mathcal{J}_{\mathcal{B}}[A_1, \bar{\Psi}_1, \Psi_1] \, \Delta_{22}[A_1, \bar{\Psi}_1, \Psi_1] \, \mathcal{J}_{\mathcal{B}}[A_1, \bar{\Psi}_1, \Psi_1] \tag{B.10}
\end{aligned}$$

abgeleitet. Für die diagrammatische Darstellung der einzelnen Terme in Gl. (B.10) siehe Fign. 2.12-2.16.

Es lassen sich nun die bekannten effektiven Theorien jeweils einer speziellen Wahl von Quark- und Gluonprojektoren zuordnen. So reproduziert man etwa die "Hard Thermal Loop" (HTL) und die "Hard Dense Loop" (HDL) effektiven Theorien durch die Projektoren (2.35) und (2.47). Es werden also im Falle von HTL (HDL) harte Quarks und Gluonen mit Impulsen $p \geq T$ (μ) ausintegriert, während die weichen Moden mit Impulsen $p \sim gT \ll T$ ($p \sim g\mu \ll \mu$) als explizite Freiheitsgrade in der effektiven Wirkung zurückbleiben. Dabei fallen viele Diagramm- klassen, die nicht zu den HTL/HDL effektiven Wirkungen gehören, aus Gründen der Impulser- haltung trivial weg. Die verbleibenden können dann nach dem bekannten HTL/HDL "Power- countingschema" [7] analysiert werden. Ebenso lässt sich die "high-density effective theory" (HDET) [100, 101, 102, 103, 104, 105] wiedergewinnen durch die Projektorenwahl (2.18) und (2.35). Im Gegensatz zur Ableitung in dieser Arbeit werden in [100, 101, 102, 103] nur Anti- quarks explizit ausintegriert (entsprechend dem Quarkprojektor (2.51)). Alle anderen Vertices, die den Effekt der harten Gluonen mit Impulsen der Ordnung μ und der Quarks fern der Fermi- kante beinhalten, sind dort "von Hand" hinzugefügt. Einige technische Probleme, die bei dieser "herkömmlichen" Ableitung auftreten, werden in Abschnitt 2.2.2 ausführlich dargelegt. Es sei hier aber nur auf ein prinzipielles Problem hingewiesen: Welche Diagramme auf diese Weise der Wirkung hinzuzufügen sind, ist sicherlich wohl definiert, wenn man z.B. die Gap-Gleichung zur subleading order ausrechnen möchte, da das Resultat bereits aus der vollen QCD bekannt

ist. Will man allerdings die noch unbekannten Korrekturen zur sub-subleading order berechnen (vom Term α in Eq. (B.2)), kann man auf diesem Weg kein systematisches Lösungsverfahren erhalten.

In dieser Arbeit wird jedoch gezeigt, dass die abgeleitete effektive Wirkung Gl. (B.10) in Kombination mit dem CJT-Formalismus [106] eine systematische und rigorose Lösung der Gap-Gleichung erlaubt. Der Hauptvorteil liegt darin, dass die Selbstkonsistenz der Lösung der Dyson-Schwinger-Gleichungen der Felder und der Propagatoren nur für die relevanten Moden der Theorie gefordert ist. Im Fall dichter, kalter Quarkmaterie kommen als relevante Quarks aufgrund des Pauli-Prinzips und der schwachen Kopplung nur solche in einer dünnen Schicht der Dicke $\Lambda_q \ll \mu$ um die Fermi-Fläche in Frage. Der Impulsaustausch über Gluonen ist durch $p \lesssim 2\mu$ beschränkt, vgl. Fig. 3.9. Dies legt für die cutoff-Parameter $\Lambda_g \gg \Lambda_q$ nahe. Aus der HDL-Theorie ist außerdem bekannt, dass man Gluonen auf der Impulsskala $p \lesssim g\mu$ mit HDLs resummieren muss, während die Resummation für Gluonimpulse $p \gtrsim \mu$ nur perturbativ kleine Korrekturen ergibt. Mit der Wahl $\Lambda_g \sim \mu$ trennt man diese beiden Regimes der Gluonen, so dass nur für die weichen, nicht-trivialen Gluonmoden eine selbstkonsistente Lösung der Dyson-Schwinger-Gleichung gefordert ist, während die harten Moden durch freie Propagatoren trivial angenähert werden können. Für die Wahl von $\Lambda_q \ll \Lambda_g$ bietet sich dann $\Lambda_q \sim g\mu$ an. Damit trägt man in der effektiven Theorie auch automatisch der Tatsache Rechnung, dass der Austausch von fast statischen, magnetischen Gluonen mit $\omega \ll p$ dominant ist, vgl. Fig. 4.1. Diese Wahl der Cutoffs hat noch einen weiteren entscheidenden Vorteil: Mit $\Lambda_q/\Lambda_g \sim g \ll 1$ hat man einen Kleinheitsparameter gewonnen. Bei der Lösung der Gap-Gleichung lassen sich alle auftretenden Terme nach Λ_q/Λ_g entwickeln und auf diese Weise rigoros power-counten. Als ein weiterer wichtiger Vorteil der Kombination der effektiven Wirkung mit dem CJT-Formalismus stellt sich schließlich heraus, dass die Gap-Gleichung im Impulsraum in verschiedene Regimes zerfällt, in denen man dann jeweils kontrollierbare Näherungen vornehmen kann, wie bspw. die Anwendung des Niederenergielimes des magnetischen Gluonpropagators.

Es lässt sich mit Hilfe der effektiven Wirkung in Kombination mit dem CJT-Formalismus die Gap-Gleichung prinzipiell zu jeder gegebenen höheren Ordnung kontrolliert lösen. So liefern die sub-subleading Beiträge α in Eq. (B.2) Korrekturen der Ordnung $O(g)$ zur Gap-Funktion gemäß $\phi \sim \mu/g^5 \exp(-c/g)[1 + O(g)]$. Ist der betreffende Koeffizient in dem $O(g)$-Term eine große Zahl vergleichbar mit $1/g$, so wäre diese Korrektur selbst im Grenzfall schwacher Kopplung wichtig. Allgemein sind diese Korrekturen höherer Ordnung notwendig, um μ kontrollierter zu physikalisch relevanten Werten herunterextrapolieren zu können, wo $g \ll 1$ nicht mehr erfüllt ist. Im Inneren von Neutronensternen etwa ist $\mu \lesssim 500$ MeV und $g \sim 1$ [13]. Als ein erster Schritt in diese Richtung wurde in dieser Arbeit erstmals der Imaginärteil und somit die Energieabhängigkeit von ϕ selbstkonsistent berücksichtigt. Dazu wurde eine komplexe Gap-Gleichung aufgestellt und mit Hilfe der effektiven Wirkung zur subleading order gelöst. Dabei wurden mehrere Korrekturen zur sub-subleading order identifiziert. Die Lösung der Gap-Gleichung zur sub-subleading order bleibt jedoch ein Projekt für die Zukunft.

Eine weitere offene Fragestellung ist die systematische Analyse aller Diagramme, die in der effektiven Wirkung (B.8) auftauchen. Ziel wäre ein konsistentes Power-counting-Schema, dass es im Fall von perturbativen Größen erlaubt, vor der eigentlichen Rechnung die Zahl der Diagramme stark zu reduzieren. In Abschnitt 2.3 wird ein erster Schritt in diese Richtung unternommen und eine erste Diagrammklasse, die der Schleifen mit internen ausintegrierten Quarkmoden und

N externen weichen Gluonenbeinen, abgeschätzt. Insbesondere wird gezeigt, dass man im Fall $\Lambda_{\mathrm{q}} \ll \Lambda_{\mathrm{gl}}$ und der Projektionsoperatoren (2.18) und (2.35) die entsprechenden HDL-Ausdrücke bis zur Ordnung $O(\Lambda_{\mathrm{q}}/\Lambda_{\mathrm{gl}})$ wiedergewinnt.

Die effektive Wirkung Gl. (B.10) stellt die bekannten effektiven Theorien für heiße und/oder dichte Quarkmaterie auf eine gemeinsame formale Basis. Sie erlaubt eine bessere Einsicht und größere Kontrolle über notwendige Näherungen und bietet den Rahmen für systematische Untersuchungen einer Vielzahl verschiedener Fragestellungen in schwach gekoppelter Quarkmaterie.

Bibliography

[1] H.D. Politzer, Phys. Rev. Lett. **30**, 1346 (1973); D.J. Gross and F. Wilczek, Phys. Rev. D **8**, 3633 (1973); Phys. Rev. D **9**, 980 (1974).

[2] J.C. Collins and M.J. Perry, Phys. Rev. Lett. **34**, 1353 (1975).

[3] A.C. Phillips, *The Physics of Stars* (John Wiley & Sons, Chichester, 1994).

[4] F. Weber, *Pulsars as Astrophysical Laboratories for Nuclear and Particle Physics* (IOP Publishing Ltd., Bristol, 1999).

[5] J.A. Pons, S. Reddy, M. Prakash, J.M. Lattimer, and J.A. Miralles, Astrophys. J. **513**, 780 (1999).

[6] P. T. Reuter, Q. Wang and D. H. Rischke, Phys. Rev. D **70**, 114029 (2004) [Erratum-ibid. D **71**, 099901 (2005)].

[7] E. Braaten and R.D. Pisarski, Nucl. Phys. B **337**, 569 (1990).

[8] J. P. Blaizot and E. Iancu, Phys. Rept. **359**, 355 (2002).

[9] M. Le Bellac, *Thermal Field Theory* (Cambridge University Press, Cambridge, 2000).

[10] M. E. Peskin and D. V. Schroeder, *An introduction to quantum field theory* (Westview Press, Oxford, 1995).

[11] K. Huang, *Quarks, Leptons and Gauge fields* (World Scientific, Singapore, 1992).

[12] D. Bailin and A. Love, *Introduction to gauge field theory* (Sussex University Press, 1986).

[13] D.H. Rischke, Prog. Part. Nucl. Phys. **52**, 197 (2004).

[14] S. Eidelman *et al.* [Particle Data Group], Phys. Lett. B **592**, 1 (2004).

[15] J.I. Kapusta, *Finite temperature field theory* (Cambridge University Press, Cambridge, 1989).

[16] R. S. Chivukula, eConf **C040802**, L010 (2004) [arXiv:hep-ph/0411198].

[17] G. 't Hooft, *Phys. Rep.* 142 (1986) 357 .

[18] D.J. Gross, R.D. Pisarski, and L.G. Yaffe, *Rev. Mod. Phys.* 53 (1981) 42 .

[19] S. Das Gupta, A. Z. Mekjian and M. B. Tsang, arXiv:nucl-th/0009033.

[20] H. Jaqaman *et al.*, Phys. Rev. C **27** 2782 (1983).

[21] A. Insolia *at al.*, Phase Transitions in Strong Interactions: Status and Perspectives, Proceedings of the 3rd Catania Relativistic Ion Studies, Acicastello, Italy (2000).

[22] W. Trautmann, Notes of NATO Advanced Study Institute, Dronten, Niederlanden (1996); Nucl. Phys. A **607** 457 (1996).

[23] J.P. Bondorf *et al.*, Phys. Rep. **257** (1995) 131.

[24] K.A. Bugaev, M.I. Gorenstein, I.N. Mishustin and W. Greiner, Phys. Rev. **C62** (2000) 044320.

[25] K.A. Bugaev, M.I. Gorenstein, I.N. Mishustin and W. Greiner, Phys. Lett. **B 498** (2001) 144.

[26] P. T. Reuter and K. A. Bugaev, Phys. Lett. B **517**, 233 (2001).

[27] K. A. Bugaev, arXiv:nucl-th/0507028.

[28] M. Creutz, *Quarks, Gluons, and Lattices* (Cambridge University Press, Cambridge, 1983).

[29] E. Laermann and O. Philipsen, Ann. Rev. Nucl. Part. Sci. **53**, 163 (2003).

[30] Z. Fodor and S. D. Katz, JHEP **0404**, 050 (2004).

[31] S. Ejiri, C. R. Allton, S. J. Hands, O. Kaczmarek, F. Karsch, E. Laermann and C. Schmidt, Prog. Theor. Phys. Suppl. **153**, 118 (2004).

[32] M. Stephanov, Acta Phys. Polon. B **35**, 2939 (2004).

[33] Proc. of the 17th Int. Conf. on Ultra-relativistic Nucleus-Nucleus Collisions, *Quark Matter 2004* (eds. Hans G. Ritter and Xin-Nian Wang), J. Phys. G, **30**, 633-1429 (2004).

[34] J. B. Kogut and M. A. Stephanov, Camb. Monogr. Part. Phys. Nucl. Phys. Cosmol. **21**, 1 (2004).

[35] B.C. Barrois, Nucl. Phys. B **129**, 390 (1977); S.C. Frautschi, report CALT-68-701, *Presented at Workshop on Hadronic Matter at Extreme Energy Density, Erice, Italy, Oct. 13-21, 1978*; for a review, see D. Bailin and A. Love, Phys. Rept. **107**, 325 (1984).

[36] K. Rajagopal and F. Wilczek, "The condensed matter physics of QCD," arXiv:hep-ph/0011333; M.G. Alford, Ann. Rev. Nucl. Part. Sci. **51**, 131 (2001); T. Schäfer, arXiv:hep-ph/0304281.

[37] I. A. Shovkovy, arXiv:nucl-th/0410091.

[38] A.A. Svidzinsky, Astrophys. J. **590**, 386 (2003).

[39] B. Link, *Phys. Rev. Lett.* 91 (2003) 101101 .

[40] K.B.W. Buckley, M.A. Metlitski, and A.R. Zhitnitsky, *Phys. Rev. Lett.* 92 (2004) 151102 .

[41] Y. Nambu and G. Jona-Lasinio, Phys. Rev. **122**, 345 (1961); Phys. Rev. **124**, 246 (1961).

[42] M.G. Alford, K. Rajagopal, and F. Wilczek, Phys. Lett. B **422**, 247 (1998); R. Rapp, T. Schäfer, E.V. Shuryak, and M. Velkovsky, Phys. Rev. Lett. **81**, 53 (1998).

[43] J. Bardeen, L.N. Cooper, and J.R. Schrieffer, Phys. Rev. **108**, 1175 (1957).

[44] Z.M. Galasiewicz, *Superconductivity and quantum fluids* (Pergamon Press, Oxford, 1970).

[45] A.L. Fetter and J.D. Walecka, *Quantum Theory of Many-Particle Systems* (McGraw-Hill, New York, 1971).

[46] M. Tinkham, *Introduction to Superconductivity* (McGraw-Hill, New York, 1975).

[47] D. Vollhardt and P. Wölfle, *The Superfluid Phases of Helium 3* (Taylor & Francis, London, 1990).

[48] G. W. Carter and D. Diakonov, Phys. Rev. D **60**, 016004 (1999); J. Berges and K. Rajagopal, Nucl. Phys. B **538**, 215 (1999); M. Buballa and M. Oertel, Nucl. Phys. A **703**, 770 (2002); F. Gastineau, R. Nebauer, and J. Aichelin, Phys. Rev. C **65**, 045204 (2002); M. Huang, P. F. Zhuang, and W. Q. Chao, Phys. Rev. D **65**, 076012 (2002).

[49] M. Buballa, Phys. Rept. **407**, 205 (2005).

[50] M. Huang, P. F. Zhuang, and W. Q. Chao, Phys. Rev. D **67**, 065015 (2003).

[51] M. Buballa and M. Oertel, Czech. J. Phys. **55** (2005) 521.

[52] M. Buballa and I. A. Shovkovy, arXiv:hep-ph/0508197.

[53] D.T. Son, Phys. Rev. D **59**, 094019 (1999).

[54] T. Schäfer and F. Wilczek, Phys. Rev. D **60**, 114033 (1999).

[55] R.D. Pisarski and D.H. Rischke, Phys. Rev. D **61**, 051501, 074017 (2000).

[56] D.K. Hong, V.A. Miransky, I.A. Shovkovy, and L.C.R. Wijewardhana, Phys. Rev. D **61**, 056001 (2000) [Erratum-ibid. D **62**, 059903 (2000)].

[57] S.D.H. Hsu and M. Schwetz, Nucl. Phys. B **572**, 211 (2000).

[58] P.W. Anderson, Phys. Rev. **130**, 439 (1963).

[59] P.W. Higgs, Phys. Lett. **12**, 132 (1964); Phys. Rev. Lett. **13**, 508 (1964); Phys. Rev. **145**, 1156 (1966).

[60] S. Elitzur, *Phys. Rev.* D 12 (1975) 3978 .

[61] S. Weinberg, *Phys. Rev. Lett.* 19 (1967) 1264.

[62] G.W. Carter and D. Diakonov, *Nucl. Phys.* B 582 (2000) 571 .

[63] D.H. Rischke, *Phys. Rev.* D 62 (2000) 034007 .

[64] R.D. Pisarski and D.H. Rischke, *Phys. Rev. Lett.* 83 (1999) 37 .

[65] M.G. Alford, K. Rajagopal, and F. Wilczek, *Nucl. Phys.* B 537 (1999) 443 .

[66] M. G. Alford, J. Berges and K. Rajagopal, Nucl. Phys. B **571**, 269 (2000).

[67] M. Ruderman, T. Zhu, and K. Chen, Astrophys. J. **492**, 267 (1998).

[68] P. W. Anderson and N. Itoh, Nature **256**, 25 (1975).

[69] T. Schafer, Nucl. Phys. B **575**, 269 (2000) [arXiv:hep-ph/9909574].

[70] M. Iwasaki and T. Iwado, Phys. Lett. B **350**, 163 (1995).

[71] T. Schäfer, Phys. Rev. D **62**, 094007 (2000);
M. Buballa, J. Hošek, and M. Oertel, Phys. Rev. Lett. **90**, 182002 (2003).

[72] A. Schmitt, Q. Wang, and D. H. Rischke, Phys. Rev. Lett. **91**, 242301 (2003); Phys. Rev. D **69**, 094017 (2004).

[73] M.G. Alford, J.A. Bowers, J.M. Cheyne, and G.A. Cowan, *Phys. Rev.* D 67 (2003) 054018 .

[74] A. Schmitt, nucl-th/0405076.

[75] T. Schäfer, *Phys. Rev.* D 62 (2000) 094007 .

[76] A. Schmitt, Q. Wang, and D.H. Rischke, Phys. Rev. D **66**, 114010 (2002).

[77] K. Iida and G. Baym, *Phys. Rev.* D 63 (2001) 074018 , Erratum *ibid.* D **66**, 059903 (2002).

[78] K. Rajagopal and F. Wilczek, *Phys. Rev. Lett.* 86 (2001) 3492 .

[79] M. Alford and K. Rajagopal, JHEP **0206**, 031 (2002).

[80] M. Huang, P.-F. Zhuang, and W.-Q. Chao, *Phys. Rev.* D 67 (2003) 065015 .

[81] F. Neumann, M. Buballa, and M. Oertel, *Nucl. Phys.* A 714 (2003) 481 .

[82] S.B. Rüster and D.H. Rischke, *Phys. Rev.* D 69 (2004) 045011 .

[83] W.V. Liu and F. Wilczek; *Phys. Rev. Lett.* 90 (2003) 047002 .

[84] E. Gubankova, W.V. Liu, and F. Wilczek, *Phys. Rev. Lett.* 91 (2003) 032001 .

[85] M.G. Alford, J.A. Bowers, and K. Rajagopal, *Phys. Rev.* D 63 (2001) 074016 .

[86] J.A. Bowers, *Ph.D. Thesis*, hep-ph/0305301.

[87] H. Müther and A. Sedrakian, *Phys. Rev.* D 67 (2003) 085024.

[88] I. Shovkovy and M. Huang, *Phys. Lett.* B 564 (2003) 205 ; *Nucl. Phys.* A 729 (2003) 835 .

[89] I. Shovkovy, M. Hanauske, and M. Huang, *Phys. Rev.* D671030042003.

[90] I. A. Shovkovy, S. B. Ruester and D. H. Rischke, J. Phys. G **31**, S849 (2005).

[91] M. Alford, C. Kouvaris, and K. Rajagopal, hep-ph/0311286.

[92] M. Huang and I. A. Shovkovy, Phys. Rev. D **70**, 051501 (2004).

[93] D. K. Hong, arXiv:hep-ph/0506097.

[94] R. Casalbuoni, R. Gatto, M. Mannarelli, G. Nardulli and M. Ruggieri, Phys. Lett. B **605**, 362 (2005) [Erratum-ibid. B **615**, 297 (2005)].

[95] M. Alford and Q. h. Wang, arXiv:hep-ph/0507269.

[96] K. Fukushima, arXiv:hep-ph/0506080.

[97] W.E. Brown, J.T. Liu, and H.c. Ren, Phys. Rev. D **61**, 114012 (2000); *ibid.* **62**, 054013, 054016 (2000).

[98] Q. Wang and D.H. Rischke, Phys. Rev. D **65**, 054005 (2002).

[99] D.f. Hou, Q. Wang, and D.H. Rischke, Phys. Rev. D **69**, 071501 (2004).

[100] D.K. Hong, Phys. Lett. B **473**, 118 (2000); Nucl. Phys. B **582**, 451 (2000).

[101] D. K. Hong, Prog. Theor. Phys. Suppl. **153**, 241 (2004).

[102] T. Schäfer, Nucl. Phys. A **728**, 251 (2003); eConf **C030614**, 038 (2003).

[103] T. Schäfer, arXiv:hep-ph/0402032.

[104] T. Schäfer and K. Schwenzer, arXiv:hep-ph/0405053.

[105] G. Nardulli, Riv. Nuovo Cim. **25N3**, 1 (2002).

[106] J.M. Cornwall, R. Jackiw, and E. Tomboulis, Phys. Rev. D **10**, 2428 (1974).

[107] J. Polchinski, arXiv:hep-th/9210046.

[108] D.B. Kaplan, arXiv:nucl-th/9506035.

[109] A. V. Manohar, arXiv:hep-ph/9606222.

[110] V. P. Gusynin and I. A. Shovkovy, Nucl. Phys. A **700**, 577 (2002).

[111] M. Kitazawa, T. Koide, T. Kunihiro and Y. Nemoto, Phys. Rev. D **65**, 091504 (2002).

[112] M. Kitazawa, T. Koide, T. Kunihiro and Y. Nemoto, arXiv:hep-ph/0502035.

[113] I. Giannakis and H. c. Ren, Nucl. Phys. B **669**, 462 (2003).

[114] K. Iida, T. Matsuura, M. Tachibana and T. Hatsuda, Phys. Rev. Lett. **93**, 132001 (2004) [arXiv:hep-ph/0312363].

[115] I. Giannakis, D. f. Hou, H. c. Ren and D. H. Rischke, Phys. Rev. Lett. **93**, 232301 (2004).

[116] R. D. Pisarski, Phys. Rev. C **62**, 035202 (2000).

[117] F.J. Wegener and A. Houghton, Phys. Rev. A **8**, 401 (1973).

[118] D.T. Son and M.A. Stephanov, Phys. Rev. D **61**, 074012 (2000).

[119] R. D. Pisarski, Nucl. Phys. B **309**, 476 (1988).

[120] H. Kleinert, Fortsch. Phys. **30**, 351 (1982).

[121] A. Gerhold and A. Rebhan, Phys. Rev. D **68**, 011502 (2003).

[122] D.D. Dietrich and D.H. Rischke, Prog. Part. Nucl. Phys. **53**, 305 (2004).

[123] C. Manuel, Phys. Rev. D **62**, 114008 (2000).

[124] D.H. Rischke, Phys. Rev. D **62**, 034007, 054017 (2000).

[125] C. Manuel, Phys. Rev. D **62**, 076009 (2000).

[126] D.H. Rischke, Phys. Rev. D **64**, 094003 (2001).

[127] R.D. Pisarski and D.H. Rischke, Nucl. Phys. A **702**, 177 (2002).

[128] R.D. Pisarski, Physica A **158**, 146 (1989).

[129] N. Nielsen, „Der Eulersche Dilogarithmus und seine Verallgemeinerungen." Nova Acta Leopoldina, Abh. der Kaiserlich Leopoldinisch-Carolinischen Deutschen Akad. der Naturforsch. 90, 121-212, (1909).

Curriculum Vitae von Philipp Tim Reuter

13.08.1975	geboren in Bonn als Sohn von I. Reuter und C. Reuter, geb. Gaa
1982-1986	Besuch der Franckeschule in Frankfurt am Main
1986-1995	Besuch des J. W. Goethe-Gymnasium in Frankfurt am Main
1995	Abitur
Sept.95-Okt.96	Zivildienst an der Katholischen Hochschulgemeinde, Frankfurt am Main
Winter 1996	Beginn des Studiums der Physik (Diplom) an der J. W. Goethe-Universität in Frankfurt am Main
23.10.1998	Vordiplom in Physik
02.07.00-01.07.01	Anfertigung der Diplomarbeit am Institut für Theoretische Physik in der Arbeitsgruppe von Prof. Dr. Horst Stöcker Titel der Diplomarbeit: „Kritische Phänomene im Statistischen Modell der Multifragmentation"
21.09.2001	Diplom in Physik
14.01.2002	Verleihung des Philipp-Siedler-Wissenschaftspreises 2002 des Physikalischen Vereins in Frankfurt am Main
Seit Herbst 2001	Wissenschaftlicher Mitarbeiter am Institut für Theoretische Physik Beginn der Arbeiten zur Dissertation in der Arbeitsgruppe von Prof. Dr. D.-H. Rischke
Seit 2005	Gutachtertätigkeit für Physical Review

Akademische Lehrer

Prof. Dr. Aßmus
Prof. Dr. Becker
Dr. Bugaev
Prof. Dr. Fink
Prof. Dr. de Groote
Prof. Dr. Dr. h. c. mult. Greiner
Prof. Dr. Haug
Prof. Dr. Hensen
Prof. Dr. Jelitto
Prof. Dr. Klein
Prof. Dr. Lüthi
Prof. Dr. Maruhn
Prof. Dr. Mäntele
AOR Dr. Reinhardt
Prof. Dr. Rischke
HD Dr. habil. Schaffner-Bielich
Prof. Dr. Schaarschmidt
Prof. Dr. Schempp
Prof. Dr. Schmidt-Böcking
Prof. Dr. Schubert
Dr. Shovkovy
Prof. Dr. Stock
Prof. Dr. Stöcker
Prof. Dr. Wang

Acknowledgements